Table of contents

« Si tu n’espères pas l’inespéré,

tu ne parviendras pas à le trouver. »

Héraclite

I. JURY MEMBERS

President

Professor Jean-Baptiste Demoulin
de Duve Institute
Université Catholique de Louvain

UCL members

Professor Luc Bertrand
Institut de recherche expérimentale et Clinique
Université Catholique de Louvain

Professor Patrick Jacquemin
de Duve Institute
Université Catholique de Louvain

External members

Professor Stéphane Germain
Center for Interdisciplinary Research in Biology
Collège de France, Paris, France

Professor Marianne Voz
GIGA
Université de Liège

Promoter

Professor Christophe E. Pierreux
de Duve Institute
Université Catholique de Louvain

Co-promoter

Professor Pierre J. Courtoy
de Duve Institute
Université Catholique de Louvain

II. ACKNOWLEDGEMENTS

Voici venu le moment des remerciements... Exprimer ma reconnaissance à tous ceux qui m'ont aidée, de près ou de loin, qui ont compté pour moi durant ces années, qui m'ont accompagnée sur le chemin de la thèse, pour quelques kilomètres ou pour une plus longue route… éveille en moi une certaine appréhension tant je crains d'en oublier certains ou de ne pas trouver les mots justes pour exprimer ce que je ressens.

Pour commencer, je tiens à remercier chaleureusement mon promoteur Christophe Pierreux. Durant ces deux années de mémoire et ces quatre années de thèse, ta compétence, tes connaissances, ta rigueur scientifique et ton exigence ont fait de moi la scientifique que je suis aujourd'hui. Disponible et toujours à l'écoute dans les moments de doute, tu as su trouver les mots justes pour me rassurer, me conseiller, me remotiver et me rendre confiance en moi. Pour tout ça, je te remercie infiniment.

Je tiens ensuite à remercier le Professeur Pierre Courtoy, pour son accueil au sein de son laboratoire. Au cours de nos discussions scientifiques, j'ai pu, grâce à ses remarques et suggestions pertinentes, profiter pleinement et avec enthousiasme de ses connaissances.

Merci à Jean-Baptiste Demoulin, Luc Bertrand et Patrick Jacquemin, respectivement président et membres de mon comité d'accompagnement. Ils m'ont suivie et accompagnée durant ces quatre années, m'ont conseillée, aidée à choisir la meilleure voie et à m'améliorer d'années en années pour arriver au bout de cette thèse. Merci également à eux d'avoir pris le temps de lire mon manuscrit de thèse et pour les questions qui ont animé la défense privée.

Merci à Stéphane Germain et Marianne Voz d'avoir accepté d'être les membres externes de mon jury, d'avoir lu et évalué mon travail ainsi que pour la discussion que nous avons eue lors de ces trois heures de défense privée.

Un grand merci au groupe « epithelial-diff », les rois de la thyroïde et du pancréas, pour le travail partagé tous les jours à vos côtés, les réunions intéressantes du lundi matin (même si pas toujours réveillés et très réactifs). Merci aussi pour les discussions, parfois scientifiques, souvent « ragoteuses » durant les pauses café

dont nous sommes restés les seuls survivants de la tradition perpétuée par nos anciens. Jona et Cha, je compte sur vous pour maintenir et assurer l'organisation des prochains team-building. ☺

Un merci plus particulier à …

Ma Minimoi… Que dire, et comment ne rien oublier? Il y a un peu plus de 3 ans, Christophe a engagé une mémorante pour travailler sur mon projet mais au niveau du pancréas, et m'a demandé de l'encadrer. Cette mémorante, c'était toi ! Petit à petit nous nous sommes apprivoisées et sommes très vite devenues inséparables. Nos ressemblances tant physiques (il parait) qu'au bench (nos bêtises) ou dans la vie t'ont très vite valu le surnom de Minimoi. L'une toujours là pour l'autre tant pour aider aux manips, raconter les dernières nouvelles, discuter projet ou papoter à n'en plus finir, mais aussi pour écouter, conseiller ou soutenir dans les moments les plus durs. A ma grande joie, nous sommes devenues amies, confidentes, sœurs et indissociables… Je garde de nos années communes au labo mes meilleurs souvenirs. Je pourrais écrire des lignes entières mais tu sais ce qu'il en est entre nous et pour tout ça, je te dis merci Minimoi. ☺

Mylah, my office buddy. You, a little lady who arrived three years ago in our group, replaced Gigi in the office that we used to share with Christophe. Of course, it was a big change for me but we managed to establish a mutually rewarding relationship. Your positivity, your enthusiasm, your patience and, most of all, your great strength to be happy and smiling no matter the situation, have been a real inspiration to me. I had never met anyone as smiling, as persevering and as motivated by their projects as you. And this, despite the thousands of kilometers that were keeping you away from your husband and family. Thanks to you, I have improved my scientific English, but also my every-day-language because of our numerous small talks every time Christophe left the office. I thank you for the work you realized for the project, but I am especially grateful for the redaction of the paper that you undertook whilst I was writing my thesis. Without you, we would never have managed it. We are now forever bounded by the future *Villacorte, Delmarcelle et al*. ☺ You will soon leave us to go back to Japan, but I hope we'll stay in touch. I wish you a lot of happiness there (or elsewhere) with your husband, future babies and all the projects you plan to realize.

Catherine, la dernière recrue d'« epithelial diff ». Ta bonne humeur, ton rire et ton aisance t'ont permis de t'intégrer rapidement au sein de notre groupe. Bonne chance pour la suite de ton parcours, je te souhaite de trouver ta voie dans la recherche et ta (peut-être) future thèse à l'unité.

Pauline, Hélo et Vivi en qui j'ai trouvé trois amies. Nous avons partagé durant ces nombreuses années nos histoires d'amour, d'enfants, de maison, de projets privés et professionnels tant au bench qu'en coin café. Merci pour ces moments. J'espère que vous trouverez votre voie et le bonheur dans vos projets futurs.

Tony, Gigi, ma GF, il n'y a pas de remerciements sans vous citer. Vous étiez les aînés à mon arrivée dans le labo. Vous m'avez initiée aux techniques de laboratoire mais aussi aux pauses-café, aux « jeudredis », aux soirées de thèse farfelues, aux papotes dans les couloirs, à l'événementiel Cell/ICP… J'ai passé avec vous des moments incroyables que je ne suis pas prête d'oublier !

Merci aussi à tous les autres membres de l'unité Cell, Pascale, Dona, Mélanie, Hélène, Louise, Manu, Freddy, Abdel, Patrick, Etienne, Audrey, Pia, Thanh, Patrick et Aimée-Lys pour leur présence au sein du labo, les échanges, les aides théoriques et techniques apportées de près ou de loin à mon projet ainsi que leur participation enthousiaste lors des événements organisés au labo. Pascale, tu as récemment intégré notre groupe. Ta rigueur, ta précision et ton ancienneté dans le labo sont un atout pour notre équipe. Hélène, j'ai découvert bien trop tard ton don pour le dessin. Tu m'as sauvée en dernière minute avec la réalisation des superbes schémas nécessaires à ma thèse, un tout grand merci.

Merci aussi aux membres du groupe LPAD avec qui nous collaborons étroitement et plus particulièrement à Sabine pour ses nombreuses connaissances techniques et son écoute attentive. Tu as toujours été présente pour moi pour m'écouter me plaindre ou me réjouir et tu as toujours su trouver les mots pour me réconforter et m'encourager. Tu as été pour moi une petite maman et une amie.

Un énorme merci à ma famille qui m'a soutenue et encouragée durant ces quatre années de thèse mais aussi durant mes études. Papa, Maman, vous avez fait de moi celle que je suis, vous m'avez permis de réaliser les études que je voulais et vous m'avez accompagnée durant toutes ces années de joie, de stress, de ras-le-bol mais surtout d'accomplissement… Vous n'avez peut-être pas toujours très

bien compris l'objet de mon travail de thèse, mais vous avez su vous adapter et me poser les bonnes questions quand il le fallait ou me laisser tranquille quand je le souhaitais pour me laisser m'en sortir seule dans les moments les plus difficiles. J'ai une chance extraordinaire de vous avoir, merci pour tout… et le reste ! ☺

Enfin, mes derniers remerciements et les plus profonds vont à mon homme, Benoît. Il n'y a pas de mots pour te dire combien je te remercie. Tu es sans conteste le plus méritant et le plus courageux pour m'avoir supportée et encouragée durant mes dernières années de thèse et plus particulièrement durant l'étape de rédaction et de défense. Ça n'a pas été de tout repos mais ta présence, tes mots et ton soutien m'ont aidée à traverser cette période particulièrement stressante. Ton arrivée dans ma vie, ainsi que ta petite tête blonde, m'ont aidée à grandir et à voir la vie sous un nouveau jour. Vos sourires et votre compréhension ont été pour moi une motivation jour après jour et m'ont donné l'envie d'y arriver… Et ça y est ! J'y suis arrivée ! :D

Merci à tous !

III. ABBREVIATION LIST

ActR: Activin receptor

ALK: Activin receptor-like kinase

AMIS: Apical membrane initiation site

aPKC: Atypical protein kinase C

AQP: Aquaporine

ATP: Adenosine triphosphate

bHLH: Basic helix loop helix

BM: Basement membrane

BMP: Bone/body morphogenetic protein

BMPR: BMP receptor

cAMP: Cyclic adenosine monophosphate

CDC42: Cell division control protein 42

CFTR: Cystic fibrosis transmembrane conductance regulator

CM: Conditioned medium

Co-Smad: Co-mediator Smad

DA: Ductus arteriosius

DIT: Di-iodotyrosine

DNA: Deoxyribonucleic acid

E: Embryonic day

EC: Endothelial cells

ECM: Extracellular matrix

eEPC: Embryonic endothelial progenitor cells

e.g.: *Exempli gratia*

ERK: Extracellular signal-regulated kinase

ESC (h or m): Embryonic stem cells (human or mouse)

FAK: Focal adhesion kinase

FBS: Fetal bovine serum

FGF: Fibroblast growth factor

FGFR: FGF receptor

Foxe1: Forkhead box E1

FRTL5: Fischer rat thyroid cell line

GAG: Glycosaminoglycans

GDF: Growth differentiation factor

GTP: Guanosine triphosphate

Hhex: Hematopoietically expressed homeobox

HUVEC: Human umbilical vein endothelial cell

Id: Inhibitor of differentiation/DNA binding

i.e.: *Id est*

IGF-1: Insulin-like growth factor

ILK: Integrin-linked kinase

I-Smad: Inhibitory Smad

I-Tg: Iodinated thyroglobulin

kDa: kiloDalton

KO: Knock-out

LE: Laminin EGF-like (repeats)

LG : Laminin globular (domain)

LN : Laminin N-terminal (domain)

MDCK: Madin Darby Canine Kidney

MIT: Mono-iodotyrosine

MIVD: Microvillus inclusion disease

NIS: Sodium/iodide symporter

Nkx2.1/Titf1: Thyroid transcription factor 1

Pax8: Paired box gene 8

PDCX/Podxl: Podocalyxin

PKA: Protein kinase A

PtdIns: Phosphatidylinositol

PTEN: Phosphatase and tensin homolog

pTFC: Progenitor of thyroid follicular cell

RGD: Arginine-glycine-aspartic acid

RNA: Ribonucleic acid

R-Smad: Receptor-activated Smad

RT-qPCR: Real time-quantitative polymerase chain reaction

SFK: Src family kinase

Shh: Sonic hedgehog

SPARC: Secreted protein acidic, cystein rich

T3: Tri-iodothyronine

T4: Tetra-iodothyronine (or thyroxin)

Tg: Thyroglobulin

TGF: Transforming growth factor

TJ: Tight junction

TPO: Thyroperoxidase

TRH: Thyrotropin-releasing hormone

TSH: Thyroid-stimulating hormone

TSHr: TSH receptor

VEGF: Vascular endothelial growth factor

VEGFR: VEGF receptor

ZO-1: Zonula occludens 1

ZONAB: ZO-1-associated nucleic acid binding protein

IV. SUMMARY

The thyroid is an endoderm-derived endocrine gland, where epithelial cells are organized in closed spheres, called follicles. Follicles are composed of an epithelial monolayer of cells, the thyrocytes, resting on a basement membrane and delineating a lumen. During embryonic development, the thyroid undergoes two opposite epithelial transitions. First, thyroid-specified polarized cells from the foregut endoderm lose polarity and form a tri-dimensional mass of undifferentiated cells. Second, after ventro-caudal, then lateral migration, the epithelial mass reorganizes into polarized epithelial monolayers, the follicles. This distinct epithelial architecture dictates the ultimate function of the organ. *A contrario*, thyroid function is impaired if the proper epithelial structure does not form or is not maintained.

In order to understand the mechanisms implicated in the formation of thyroid follicles (folliculogenesis), I focused on reciprocal juxtacrine communications between epithelial cells and their environment, and in particular with endothelial cells from blood vessels. In our first study, we showed that during the reorganization of the thyroid mass into polarized monolayers, epithelial cells are closely apposed to endothelial cells. Genetic inactivation of Vegfa (Vegfa^{KO}) in thyrocytes progenitors revealed impaired recruitment of endothelial cells around and in the thyroid. Reduced endothelial cell density in the thyroid prevented folliculogenesis, suggesting that endothelial cells instruct the developing thyroid epithelium to form follicles. Using an *ex vivo* culture system of embryonic thyroid, we demonstrated that the instructive role of endothelial cells on thyroid epithelial cells is contact-independent and can be mimicked with medium conditioned by embryonic endothelial progenitor cells (eEPC).

We initiated two projects to understand the mechanisms of folliculogenesis: a candidate-based approach focusing on BMP signaling and a biochemical approach to characterize the folliculogenic activity present in conditioned medium. Similarly to Vegfa^{KO}, thyroid-specific inactivation of *Smad1* and *Smad5* (Smad1/5^{dKO}) displayed defective folliculogenesis. Despite normal endothelial cell density, Smad1/5^{dKO} thyroid expressed lower levels of selected endothelial-specific markers and showed reduced expression of *Vegfa*. Moreover, both Vegfa^{KO} and Smad1/5^{dKO} showed impaired basement membrane assembly,

suggesting that folliculogenesis might depend on basement membrane formation. The second approach revealed that medium conditioned by eEPC rescue the folliculogenesis defect of Smad1/5^{dKO} and of Vegfa^{KO} thyroids, indicating that folliculogenic activity from the conditioned medium acts downstream of BMP signaling and of endothelial cells. We demonstrated that eEPC express, produce and secrete in the culture medium high quantities of laminin α1, β1 and γ1. Furthermore, heterotrimeric laminin 111 was deposited and weaved around thyroid explants in culture, and folliculogenic activity of conditioned medium was abrogated when laminin α1 was silenced in eEPC. We propose that epithelial Smad1/5 signaling and endothelial cells recruited to the thyroid control folliculogenesis via follicles basement membrane assembly.

Dans la thyroïde, une glande endocrine dérivée de l'endoderme,les cellules épithéliales sont organisées en structures sphériques fermées, appelées follicules. Les follicules sont composés d'une monocouche de cellules épithéliales, les thyrocytes, reposant sur une membrane basale et délimitant une lumière. Durant le développement embryonnaire, la thyroïde subit deux transitions épithéliales opposées. Premièrement, les cellules polarisées du tube primitif perdent leur polarité et forment un amas tridimensionnel de progéniteurs thyroïdiens non différenciés. Ensuite, après migration ventro-caudale et puis latérale, la masse épithéliale se réorganise en monocouches de cellules épithéliales polarisées, les follicules. Cette architecture particulière est requise pour la fonction de l'organe. Au contraire, sa fonction est altérée si les follicules ne se forment pas correctement ou ne sont pas maintenus.

Dans le but de comprendre les mécanismes impliqués dans la formation des follicules thyroïdiens (folliculogenèse), je me suis concentrée sur le réseau de communications juxtacrines réciproques entre les cellules épithéliales et leur environnement, plus particulièrement avec les cellules endothéliales des vaisseaux sanguins. Dans une première étude, nous avons montré que, durant la réorganisation de l'amas thyroïdien en monocouches polarisées, les cellules épithéliales sont étroitement apposées aux cellules endothéliales. L'inactivation génétique de *Vegfa* ($Vegfa^{KO}$) dans les progéniteurs de thyrocytes entraine un défaut de recrutement des cellules endothéliales autour et dans la thyroïde. A son tour, la réduction de la densité endothéliale dans la thyroïde perturbe la formation des follicules, suggérant que les cellules endothéliales instruisent l'épithélium thyroïdien à former des follicules. A l'aide d'un système de culture de thyroïde embryonnaire *ex vivo*, nous avons démontré que le rôle instructeur des cellules endothéliales sur les thyrocytes est indépendant d'un contact cellulaire et peut être reproduit avec du milieu conditionné par des progéniteurs de cellules endothéliales embryonnaires (eEPC).

Nous avons initié deux projets pour comprendre les mécanismes de la folliculogenèse: une approche « candidat » se basant sur les BMPs et une approche biochimique visant à caractériser le milieu conditionné. De manière similaire au $Vegfa^{KO}$, l'inactivation thyroïde-spécifique de *Smad1* et *Smad5* ($Smad1/5^{dKO}$) entraîne un défaut de folliculogenèse. Bien que la densité épithéliale soit normale, la thyroïde de $Smad1/5^{dKO}$ exprime des quantités réduites de

marqueurs endothéliaux ainsi que de *Vegfa*. De plus, tant Vegfa^{KO} que Smad1/5^{dKO} présentent un défaut d'assemblage de la membrane basale, suggérant que la folliculogenèse pourrait dépendre de la présence de cette structure. La seconde approche a révélé que le milieu conditionné par les eEPC corrige le défaut de folliculogenèse des thyroïdes Vegfa^{KO} et Smad1/5^{dKO}, indiquant que l'activité folliculogénique du milieu conditionné agit en aval de la signalisation BMP et des cellules endothéliales. Nous avons démontré que les eEPC expriment, produisent et sécrètent dans le milieu de culture de grandes quantités de laminine α1, β1 et γ1. De plus, la laminine 111 est déposée et assemblée autour d'explants thyroïdiens en culture, et l'activité folliculogénique du milieu conditionné est abolie lorsque l'expression de la laminine α1 est diminuée dans les eEPC à l'aide de shRNA. En conclusion, nous proposons que la signalisation épithéliale Smad1/5 et le recrutement des cellules endothéliales dans la thyroïde contrôlent la folliculogenèse via l'assemblage de la membrane basale folliculaire.

V. INTRODUCTION

1. The thyroid gland

1.1. Histology

The thyroid gland is an endocrine organ composed, in mammals, of two lobes connected by an isthmus and situated on both sides of the trachea, at the base of the neck (Figure 1 A.). Two endoderm-derived cell types are found in the thyroid: the follicular cells, also called thyrocytes, originating from the midline endodermal thyroid anlage, and the C-cells deriving from the fourth pharyngeal pouches as the ultimobranchial bodies (De Felice and Di Lauro, 2004; Kameda et al., 2007).

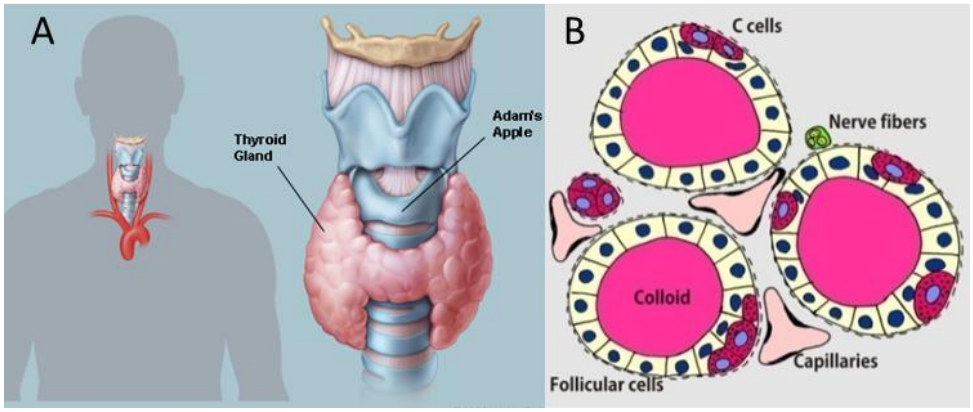

Figure 1. Thyroid localization, shape and organization. A. The thyroid is situated at the base of the neck, in front of the trachea and is composed of two lateral lobes linked by the isthmus. B. Organization of the various cell types in the thyroid. Thyrocytes or follicular cells are organized in follicles and delineate a lumen containing the colloid. C-cells are present in the stroma or closely associated with the follicular epithelium. Capillaries and nerves are scattered all around follicles (Fernández-Santos et al., 2012).

Other non-epithelial cell types present in adult thyroid include endothelial cells and pericytes of blood vessels, mesenchymal cells and nerve cells. Thyrocytes are organized in spherical structures called follicles. These structures consist of a monolayer of polarized thyrocytes facing a gel-filled space, the colloid (Figure 1 B.). Follicles allow synthesis, storage and controlled release of thyroid hormones:

tri-iodothyronine (T_3) and thyroxine (T_4). T_3 and T_4 are essential for the body as they regulate metabolism, growth and development, body temperature and are also required for brain maturation. C-cells secrete another hormone, calcitonin, which is implicated in calcium homeostasis.

When plasma T_3 and T_4 levels are low, thyroid stimulating hormone (TSH) released from the pituitary stimulates the synthesis of new hormones. Synthesis requires import of iodide into the cell, its incorporation into thyroglobulin (Tg), the apical capture and proteolytic excision of hormonogenic peptides at the extremities of iodinated thyroglobulin (I-Tg) and basolateral release of T_3 and T_4 into the bloodstream. For the first step, iodide is taken up from blood capillaries and transported into thyrocytes via the sodium-iodide symporter (NIS) localized at the basal pole. NIS transports two sodium (Na^+) ions and one iodide (I^-) ion into the thyrocyte. The energy required for iodide import is produced by the Na^+/K^+ ATPase that generates a gradient of Na^+ concentration. I^- next crosses the apical membrane via the pendrin transporter and is oxidized by thyroperoxidase (TPO) in the colloid. This activity requires H_2O_2 to be optimal. Thyroglobulin, assembled in the endoplasmic reticulum, processed in the Golgi and transported to the apical surface in small vesicles, is released in the colloid. Iodine organification, which corresponds to the covalent binding of iodine to tyrosyl residues of thyroglobulin, allows the formation of mono-iodotyrosine (MIT) and di-iodotyrosine (DIT) which are coupled again by TPO to form tri-iodothyronine (T_3) and tetra-iodothyronine or thyroxin (T_4). I-Tg is then stored in the colloid, a viscous substance filling the follicular lumen, until utilization. Following stimulation by TSH, which binds to the TSH receptor (TSHr) at the basal pole of the thyrocyte, I-Tg is captured by endocytosis, via formation of pseudopods, and hydrolyzed by proteases in lysosomes. This allows the release of thyroid hormones (T_3 and T_4) from the Tg backbone and their delivery into the circulation via basal transporters such as monocarboxylate transporter 8 (MCT8) (Figure 2)(Colin et al., 2013; Dunn and Dunn, 2001). The human gland secretes about 100nmol of T_4 and about 7 nmol of T_3 into the blood per day. The concentration range of free active T_4 is 9-25pmol/L and T_3 is 4-8pmol/L (Kolpak et al., 2015). The majority of T_3/T_4 is bound to proteins in the blood and is thus inactive. Once T_3/T_4 levels are normalized, they exert a negative feedback on the hypothalamo (thyreotropin releasing hormone, or TRH)

hypophyseal/pituitary (TSH) axis, thereby decreasing TRH and TSH release. This regulation also depends on iodine concentration in the thyrocytes.

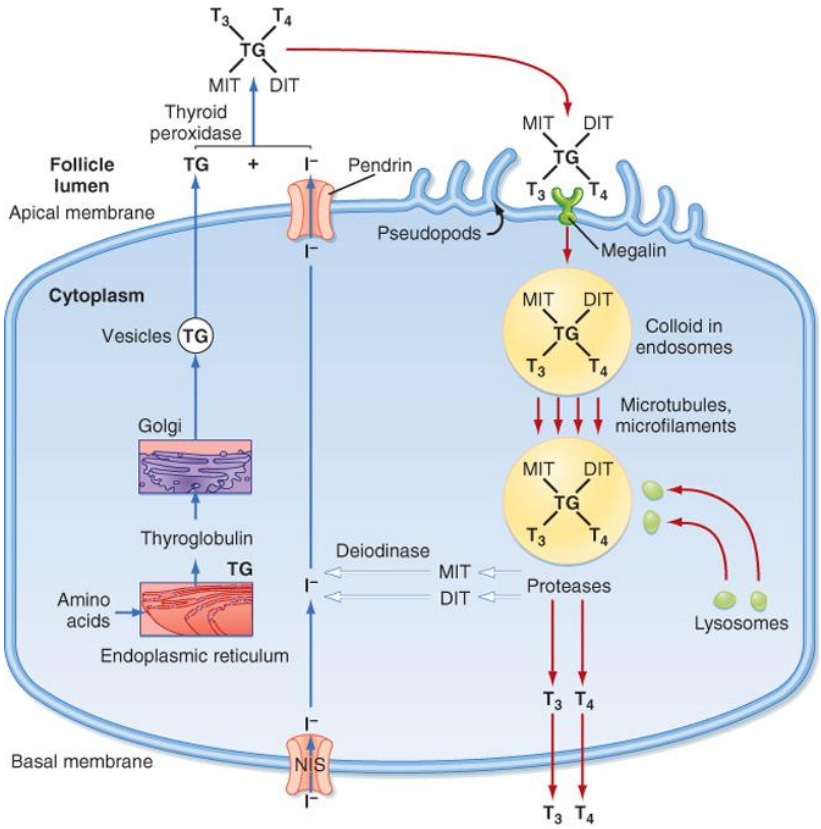

Figure 2. Thyroid hormone synthesis. Thyrocytes synthesize Tg and capture iodide, which are then transported into the lumen. Iodide is oxidized by TPO and incorporated to Tg at the apical membrane and stored in the colloid as I-Tg. Following TSH stimulation (not depicted), I-Tg is endocytosed into lysosomes where T_3 and T_4 are released by cathepsins. Hormones are finally released at the basal pole in the extracellular environment to reach the blood vessels (Berne and Levy Physiology, 6th Edition).

Follicles can be either in active or hypofunctioning state. This latter is characterized by a decrease of pendrin and TPO expression and an absence of Tg in colloid. The capillary network is also thinner around hypofunctioning follicles. On the contrary, active follicles are surrounded by larger capillaries and close contacts exist between epithelial follicular cells and the endothelial cells of blood

vessels. These contacts allow exchange between both cell types: capture of iodide and release of thyroid hormones. Active follicles surrounded by blood capillaries can thus be referred to as “angio-follicular units” (Colin et al., 2013; Gérard et al., 2002).

1.2. Development/morphogenesis

1.2.1. Developmental steps

As mentioned, thyroid is composed of two types of endocrine cells: follicular cells and parafollicular C cells. These cells have different embryonic origins but will reach the same location. Although a continuous process, mouse thyroid development can be divided into various steps: specification, budding, migration, lobulation, folliculogenesis and differentiation. It starts at embryonic (E) day 8.5, which is 8.5 days after fertilization, and continues throughout gestation until delivery (E19 or P0). Human thyroid development involves very similar steps but occurs on a longer time scale, from E20 to E70 (Trueba et al., 2005).

Specification and budding (E8.5-E10.5)

At E8.5, a small group of cells from the foregut pharyngeal endoderm start to express the transcription factors Nkx2.1, Foxe1, Pax8 and Hhex: they form the midline thyroid primordium (Figure 3 A.). These cells are specified to undertake the thyroid developmental program (De Felice and Di Lauro, 2004) and are in close contact with the aortic sac, a large vessel from which the pharyngeal arch arteries will later develop (Figure 3 B.). The proximity of the aortic sac suggests that this structure plays an essential role for thyroid primordium specification. In late E9.5, the thyroid primordium is enlarged and the endoderm evaginates and expands ventrally into the surrounding mesenchyme. This step is called thyroid budding. Surprisingly, thyroid bud growth is not due to cell proliferation but rather triggered by recruitment of new progenitor cells from the endoderm adjacent to the primordium (De Felice and Di Lauro, 2004; Fagman et al., 2006).

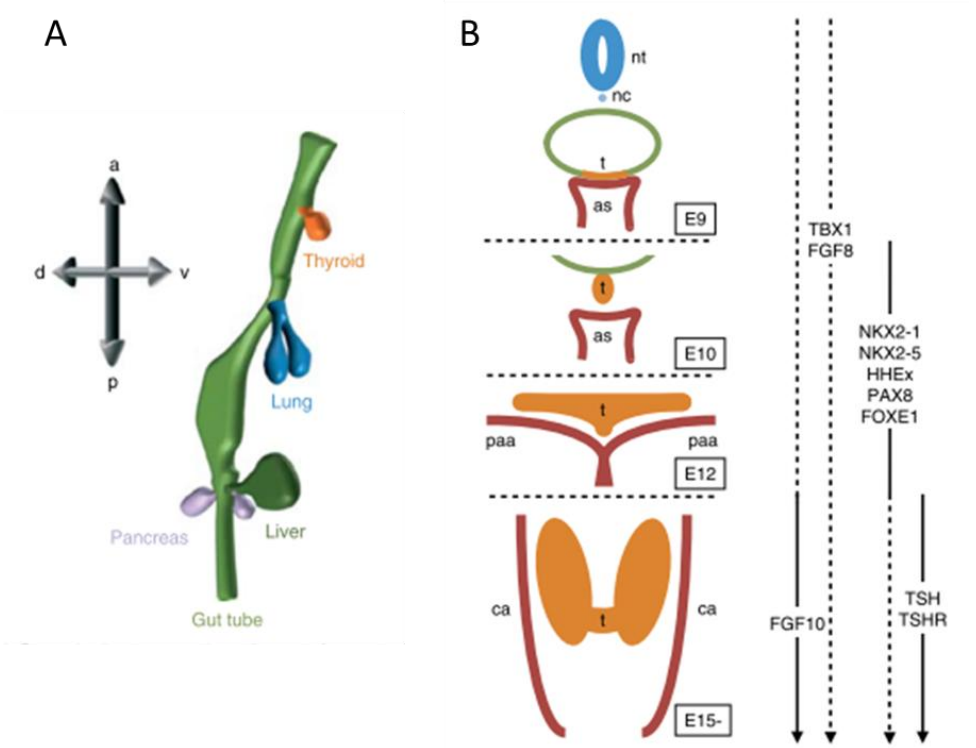

Figure 3. Thyroid development from the endoderm. A. Localization of different endoderm-derived organs along the antero-posterior axis. Similarly to lung (blue), liver (green) and pancreas (purple), thyroid (orange) is specified from the primitive endoderm or primitive gut tube (green) and buds ventro-caudally. B. Schematic representation of thyroid development stages in transversal view. At E9, the thyroid primordium ('t', orange) specifies from the gut tube (green), co-expresses Nkx2.1, Pax8, Hhex and Foxe1 and is in close contact with aortic sac ('as', red). Neural tube ('nt') and notochord ('nc') are localized dorsally to the primitive gut tube. At E10, thyroid progenitors migrate in the adjacent mesenchyme and form a bud ('t'). At E12, the thyroid expands and migrates laterally along the course of pharyngeal arch arteries ('paa'). Finally, at E15, thyroid has reached its final localization and shape: two lobes connected by an isthmus ('ca': carotid arteries). On the right, arrows represent expression of factors implicated in thyroid development. Dashed lines mean that these implications are not well characterized in development (Fagman and Nilsson, 2011).

Bud disconnection and migration (E10.75-E11.5)

After E10.5, the bud elongates and invades the adjacent mesenchyme in a ventro-caudal direction (De Felice and Di Lauro, 2011). The transcription factor

Foxe1 is implicated in this migratory process (De Felice and Di Lauro, 2004). Migration results in a thinning of the connection between the bud and pharyngeal endoderm. The last connection between developing thyroid and pharyngeal floor, the thyroglossal tract, disappears at E11.5 so that the bud is entirely disconnected from the pharyngeal endoderm (Figure 3 B.). At this stage, some blood vessels appear around the thyroid primordium. At the same time, two endodermal evaginations arise from the fourth pharyngeal pouches localized rostrally and laterally and give rise to the ultimobranchial bodies. These two groups of cells initiate a caudal migration on each side of the developing trachea. They express Nkx2.1 and will later give rise to the parafollicular C cells (Fagman et al., 2006).

Thyroid bilobation and fusion with ultimobranchial bodies (E12.5-E13.5)

At E12.5, the spherical thyroid primordium has reached a ventral position, in front of the trachea. Proliferative activity is detected in the primordium and this will allow the initiation of bilobation by expansion and migration. At E13.5, thyroid expansion and migration has generated two lobes located on each side of trachea but still connected by the isthmus (Figure 3 B.). Migration is probably guided by the third pharyngeal arteries. Interestingly, the bilateral migration path of the thyroid midline primordium and the descending path of the ultimobranchial bodies will converge and the two progenitor populations will mix at the meeting points thereby forming the two lateral lobes (Fagman et al., 2006).

Morphogenesis and differentiation (E14.5-E17.5)

At E14.5, the thyroid has acquired its definitive anatomical shape and position. It will continue to expand by proliferation, and most importantly, epithelial cells will organize into follicles (see section 1.1.) and C cells will disseminate into the thyroid parenchyma. The mechanisms of cell organization in follicles were the focus of my thesis and will be explained in the results section. At E17.5, thyroid has almost reached its final size and blood vessels encircle individual follicles. During this period, thyroid progenitors differentiate and start to express Tg, TPO, NIS and TSH receptor. Tg accumulates in the lumen and T_4 is detected as early as E16.5 (De Felice and Di Lauro, 2004; Fagman et al., 2006).

1.2.2. Thyroid specific transcription factors

Thyroid organogenesis perturbations lead to hypoplasia, ectopy or agenesis in newborns. These conditions, collectively named “thyroid dysgenesis”, are responsible for 85% of congenital hypothyroidism, a condition that affects one out of 3500 newborns worldwide. As the cause of hypothyroidism is mainly due to sporadic mutations, it is important to identify genes implicated in thyroid development and to understand their mode of action (De Felice and Di Lauro, 2004). Embryonic thyroid organogenesis relies mainly on 4 transcription factors - Nkx2.1, Pax8, Hhex and Foxe1 - which are expressed from the thyroid specification step and are maintained in adults, where they control thyroid function (Figure 3 B.).

Titf1/Nkx2.1 (thyroid transcription factor 1)

Nkx2.1 is expressed in thyrocytes, in C cells but also in the trachea and lung epithelium. In the thyroid, it is responsible for Tg, TPO and TSHr expression (Figure 4). Nkx2.1 is not required for thyroid primordium specification and budding, but thyroid primordium cells rapidly degenerate and the bud disappears by E12-13 in Nkx2.1 null or knockout (KO) mice. Furthermore, $Nkx2.1^{KO}$ has no C-cells and impaired lung morphogenesis so that mice die at birth (De Felice and Di Lauro, 2004; Kusakabe et al., 2006). Seven phosphorylation sites (serine) presenting homology to CKII, protein kinase C or microtubules-associated protein kinase have been identified in Nkx2.1 sequence as important for transcriptional activation by NKX2.1 *in vitro* (Zannini et al., 1996). *In vivo*, these same sites are important for normal follicular organization (Silberschmidt et al., 2011). This suggests that extracellular signals, which allow post-translational modification of Nkx2.1, are probably implicated in thyroid follicle morphogenesis.

Pax8 (paired box gene 8)

Pax8 is expressed in thyroid, kidney and nervous system but is absent from the C cells and their progenitors. It directly interacts with the transcription factor Nkx2.1 and regulates the expression of thyroid-specific genes: Tg, TPO and NIS (Figure 4). Genetic inactivation of Pax8 in mouse embryo leads to growth retardation and death within the first 2-3 weeks. The thyroid is severely affected as no thyrocytes can be detected and the gland is only composed of C-cells. This

means that Pax8 is required for the survival of thyroid progenitors but not for their specification as thyroid primordium is normal (De Felice and Di Lauro, 2004; Mansouri et al., 1998). Upon conditional deletion of Pax8 in adults, mice develop severe hypothyroidism due to a reduced gland size and defective expression of differentiation genes. Further analysis of $Pax8^{KO}$ mice revealed downregulation of the anti-apoptotic factor Bcl2: Pax8 positively regulates Bcl2 (Marotta et al., 2014). In thyroid FRTL-5 cells, tumor protein 53-induced nuclear protein 1 (tp53inp1), a positive regulator of apoptosis, is a transcriptional target of Pax8. Following Pax8 deletion, tp53inp1 is upregulated and stimulates apoptosis thereby providing an explanation for thyroid size reduction (Di Palma et al., 2013). Recently, Wnt4 was also identified as a new target of Pax8 transcription factor in FRTL-5 cells and was demonstrated to be important for maintenance of the epithelial phenotype of thyrocytes (Filippone et al., 2014).

Interestingly, transient coexpression of Pax8 and Nkx2.1 in mouse (Antonica et al., 2012; Ma et al., 2013) or human embryonic stem cells (mESC or hESC) (Ma et al., 2015) induces the expression of thyrocyte-specific differentiation genes such as NIS, TPO, Tg and TSHr. Further culture in matrigel with TSH potentiates these effects and follicular structures acquire the ability to organify iodide (Antonica et al., 2012; Ma et al., 2013; Ma et al., 2015). These experiments support the strong involvement and critical role of Nkx2.1 and Pax8 in thyroid development.

Hhex (hematopoietically expressed homeobox)

Hhex is expressed in thyroid but also in the liver, thymus, pancreas and lungs. In Hhex-null embryos, the thyroid primordium is present but at E10, thyroid budding is impaired and this results in absence of thyroid, or hypoplastic thyroid still connected to the floor of the pharynx. Embryos die before E15.5 due to forebrain development defects (De Felice and Di Lauro, 2004).

Foxe1 (thyroid transcription factor 2)

Foxe1 is first detected in all endodermal cells of the foregut, then restricted to thyroid, palate, esophagus, tongue and epiglottis at later stages. Foxe1-null embryos develop normally but die within 48h after birth and display a small thyroid still attached to the pharyngeal floor or no thyroid at all. Foxe1 is not

required for the budding stages but is important to promote migration of follicular precursors (De Felice and Di Lauro, 2004).

Nkx2.1, Pax8, Foxe1 and Hhex form a strong regulatory network

In summary, the co-expression of these four transcription factors in endodermal cells specifies the thyroid fate. These gene products have important role in thyroid development but also in adult although they are not individually required for the initial steps of morphogenesis, specification and early budding. Several evidences indicate that thereafter, the four transcription factors form a robust network via reciprocal-cross regulation: every transcription factor induces or maintains the expression of another one (Figure 4). For example, in $Pax8^{KO}$ embryos, the expression of Foxe1 and Hhex is reduced. Hhex promoter contains binding sites for Pax8, but also for Nkx2.1, these two being major activators of Hhex. As a result, Pax8, Nkx2.1 together with Hhex, control Foxe1 expression. Foxe1 is at the end of this transcriptional cascade as $Foxe1^{KO}$ expresses normal level of the three transcription factors. Once initiated, this network is self-maintained; for example, Hhex maintains the expression of Nkx2.1, Pax8 and Foxe1 (Fagman and Nilsson, 2010; Parlato et al., 2004).

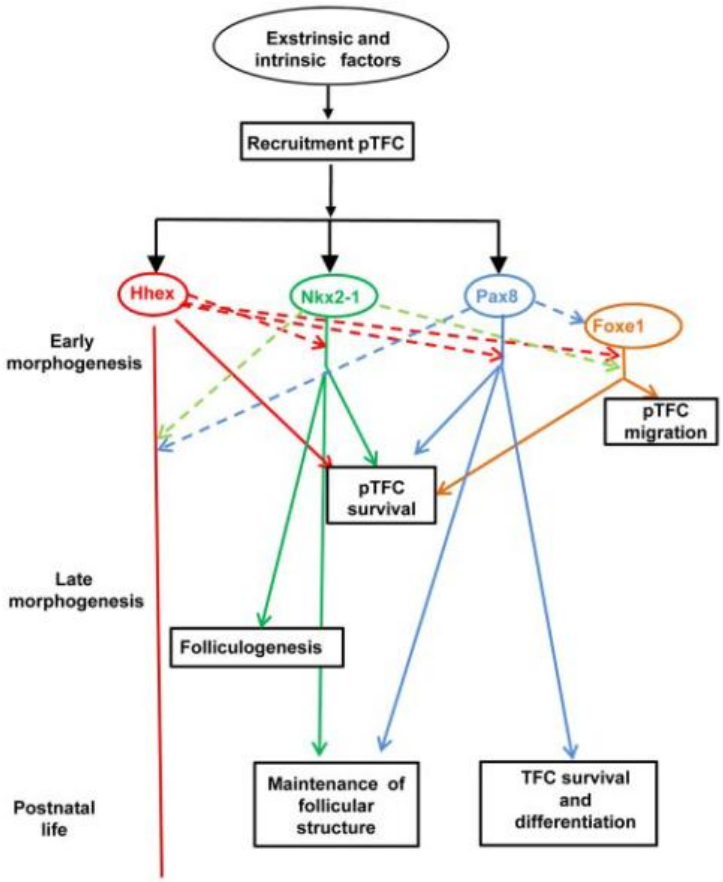

Figure 4. Interactions and functions of Nkx2.1, Pax8, Foxe1 and Hhex during thyroid development and postnatal life. Dashed arrows represent transcription regulation, initiation or maintenance, between transcription factors; solid arrows indicate control of important steps in thyroid morphogenesis and function. ('pTFC': progenitor of thyroid follicular cells) (De Felice and Di Lauro, 2011).

1.2.3. Signaling pathways implicated in thyroid development

Few other genes have been demonstrated to play important role in thyroid organogenesis. For example, there is no known gene controlling specification and budding during early thyroid development. It has been suggested that Nodal, Fgf4 or members of the GATA or Sox family could play a

role in the initial specification of thyroid (De Felice and Di Lauro, 2007). Here, I will shortly present signaling pathways for which a role has been demonstrated.

TSH receptor (TSHr)

TSHr is G protein-coupled receptor expressed at the basal pole of thyrocytes from E14 onwards and maintained throughout adult life. Binding of TSH to its receptor is an important regulator of thyroid growth in postnatal life, probably via activation of the cAMP pathway. As already described (see section 1.1), TSH/TSHr signaling is implicated in late stages of thyroid organogenesis by stimulating the expression of TPO and Nis, and the synthesis and production of thyroid hormones in adults.

$TSHr^{KO}$ mice have no particular phenotype during embryonic life while adult mice display severe hypothyroidism associated with thyroid hypoplasia (De Felice and Di Lauro, 2004). A similar role for TSHr was found in zebrafish (Opitz et al., 2011). In thyroid cell culture, addition of TSH increases the production of thyroid hormone. It also promotes the expression of insulin growth factor 1 (IGF-1) and of vascular endothelial growth factor (VEGF) which act on thyroid endothelial cells to initiate angiogenesis (Eggo et al., 2003). Such studies demonstrate the important role of TSHr to generate and maintain a functional thyroid gland.

Sonic hedgehog (Shh)

Shh belongs to the hedgehog family, together with Indian and Desert hedgehog. Shh is a soluble ligand, which binds to Patched (Ptc) receptor. Ligand binding relieves the inhibitory effect of Ptc on Smoothened (Smo), another transmembrane protein, and the intracellular signaling is activated via the Glioblastoma transcription factors (Gli). Shh controls cell growth, cell specialization, and the normal shaping of the body. This protein is important for development of the brain, eyes, limbs, and many other parts of the body. Shh is also a major regulator of foregut development since in Shh^{KO} mice, the esophagus, trachea and pancreas are affected. Interestingly, all epithelial cells of the foregut endoderm express Shh, except those that will give rise to the thyroid primordium and the ventral and dorsal pancreas. In the absence of Shh, thyroid primordium develops normally but the lobulation process is impaired as the gland fails to

separate into two distinct lobes and form a single midline tissue mass. Moreover, loss of Shh in the pharyngeal endoderm leads to ectopic thyroid tissue in the respiratory tract. Shh could thus restrict the site of thyroid specification and budding (Fagman et al., 2004).

Fibroblast growth factor (FGF)

The large mammalian FGF family comprises 18 ligands, which bind to 4 different transmembrane tyrosine kinase receptors. FGF are secreted glycoproteins generally sequestered in the extracellular matrix (ECM) and released from ECM by proteases. Free FGF are bound close to the cell surface by heparin sulfate proteoglycans and can interact with their receptors. Binding induces receptors dimerization and transphosphorylation. Adaptor proteins are then recruited and different signaling pathways are activated such as PKC, Akt or Ras/ERK pathways. FGF signaling regulates various biological activities such as proliferation, survival, migration and differentiation. Usually, FGF ligands are expressed in the mesenchyme while receptors are mostly found on epithelial cells (Turner and Grose, 2010). During thyroid development, Fgfr2b is expressed in the bud at E11. Genetic deletions of Fgfr2b or of its ligand Fgf10 result in thyroid agenesis. This indicates that the Fgf10/Fgfr2b interaction is critical for thyroid organogenesis (Ohuchi et al., 2000; Revest et al., 2001). Further evidence for the implication of FGF in thyroid development comes from deletion of Tbx1 (T-box protein 1). Tbx1 is a transcription factor expressed in the mesoderm adjacent to the thyroid primordium, where it controls Fgf8 expression. Tbx1 inactivation also causes thyroid hypoplasia by defective Fgf8 production. Tbx1 and Fgf8 are both required for early thyroid primordium size (Lania et al., 2009).

Ephrin

Ephrin receptors (Eph) and ephrins (ligands) are expressed in most embryonic tissues. The receptors have tyrosine kinase activity and interact with cell surface-bound ephrins from another cell. Receptors and ligands are grouped into class A or B, based on sequence similarities and binding preference. The Eph/ephrin signaling can be bidirectional with a forward signaling downstream of the Eph receptor and a reverse signaling downstream the ephrin ligand (Figure 5 A.). They are implicated in various cellular processes such as migration, repulsion or attraction (Klein, 2012). In the thyroid, EphA4 is expressed at all stages of

thyrocyte development and in mature follicular cells, but also in C-cell progenitors in the ultimobranchial bodies. However, EphA4 expression in C-cells is lost before the fusion of ultimobranchial bodies with the thyroid buds. Embryonic EphA4 mutants have no particular thyroid phenotype while EphA4^{KO} adult mice display flattened thyrocytes and smaller follicles than the control. Interestingly, when the intracellular domain of EphA4 is replaced by EGFP (enhanced green fluorescent protein), forward signaling is impaired and this results in larger follicles and reduced number of C-cells, which remain localized in the center of the lobes without dispersing. These data suggest that forward and reverse signaling of EphA4 control follicle formation and C-cells dispersion (Figure 5 B.) (Andersson et al., 2011).

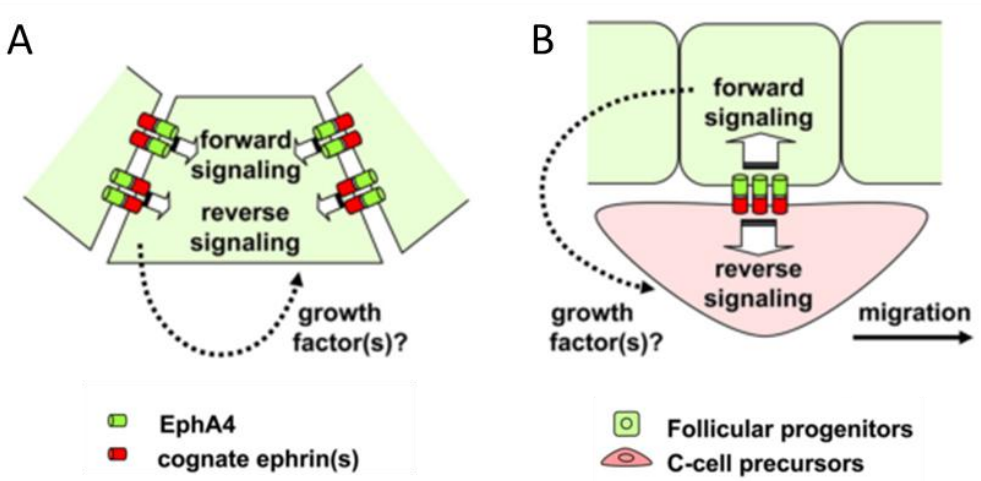

Figure 5. Model of EphA4 signaling in thyroid cell:cell interactions. A. Reciprocal interaction between EphA4 and its cognate ephrins in thyroid follicular cells modulate follicle formation by forward and reverse signaling. B. C-cell ephrins bind to thyrocytes EphA4. C-cell number and dispersion are controlled by forward signaling while reverse signaling has not yet been characterized (Andersson et al., 2011).

Blood vessels

Blood vessels are tubes of the circulatory system that transport blood throughout the human body. They are composed of endothelial cells forming a single cell layer that rests on a basement membrane and regulates exchanges between the bloodstream and the surrounding tissues. They form

during development, from mesoderm-derived angioblast precursors. First, endothelial cells differentiate from angioblasts and organize in a primitive vascular network; a process called vasculogenesis. Subsequent sprouting of new vessels from a preexisting vessel is called angiogenesis. Endothelial cells are activated and regulated by pro-angiogenic signals, among which vascular endothelial growth factors (VEGF) is the most potent (Lohela et al., 2009).

VEGF are secreted homodimeric glycoproteins belonging to the platelet-endothelial growth factor (PDGF) family. In mammals, 5 VEGF genes have been described: VEGF (or VEGF-A) which give rise to different isoforms after splicing, VEGF-B, VEGF-C, VEGF-D and placental growth factor (PlGF). They can bind to three tyrosine kinase receptors, VEGFR1 (Flt-1), VEGFR2 (KDR or Flk-1) and VEGFR3 (Flt-4), with different affinities. Although VEGFR2 is the main endothelial cell receptor triggering cellular responses (migration, proliferation, permeability,…), VEGFR1 has a more elusive role and would act as a decoy receptor sequestering VEGF ligands. VEGFR3 is mostly involved in the regulation of lymphatic endothelial cells. Two co-receptors are also known to modulate VEGF activity: neuropilin-1 and 2 (Haigh, 2008; Robinson and Stringer, 2001).

Besides their fundamental role of nutrient and oxygen delivery to tissues, signals from endothelial cells have recently been recognized as important regulators of organ formation, growth and differentiation, by providing signals in a paracrine, also called angiocrine fashion (Ramasamy et al., 2015). During my thesis, I studied the perfusion-independent role of endothelial cells during thyroid follicle formation.

2. Lumen formation and polarity

Thyroid, as many epithelial organs, is composed of polarized epithelial cells organized in monolayers surrounding a lumen. In general, the organization of epithelial cells in monolayers is important for organ function at the interface between internal and external milieu. Monolayers can form simple open tube (intestine), highly branched and open tube (lung, pancreas) or closed and independent spheres, called follicles like in the thyroid.

2.1. Polarized epithelium

Polarization is a cellular process required for tubulogenesis and folliculogenesis. Epithelial cell polarization involves asymmetrical organization of cell surface, organelles and cytoskeleton. This polarity provides cell poles or membranes with different structure, composition and function. Three domains are distinguished. The basal pole is in contact with the basement membrane (or basal lamina) of the extracellular matrix through receptors such as integrins (see section 3.2.1.) and is exposed to regulatory signal (eg TSH). The lateral domain links neighboring cells via junctional complexes such as the tight junction, the adherens junction and desmosomes. Basal and lateral domains are often called basolateral domain, as they are not separated by a physical frontier. On the contrary, the tight junction physically separates the basolateral membrane from the third domain or apical pole, specialized in absorption and/or secretion. The tight junction is a strict frontier that prevents phospholipids and proteins from apical and basolateral domains to mix. Moreover, this junction seals the epithelial cells to create a barrier between the external and the internal milieu. However, depending on its protein composition, paracellular transport of ions and water can occur through the tight junction. The tight junction also interacts with intracellular protein involved in polarity development (PAR3, aPKC), recruits proteins implicated in proliferation or differentiation and regulate gene expression (Balda and Matter, 2009). Structurally, the apical pole faces the lumen of the tube or follicle and can present a unique cilium and a multitude of microvilli (Figure 6).

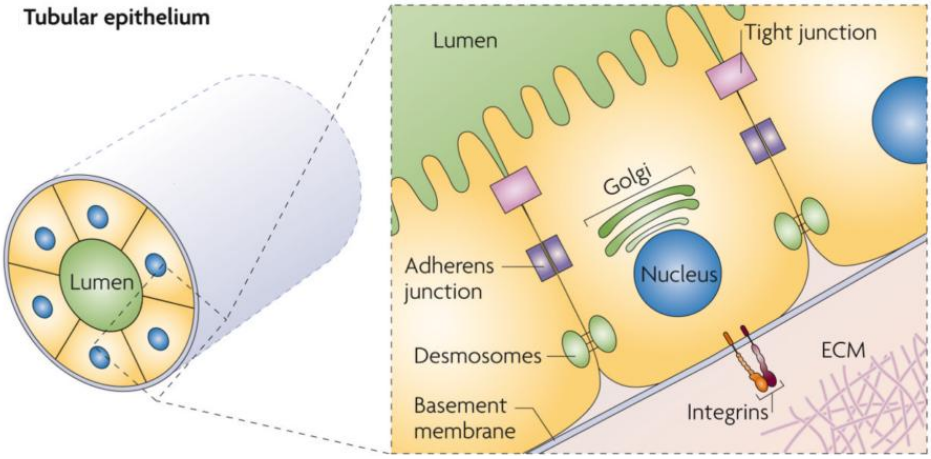

Figure 6. Organization of polarized cells. Cell surface is separated in three domains: the apical pole facing the lumen, the lateral domain connecting adjacent cells through adherens junctions, tight junctions and desmosomes and the basal pole contacting the basement membrane and extracellular matrix through integrins (Bryant and Mostov, 2008).

Establishment and maintenance of polarity depend on three protein complexes: the PAR (CDC42-PAR3-PAR6-aPKC) complex, the Crumbs (Crb-PALS-PATJ) complex and the Scribble (Scrib-Dlg-Lgl) complex. The PAR and Crumb complexes are localized at, and promote the development of apical pole while the Scribble complex is confined and acts at the basolateral surface (Figure 7). Polarity complexes antagonize each other to maintain the asymmetry. For example, aPKC from the PAR complex restricts by phosphorylation Lgl from entering into the apical domain.

In addition to polarity protein complexes, phospholipids are also distributed differentially at the membrane. Phosphatidylinositols (PtdIns) are phosphorylated lipids of which two are essential for polarity: PtdIns(3,4,5)P_3 and PtdIns(4,5)P_2. These phosphorylated lipids are generated by the action of PtdIns kinases, among which Ptdns-3 kinase is the best studied. An interesting phosphatase, PTEN can dephosphorylate PtdIns(3,4,5)P_3 and generate PtdIns(4,5)P_2. Since PTEN is localized and active at tight junctions, it produces PtdIns(4,5)P_2 at the apical pole and segregate if from PtdIns(3,4,5)P_3 which is

exclusively found at the basolateral surface (Gassama-Diagne et al., 2006; Martin-Belmonte et al., 2007; Martín-Belmonte and Rodríguez-Fraticelli, 2009).

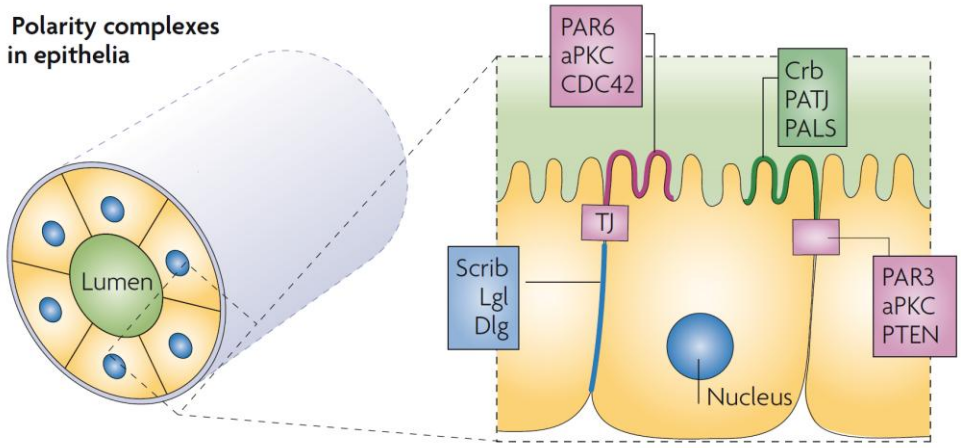

Figure 7. Segregation of polarity proteins within the cell surface. The polarity complex Scribble (Scrib-Lgl-Dlg) is situated at the basolateral membrane while the Crumbs (Crb-PATJ-PALS) complex is at the apical membrane.The PAR complex is separated in two groups; PAR6, aPKC and CDC42 is at apical membrane and PAR3, aPKC and PTEN is at tight junctions (Bryant and Mostov, 2008).

Upon individualization of apical and basolateral domains, these membrane domains will be equipped with proteins essential for the function of the organ. In the thyroid, NIS and Na^+/K^+ ATPase will be targeted to the basal domains and will not be able to reach the apical domain. On the contrary, Pendrin will be targeted to the apical domain.

2.2. Structural mechanisms of polarity: lessons from tubulogenesis

Tube formation implies the assembly of epithelial cells around a central lumen. Several mechanisms to form simple epithelial tubes have been described and can be grouped in two major groups. The first one requires remodeling of an already polarized epithelium to surround a luminal space. In the second one, luminal space will be created *de novo* from non-polarized epithelial cells.

Lumen formation from polarized epithelia

Tube formation from epithelial cells already polarized can occur by wrapping or budding.

A. *Wrapping* is the curling or invagination of an epithelial sheet and subsequent fusion of the cells to create a lumen, completely separated upon pinching from the original epithelium (Figure 8 A.). Wrapping occurs for example during neural tube formation from the polarized ectoderm.

B. *Budding*, similarly to wrapping, is the perpendicular in- or e-vagination of the cells from the epithelium plane. In this case, cells from the newly formed elongated structure do not separate from the epithelium of origin and remain contiguous with this latter. This budding process can occur iteratively. Lumen of new branches being a direct extension of the parental lumen (Figure 8 B.). Elaboration of highly branched epithelial organs such as the lungs occurs by budding.

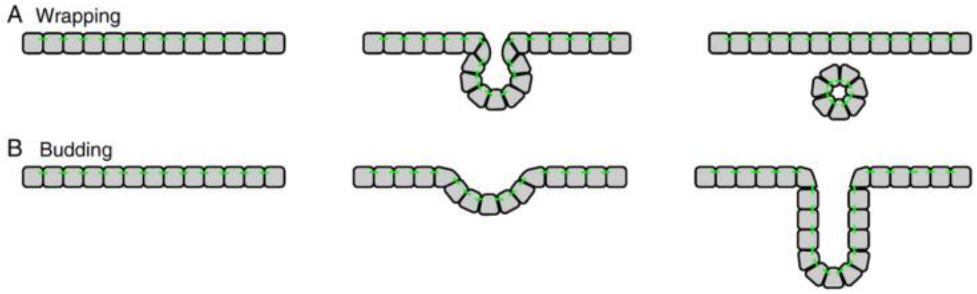

Figure 8. Two basic structural mechanisms of tube formation from preexisting polarized epithelia: A. Wrapping. B. Budding (green: intercellular tight junctions of polarized cells) (Andrew and Ewald, 2010).

De novo lumen formation

De novo lumen formation implies that tube will form from aggregates of cells or from single aligned cells that do not initially show apico-basal polarity. Instead, cells will polarize concomitantly with tube formation. Three mechanisms can be distinguished: cord hollowing, cell hollowing and cavitation (Andrew and

Ewald, 2010; Iruela-Arispe and Beitel, 2013; Lubarsky and Krasnow, 2003; Sigurbjörnsdóttir et al., 2014).

C. *Cord hollowing* is the formation of a lumen between cells organized in a thin or thick cord and does not require cell death. This mechanism involves the formation of intracellular small lumina which will fuse with one region of the membrane and create the apical pole (Figure 9 C.). Such process requires partial disruption of cell-cell contacts where the future apical pole develops. In thick cord of cells, i.e. a mass, a more important reorganization of the cells is also necessary. The new space created in between the cells must be filled with solutes and ions. The zebrafish gut and the mouse pancreas, in the initial steps of its development, acquire their lumen via cord hollowing.

D. *Cell hollowing* is similar to the cord hollowing but starts within cells and is mainly observed during capillaries formation. In the cytoplasm, small vesicles appear and fuse together to create a large intracellular lumen corresponding to an internal apical compartment. Connection of the intracellular lumina from adjacent cell will create an intracellular tube (Figure 9 D.). In cell hollowing, vesicles target a central position in the cell and organize an internal apical compartment.

E. *Cavitation* is the polarization of cells localized at the periphery of a mass and elimination of the central cells by apoptosis to create a luminal space. This event was erroneously reported to occur *in vivo* during salivary gland development (Figure 9 E.). Despite the presence of this process in numerous reviews on tubulogenesis, we do not believe it actually occurs *in vivo*.

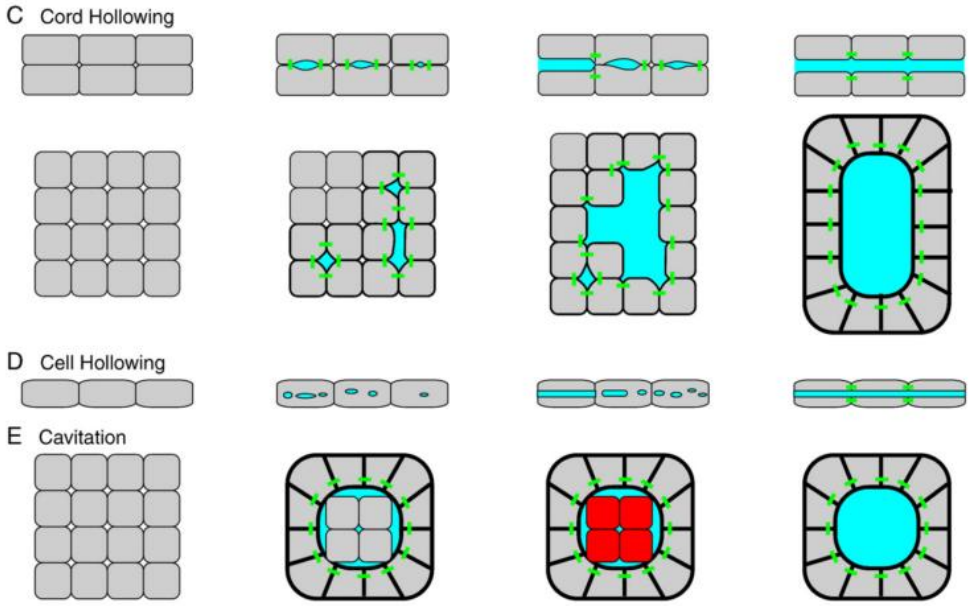

Figure 9. Structural mechanisms of *de novo* lumen formation. C. Cord Hollowing. D. Cell Hollowing. E. Cavitation (green: intercellular tight junctions of polarized cells, blue: lumen, red: apoptotic cells) (Andrew and Ewald, 2010).

Whatever the original mechanism, after formation of a tube, changes in cell shape, arrangement, division or recruitment are implicated to allow tube growth and elongation (Andrew and Ewald, 2010; Lubarsky and Krasnow, 2003; Sigurbjörnsdóttir et al., 2014).

Lumen formation in the thyroid has not been studied in details and is amazingly never discussed in the abundant literature on lumen formation. Analysis of thyroid development reveals that non-polarized cells first form a mass, which progressively reorganizes in independent polarized monolayers, suggesting *de novo* lumen formation (Fagman et al., 2006; Hick et al., 2013). Cell organization in follicles is the focus of my thesis and will be explained in the results section.

Cellular processes leading to lumen formation are driven by intrinsic program but are controlled by extrinsic cues from the environment. In the next section, I will introduce the key role of the extracellular matrix in epithelial morphogenesis.

3. The role of extracellular matrix in epithelial morphogenesis

The function of every epithelial cell in our organs depends on its polarity but also on the typical architecture or organization of these cells within the organ. Acquisition and maintenance of the desired architecture and function depends on contacts and interactions with neighboring cells but also with the stromal environment. The stroma, or connective tissue, is composed of other cell types, such as fibroblasts, pericytes, endothelial cells and nerve cells (Goruppi and Dotto, 2013), and of extracellular matrix (ECM) components and includes soluble proteins or growth factors when trapped in the ECM.

During embryogenesis, the interaction between epithelial cells and the stroma, sometimes historically called mesenchyme, is important for morphogenesis and differentiation. The instructive role of the stromal tissue was demonstrated several decades ago by elegant recombination experiments using isolated tissues from the mammary gland and other organs (Figure 10). For example, mammary gland mesenchyme recombined with epithelial tissue such as the epidermis, will induce typical mammary branching of the epidermis. Conversely, mammary gland epithelium recombined with salivary gland mesenchyme adopts a salivary gland architecture (Nelson and Bissell, 2006). This demonstrates the flexibility of epithelial cells and the critical instructive role of the environment.

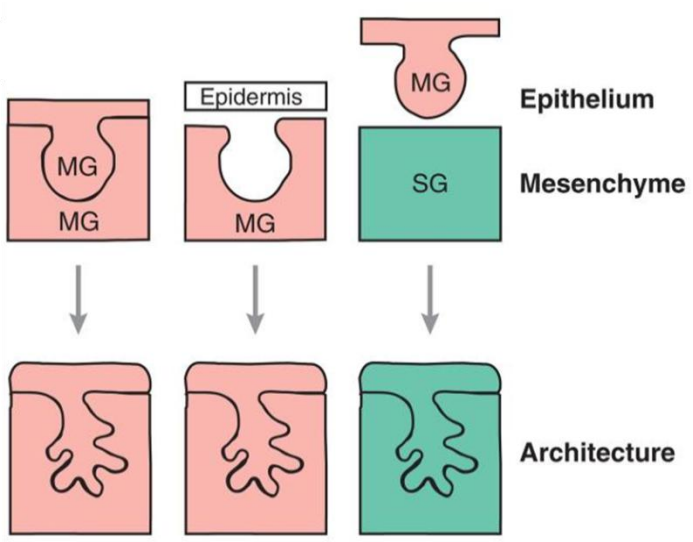

Figure 10. Epithelial/mesenchymal recombination experiments. Mammary gland (MG) mesenchyme instructs epidermis to adopt mammary gland architecture and differentiation, while mammary epithelium is instructed by salivary gland (SG) mesenchyme to form a salivary epithelial tree (Nelson and Bissell, 2006).

In the following sections, I will present the components of the ECM that are secreted by epithelial or stromal cells and provide structural and biochemical support to the neighboring cells. Note that ECM is produced by cells and in turn instructs, modulates signaling to cells. First, ECM serves as a storage site for soluble factors like growth factors, cytokines, chemokines or enzymes. Remodeling enzymes can modulate the biological activity, availability or presentation of these factors to their cell surface receptors. Secondly, interaction of ECM proteins with cellular receptors, like integrins, can affect cell adhesion, migration, differentiation, proliferation or survival via outside-in signal transduction cascade (Aszodi et al., 2006). ECM also plays a role in fin tissue regeneration in zebrafish (Govindan and Iovine, 2015), expansion and branching of epithelial tissues in lungs and salivary glands (Harunaga et al., 2014), but also in establishment and maintenance of epithelial polarity (Manninen, 2015).

3.1. Extracellular matrix components

In mammals, one can distinguish two parts in the ECM: the interstitial matrix and basement membrane (BM). I will mainly focus on the BM, a 50-100 nm thick sheet-like extracellular matrix separating epithelial cells, like thyroid follicular cells, from the stroma. The molecular architecture and composition of the ECM is heterogeneous and varies depending on the organs (e.g. skin *versus* kidney), the tissue compartments (e.g. endocrine *versus* exocrine pancreas), but also the developmental stages (embryonic *versus* adult) and physiological states (e.g. normal *versus* fibrotic). Two major categories of macromolecules are present in ECM: polysaccharides chains, called *glycosaminoglycans* (GAGs), which are covalently linked to proteins and form *proteoglycans*, and fibrous and non-fibrous proteins including *collagens*, *elastin, fibronectin* and *laminins*. Both have structural and adhesive functions and are organized in a highly dynamic 3D meshwork, due to constant remodeling controlled by fine regulation of ECM synthesis and degradation (Aszodi et al., 2006).

3.1.1. Glycosaminoglycans and proteoglycans

Glycosaminoglycans are composed of a repetition of disaccharide units. These disaccharides consist of a glucuronic acid and N-acetyl-glucosamine or -galactosamine that can be modified (most frequently by addition of sulfate groups). Several types of glycosaminoglycans exist: hyaluronan, dermatan-sulfate, heparin-sulfate, chondroitin-sulfate and keratan-sulfate. Covalent linking of glycosaminoglycans to side chains of a protein generates proteoglycans such as syndecans, glypicans, perlecans and aggrecans. With their numerous negative sulfate groups on their surface, proteoglycans retain water thus form a highly hydrated gel that can resist compressive forces applied on the matrix. For example, Warthon's jelly is a gelatinous substance, composed mainly of highly hydrated hyaluronan surrounding the umbilical cord blood vessels, which confers insulation and protection against eventual pressures. Another function of proteoglycans like heparin-sulfate is related to the binding and storage and regulation of growth factor signaling activity (FGF, VEGF or cytokines) (Kim et al., 2011).

3.1.2. Elastin

Elastin is a non-glycosylated fibrous protein that gives elasticity and resilience to flexible tissues. It is found in ECM of many tissues such as arteries, lungs, or skin to confer elasticity needed for their function or role. There is only one gene in humans coding for tropoelastin, a protein rich in proline and glycine. In the extracellular matrix, tropoelastin self-associates and cross-links via lysine bonds to form insoluble elastin polymers. Elastin synthesis stops at puberty but due to its stability (half-life of approximately 70 years), it remains present throughout life. However, elastins can be degraded by elastase after inflammatory reaction, fragmented by physical damages such as burns and sun damage or as a result of aging. Loss of skin elasticity is illustrated by wrinkles (Aszodi et al., 2006) (Molecular Biology of the Cell, 4th Edition; Weiss, 2011).

3.1.3. Fibronectin

Fibronectin is a fibrillar glycoprotein important for migration and differentiation, also expressed from a single gene. However, alternative splicing produces 20 transcript variants. Fibronectins form parallel dimer joined by a disulfide bond at the C-terminal. Each monomer is composed of type I, type II or type III repeats that allow fibronectin interactions with different ECM proteins such as collagen, heparin or thrombospondin. These repeats also mediate interaction of fibronectin with cell receptors named integrin through the RGD (Arg-Gly-Asp) peptide. Fibronectin thus acts as a scaffold for the assembly of other ECM proteins and is also involved in cell adherence to ECM (Kostourou and Papalazarou, 2014) (Molecular Biology of the Cell, 4th Edition).

3.1.4. Collagens

Collagens, the most abundant fibrous proteins in mammals, consist of three polypeptide chains, called α chains (115kDa per chain), coiled around each other in a superhelix. Collagens are composed of Glycine-X-Y repeats with residues often hydroxylated (commonly proline and lysine). About 25 distinct collagen α chains have been identified but only 27 combinations of collagens chains have been identified. Each collagen type has its own structure and is found in particular organs. For example, type I collagen is abundant and plays a role in skin, bones or cornea formation while type III is found in cardiovascular system.

Type IV collagen is a non-fibrillar collagen and will be detailed below. Collagen synthesis and production is complex and requires the activity of different intracellular and extracellular enzymes for correct assembly of the typical mature fibrillar collagen. Mutations in collagen genes can cause several diseases as for example *osteogenesis imperfecta* when collagen type I is mutated.

Collagen acts as structural support and binds other ECM proteins as well as secreted growth factors, signal receptors or adhesion molecules present in the extracellular environment. In contrast to GAG and proteoglycans, which resist compressive forces, collagen fibrils resist tensile forces (Aszodi et al., 2006; Kim et al., 2011) (Molecular Biology of the Cell, 4th Edition).

Type IV Collagen is a particular one that does not form fibers but a network specific of basement membrane. Six genes encoding isoforms of type IV collagen exist (α1 to α6). These isoforms form a central triple helix with globular domains at their N- (NC1 domain) and C-terminal (7S domain). After chain trimerization and secretion, two such protomers form a dimer via their NC1 domains to become a NC1 hexamer. Then, four dimers interact at the glycosylated C-terminal 7S region to form the so-called tetramers. A scaffold evolves into a suprastructure with end-to-end associations as well as lateral associations between tetramers (Figure 11).

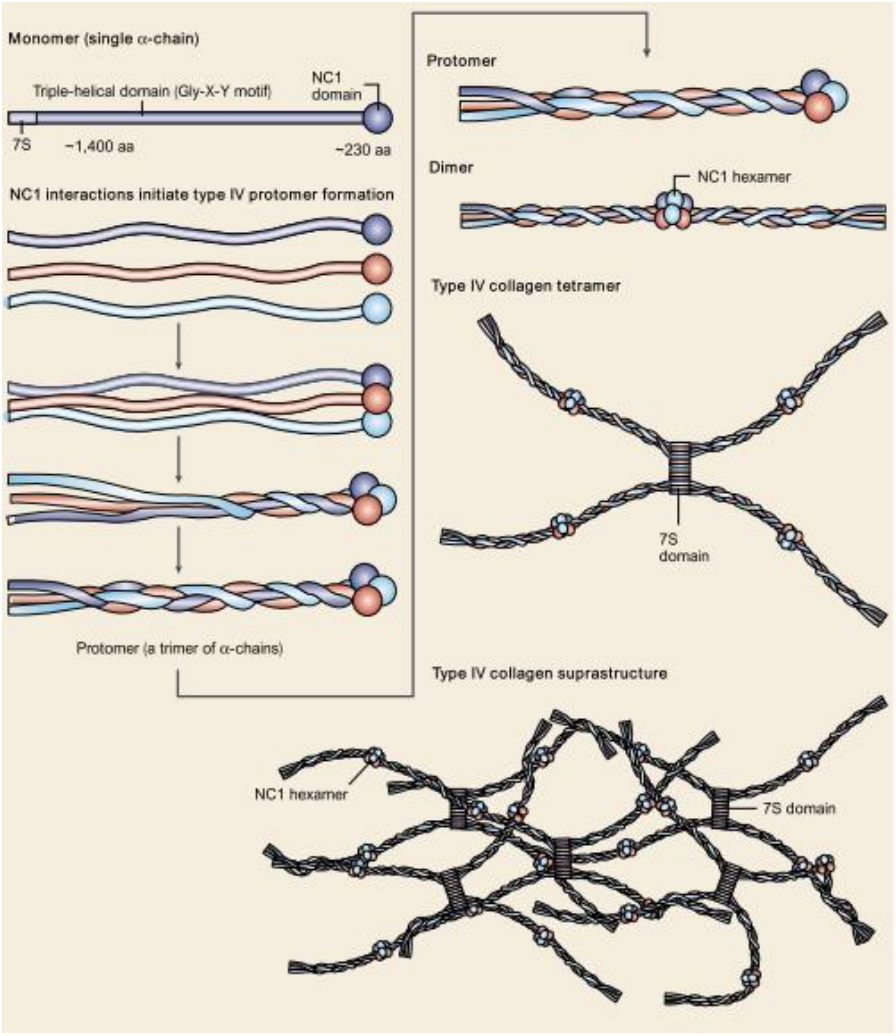

Figure 11. Type IV collagen network formation. Protomers (trimer of α-chains) are assembled by interactions between NC1 domains to form dimers. Four dimers assemble into tetramer by 7S domains interaction. Collagen IV forms a bi-dimensional and irregular network (Kalhuri, 2003).

The type IV collagen network will be interconnected with the laminin network and form the basal lamina or basement membrane (BM) (Kalhuri, 2003). Other proteins such asnidogen and perlecan are also enriched in the BM. BM plays a role in epithelial polarity establishment and maintenance during

embryonic development and in adult. It is also a barrier that carcinoma cells have to cross or degrade before invasion and metastasis.

3.1.5. Laminins

Laminins are glycosylated heterotrimeric proteins composed of one α, one β and one γ chain that are assembled through a central coiled coil and held together by disulfide bonds. There are five different α chains (200 to 400kDa), four β chains and three γ chains (120 to 200kDa); hence trimers have a size comprised between 400 and 800kDa. Among 60 theoretical trimers possibilities, only 16 combinations of trimers have been identified (Domogatskaya et al., 2012; Yurchenco, 2015). Laminin nomenclature is based on composition of the chains used; for example, laminin 511 is composed of α5, β1 and γ1 chains (Aumailley, 2013).

In addition to the long coiled coil domain common in the three chains, the α chain has a long C-terminal globular G domain containing five LG subdomains named LG1 to LG5. These LG subdomains are involved in binding to integrin receptors, through LG1-3, or to dystroglycan, through LG4-5. The N-termini of the three chains are called short arms and vary in length mainly due to the number of laminin type epidermal growth factor like (LE) repeats located between globular L domains. The globular laminin N-terminal (LN) domain found at the extremities of the three chains (Figure 12 A.) is essential for the self-assembly of the laminin network (Figure 12 B.) and for interaction with other BM proteins such as nidogen or perlecan. The three chains are synthesized in the cell and dimerization of β and γ chains occurs before incorporation of the α chain. Specific interactions in the coiled coil domain limit the number of allowed heterotrimer combinations and control intracellular trimer assembly. Laminins are then secreted as trimers in the ECM or basal lamina where they will form the scaffold for other ECM components (Domogatskaya et al., 2012; Kostourou and Papalazarou, 2014; Yurchenco, 2015).

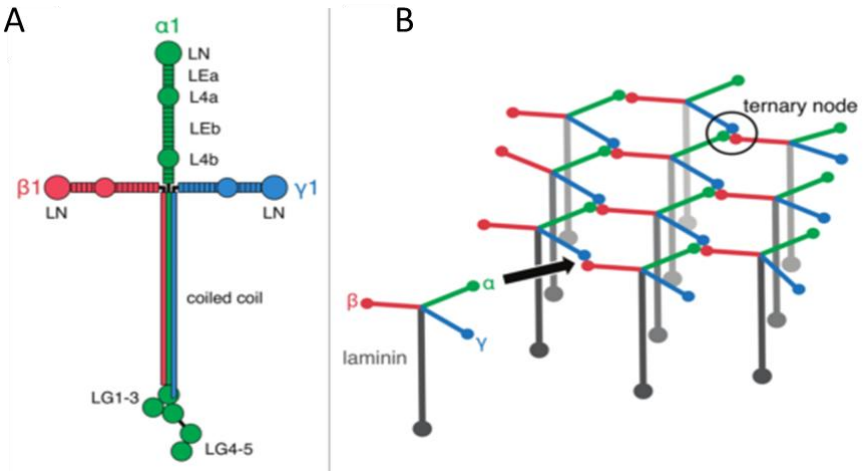

Figure 12. Schematic representation of laminin 111 heterotrimer and self-assembly in network. A. Two-dimensional model of a single laminin 111 is composed of α1, β1 and γ1 chains, which interact through their coiled coil domains. The short arms of the three chains contain LN and L globular domains and laminin epithelial growth factor like (LE) repeats. The C-terminus of α chain comprises five globular (LG) domains. B. Three-dimensional model of a basement membrane where laminins heterotrimers self-assemble outside the cell and form a network by binding to other heterotrimers via their LN domains (Hohenester and Yurchenco, 2013).

Combinations of laminin chains can be ubiquitous or tissue-restricted, found in embryo or in adult. For example, laminin 111 is rather ubiquitous in developing organs in embryos while it is restricted to a small subset of BM in adult tissues. In contrast, laminin 511 and 521 progressively replace laminin 111 and are the most ubiquitous isoforms in adult (Aumailley, 2013). Laminins are important for early embryonic development. Deletion of β1 or γ1 chains leads to early embryonic death (E5.5) due to total lack of BM and tissue disorganization. Inactivation of α1 causes embryonic lethality at E6.5-7, while the absence of α5 chain leads to multiple developmental defects (defective salivary gland morphogenesis and renal agenesis) and embryos die *in utero* between E13 and E17 (Domogatskaya et al., 2012; Kostourou and Papalazarou, 2014; Li et al., 2002; Yurchenco, 2015).

Endothelial cells of blood vessels are also surrounded by basement membrane, which is composed of the same components as epithelial BM. The

major endothelial type IV collagen is composed of α1α1α2 chains while laminins α4 and α5 (and in some cases α2) chains are the major isoforms expressed by endothelial cells (Yousif et al., 2013).

3.1.6. Nidogen

As compared to other ECM components, nidogen is a small glycoprotein that exists in two isoforms, nidogen-1 and -2. It is a rod-shape protein with three globular domains (G1, G2, G3). Nidogen interacts with other components of BM to stabilize it. It connects the networks formed by collagens and laminins and may also play a role in cell interactions with the ECM (Miosge et al., 2001).

3.2. Cell receptors for ECM

ECM proteins can bind to different transmembrane receptors of which integrins and dystroglycans are the most important.

3.2.1. Integrins

Integrins, the best studied receptors of ECM proteins are heterodimeric transmembrane receptors composed of one of the 18 α possible subunits and one of the 8 β subunits, non-covalently assembled into 24 combinations. The specific integrin expressed at the cell surface dictates which ECM substrate the cell will be able to bind. Integrins are classified into collagen, laminin, RGD and leukocyte receptors (Figure 13). Their roles in development of many organs such as salivary gland, lung or pancreas, have been determined using KO mice (Pozzi and Zent, 2011).

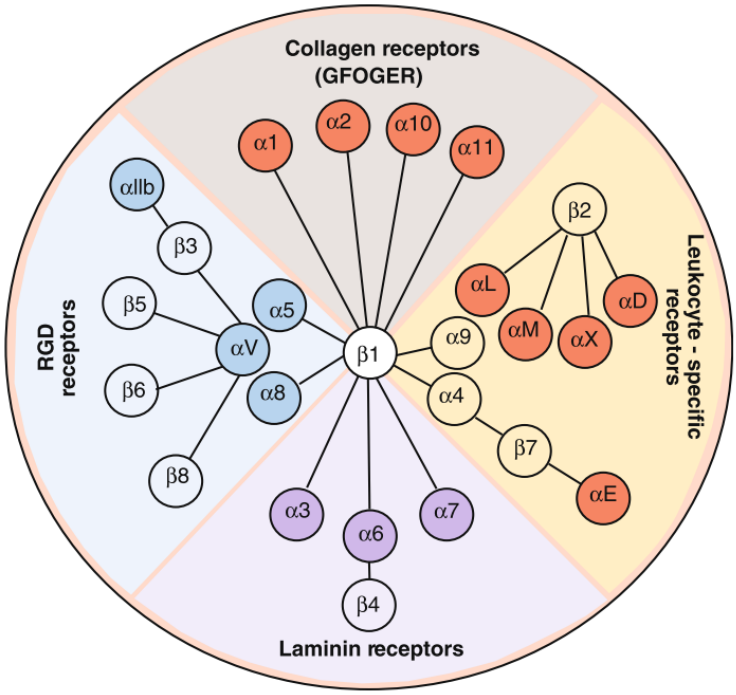

Figure 13. Integrins are heterodimeric receptors forming a large family. α subunits associate with different β subunits to form specific receptors for collagen, laminin, leukocyte or RGD ligand (Barczyk et al., 2010).

The α and β subunits consist of an extracellular part composed of several domains that support the integrin head involved in ligand binding (see section 2.1.; Figure 6). Both subunits also contain a transmembrane domain and a cytoplasmic domain, through which the β subunit can interact with actin cytoskeleton or with kinases (Kim et al., 2011). Heterodimerization occurs intracellularly, before delivery at its final basal destination. Expression of the α subunit is limiting and will determine the amount of receptor that will go to the cell surface(Barczyk et al., 2010).

3.2.2. Dystroglycan

Dystroglycan is a glycosylated protein, which is cleaved in two associated subunits, α (N-terminal region) and β (C-terminal region). α-dystroglycan is an extracellular protein, which binds to several extracellular ligands, especially laminins. β-dystroglycan, a transmembrane protein, associates with dystrophin

glycoprotein complex (DGC), which is able to bind F-actin (Domogatskaya et al., 2012).

3.3. Assembly of ECM components into a basement membrane

The assembly of the BM starts when secreted laminin heterotrimers self-assemble into a polymeric network and bind to the cell surface via their LG domains through the ECM receptors, integrins and dystroglycan. This laminin network forms an initial scaffold for other matrix proteins and most importantly for the collagen type IV network. These two networks interact through nidogen, agrin and perlecan (Figure 14) (Morrissey and Sherwood, 2015; Pöschl et al., 2004).

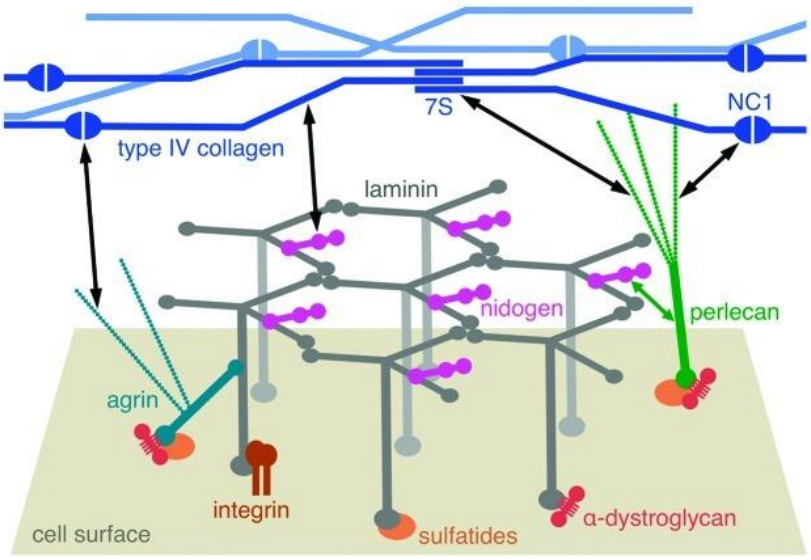

Figure 14. Assembly of the basement membrane and interacting proteins. Laminin network interacts with collagen type IV network via agrin, perlecan and nidogen proteins. Laminin binds to cell surface through integrin or α-dystroglycan receptors (but also with sulfatides, not described) (Hohenester and Yurchenco, 2013).

Not all BM constituents are required for the assembly of BM. For example, it was demonstrated that the collagen type IV α1 and α2 chains were not necessary for the deposition of BM in mouse early development. However,

collagen type IV is essential for the structural and functional integrity of basement membrane. This was especially demonstrated in Reichert's membrane where defect of BM causes insufficient barrier between maternal and embryonic environments and by consequence, excessive bleeding into the yolk sac cavity (Pöschl et al., 2004).

An elegant study demonstrated that epithelial cysts grown in matrigel undergo rotational motions at rates of 15-20 μm/h with a full revolution (360°) every 4 hours. These rotations are dependent on polarity proteins as well as on microtubules. A direct relationship was noted between rotations and assembly of basement membrane proteins, especially laminins. Blocking rotational motion prevented weaving of the exogenous matrix around the 3D cystic structure (Wang et al., 2013).

In vivo, BM assembly occurs at the base of most epithelial cells, but also of endothelial cells. Two BM thus exist between epithelial and endothelial cells. In kidney glomeruli, the BM from epithelial cells (podocytes) and from endothelial cells come in close contact and fuse to form a stable and robust BM that serves for ultrafiltration (Molecular Biology of the Cell, 4th Edition).

3.4. Signaling

Two opposite directions of signaling can be transduced through integrins. Upon extracellular ligand binding, integrins undergo a conformational change resulting into clustering in focal adhesions and this lead to *outside-in* signaling controlling cell polarity, survival and proliferation, cytoskeletal organization and gene expression. Upon action of intracellular proteins (FAK, ILK, talin), integrins undergo a conformational change leading to *inside-out* signaling. This conformational change triggers signals for cell migration, adhesion and ECM assembly. (Figure 15). Both events are often closely linked (Barczyk et al., 2010; Shattil et al., 2010).

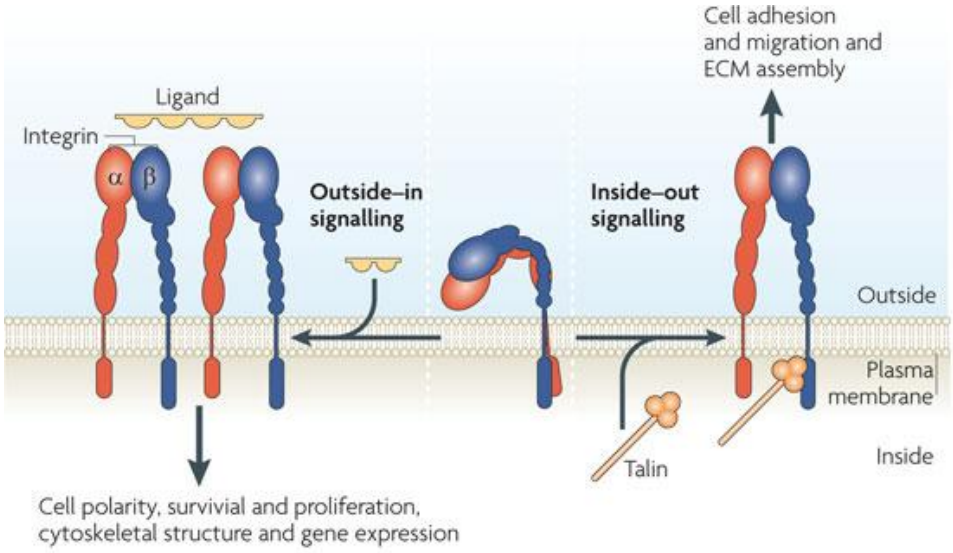

Figure 15. Integrin signaling. At left, upon binding with extracellular ligand from the ECM, integrins undergo a conformational change and clustering, which results in outside-in signaling controlling cell polarity, survival and proliferation, or change in cytoskeletal structure and gene expression. At right, after activation by intracellular proteins (e.g. talin), integrins undergo a conformational change and induce *inside-out* signaling acting on cell adhesion, migration and ECM assembly (Shattil et al., 2010).

Outside-in signaling is the most common and best studied. Upon ECM binding, integrins undergo clustering that concentrates intracellular components involved in signaling. Integrin clustering linked to ECM and intracellular signaling protein is called a focal adhesion. Intracellular signaling, initiated downstream of integrins, implicates tyrosine kinases such as FAK (focal adhesion kinase), Src or ILK (integrin-linked kinase). FAK activation leads to autophosphorylation and recruitment of Src, which further phosphorylates FAK and other binding partners. Among FAK targets, the Rho family of small GTPases (Rac1, Cdc42 and RhoA) links focal adhesion to the actin cytoskeleton (Kim et al., 2011; Yurchenco, 2011).

Laminin signaling via integrin is required for development of many epithelial organs. During salivary gland and lung development, an antibody blocking the interaction between laminin and its dystroglycan receptor caused morphogenesis and branching defects (Durbeej et al., 2001). Similarly, laminin α5 was shown in the submandibular gland to be required for cell organization and

lumen formation via its interaction with integrin β1 (Rebustini et al., 2007). During lung development, integrin β1 was demonstrated to be required for lung branching morphogenesis, alveoli formation and homeostasis (Plosa et al., 2014).

ECM components, especially laminins, can also play a role in differentiation of epithelial organs. *In vitro* culture of pancreatic islets (mostly β cells) or insulinoma cells revealed that β cells do not produce basement membrane proteins. However, β cells recruit endothelial cells around and within islets by producing angiogenic VEGF-A. Recruited endothelial cells secrete and form a basement membrane adjacent to the β-cells. In this endothelial-derived basement membrane, laminin 111 was identified to promote integrin β1-dependent proliferation of the β-cell and insulin gene expression. This process depends on laminin deposition since in the absence of basement membrane ($Vegfa^{KO}$) exogenous laminin can rescue cell proliferation and insulin expression (Nikolova et al., 2006).

3.5. Extracellular matrix in *de novo* lumen formation

MDCK (Madin Darby Canine Kidney) cells have been widely used as an *in vitro* model of lumen formation. Moreover, gene silencing technology in MDCK allowed the identification of many proteins involved in *de novo* lumen formation and a better understanding of this process. *De novo* lumen formation in MDCK can be divided in three different events: orientation, polarization and lumen expansion.

3.5.1. Cell-ECM interaction and orientation

Many studies have demonstrated the importance of extracellular matrix in the acquisition of correctly oriented apico-basal polarity of epithelial cells. Indeed, MDCK cells cultured in suspension form cysts with apical proteins localized at the cell surface in contact with the culture medium. This is called an inverted polarity. However, if these “inverted” cysts are then placed in collagen gel, MDCK cells reverse polarity and apical poles develop towards the center of the cysts (Wang et al., 1990). If directly seeded in collagen type I gel, MDCK form cyst with the apical pole immediately oriented towards the center of the cyst. This correct orientation depends on laminin assembly around the cystic structure. Indeed, culture of MDCK cells dominant-negative for Rac1 in collagen gel forms

cysts with an inverted polarity that do not assemble laminin. Addition of exogenous laminin to these Rac-1 dominant negative cysts corrects the apico-basal polarity (O'Brien et al., 2001). It was further shown that blocking β1 integrin interaction with the ECM using an antibody (AIIB2) inhibits cyst and lumen formation in MDCK cultured in collagen (Figure 16) (Ojakian and Schwimmer, 1994; Yu et al., 2005). These crucial studies thus established that initial contact with collagen type I gel promotes polarized laminin secretion and assembly around the cyst. Then, laminin binding to integrin β1 receptor triggers MDCK epithelial cells to develop a centrally-localized apical domain.

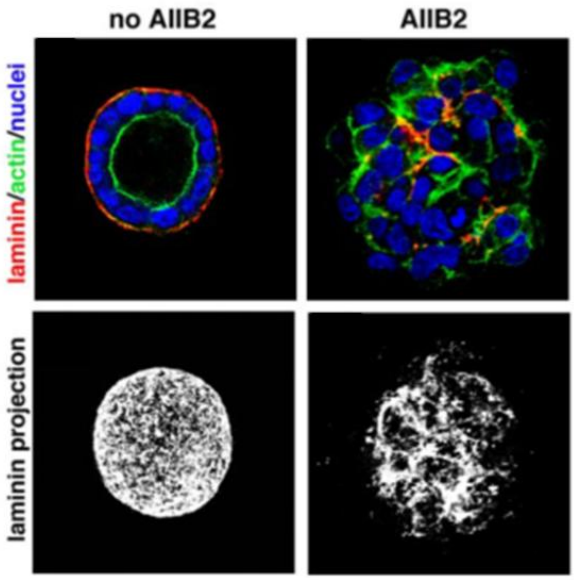

Figure 16. β1 integrin-dependent lumen formation in MDCK cells. MDCK cells grown in matrigel organize in cyst-like structure with a well-developed apical pole (actin, green) and surrounded by a basement membrane (laminin, red). Addition of an integrin β1 blocking antibody (AIIB2) blocks cell polarization and lumen formation. 3D laminin projection shows the homogeneous organization of laminin around the cystic structure in control while, it is altered and irregular in the presence of AIIB2 blocking antibody (Yu et al., 2005).

3.5.2. Polarization and lumen formation

The polarity complexes PAR, Crumbs and Scribble cooperate with many other proteins to regulate apical trafficking and lumen formation. When seeded in

collagen, a MDCK cell has its apical membrane determinant gp135/podocalyxin (PDCX) mixed with basal determinants in contact with the ECM at the cell surface. After cell division, a cell-cell contact is created where basal determinants accumulate. Concomitantly, laminin is produced and secreted towards the ECM to build a basement membrane. Upon signal from the basement membrane, PDCX and Crumbs3 accumulate in Rab8/11a positive vesicles, which are directed to the cell-cell contact to initiate the lumen at a region called the "apical membrane initiation site" (AMIS). The AMIS is demarcated by aPKC and PAR3 proteins, and several other proteins (Rab11, Rabin8α, Rab8, myosin 5B and F-actin) are implicated in the transport and fusion of the vesicle with the AMIS. Annexin 2, recruited by enriched apical PIP_2, participates in the Cdc42 control of vesicle exocytosis to the AMIS. The AMIS matures in a "pre-apical-patch", an early apical domain between adjacent cells not yet opened. PAR3, aPKC and exocysts subunits relocalize to tight junctions (Figure 17) (Bryant et al., 2010; Datta et al., 2011; Overeem et al., 2015).

Even if MDCK is the best studied *in vitro* system for *de novo* lumen formation, other culture systems also provide important information. In mammary epithelial cells, an important role has been attributed to microtubules. Microtubules and actin microfilaments are important cytoskeleton components for cell shape, cell organization, and intracellular vesicular transport. In mammary epithelial cells cultured in 3D, microtubules are aligned along the apico-basal axis and control the endocytic removal of apical proteins from the surface of the cell in contact with collagen and their release at the opposite, developing apical face (Akhtar and Streuli, 2013).

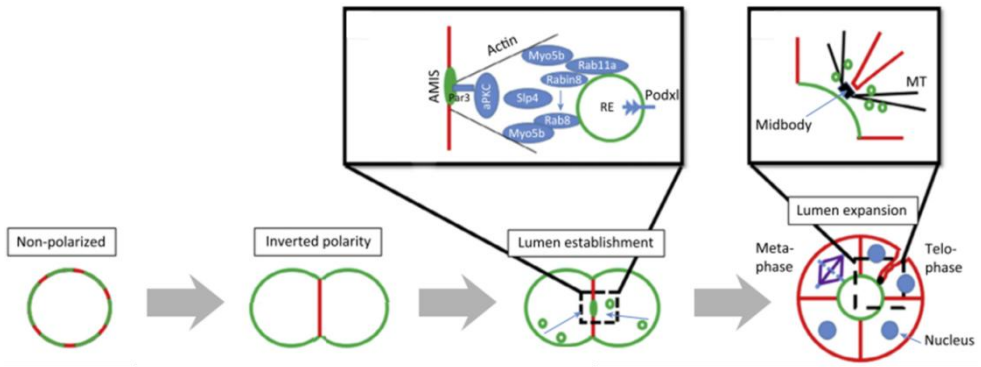

Figure 17. Schematic representation of *de novo* lumen formation and proteins involved. Initially, MDCK cells seeded in collagen are non-polarized. After a first division, basal determinants accumulate at the junction and podocalyxin (Podxl, one of apical determinants green) is excluded from that membrane and only localize at the ECM-contacting membrane (inverted polarity). Podxl is then internalized and accumulates in Rab8/11 positive vesicles, which are targeted to a region between adjacent cells that forms the apical membrane initiation site (AMIS). The AMIS becomes the pre-apical patch and polarity proteins acquire their correct localization. Fine control of vesicle delivery via Rab8/11 together with Myosin 5b allows lumen opening and expansion (Basal determinants, red) (Overeem et al., 2015).

In addition to investigations on lumen formation in epithelial cells, polarization and lumen formation of endothelial cells (EC) have also been intensively studied. In endothelial cells, integrin interaction with ECM activates Rac1 and Cdc42 GTPases as well as Src kinases. Cdc42 and Src kinases cooperate to phosphorylate and activate Pak2 and Pak4, which will stimulate ERK-dependent lumen formation. In parallel, angiogenesis can be stimulated by phorbol esters and this is mediated by PKCε-dependent phosphorylation of Src kinases (Koh et al., 2008; Koh et al., 2009). Together, these kinases control the cytoskeleton.

3.5.3. Lumen expansion

Once a lumen has been formed, it needs to expand to acquire the appropriate diameter to fulfill its function. Lumen expansion depends on fluid accumulation in the lumen, and is thus regulated by pumps (e.g. Na^+/K^+ ATPase), transporters (e.g. CFTR; cystic fibrosis transmembrane conductance regulator) and channels (e.g. AQP; aquaporin). It can also be modulated by ion permeability

(paracellular transport) at tight junctions (Bryant and Mostov, 2008). In MDCK, it was shown that CFTR is recruited at the apical membrane for fluid transport (Ferrari et al., 2008) and that inhibitors of CFTR reduce cyst lumen size (Yang et al., 2008).

These observations were corroborated by studies in zebrafish and salivary glands. In zebrafish, single gut lumen formation is controlled, among others, by Na^+/K^+ ATPase and CFTR (Bagnat et al., 2007). This fluid accumulation in the developing lumen results from activation of CFTR, and thus chloride injection (Bagnat et al., 2010). Similarly, ductal growth in the developing mouse salivary gland depends on CFTR activation by parasympathetic stimulation (Nedvetsky et al., 2014).

Another important parameter in lumen expansion and maintenance is electrostatic repulsion. Hence, to avoid lumen collapse after opening, proteins localized at apical lumen (podocalyxin, mucin 1) are glycosylated or sialylated, resulting in highly negatively charged extracellular domains, which act as anti-adhesive molecules (Datta et al., 2011; Iruela-Arispe and Beitel, 2013).

3.6. Role of the ECM in thyroid development

The role of extracellular matrix proteins in thyroid development or tridimensional organization has not been studied *in vivo* but several observations have been made in *in vitro* culture systems. Adult thyroid tissue fragments cultured in collagen type I retain their 3D follicular structures with apical microvilli and basal lamina (Toda et al., 2001). Moreover, these in vitro cultured follicles will remain functional for a long period of time if they are cultured with sufficient oxygen supply (3D air-liquid culture) (Toda et al., 2011; Toda et al., 2002). Similarly to MDCK cells, thyroid porcine cells grown in suspension form cyst-like structure and develop their apical pole facing the culture medium. Upon transfer in type I collagen, these inverted cysts correct polarity within 3 days so that the apical pole will now face the internal lumen (Chambard et al., 1981; Mauchamp et al., 1998). Finally, as already mentioned, transient but concomitant expression of Nkx2.1 and Pax8 in embryonic stem cells (ESC) allows their differentiation into thyrocyte progenitors. Upon transfer and culture in extracellular matrix (matrigel), these thyrocyte progenitors further differentiate and organize in 3D follicles able to

organify iodide (Antonica et al., 2012). Although nothing has been described *in vivo*, all these *in vitro* observations support a role for ECM in thyroid morphogenesis.

4. Bone morphogenetic proteins signaling

4.1. Ligands

Bone Morphogenetic Proteins (BMPs) are soluble growth factors named after their role in cartilage and bone formation. Since these original discoveries, BMPs have been implicated in many different organs during embryonic development but also in adult tissue homeostasis and disease. Hence, Body Morphogenetic Proteins is a more appropriate name.

BMPs are 20 different proteins belonging to the Transforming Growth Factor-β family. This family also includes TGF-βs (3 isoforms), activins (3 isoforms), inhibins, Growth Differentiation Factors (GDFs), Glial Derived Neurotrophic factor (GDNFs), Nodal, Lefty and anti-Müllerian hormone. BMPs, phylogenetically closer to GDFs, are subdivided into 4 groups based on their structures and functions. BMP-2 and -4 form one group ("BMP-2/4 group"). BMP-5, -6, -7 (previously called OP-1; osteogenic protein-1) and -8 (OP-2) form the second group ("OP-1 group"). GDF-5, -6 (BMP-13) and GDF-7 (BMP-12) form the third group (GDF-5 group). BMP-9 and -10 form the fourth group. BMPs have distinct spatiotemporal expression profiles and their affinities to receptors define their biological activities (Miyazono et al., 2010; Miyazono et al., 2005). BMPs are synthesized as precursors containing a N-terminal signal peptide, a prodomain for folding and secretion and the C-terminal mature peptide. Dimers of precursors are formed in the cytoplasm, and require stabilization by disulfide bonds. Dimers are then cleaved by convertases to generate N- and C-terminal fragments, the latter being capable of binding to its receptor (Harrison et al., 2011; Wang et al., 2014).

BMPs function in a continuous dose-dependent manner. Indeed, after secretion from the producing cell, BMP diffuse and generates a gradient. During Drosophila development, type IV collagen interacts with BMPs (Dpp in drosophila) in the extracellular space. This interaction increases Dpp signaling in the whole

embryo by promoting gradient formation or restricts the signaling in the ovary by sequestration of Dpp (Ramel and Hill, 2012; Wang et al., 2008).

4.2. Receptors

Two types of TGF-β/BMP receptors exist: type I and type II. There are seven type I receptors (ALK1-7) among which three can bind BMPs and four type II receptors, three of which can interact with BMPs (Table 1).

Receptors	**Ligand**
Type I	
ALK1	TGF-β/BMP (9-10)
ALK2 = ActR-1A	BMP (6-7-9-10)/Activin
ALK3 = BMPR-1A	BMP(2-4)
ALK4= ActR-1B	TGF-β/Activin
ALK5= TβRI	TGF-β
ALK6 = BMPR-1B	BMP (2-4/GDF5)
ALK7	TGF-β
Type II	
BMPR-2	BMP
ActR-2A	BMP/Activin
ActR-2B	BMP/Activin
TβRII	TGF-β

Table 1: Receptors of the TGF-β family and their interaction with ligands. Receptors are classified in two groups, type I (ALK1-7) and type II (BMPR-2, ActR-2A, ActR-2B, TβRII) and can bind TGF-β, BMPs or Activin ligands (based on (Miyazono et al., 2010; Wang et al., 2014)).

Given the number of receptors and ligands, many different combinations of type I and type II receptor pairing and of ligand-receptors can occur and hence create a huge diversity in signaling properties (Wu and Hill, 2009).

Receptors are composed of a short extracellular ligand-binding domain, a transmembrane domain and an intracellular domain with serine/threonine kinase activity for signaling (Wang et al., 2014).

4.3. Smad proteins

The main intracellular mediators of TGF-β/BMP signaling pathway are called the Smads. Smad proteins are conditional transcription factors containing two globular domains connected by a linker region. The N-terminal domain, or Mad homology domain 1 (MH1), can bind DNA. The C-terminal domain, or MH2, mediates protein-protein interaction with receptors, DNA binding cofactors or chromatin modifying enzyme (Macias et al., 2015). Smad proteins can be grouped in three classes: R-Smads are activated by the receptors after ligand binding; Smad2 and Smad3 are activated upon TGF-β binding; while Smad1, 5 and 8 are activated after BMP binding. The Co-Smad, Smad4, is common to TGF-β and BMP signaling and associates with activated R-Smads. The I-Smads, Smad 6 and 7, inhibit Smad signaling.

4.4. Signaling

Two main signaling pathways can be activated following BMP binding to receptors: the canonical Smad pathway and the non-canonical pathway that triggers activation of proteins from the MAPK family, PI3K/Akt, or from the Rho family of GTPases. I will focus on the canonical Smad signaling pathway downstream of BMP.

In the canonical pathway, BMP binding to its receptor induces the formation of a heterotetrameric complex of two dimers of type I and type II receptors (Figure 18). Once in close contact, the constitutively active type II receptor phosphorylates the type I receptor at a particular domain rich in glycine and serine. Type I receptor becomes activated and phosphorylates the receptor-regulated Smads (R-Smads) at a C-terminal SSXS motif. R-Smads then associate with the Co-mediator Smad4 (Co-Smad), and activated heteromeric Smad complexes translocate to the nucleus where they bind upstream regulatory sequences to target genes and regulate their transcription (Wang et al., 2014).

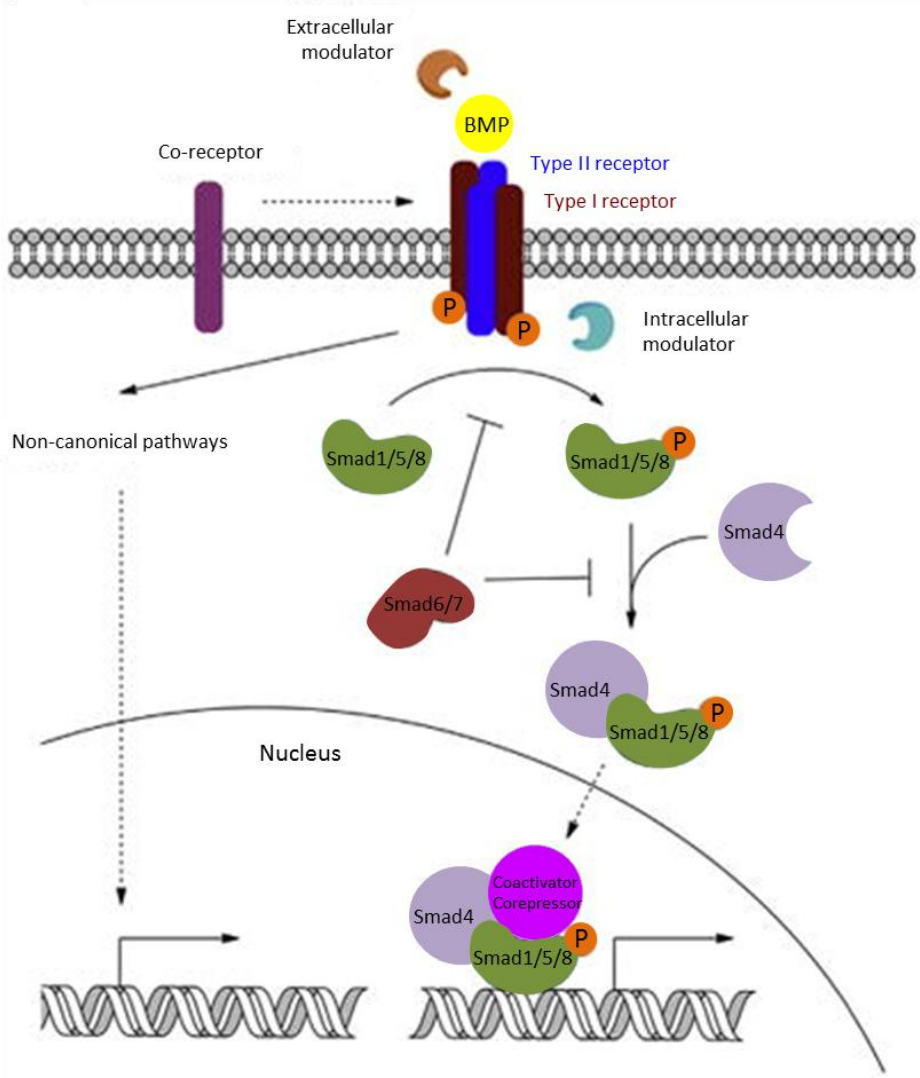

Figure 18. BMP signaling pathway. Binding of BMP ligand to heterotetrameric type I and II receptors induces non-canonical pathways and phosphorylation of R-Smad (Smad1/5/8). Phosphorylated R-Smad interacts with Smad4 and translocates to the nucleus to regulate gene transcription in association with transcriptional coactivators or corepressors. Activity of the pathway can be modulated by co-receptors (Endoglin) or extracellular (Noggin) and intracellular (Smad6/7) modulators (Wang et al., 2014).

Smads activated by TGF-β bind to Smad-binding elements (SBEs; AGAC or GTCT sequence) in the promoter of target genes, while Smads activated by BMPs

bind usually to the GCCGnCGC (GC-rich) sequence in regulatory regions of target genes. Among the various BMP target genes, the best studied belong to the Id (inhibitor of differentiation or inhibitor of DNA binding) family that contains 4 members (Id1-4). These HLH factors are negative regulators of cell differentiation and positive regulators of cell proliferation through inhibitory complex formation with bHLH transcription factors.

Once turned on, TGFβ/BMP signaling must be turned off. One mechanism is based on the increased expression of target genes Smad6 and Smad7 (I-Smads), which trigger feedback inhibition on the pathway by various means. Smad6 inhibits BMP signaling while Smad7 inhibit both TGF-β/BMP and activin pathways. Upon expression, I-Smads interact with type I receptor and prevents the interaction of R-Smad with the receptor. I-Smads also associate with R-Smad and prevent formation of the signaling complex between R-Smad and Co-Smad. Moreover, I-Smads can inhibit transcription of certain genes in the nucleus. In this compartment, Smurf, an ubiquitin ligase, can bind I-Smads and induce their nuclear export, thereby facilitating interaction with type I receptor and with cytoplasmic R-Smad (see above). In addition, I-Smad will also bring the ubiquitin ligase Smurf in close contact with the receptor and the R-Smad and mark these for proteasome-dependent degradation. Lastly, I-Smads can turn off receptor signaling by triggering dephosphorylation of receptors via protein phosphatases I (PPI) (Miyazono et al., 2010; Miyazono et al., 2005). Another mechanism to regulate TGFβ/BMP signaling is the nuclear export of Smad2/3 upon dephosphorylation by the phosphatase PPM1a which thus stops TGFβ signaling. Dephosphorylated Smads are recognized by RanBP3, a nuclear protein promoting export of the Smad from the nucleus (Dai et al., 2010; Lin et al., 2006).

4.5. BMPs in development

The role of BMP signaling in development has been studied in mice by genetic inactivation of BMPs, their receptors or downstream Smads. Defects in bones, heart, blood vessels, liver or lungs have been described which indicate that BMPs control cell growth, differentiation and apoptosis and support the appellation “body morphogenetic proteins”. Below, I will describe selected examples of the role of BMP in development.

The respiratory system (trachea and lungs) and the upper digestive tract (esophagus) derive from a single tube, the anterior foregut. Finely regulated processes, such as cell specification, are required to produce these two distinct tubes. Cells in the ventral part of the foregut endoderm tube, which will give rise to the respiratory system, are $NKX2.1^{+}$ and $SOX2^{-}$. Conversely, endodermal cells in the dorsal part of this tube are $NKX2.1^{-}$ and $SOX2^{+}$. BMP signaling controls the establishment of these two territories of the foregut tube (Domyan et al., 2011). Following inactivation of BMP receptors 1a and 1b, formation of the two tubes from the foregut tube does not occur and the foregut remains a single tube. In the tube, cells display by default the characteristic expression pattern of the esophagus: $NKX2.1^{-}$ and $SOX2^{+}$. This indicates that BMP signaling is required for trachea/lung specification. Based on the reciprocal antagonism described for NKX2.1 and SOX2, inactivation of SOX2 was performed in $BMPR1a/1b^{KO}$ mice. Triple KO embryos exhibited a separated trachea and esophagus, similar to controls. They further demonstrated that BMP signaling via BMPr1a/1b represses SOX2 expression, thereby allowing NKX2.1 expression in the ventral part of the foregut tube and thus promoting trachea formation (Domyan et al., 2011).

BMPs also play a critical role in ductus arteriosus (DA) closure. DA is a bypass conduit from the pulmonary artery to the aorta, operational only during fetal life to prevent blood passage via the non-functioning, non-ventilated lungs. At birth, transition to a pulmonary circulation requires rapid closure of the DA. The DA closure occurs in two steps: first, functional (initial) closure by a smooth muscle contraction, then anatomical (definitive) closure by a remodeling of endothelial cells in the DA lumen. BMP9 and 10 are circulating BMPs implicated in vascular development. $BMP9^{KO}$ embryos injected with a BMP10 neutralizing antibody showed impaired DA closure (Levet et al., 2015). The authors demonstrated that BMP9 and 10 stimulate the expression of fibronectin and of genes involved in endothelial-to-mesenchymal transition (EndMT). They propose a model in which high circulating BMP9 and 10 at birth trigger remodeling of DA endothelial cell in intimal cell, which lose cell-cell contacts, become mesenchymal and produce matrix deposition.

BMPs are also involved in angiogenesis which is the extension of new blood vessels from an existing vessel. First evidence came from the inactivation of Smad5 in mice, which leads to embryonic death at E10.5-11.5 due to defects in

angiogenesis (Yang and Chiba, 1999). A more recent study illustrates the role of BMP pathway in angiogenic sprouting (Moya et al., 2012). Upon VEGFa-dependent angiogenic stimulation, an endothelial cell becomes tip cell, while neighboring cells become stalk cells. The tip cell induces Dll4-Notch signaling in adjacent cells resulting in repression of tip cell characteristics in the adjacent stalk cells. By using mouse KO for Smad1 and Smad5 in endothelial cells, authors observed excessive angiogenic sprouting due to increased number of tip cells and decreased number of stalk cells. This observation was explained by cooperation between BMP-mediated Smad signaling and Notch signaling to maintain non-tip cells in the stalk cell state. BMP signaling is thus an important player together with Notch and VEGF in angiogenesis fine-tuning during development (Moya et al., 2012).

Although nothing is known about the implication of BMP in thyroid development, these selected examples suggest that they are active in the foregut, and could play a role in thyroid organogenesis, probably through angiogenesis or ECM deposition.

VI. AIMS OF THE WORK

The thyroid gland is composed of epithelial monolayers forming closed independent structures surrounding a lumen, the follicles. Formation of follicles occurs by reorganization of a tri-dimensional mass of non-polarized epithelial cells derived from the endoderm. Our lab is interested in the mechanisms driving folliculogenesis, more specifically in the communication between epithelial cells and the environment, in which endothelial cells are an important component.

When I joined this project, the working hypothesis was that endothelial cells, initially localized around the mass but progressively invading the thyroid mass, could be an important player in folliculogenesis. Indeed, in $Vegfa^{KO}$ thyroid, recruitment of endothelial cells was reduced and this was accompanied with defective follicle formation. Culture of thyroid explants depleted of endothelial cells also impaired folliculogenesis. Interestingly, and this is where I started to be involved in the project, defective folliculogenesis in thyroid explants could be rescued by addition of endothelial progenitors cells (eEPC) or their conditioned medium. These observations indicated that endothelial cells instruct epithelial cells to organize in follicles through secretion of a soluble factor (Delmarcelle et al., 2014; Hick et al., 2013).

My main objectives were to characterize the conditioned medium and to identify the folliculogenic factor(s) in order to understand the molecular and cellular mechanisms controlling folliculogenesis. Understanding cell-cell communications and the mechanisms involved in epithelial monolayers organization is not only important for developmental biology but also for medicine. Indeed, upon transformation, polarized epithelial cells in monolayers lose their polarity and proliferate to form a tridimensional mass. Carcinomas will then recruit endothelial cells and reciprocal communications will be initiated.

Characterization of the conditioned medium was facilitated by improvements of our thyroid culture system (Delmarcelle et al., 2014). We thus microdissected and cultured a homogenous tissue, the thyroid lobes at E14.5. This culture system was instrumental to biochemically characterize the conditioned medium but also to test implication of candidate molecules/signals in folliculogenesis. My work progressively merged with another project from the lab,

aiming at understanding the role of BMP-Smad1/5 signaling in thyroid folliculogenesis. We demonstrated that conditioned medium could rescue the defective folliculogenesis of $Vegfa^{KO}$ but also of $Smad1/5^{dKO}$. Combined progress in these two projects allowed us to identify laminins, a major component of the basement membrane, as a potent profolliculogenic factor. These results are the subject of my main scientific paper (Villacorte*, Delmarcelle* et al., in revision).

VII. RESULTS

1. Reciprocal epithelial:endothelial paracrine interactions during thyroid development govern follicular organization and C-cells differentiation

Anne-Christine Hick, Anne-Sophie Delmarcelle, Mahé Bouquet, Sabrina Klotz, Tamarra Copetti, Céline Forez, Patric Van Der Smissen, Pierre Sonveaux, Jean-François Collet, Olivier Feron, Pierre J. Courtoy, Christophe E. Pierreux

This work supported the thesis project of a previous PhD student from the lab, Anne-Christine Hick. I contributed to finalize this work and to perform experiments requested by the reviewers. Characterization of the conditioned medium was initiated, by studying the nature and the size of the folliculogenic factor. Other experiments were also performed to evaluate the role of the conditioned medium on the phosphorylation status of Nkx2.1.

Developmental Biology 381 (2013) 227–240

Contents lists available at ScienceDirect

Developmental Biology

journal homepage: www.elsevier.com/locate/developmentalbiology

Reciprocal epithelial:endothelial paracrine interactions during thyroid development govern follicular organization and C-cells differentiation

Anne-Christine Hick [a], Anne-Sophie Delmarcelle [a], Mahé Bouquet [a], Sabrina Klotz [a], Tamara Copetti [b], Celine Forez [a], Patrick Van Der Smissen [a], Pierre Sonveaux [b], Jean-François Collet [a,c], Olivier Feron [b], Pierre J. Courtoy [a], Christophe E. Pierreux [a,*]

[a] de Duve Institute, Université catholique de Louvain (UCL), B-1200 Brussels, Belgium
[b] Pole of Pharmacology and Therapeutics, IREC Institute, Université catholique de Louvain (UCL), B-1200 Brussels, Belgium
[c] WELBIO, B-1200 Brussels, Belgium

ARTICLE INFO

Article history:
Received 17 September 2012
Received in revised form
25 March 2013
Accepted 9 April 2013
Available online 21 May 2013

Keywords:
Thyroid
VEGF-A
Follicles
Polarity
C-cells
Endothelium
Epithelium
Explants
Paracrine control

ABSTRACT

The thyroid is a highly vascularized endocrine gland, displaying a characteristic epithelial organization in closed spheres, called follicles. Here we investigate how endothelial cells are recruited into the developing thyroid and if they control glandular organization as well as thyrocytes and C-cells differentiation. We show that endothelial cells closely surround, and then invade the expanding thyroid epithelial cell mass to become closely associated with nascent polarized follicles. This close and sustained endothelial:epithelial interaction depends on epithelial production of the angiogenic factor, Vascular Endothelial Growth Factor-A (VEGF-A), as its thyroid-specific genetic inactivation reduced the endothelial cell pool of the thyroid by >90%. Vegfa KO also displayed decreased C-cells differentiation and impaired organization of the epithelial cell mass into follicles. We developed an *ex vivo* model of thyroid explants that faithfully mimicks bilobation of the thyroid anlagen, endothelial and C-cells invasion, folliculogenesis and differentiation. Treatment of thyroid explants at e12.5 with a VEGFR2 inhibitor ablated the endothelial pool and reproduced *ex vivo* folliculogenesis defects observed in conditional Vegfa KO. In the absence of any blood supply, rescue by embryonic endothelial progenitor cells restored folliculogenesis, accelerated lumen expansion and stimulated calcitonin expression by C-cells. In conclusion, our data demonstrate that, in developing mouse thyroid, epithelial production of VEGF-A is necessary for endothelial cells recruitment and expansion. In turn, endothelial cells control epithelial reorganization in follicles and C-cells differentiation.

Introduction

In mammals, the thyroid is a composite endocrine gland that produces both thyroid hormones, by thyrocytes organized as follicles, and calcitonin in scattered C-cells. Follicular cells originate from the primitive endoderm as a thickening in the ventral wall of the primitive pharynx around embryonic day (e)8–e8.5. Invagination forms the thyroid bud that separates from the endoderm at e11.5 and starts expanding bilaterally. Final shaping in two lobes connected by a narrow isthmus is achieved by e15. At the same time, prefollicular structures appear by polarization of epithelial cells, and genes involved in thyroid hormones synthesis are induced (De Felice and Di Lauro, 2004). The second type of endocrine cells, C-cells, originates from the fourth pharyngeal pouches. They migrate as two groups of cells called the ultimobranchial bodies, and intermix with the thyroid cells of each lobe at e13.5 (Kameda et al., 2007). In adult, thyrocytes transport iodine from the basolateral to the apical cell membrane, where thyroperoxidase ensures thyroglobulin iodination. Upon stimulation by TSH (thyroid-stimulating hormone), thyrocytes endocytose iodinated-thyroglobulin into lysosomes where T4 and T3 are excised to be eventually exported into the circulation (Dunn and Dunn, 2001). The thyroid gland is highly vascularized and the intimate association between follicles and blood capillaries, referred to as angio-follicular units, is crucial for thyroid hormone synthesis and release (Gerard et al., 2002).

Congenital hypothyroidism (CH) is the most prevalent endocrine disorder among children, with an incidence of 1/3000–4000 (Toublanc, 1992). Untreated CH causes dwarfism and severe intellectual disability. Accurate thyroid development is therefore an absolute requirement for central nervous system and whole body development (Morreale de Escobar et al., 2000).

* Corresponding author. Fax: +32 2 764 75 43.
E-mail address: christophe.pierreux@uclouvain.be (C.E. Pierreux).
URL: http://www.deduveinstitute.be/epithelial.php (C.E. Pierreux).

0012-1606/$ - see front matter © 2013 Elsevier Inc. All rights reserved.
http://dx.doi.org/10.1016/j.ydbio.2013.04.022

A regulatory network of four transcription factors, all expressed by epithelial cells, controls thyroid development: Nkx2.1, Pax8, Foxe1 and Hhex. Individual knockout of each of these transcription factors severely impairs thyroid development (for a review, De Felice and Di Lauro, 2004). Interestingly, Nkx2.1 inactivation in adults shows its essential role for the maintenance of thyroid architecture and function (Kusakabe et al., 2005). Moreover, folliculogenesis is impaired in thyroids expressing a non-phosphorylable Nkx2.1 protein (Silberschmidt et al., 2011). Recently, two studies also reported the involvement of microRNAs in follicular organization (Frezzetti et al., 2012; Rodriguez et al., 2012). Besides these intrinsic controls, a role for epithelial: mesenchymal interactions has been uncovered in thyroid development, like in other endoderm-derived glands (Hick et al., 2009). For example, Tbx1 (T-box transcription factor), expressed in the mesoderm surrounding the thyroid, is a direct regulator of Fgf8 expression. Tbx1 gene inactivation causes thyroid hypoplasia, limited to a single lobe, and absence of ultimobranchial bodies, thus of C-cells (Liao et al., 2004). Artificial reexpression of mesenchymal Fgf8 from the Tbx1 locus rescues the size defect of the thyroid primordium, demonstrating the central role of mesenchyme for overall thyroid development (Lania et al., 2009). At the onset of thyroid development, Shh is remarkably absent from endodermal cells that will give rise to the thyroid primordium, but is well-expressed in the adjacent pharyngeal endoderm. However, Shh has been demonstrated to be involved in thyroid bilobation (Fagman et al., 2004). To our knowledge, no extrinsic cue has been shown to specifically control follicle formation.

Blood vessels have long been considered as a passive tubular network delivering oxygen and nutrients. According to this view, "vasculature follows organ development". However, an instructive view of the endothelium has recently emerged in developmental or disease processes, either by physical (contact) or chemical (paracrine) interactions with the epithelium (Cleaver and Melton, 2003; Cleaver and Dor, 2012). For example, hypervascularization of the pancreas promotes endocrine differentiation at the expense of the acinar cells (Lammert et al., 2001). We have further shown that endothelial cells are specifically recruited near the trunk cells of the pancreatic epithelium due to their high expression of vascular endothelial growth factor-A (VEGF-A), as compared to tip cells. This precise localization prevents exocrine differentiation of trunk cells, thereby restricting exocrine differentiation to tip cells (Pierreux et al., 2010). In the developing lung, endothelial cells are required to determine airway branching morphogenesis (Lazarus et al., 2011). Dosage seems critical since either deletion or overexpression of Vegfa in kidney glomeruli likewise impact on endothelial development and impair the establishment and maintenance of the glomerular filtration barrier (Eremina et al., 2003).

Several studies reported potential roles of the vasculature during early thyroid development. Rather intriguing is the close proximity between endoderm thickening specified to the thyroid primordium and the aortic sac, without any mesenchymal cell interposition (Fagman et al., 2006). It has been postulated that arch arteries could serve as guiding tracks for thyroid progenitors as they migrate towards the ultimobranchial bodies (Fagman et al., 2006; Alt et al., 2006). Interestingly, cardiac anomalies such as Di George's syndrome represent the most recurrent birth defects associated with thyroid dysgenesis and congenital hypothyroidism (Olivieri et al., 2002; Liao et al., 2004). Deletion of the Tbx1 gene in mice, which has been associated with Di George's syndrome, also causes defects of aortic arch and outflow tract heart associated with thyroid hemi-agenesis and hypocalcemia (Liao et al., 2004). Whether association of cardiac and thyroid malformations is due to the lack of a common biochemical regulator (for example the transcription factor Isl1 is expressed in both thyroid and heart progenitors) or interruption of reciprocal interactions between the two structures remains unknown (Fagman and Nilsson, 2009).

Detailed knowledge of organ morphogenesis should therefore include the precise analysis of epithelial and endothelial development, and their reciprocal communications. Here, we investigated the role of endothelial cells during thyroid gland development. We first show that endothelial cells are recruited in response to epithelial production of VEGF-A. The functional role of blood capillaries was next studied in thyroid-specific Vegfa knockout, and in an original *ex vivo* culture system of the thyroid. Our results show that endothelial cells are necessary for the organization of the thyroid epithelial cell mass into follicles and for normal calcitonin expression.

Materials and methods

Animals

Vegfa-floxed and Pax8-cre mice were obtained from N. Ferrara (Genentech) (Gerber et al., 1999) and (Bouchard et al., 2004), respectively. All other mice were of the CD1 strain. Mice were raised and treated according to the principles of laboratory animal care of the University Animal Welfare Committee.

Dissection and culture of thyroid explants

Thyroid explants were microdissected from e12.5 mouse embryos and included tissue localized rostral to the pharyngeal arch arteries, containing the trachea but not the oesophagus. Explants were cultured on microporous membranes, floating on M199 medium supplemented with 10% fetal calf serum (FCS), 100 U/ml penicillin, 100 μg/ml streptomycin, 0.25 μg/ml fungizone and 2 mM glutamine (van Eyll et al., 2004), renewed every other day. SU5416 (VEGFR2 kinase inhibitor III, Calbiochem/VWR) was dissolved in DMSO as 10 mM stock solution and added at 5 μM in the culture medium. Control explants were exposed to the same concentration of vehicule as the test samples. Bright field and fluorescence images of cultured explants were acquired with a Zeiss Discovery V12 stereomicroscope.

Endothelial progenitor cells (EPCs)

Embryonic EPCs were produced as described (Sbaa et al., 2006) and cultured on gelatin-coated dishes containing DMEM (cat # 42430, Gibco) supplemented with 20% non-decomplemented FCS, 100 U/ml penicillin, 100 μg/ml streptomycin and 100 μM non-essential amino acids. To stably express TOMATO FP, the cells were infected with pHIV-TOMATO (Addgene) using lentiviral approach disclosed elsewhere (Taulli et al., 2005). Cells were trypsinized with Tryple Express (Invitrogen). For rescue experiments, 60,000 eEPCs were added on the center of the filter with the explants. To collect conditioned medium (c.m.), 50–70% confluent cells were incubated for 16 h in M199 medium without serum (6 ml for a 7.8-mm^2 dish). Supernatant was first centrifuged at 850g for 5 min to remove floating cells or large debris, then at 17000g for 20 min and finally concentrated by centrifugation at 1900g for 5 min in Amicon Ultra, 5 or 50 K units. Non-conditioned M199 medium was also concentrated in parallel and used as negative control. 10-x concentrated medium was supplemented with 10% FCS before use. For proteolytic digestion, 10-x concentrated c.m. was incubated for 2 h at 37 °C with 0.5 mg of pronase/ml (Sigma), which was then washed out by 6 cycles of dilution with M199/concentration on Amicon filter unit. For gel filtration, 50 μl of 40-x concentrated c.m. was loaded on a Superdex-200 gel filtration column (GE Healthcare) equilibrated with buffer A

(25 mM Hepes, pH 7.1, 100 mM NaCl) at a flow rate of 0.5 ml/min, and two-ml fractions were collected in 220-μl of 10-x non-conditionned M199 medium. Fractions were further concentrated 2-fold on Amicon Ultra-4, 5 K units before assessing biological activity in the presence of 10% FCS. To determine the molecular weight range of the fractions, the Superdex-200 column was calibrated with following standards: thyroglobulin (670 kDa), IgG (158 kDa), ovalbumin (44 kDa), myoglobin (17 kDa) and vitamin B12 (1.35 kDa).

In situ hybridization

Mouse embryos were fixed overnight at 4 °C by 60% ethanol, 30% formaldehyde and 10% acetic acid before paraffin embedding. Digoxigenin-labeled antisense RNA probes for Vegfa and VEGF Receptor type 2/Fetal liver kinase 1 (Vegfr2/Flk1) are described elsewhere (Pierreux et al., 2010). Nkx2.1 probe was kindly provided by R. Di Lauro. cDNAs spanning nucleotides 44–243, 171–424 and 1265–1473 of mouse sequences coding for Pax8, Foxe1 and Hhex, respectively, were amplified to generate antisense probes. In situ hybridization was performed on 16μm-thick sections as described (Jacquemin et al., 2003). Whole-sample images were acquired using a Zeiss Mirax Midi fluorescence microscope.

Immunolabeling

For whole-mount immunolabeling, dissected thyroids were fixed by 4% formaldehyde in PBS for 1 h at 4 °C and processed as described (Pierreux et al., 2006). Immunofluorescence on sections from embryos or explants was performed as described (Pierreux et al., 2006). For immunofluorescence after in situ hybridization, sections were treated as described (Gaide Chevronnay et al., 2008). Antibodies and dilutions are described in Supplementary Table 1. Nuclei were counterstained with Hoechst (Sigma) in PBS during incubation with the secondary antibodies. Secondary antibodies were coupled to Alexa-488, −594 or −647, as appropriate (Invitrogen). For peroxidase staining, the envision system (Dako) was used. Fluorescence on sections was observed with a Zeiss Axiovert 200 inverted fluorescence microscope or with a Zeiss Cell Observer Spinning Disk (COSD). Whole-mount immunolabeled tissues were dehydrated gradually in methanol, cleared and mounted in methylsalicylate (Sigma) and examined with a Zeiss LSM510 multiphoton microscope using its dedicated software for three-dimensional projections.

For quantification of calcitonin-expressing cells, we counted labeled cells on every tenth 7-μm section of each lobe of the whole thyroid gland (approximately seven sections per lobe of three individuals). Numbers were integrated per distance interval to provide an estimate of total c-cell number in each lobe as a function of tissue depth. For quantification of PHH3-expressing cells, we counted labeled cells on every fifth 8-μm section of each lobe of the whole thyroid gland (approximately twenty sections). Numbers were integrated per distance interval to provide an estimate of total cell number per thyroid lobe. Further normalization to 100-μm thickness prevented bias due to lobe size variations.

For quantification of number and size of ezrin-labeled structures, samples were analyzed using the LSM510 (Zeiss) confocal microscope. Z-stacks of 12 to 27-μm thick optical sections were recorded at high resolution (63/1.40 oil Plan-Apochromat) under optimal conditions to fulfill Nyquest sampling criteria. To avoid analysis of the same ezrin+structure, only every tenth section in the z-stack was analyzed. Analysis was performed with AxioVision 4.8.2 software (Zeiss). To prepare the binary mask for analysis, images were thresholded in a fixed intensity window (20→255) and very small dots, at the limit of microscopic detection (surface < 4 pixels) were cleaned away. Retained structures on the binary image were filled and surface measured on all selected images. Statistical tests were performed with SYSTAT (version 10, SPSS).

Real-time RT-PCR

Total RNA was extracted from embryonic thyroid lobes or cultured explants using Trizol reagents (Invitrogen) in combination with Phase Lock Gel™ (Invitrogen). RNA (0.5 μg) was reverse-transcribed with random hexamers using Moloney Murine Leukemia Virus or Avian Myeloblastosis Virus reverse transcriptase (Invitrogen). Real-time quantitative PCR was performed by using KAPA™ SYBR® Fast qPCR kit (Sopachem). Primers sequences are described in Supplementary Table 2. Relative changes in target gene/β-actin mRNA ratio were determined by transformation of threshold cycles to absolute mRNA numbers (Pierreux et al., 2006) or using the ΔΔct method using β-actin as the reference gene.

Electron microscopy

Control and cKO e18.5 thyroid lobes were rapidly rinsed with 155 mM NaCl, fixed by 2% (v/v) glutaraldehyde in 0.1 M sodium cacodylate buffer, pH 7.4, for 30 min at 4 °C, and washed again thrice for 10 min with 50 mM Tris–HCl, pH 6.0. Cells were post-fixed with 1% (w/v) OSO_4–2%$KFe(CN)_6$ solution, stained en bloc with 1% uranyl acetate for 2 h and pelleted in 2% agar. Pellets were dehydrated in graded ethanol and embedded in Spurr. Ultrathin (70 nm nominal) sections were obtained with a Reichert ultramicrotome (Reichert), collected on rhodanium 400 mesh grids and contrasted with 3% uranyl acetate followed by lead citrate, each for 10 min. Grids were washed with water, dried, and examined in a FEI CM12 electron microscope operating at 80 kV.

Statistical analysis

Statistical analysis was performed using two-tailed Student's *t*-test, except for ezrin+structures quantification, where Kolmogorov–Smirnov and Sign-test were used. Data are presented as mean ± s.e.m.

Results

Endothelial cells closely surround thyroid epithelium during development

Most studies investigating thyroid development have focused on epithelial development as an autonomous process. Here, we addressed thyroid epithelial development within its environment. Given that the thyroid is a highly vascularized endocrine organ, we focused on the role of blood vessels during thyroid development with emphasis on folliculogenesis. To these aims, we first determined the spatial organization of endothelial cells in relation to epithelial cells from the early stages of thyroid bud development (Fig. 1). We identified endothelial cells by immunofluorescence for Platelet and Endothelial Cell Adhesion Molecule (PECAM or CD31) and thyroid epithelial cell nuclei using antibodies to Nkx2.1 (TTF-1). We found that, at e12.5, endothelial cells are localized around the single thyroid epithelial cell mass derived from the endoderm bud. From e13.5, the abundance of endothelial cells increases and they progressively migrate in-between Nkx2.1+ epithelial cells. Vascular density culminates around e16.5, a time at which almost every epithelial cell is in contact with an endothelial cell (Fig. 1A). Tridimensional analysis of whole-mount immunolabeled thyroids at e12.5 and e16.5 confirmed these observations (supplementary Movies 1 and 2). In parallel, we monitored thyroid folliculogenesis,

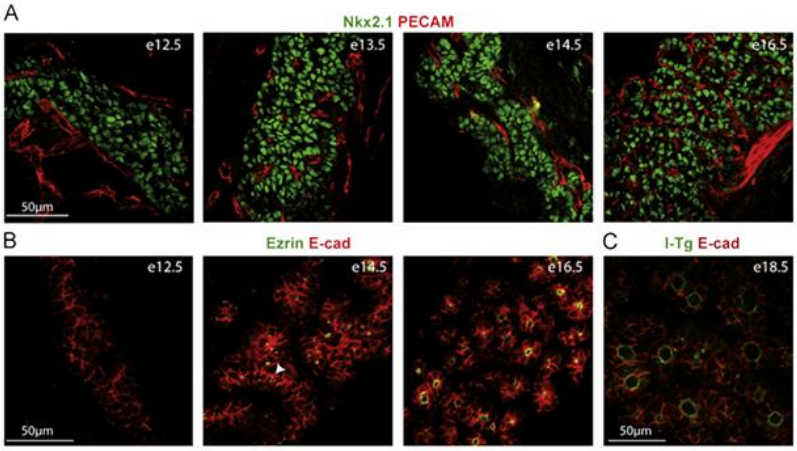

Fig. 1. Endothelial cells closely surround the thyroid mass, then epithelial follicles, which start producing thyroid hormones. Immunolabeling of control thyroid sections from e12.5 to e16.5 ((A), (B)) or at birth (C). (A) Topological relation between the thyroid epithelium and blood capillaries. At the thyroid bud stage (e12.5), endothelial cells (PECAM, red) closely surround the epithelial cell mass (Nkx2.1, green). During subsequent development, endothelial cells progressively invade the expanding cell mass, and generate therein a dense capillary network that eventually surrounds all individualized follicles at e16.5. Panels at e12.5 and e16.5 show frames selected from Supplementary Movies 1 and 2, respectively. (B) Polarization of thyrocytes. The e12.5 thyroid bud is composed of a mass of non-polarized epithelial cells (E-cad+; Ezrin−). Small intracellular dots labeled for ezrin appear at e14.5, sometimes seen as doublets just underneath both sides of an epithelial contact (arrowhead), but no lumen is detectable. At e16.5, essentially all epithelial cells are organized in follicular-like structures or "rosettes", made of polarized monolayers, with apical ezrin delineating microlumina, which expand thereafter (see (C)). (C) Differentiation of thyrocytes. At birth, follicular cells (E-cad+) are apically labeled for iodothyroglobulin (T4 antibodies). See also Fig. S1 in the supplementary material.

i.e. acquisition of epithelial cell polarity, using antibodies to the subapical marker, ezrin, in combination with the epithelial plasma membrane marker, E-cadherin. At e12.5, the thyroid bud consists of a mass of epithelial cells with no visible ezrin staining (Fig. 1B). This multilayered epithelium thus totally lacks apico-basal polarity and luminal structure (Fig. 1A and B), as in the pancreas and submandibular buds (Hick et al., 2009). With development, the thyroid bud expands and the first sign of polarization appears around e14.5 with small clusters of ezrin, sometimes seen as doublets just underneath both sides of an epithelial contact (arrowhead, Fig. 1B). From e16.5, epithelial cells are reorganized in small clusters ("rosettes"), with ezrin labeling at the apical membrane delineating small lumina (Fig. 1B). Similar results were obtained using an antibody recognizing the tight junction scaffold, ZO-1 (see Fig. S1 in the supplementary material). Subsequently, as lumina dilate, "rosettes" form follicles, i.e. continuous independent monolayer sheets surrounding a closed compartment where thyroglobulin is vectorially discharged and converted into iodothyroglobulin (Fig. 1C). Thus, during thyroid morphogenesis and folliculogenesis, endothelial cells initially surround a mass of non-polarized epithelial cells. As they invade this mass, epithelial cells concomitantly organize in pre-follicular "rosettes". By the end of gestation, a dense network of capillaries intimately embraces all polarized thyroid follicles. These data suggested that thyroid epithelial cell organization into follicles might be concerted with endothelial cells development.

Supplementary material related to this article can be found online at http://dx.doi.org/10.1016/j.ydbio.2013.47.002.

Vegfa/Vegfr2 are strongly expressed during thyroid development

Since VEGF-A is a major regulator of blood vessels development, we quantified the expression of the VEGF family members and of their receptors (VEGFRs) in the thyroid from e14.5 to e17.5. Among the VEGF ligands, the expression of Vegfa mRNA was the highest and increased with thyroid development (Fig. 2A). Among its receptors, Vegfr2, the main VEGF-A receptor involved in blood vessels angiogenesis, also showed the highest mRNA expression level in the thyroid. We thus mapped Vegfa- and Vegfr2-expressing cells using in situ hybridization (ISH). Analysis of e14.5 whole embryo sections showed a strong Vegfa expression in the thyroid gland, actually displaying the highest signal in the entire body section (Fig. 2B, boxed region). To define cells that so actively expressed Vegfa, we identified epithelial and endothelial cells on the same section as used for ISH, using double immunofluorescence for E-cadherin and PECAM, respectively. High magnification of the thyroid region demonstrated that Vegfa signal was exclusively detected in E-cadherin+ thyroid epithelial cells and not in adjacent endothelial cells (Fig. 2B and Fig. S2 in the supplementary material). Of note, epithelial cells originating from the ultimobranchial bodies were devoid of Vegfa expression (asterisks in Fig. 2B). Analysis of the adjacent section, hybridized with a Vegfr2 antisense probe, revealed a complementary endothelial-like expression pattern (Fig. 2B, lower panels). The endothelial identity of the Vegfr2 signal was confirmed by co-immunolabeling with the PECAM antibody, thereby demonstrating that only endothelial cells expressed Vegfr2. The complementary expression pattern of Vegfa and Vegfr2, also observed at e16.5 (see Fig. S2 in the supplementary material), strongly suggested that the epithelial cell-derived VEGF-A was a *primum movens* to attract and retain endothelial cells into the epithelial mass.

Epithelium-derived VEGF-A is necessary for endothelial cells recruitment and expansion

To test for a key role of VEGF signaling in endothelial cell recruitment and blood vessels development in the developing

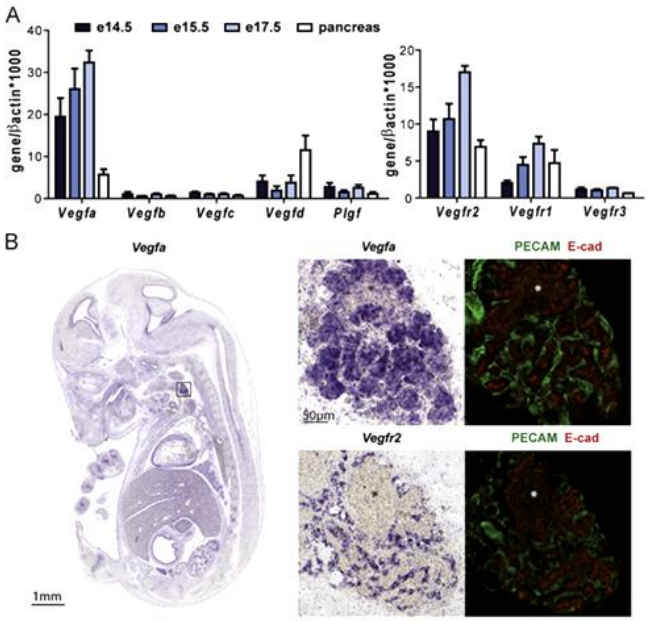

Fig. 2. The developing thyroid strongly expresses Vegfa and is closely associated with Vegfr2-expressing endothelial cells. (A) Q-PCR profiling of VEGF family ligands and receptors. Vegfa and Vegfr2 are most expressed during thyroid development where expression increases from e14.5 to e17.5. (B) Vegfa and Vegfr2 localization by in situ hybridization and immunolabeling. At left, hybridization of the antisense probe for Vegfa on an e14.5 embryo shows the highest intensity in the thyroid region (boxed; enlarged at right). On the same section shown at upper right, the Vegfa pattern coincides with epithelial cells (E-cad; red), and is fully dissociated from endothelial cells (PECAM; green). At lower right, pattern for Vegfr2 mRNA is complementary to that of Vegfa and perfectly overlaps with endothelial cells (PECAM, green). All asterisks mark the cluster of epithelial cells originating from ultimobranchial bodies (E-cad+; Vegfa-). See also Fig. S2 in the supplementary material.

thyroid, we inhibited VEGF-A production by specific inactivation of floxed Vegfa alleles in the thyroid epithelium. To this end, Pax8-Cre mice, which express Cre recombinase in the thyroid, were mated with Vegfa-loxP mice. Recombination efficiency was evaluated by LacZ staining and its effect was evaluated by in situ hybridization and by RT-qPCR (Fig. 3). The double heterozygous $Pax8^{Cre/+}$;$VEGFA^{flox/+}$ males used in this study were first mated with ROSA-stop-LacZ females. Analysis of the neck of e13.5 embryos revealed strong and uniform β-galactosidase activity limited to both thyroid lobes and their isthmus, demonstrating efficient and selective Cre recombinase activity in the thyroid (Fig. 3A). Double heterozygous males were crossed with $VEGFA^{flox/flox}$ females to obtain thyroid-specific VEGFA deficient embryos: $Pax8^{Cre/+}$;$VEGFA^{flox/flox}$ or conditional KO (cKO). Using RT-qPCR, we measured Vegfa mRNA levels, as well as those of the endothelial-specific Vegfr2 and Ve-cadherin, in microdissected thyroids from newborns (P0). In cKO newborns, Vegfa expression was decreased by more than 90% ($p<0.001$, $n=5$) (Fig. 3B). The strong decrease in Vegfa expression was accompanied by a large reduction in the endothelial-specific Vegfr2 (−80%, $p<0.001$, $n=7$) and Ve-cadherin (−70%, $p<0.001$, $n=7$) mRNAs. Heterozygous ($Pax8^{Cre/+}$;$VEGFA^{flox/+}$) newborns displayed only mild reduction in Vegfa, Vegfr2 and Ve-cadherin expression (around 30% for the three tested genes, $p<0.001$, $n=5$ for Vegfa and $n=7$ for Vegfr2 and Ve-cadherin).

To verify that the decrease in Vegfa mRNA was specific to the thyroid epithelium, we performed in situ hybridization on e14.5 embryos. This analysis revealed that Vegfa expression was ablated in the thyroid epithelium of cKO but not in adjacent submandibular glands (Fig. 3C and Fig. S3). Of note, Pax8-driven Cre also inactivated VEGF-A production in the kidney (see below). In line with RT-qPCR data, strongly reduced Vegfa expression in e14.5 cKO thyroids was accompanied by a much weaker and more spatially restricted Vegfr2 signal on the adjacent section, demonstrating strong impairment of microvessel survival and/or angiogenesis (Fig. 3C). Whole-mount immunolabeling of PECAM control and cKO thyroids at e17.5 confirmed the decreased blood vessels density, as illustrated by z-stacks of confocal sections followed by three-dimensional reconstructions. Importantly, apoptosis was not detected at any developmental stage in cKO embryos (data not shown). Altogether, these results demonstrated that Vegfa produced by thyroid epithelial cells is necessary for the recruitment of endothelial cells and for the development of a dense network of blood vessels around the epithelial cells.

VEGFA conditional knockout mice die perinatally, presumably due to renal failure

Mutant offspring were observed at the expected Mendelian frequency up to birth, but all cKO died during their first postnatal day, preventing analysis of thyroid function. Analysis of epithelial cell proliferation in cKO thyroids was normal at e15.5 (data not shown), but showed qualitative and quantitative differences at e17.5. Qualitatively, proliferating cells identified by labeling for

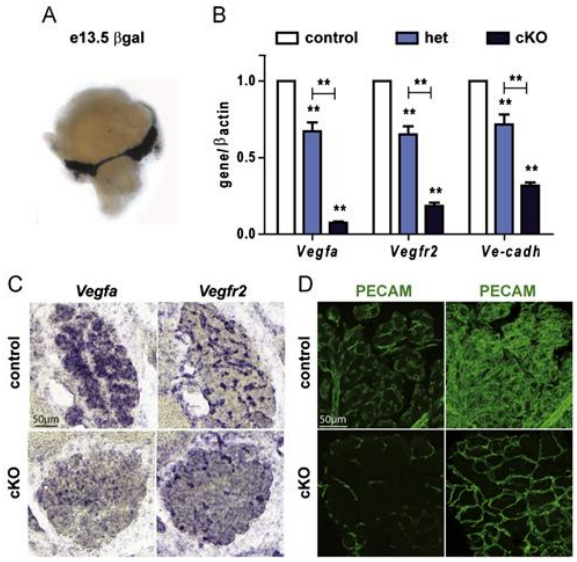

Fig. 3. Thyroid-specific Vegfa KO demonstrates that recruitment and expansion of endothelial cells depends on production of VEGFA by epithelial cells. (A) Targeting and efficiency of Cre recombinase activity. β-galactosidase (lacZ) staining of $Pax8^{Cre/+}$ thyroid gland demonstrates efficient Cre recombinase activity in the thyroid lobes and isthmus as early as e13.5. (B) Efficiency of Vegfa inactivation by RT-qPCR. Loss of one (heterozygote; het) or two (homozygote or Vegfa conditional knockout; cKO) Vegfa alleles causes a dose-dependent reduction in the expression of Vegfa, and of the endothelial markers Vegfr2 and Ve-cadherin in newborns (values are means ± s.e.m. $^{**}p < 0.001$). (C) Efficiency of Vegfa inactivation as shown by in situ hybridization. Serial sections of control (upper row) or cKO e14.5 thyroids (lower row). cKO abrogates Vegfa antisense probe hybridization and decreases that for Vegfr2. (D) Decreased endothelial cell density in Vegfa cKO. Whole-mount immunolabeling for PECAM (green) of e17.5 control (upper row) and cKO thyroids (lower row). Left, individual confocal sections; right, 3D reconstruction from 43 confocal images (projection from 43-μm total thickness). In Vegfa cKO, thyroid microvascular density is strongly reduced.

phosphohistone-H3 were widespread within the control epithelium, but preferentially found at the periphery of cKO glands (see Fig. S4). This corresponded to a two-fold reduction in the number of pHH3+ cells in cKO (1200 ± 100 vs 580 ± 70 PHH3+cells/100 μm thickness, $p < 0.01$). Nevertheless, this late decrease had no visible effect on cKO thyroid size at birth.

We thus suspected that early death of cKO newborns was due to renal failure. Indeed, besides expression in the thyroid gland, Pax8 is also expressed in the kidneys and homozygous deletion of Vegfa in glomeruli (using nephrin-Cre) results in perinatal lethality due to abortive build-up of the glomerular filtration barrier (Eremina et al., 2003). In the kidneys of cKO newborns, ablation of Vegfa expression was confirmed by RT-qPCR, and PECAM immunofluorescence disclosed a severe loss of endothelial cells in glomeruli, with abortive architecture as shown by conventional histopathology (see Fig. S5). Adults heterozygous for the deletion of Vegfa in the thyroid showed normal follicle shape and size, proper vascularization and iodothyroglobulin production (see Fig. S6 Moreover, heterozygotes and controls showed no significant difference for thyroxin serum levels (5.6 ± 0.2 vs 6.0 ± 0.2 μg/dl, $n=15$ and 26, respectively) and TSH levels (130 ± 20 vs 100 ± 30 pg/ml, respectively, $n=7$).

Effect of vascular density on the dual thyroid endocrine function

The thyroid gland is a composite organ with dual endocrine function: production of thyroid hormones by thyrocytes organized into follicles, to finely tune global body metabolism; and secretion of calcitonin by scattered C-cells, as part of calcium homeostasis. To evaluate the role of blood vessels in thyroid embryonic development, we first measured the expression level of the four thyroid-specific transcription factors (Nkx2.1, Pax8, Foxe1 and Hhex) by RT-qPCR at P0 and analyzed their expression pattern by in situ hybridization at e14.5 (Fig. 4A and C). While Nkx2.1, Foxe1 and Hhex had the same level and expression pattern in cKO and control thyroids, Pax8 expression level was increased by almost 40% in cKO and heterozygote thyroids at birth ($p < 0.05$, $n=7$). Nevertheless, its expression pattern, confined to the epithelium, was comparable between control and cKO embryos (Fig. 4C).

We then analyzed the mRNA expression of differentiation markers in cKO thyroids at birth. Thyroperoxidase (Tpo), thyroglobulin (Tg) and TSH receptor (Tshr) expression were slightly modified (−30, −20 and +30%, respectively, $p < 0.01$, $n=7$), Na^+/I^- symporter (Nis) expression was unaffected and immunolabeling of iodothyroglobulin showed a normal localization (Fig. 4B and D). Altogether, these data indicate that reduced blood vessels density is not detrimental to thyrocytes differentiation. Unexpectedly, RT-qPCR showed a 2-fold reduction in calcitonin expression (−55%, $p < 0.001$, $n=7$) in cKO thyroids. This decrease could reflect a lower number of C-cells, a reduced expression of calcitonin in all the C-cells, or both. To distinguish between these hypotheses, we performed immunolabelling and in situ hybridization for calcitonin. To quantify the number of C-cells, three controls and three cKO thyroids at P0 were immunolabeled with an anti-calcitonin antibody and calcitonin-producing C-cells were counted in serial sections of both lobes. The average number of C-cells per 100-μm

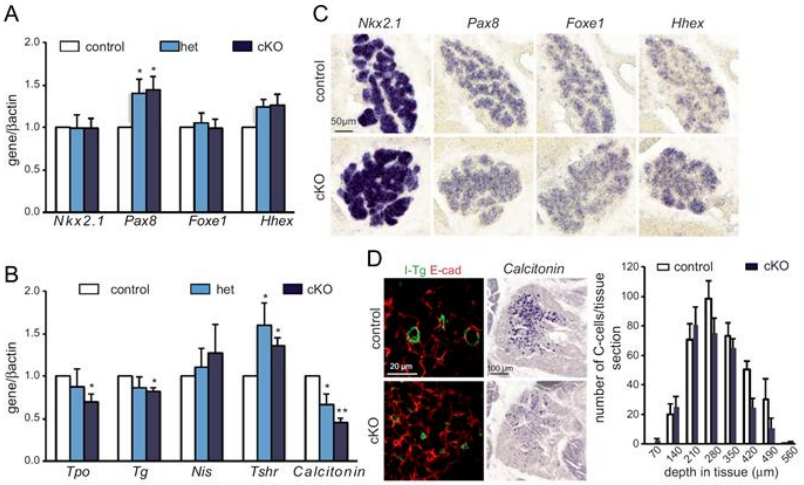

Fig. 4. Reduction in vascular density does not prevent thyrocyte differentiation but impairs calcitonin expression. (A) Thyroid-specific transcription factor analysis by RT-qPCR. Except for a slight increase of Pax8 expression level in Vegfa cKO and heterozygote thyroids ($^{*}p < 0.05$), the expression of Nkx2.1, Foxe1 and Hhex does not change in cKO newborns. (B) Differentiation marker analysis by RT-qPCR. In cKO P0 thyroids, the expression levels of thyroperoxidase (Tpo), thyroglobulin (Tg) and thyrotropin receptor (Tshr) are only marginally affected, but that of calcitonin is reduced by 50% ($^{*}p < 0.01$, $^{**}p < 0.001$). (C) Localization of transcription factors by in situ hybridization. The expression pattern of the four thyroid-specific transcription factors is comparable in e14.5 control and Vegfa cKO thyroids. (D) Imaging and quantification of endocrine differentiation. Immunolabeling (e17.5) and in situ hybridization (e18.5) on control and cKO thyroid sections. Although follicular differentiation is impaired by Vegfa cKO (see below), apical iodothyroglobulin production is qualitatively preserved, in line with RT-qPCR data (panel B). The number of calcitonin-expressing C-cells and their distribution within the lobes is not affected in cKO, but calcitonin mRNA level in each cell is significantly reduced, confirming RT-qPCR data (panel B).

tissue slice of thyroid tissue was not statistically different in control and cKO ($794 \pm 75{,}5$ vs $687 \pm 83{,}2$; $p = 0.128$), and their distribution in the whole lobes was comparable (Fig. 4D). In situ hybridization for calcitonin mRNA also revealed a similar number and scattering of calcitonin-expressing cells throughout the epithelium of e18.5 cKO embryos, as compared to controls (Fig. 4D). However, the intensity of calcitonin mRNA staining was clearly weaker in cKO thyroids. Altogether, these data indicated that blood vessels do not influence C-cell number in the thyroid, but control the level of calcitonin expression by C-cells.

Vascular density controls epithelial reorganization and follicle formation in vivo

Having noted that follicular differentiation was modestly affected in cKO mice (Fig. 4), we thus carefully analyzed the impact of decreased vascular density on thyroid epithelial morphogenesis. This analysis was started at e15.5, the stage at which thyroid epithelial cells have normally initiated their reorganization from a non-polarized multilayer cell mass into pre-follicular "rosettes" structures, concomitant with invasion by endothelial cells (Fig. 5A). Epithelial cell polarization and organization into "rosettes" were analyzed using ezrin and E-cadherin immunolabeling. Control thyroids showed both intracellular ezrin+ vesicles (arrow in Fig. 5A), and larger ezrin+ structures shared by several epithelial cells (arrowhead in Fig. 5A), indicating intracellular build-up of an apical domain followed by coordinated apical fusion to form a lumen. In contrast, the Vegfa cKO epithelium appeared on sections as a multilayered epithelial mass (Fig. 5A′), suggesting a general reorganization defect, without any demonstrable "rosette"', and bearing much smaller ezrin+ dots that had apparently not fused into lumina (arrows in Fig. 5A′). Moreover, immunolabeling for the tight junction marker, ZO-1, better evidenced coalescence of several apical domains in WT (arrowhead at Fig. 5B), and revealed perturbed polarization of cKO epithelial cells, with only short ZO-1+ stretches between two adjacent membranes (Fig. 5B and B′). We finally looked at defective polarization in cKO from the basolateral membrane perspective. While the key component of basement membranes, laminin, was readily labeled around all "rosettes" in WT, it was mainly restricted to the periphery of cKO thyroids (Fig. S7). Altogether, these data indicated that a severe decrease of endothelial cell density strongly impacted on the organization of thyroid epithelial cells into pre-follicular "rosettes", resulting in persistence of a multilayered cell mass with defective polarization and apical lumen formation.

At birth, the difference in glandular organization between control and cKO thyroids was even more dramatic. As expected, control thyroid epithelial cells, surrounded by a dense vascular network, formed large follicles, i.e. polarized epithelial monolayers with continuous ezrin labeling at the apical pole of several cell profiles, and laminin at each basal pole (Fig. 5C–E). In contrast, the overall epithelial organization of cKO at birth, when based on E-cadherin labeling alone, could not be distinguished from that at e15.5 (compare E-cadherin staining in Fig. 5A′ and C′): thyroid epithelial cells remained clustered as a mass with few interspersed endothelial cells. Ezrin+ structures were smaller and more abundant (Fig. 5C′–E′). Quantification of the size and the number of ezrin+ structures in three controls versus cKO glands at P0 confirmed this conclusion (Fig. 5F; mean size: 18 ± 30 vs $7 \pm 10\ \mu m^2$, $n = 436$ and 523, $p < 0.0001$ by the Kolmogorov–Smirnov test; number of: 19 ± 6 vs 44 ± 18 ezrin+ structures per section, $n = 10$ confocal sections, $p < 0.05$ by the ranked sign test).

These observations suggested that the defective organization of epithelial cells into follicular structures involved impairment of

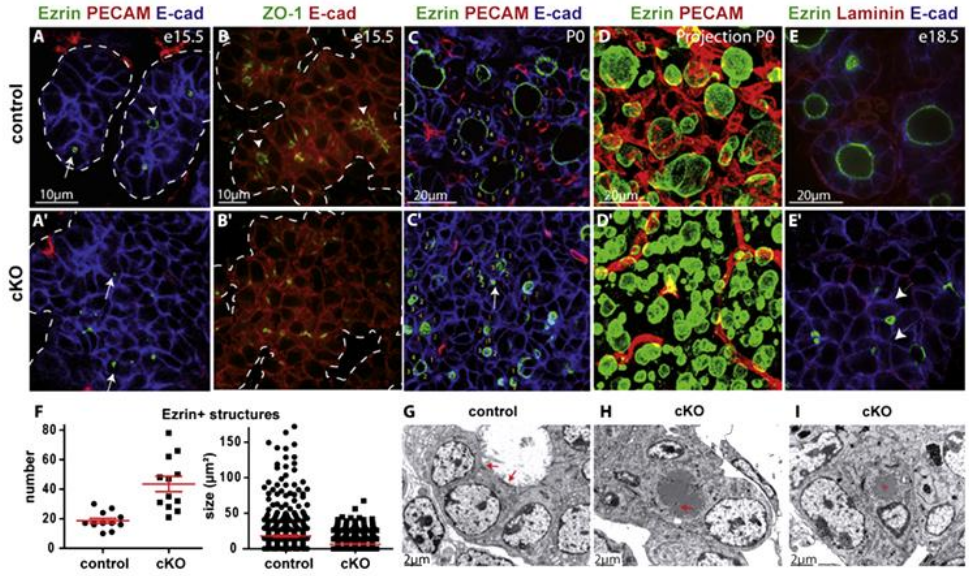

Fig. 5. In vivo reduction in vascular density impairs epithelial reorganization and follicle formation. Representative immunofluorescence views of control ((A)–(E)) and cKO ((A')—(E')) thyroid sections or full projections over 18.5 µm ((D), (D')). ((A)–(B)) At e15.5, control epithelial masses (E-cad+; dotted lines) have started to form pre-follicular structures or "rosettes". Concerted polarization of epithelial cells is also initiated, as demonstrated by pluricellular apical ezrin+ structures and ZO-1 belts (arrowheads in (A), (B)). In contrast, the epithelium of Vegfa cKO thyroids remains a mass of non-polarized cells with random small intracellular ezrin dots (arrows in A') and rare, exclusively bicellular ZO-1 staining (B'). ((C)–(E)) Around birth, control thyrocytes (E-cad+) are organized into follicles, where ezrin delineates well-defined apical lumina shared by 7 to 9 cells per profile (numbered in (C)), showing multiple contacts with blood capillaries (PECAM+). The enlarged size of closed lumina and the density of surrounding microvasculature are best appreciated by the full projection at (D). In cKO, thyrocytes are still clustered as a multilayered mass, wherein only a minority of cells have engaged into the formation of small ezrin+ structures, shared by 2 to at most 4 cells per profile (numbered in (C')). Other cells show intracellular ezrin dots (arrow in (C')), which mimick those seen at e15.5 in controls (arrow in (A)). ((D), (D')) 3D reconstruction of 50 confocal images evidences a higher number of smaller ezrin+ structures between fewer vessels in Vegfa cKO. ((E), (E')) Opposite localization of apical cellular (ezrin) and basal extracellular (laminin) markers in WT confirms full thyrocyte polarity in independent follicles. In cKO, epithelial cells (E-cad+) exhibit defective apico-basal polarization: cells displaying ezrin at one pole do not assemble laminin at the opposite pole, and vice versa (arrows in (E')). (F) Quantification of the number and size of ezrin+ structures at birth. As compared to controls, the number of ezrin+ profiles per section in cKO glands is twice higher but their mean size is twice smaller, exceptionally reaching 50 µm², as opposed to ~150 µm² in controls. ((G)–(I)) Transmission electron microscopy at e18.5. (G) A control follicle, composed of at least 5 polarized thyrocytes in this part of the section, surrounds a closed lumen (tight junctions at the upper part of the lateral membrane marked by arrows) into which numerous microvilli project. (H) In cKO thyroids, follicular structures are smaller due to fewer cells, displaying apical differentiation (tight junctions) and shared lumen with microvilli. (I) Some cKO cells exhibit apparently similar structures (red asterisk), yet entirely intracellular (no visible junction).

intracellular expansion and concerted coalescence of ezrin+ vesicles, normally allowing lumen expansion. Closer analysis of ezrin+ structures confirmed that lumina were shared by ~8 cell profiles per WT section (roughly 40/follicle) vs ~3 profiles (>10/follicle) in cKO (see numbers in panels C, C'). Moreover, intracellular ezrin+ vesicles were still observed in some cells of cKO thyroids at P0 (arrow in Fig. 5C'), but never in WT. To better visualize this difference, orthogonal views showed large ezrin+ lumina in the control, while in cKO newborns these structures appeared smaller or collapsed at light microscopic resolution (short arrows in Fig. S8).

However, transmission electron microscopy on e18.5 glands showed that the ezrin+ apical staining shared by ~3 cells in cKO (Fig. 5C') were actually small lumina with microvilli (Fig. 5H). Moreover, epithelial cells forming these small structures had developed tight junctions indicating that some Vegfa cKO epithelial cells were still competent for acquiring and developing an apical domain, yet they did not all do so (arrow in Fig. 5G and H). Projection of tight junctions into the lumen of the fewer smaller "rosettes" in cKO was a distinctive feature from WT follicles, where tight junctional belts were clearly positioned below the average level of the apical membrane. Despite the ability of these cells to acquire apical characteristics, their basal pole visualized by laminin staining was still abnormal, failing to continuously circumscribe "rosettes"/follicles (Fig. 5E and E'). Nevertheless, several cKO epithelial cells did not succeed to polarize, as demonstrated by the persistence of intracellular vesicles (asterisk in Fig. 5I) and the absence of tight junctions. In conclusion, the reduction in vascular density in VEGFA cKO thyroids impaired the general reorganization of the epithelial mass into monolayers by altering polarization, as evidenced by lack of defined basal pole and reduced coordinated assembly of apical pole (<4 cell profiles per shared lumen).

Thyroid development is reproduced in culture: bilobation, differentiation, polarization and vascularization

Arguably, a trivial explanation for the observations reported so far could be the lack of adequate supply of oxygen and nutrients. To rule out this explanation and to better understand how endothelial cells themselves impacted on the development of thyroid epithelial and C-cells, we set up an original ex vivo explant culture system of the thyroid. Based on our expertise of pancreatic explant culture, we dissected e12.5 embryos and isolated the

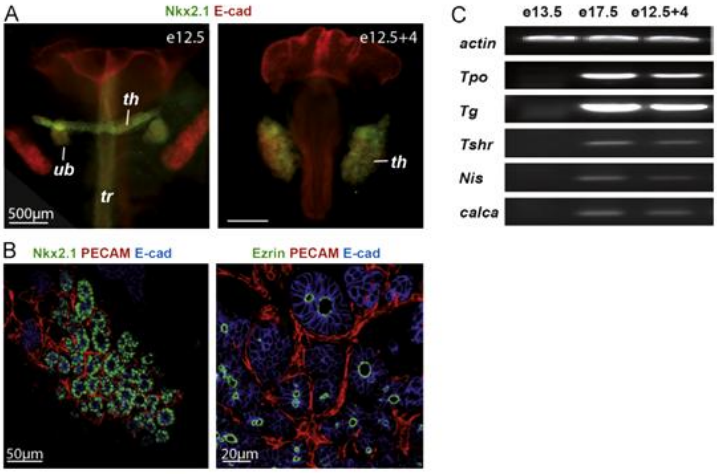

Fig. 6. Key steps of thyroid development are reproduced ex vivo: bilobation, vascularization, polarization and folliculogenesis, and dual endocrine differentiation. (A) Expansion and bilobation. Whole-mount immunolabeling of e12.5 thyroid explants before and after 4 days of culture. At e12.5, the thyroid midline anlage (th; E-cad+, Nkx2.1+) is positioned ventrally to the trachea (tr; E-cad+ only), while the ultimobranchial bodies (ub; E-cad+, Nkx2.1+) are lateral and caudal. After 4 days ex vivo, the thyroid midline anlage has migrated laterally and fused with the ultimobranchial bodies to form two lobes on each side of the trachea. (B) Vascularization, polarization and folliculogenesis. After 4 days ex vivo, almost all epithelial cells are polarized (ezrin+) and organized in follicular structures closely surrounded by a capillary network (PECAM +), despite lack of blood flow. Panel at left shows a frame selected from Supplementary Movie 3. (C) Dual endocrine differentiation. PCR profiling of differentiation markers in the cultured thyroid explants. After 4 days ex vivo (e12.5+4), expression of thyroperoxidase (Tpo), thyroglobulin (Tg), TSH receptor (Tshr), Na^+I^- symporter (Nis) and calcitonin a (calca), undetectable one day after culture onset (e13.5), was comparable to that observed in vivo (e17.5).

upper part of the trachea, where the thyroid primordium lies. At this stage, the thyroid primordium is composed of an elongated mass of non-polarized epithelial cells that has not yet fused with the ultimobranchial bodies (Figs. 1 and 6A). Such explants were placed on a filter at the interface between air (above the filter) and the medium (below the filter). After 24 h in culture, two thyroid lobes had formed on each side of the trachea and continued to expand ex vivo (up to 4 days; see Fig. S9). Whole-mount immunolabeling for Nkx2.1 after 4 days in culture confirmed the presence of two lobes, on each side of the trachea (Fig. 6A). Macroscopically, this ex vivo culture system thus reproduced in vivo morphogenic movement and expansion of the thyroid anlage, despite dissociation from the circulation and isolation from all distant endocrine or nervous signals.

Confocal analysis of the thyroid lobes at the end of the culture showed that most thyrocytes nuclei, labeled for Nkx2.1, were closely apposed to endothelial structures, and circumferentially organized around a hypothetical center (Fig. 6B). Moreover, series of confocal pictures along the z axis revealed that the epithelial cells were organized in "3D spheres", surrounded by a dense capillary network (see Supplementary Movie 3). Triple immunolabeling for the (sub)apical marker ezrin, E-cadherin and PECAM, demonstrated that thyrocytes had acquired full polarization, in the absence of any blood supply, with the (basal) pole close to PECAM + blood vessels, and the opposite (apical) pole concentrating the ezrin signal and delineating a lumen (Fig. 6B).

Supplementary material related to this article can be found online at http://dx.doi.org/10.1016/j.ydbio.2013.47.002.

RT-PCR further confirmed that explant culture allowed for undistinguishable differentiation of thyrocytes and C-cells as in vivo. As compared to undifferentiated e13.5 thyroids, and similarly to differentiated e17.5 thyroids, e12.5 explants cultured for 4 days showed induction of all tested thyrocytes differentiation markers Tpo, Tg, Tshr, and Nis (Fig. 6C). Moreover, induction of calcitonin expression in the explants indicated that C-cells derived from ultimobranchial bodies had not only migrated into, and scattered within, the thyroid primordium, but also engaged their differentiation program during culture (Fig. 6C). Taken together, these results validated our culture system, which faithfully recapitulated all key steps of in vivo thyroid development, thus providing an adequate and powerful model to directly test the role of endothelial cells during thyroid development.

Pharmacological ablation of endothelial cells in explants reproduces the in vivo effects of VEGFA cKO on epithelial reorganization and follicle formation

To test the role of endothelial cells on thyroid development, we used the specific inhibitor of VEGFR2/Flk-1 tyrosine kinase, SU5416. Addition of SU5416 to the culture medium of thyroid explants removed essentially all PECAM+ endothelial cells, as shown in the three-dimensional reconstruction on 29-µm thickness (red in Fig. 7A). As expected from the expression pattern of VEGFR2 (Fig. 2B), the inhibitor specifically affected endothelial cells. Indeed, thyroid explants cultured for 16 h with SU5416 showed extensive apoptosis restricted to endothelial cells, as revealed by co-immunolabeling for active caspase-3 and PECAM Fig. S10). This treatment did not affect epithelial Vegfa expression in the thyroid buds, as measured by RT-qPCR (90% ± 7% of control explants; $n=4$). Visualization of the (sub)apical marker ezrin in 3D reconstructions revealed large spheres in the untreated explants but smaller structures in treated ones (green in Fig. 7A), exactly as in cKO embryos (compare with Fig. 5). Double immunofluorescence for E-cadherin and ezrin revealed that reorganization of the

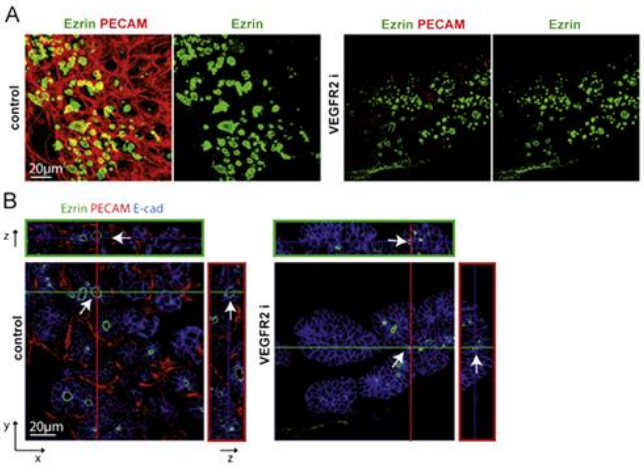

Fig. 7. *Ex vivo* ablation of endothelial cells impairs follicle formation. Whole-mount immunolabeling of control or treated explants (VEGFR2 inhibitor SU5416). (A) 3D reconstruction from a Z-stack of 79 confocal images (every 0.37 µm). The dense endothelial cells network (PECAM+, red) is absent when explants are cultured in the presence of the VEGFR2 inhibitor (VEGFR2i). Structures labeled by ezrin are much smaller. (B) Corresponding orthogonal views better show that VEGFR2i causes maintenance of multilayering and the lack of large lumina, abundant in untreated controls, with ezrin mostly limited to intracellular dots (arrows). Upper rectangles boxed in green correspond to XZ reconstructions from positions indicated by horizontal green lines in the central XY squares. Right rectangles boxed in red correspond to to YZ reconstructions at the red vertical red lines. See also Fig. S7 in the supplementary material.

epithelial mass was strongly impaired by SU5416: epithelial cells remained clustered as compact masses failing to organize into polarized monolayers surrounding shared lumina. This was evidenced by ezrin-labeled structures, which remained as intracellular dots or formed smaller lumina shared by much fewer cells (arrows in Fig. 7B). Altogether, these data showed that in vitro ablation of endothelial cells reproduced the morphogenic defects of cKO VEGFA in vivo, thus confirming the importance of VEGFA–VEGFR2 interaction in thyroid development and demonstrating the direct instructive role of endothelial cells, independently of blood supply.

Exogenous endothelial cells rescue folliculogenesis and calcitonin production in vitro

As a complementary test for a direct role of endothelial cells, we attempted to rescue the two key defects observed in the Vegfa cKO and SU5416-treated explants – follicular organization and calcitonin expression – by addition of exogenous embryonic endothelial progenitor cells (eEPCs). Two mechanisms were addressed: (i) direct contact or proximity of endothelial cells; and (ii) release of endothelial-derived factor(s). To this end, thyroid explants were treated with SU5416 for 40 h to eliminate all endogenous endothelial cells, or left untreated (control). eEPCs stably expressing the tomato fluorescent protein were then added to the SU-treated explants on the filter and co-culture was extended for another 56 h. To test for contact-independent, endothelial-derived secreted factor(s), we added instead culture medium conditioned by eEPCs for 16 h and concentrated 10 times. At the end of the culture (day 4), Vegfr2 expression level was measured by RT-qPCR (Fig. 8A) and ablation of endothelial cells in SU5416-treated explants was confirmed by PECAM immunofluorescence (Fig. 8C). Since Vegfr2 is not expressed by eEPCs, we measured instead the expression of Tie2, a known tyrosine kinase receptor of these cells. Tie2 expression level was similar in control (untreated explants) and SU5416-treated explants supplemented with eEPCs (Fig. 8A). Tomato fluorescence was used to visualize the eEPCs during and at the end of the culture (Fig. S11).

We thus tested if – and to what extent – exogenous endothelial progenitor cells or their conditioned media could faithfully rescue follicle formation. Macroscopic and confocal analyses revealed that both treatments were effective to induce follicle formation (Fig. 8C and Fig. S11, compare with Fig. S9). In VEGFR2i-treated explants cultured in direct contact with eEPCs, the thyroid epithelium formed not only large follicular structures, but these were even larger than in control explants. Combined ezrin, laminin and E-cadherin immunolabeling showed that eEPCs had restored the ability of epithelial cells to organize as monolayers and to acquire apico-basal polarity, although less regularly than in controls (Fig. 8C). Interestingly, no correlation was observed between the localization of these structures in the thyroid lobes and the proximity with Tomato-labeled eEPCs (see. Fig. S11), suggesting that direct epithelial:endothelial contact was not required to induce follicle formation. In line with this observation, eEPCs-conditioned medium (c.m.) was also able to rescue the formation of follicular structures composed of polarized epithelial cells in thyroid lobes totally devoid of endothelial cells (Fig. 8C). Again, c.m.-induced folliculogenesis was exacerbated as compared to control explants, pointing to a dosage effect or to the need of a proper balance of agonistic and antagonistic factors. Altogether, these experiments indicated that thyroid follicle formation requires endothelial-derived molecule(s), rather than epithelial: endothelial contacts.

As a preliminary characterization of the "folliculogenic" activity present in the medium conditioned by the eEPCs, we first tested if it was dependent on proteins, based on inactivation by boiling and sensitivity to proteolysis. The concentrated c.m. was thus boiled for 30 min or left on ice (as positive control of activity). Alternatively, concentrated c.m. was incubated with pronase, a powerful proteases cocktail, or with PBS (as a control) at 37 C for 2 h. Biological activity was then tested on VEGFR2i-treated explants by

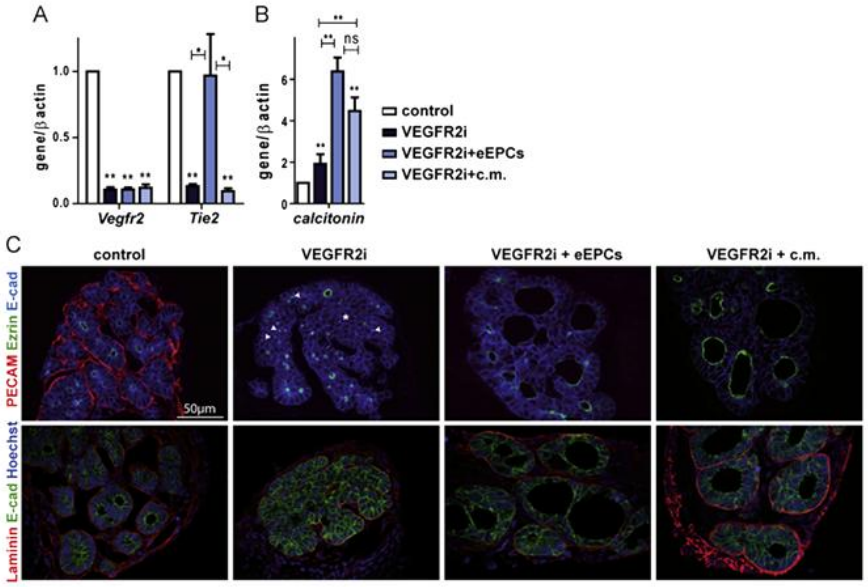

Fig. 8. Induction of follicle formation and calcitonin expression, in thyroid explants with endothelial cell ablation, by exogenous factor(s) derived from embryonic endothelial progenitor cell (EPC). E12.5 thyroid explants were first treated with the VEGFR2 inhibitor (VEGFR2i) for 40 h to ablate endogenous endothelial cells, washed, then incubated for 2 days with either exogenous endothelial progenitor cells (EPCs), or their concentrated conditioned media (c.m.). ((A), (B)) RT-qPCR analysis. (A) Treatment of e12.5 thyroid explants with VEGFR2i causes a strong reduction in Tie2 and Vegfr2 expression, two endothelial markers. Subsequent addition of EPCs restores Tie2 but not Vegfr2 expression. (B) Calcitonin expression is enhanced by EPCs or their conditioned medium. (C) Immunolabeling. In untreated control explants, epithelial cells (E-cad+) are polarized (apical ezrin, upper row; basal laminin, lower row) and organized in follicles surrounded by a microvascular network (PECAM+). VEGFR2i ablates endothelial cells, and prevents thyrocyte polarization (asterisk on multilayered mass) and lumen coalescence (arrowheads). Subsequent incubation of VEGFR2i-treated explants with EPCs or their c.m. accelerates enlargement of polarized follicles as compared to untreated controls.

morphological changes in thyroid lobes, as a semi-quantitative assay. Both treatments strongly decreased (if not abrogated) the folliculogenic activity (Fig. S12A), indicating the proteinaceous nature of the folliculogenic factor(s). We next determined by gel filtration the corrersponding molecular weight range. To this aim, concentrated c.m. were resolved by a calibrated Superdex S200 column. Two well-separated fractions displayed a folliculogenic activity: one at very low-molecular weight, around 6 kDa, and another one at high-molecular weight (fraction 2: 540–180 kDa) (Fig. S12B). As in another experiment, fraction 1 (1600-540) contained as much activity as fraction 2, the active factor could be larger than 500 kDa. In addition, high-speed ultracentrifugation of the c.m. disclosed partial activity in both soluble and sedimentable material; their combination restored initial potency (data not shown). These data suggest several possibilities on the nature of the "folliculogenic" factor(s) produced by the endothelial progenitor cells: (i) two different proteins (a very small and a very large one); (ii) a single protein that can exist as a monomer or associate onto a large complex; (iii) and either form adsorbed onto sedimentable particles. Further work is clearly needed to clarify this issue.

Since VEGFA cKO causing 90% depletion of endothelial cells was associated with a 50% decrease in calcitonin expression, we next tested if calcitonin expression was also altered in SU5416-treated explants and could be rescued by eEPCs or their conditioned medium. Surprisingly, normalized calcitonin expression level was increased two-fold in explants upon SU5416-treatment. As compared to SU5416-treated explants, addition of eEPCs or their conditioned medium was sufficient to induce a 2-to-3-fold increase in calcitonin expression (Fig. 8B). Altogether, these data indicated that during thyroid development, endothelial cells also promote calcitonin expression by C-cells, by a contact-independent, paracrine mechanism.

Discussion

In the present work, we first show that the midline thyroid anlage initially expands from the endoderm as a mass of non-polarized epithelial cells, surrounded by endothelial cells. As these progressively invade the mass, epithelial cells reorganize into monolayers that polarize into follicles. Exuberant development of endothelial cells showing intimate contacts with epithelial cells, combined with strong expression of Vegfa in epithelial cells and Vegfr2 in endothelial cells, reflect coordinated reciprocal interactions. Specific inactivation of floxed Vegfa alleles in the thyroid epithelium, decreasing endothelial cells density by ~90%, impairs both follicles formation and C-cells differentiation. In an original *ex vivo* system of thyroid explants that faithfully recapitulates in vivo development, endothelial cells ablation by the VEGFR2 inhibitor SU5416 mimicks the effects of cKO by impairing follicular differentiation. Conversely, co-culture of endothelial-depleted explants with embryonic endothelial progenitor cells (eEPCs), or their conditioned medium, exacerbates follicular reorganization

and C-cells differentiation. Altogether, these data suggest that reciprocal paracrine interactions between epithelial (VEGF-A) and endothelial cells – via still unknown factor(s) - drive formation of follicles and differentiation of C-cell progenitors.

Origin of the cross-talk: VEGFA expression and endothelial response. The developing thyroid gland shows the highest Vegfa expression in the embryo, in line with its high vascularization at the adult stage. Whether high Vegfa expression is induced by low oxygenation via HIF, or via HIF-independent signals such as polarization or thyroid-specific transcription factors, remains an open question. Three mechanisms can be envisaged. First, strong hypoxia within the epithelial mass could induce accumulation of Hypoxia-induced factor-1 (HIF1A), known to activate the expression of Vegfa (Fong, 2009). However, this explanation does not account for the low Vegfa expression in the submandibular buds (Fig. S3). Second, when breast epithelial cells cultured in 3D matrices form disorganized structures, they express high levels of Vegfa; conversely, restoration of polarity decreases Vegfa expression, thus their ability to recruit endothelial cells. In this cellular model, these effects depended neither on HIF1 expression level nor on its activity (Chen et al., 2009). Conceivably, high Vegfa expression in the thyroid primordium could simply be linked to the lack of organization or polarity in the thyroid epithelial mass. However, this is unlikely to account for in vivo observations reported here, since Vegfa level actually *increased* during polarization. Third, Vegfa expression could be autonomously driven by thyroid-specific transcription factors. A good candidate is Pax8 whose expression pattern, restricted to the thyroid and kidney, correlates with that of Vegfa (Fig. 2B). Whatever the mechanism responsible for Vegfa expression, thyroid-specific inactivation of Vegfa causes a dramatic reduction in vascular density. We conclude that, throughout its development, the thyroid epithelium controls the recruitment, invasion and expansion of endothelial cells via the secretion of VEGF-A (Fig. 9). The reciprocal role of endothelial cells on epithelial differentiation was evidenced both in vivo, using Vegfa cKO, and in vitro (thyroid explants) by loss-of-function (full endothelial ablation by SU5416) and gain-of-function (exacerbated lumen formation in ablated explants by exogenous eEPCs or their conditioned medium).

Coordination between thyrocytes and C-cells. The preserved migration and abundance of C-cells in cKO thyroids is remarkable, even though calcitonin expression level was decreased by 50% in newborns. Paracrine mechanism(s), originating from epithelial or endothelial cells with which they are closely intermingled must regulate calcitonin expression. We cannot discriminate between the two possibilities, as follicles are not formed and endothelial cells are absent in the Vegfa cKO. A recent study suggests that Ephrin signaling from the follicular cells is important for C-cells generation (Andersson et al., 2011).

Paracrine signals control the thyrocyte pool expansion. A previous report noted that proliferating cells are mainly found at the periphery of e15.5 thyroid bud, but scattered throughout the gland at e17.5 (Fagman et al., 2006). We confirmed this observation in WT thyroid, and provide an explanation in Vegfa cKO. Upon conditional depletion of endothelial cells, proliferation occurred normally at the periphery of thyroid masses at e15.5, and so remained at e17.5, with a two-fold reduction in the total number of proliferating cells at that stage. The restricted peripheral localization of proliferating cells in the cKO thyroids at e17.5 implies that normal epithelial cell proliferation depends on environmental signals, from the adjacent mesenchymal or endothelial cells. Defective epithelial reorganization of the compact mass in cKO thyroids prevented to form individualized "rosettes" and growing follicles closely surrounded by endothelial cells, could only expose peripheral cells to this proliferating signal. The identity and source of this signal remains to be discovered. Good candidates could be mesenchymal FGFs, found to be important for thyroid development (Revest et al., 2001; Ohuchi et al., 2000). Moreover, in the pancreas, endothelial cells have been shown to sustain mesenchymal survival and production of FGF10, required for epithelial proliferation (Jacquemin et al., 2006). Likewise, we propose that in the thyroid, endothelial cells are required to

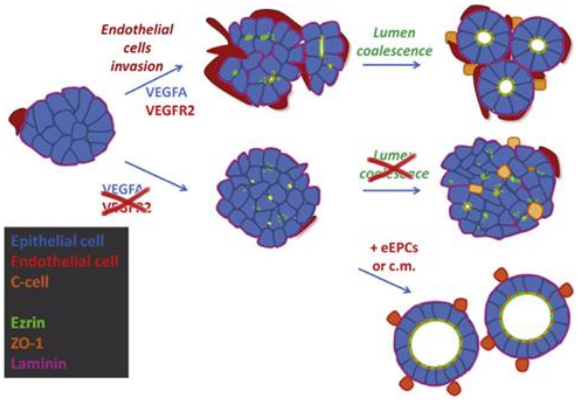

Fig. 9. A working model: role of endothelial cells in thyroid follicle formation and C-cells differentiation. VEGFA released by thyroid epithelial cells (blue) triggers VEGFR2+ endothelial cells (red) to invade the epithelial mass. Reorganization of the mass goes along with the appearance of ezrin+ structures (green) that coalesce to form early lumina. Follicles, i.e. monolayers of polarized epithelial cells, with ezrin (green) at the apical pole and laminin (purple) at the basal pole, are thus formed and remain surrounded by a dense microvascular network. C-cells (orange) are scattered between follicles. In the absence of Vegfa expression (in vivo cKO) or VEGFR2 activity (*ex vivo* inhibition), endothelial cells density is reduced. Epithelial cells remain as a multilayered mass and cannot efficiently polarize, thus harboring more numerous smaller ezrin+ structures that fail to coalesce. In cKO, C-cells are still scattered within the epithelial mass but express less calcitonin (light orange). Conversely, when explants with ablated endogenous endothelial cells are rescued by eEPCs or their conditioned medium (c.m.), folliculogenesis is accelerated and calcitonin expression is enhanced (dark orange).

promote the reorganization of the epithelial cell mass and thereby allow contact of epithelial cells with mesenchymal cells.

Reorganization defect. Thyroid buds in cKO newborns or explants with ablation of endothelial cells by SU5416 remained as a compact mass where epithelial cells displayed impaired polarization. To monitor the formation of an apical domain, we used ezrin immunolabeling. In control thyroids, ezrin-labeled structures were observed intracellularly up to e15.5, then fused coordinately to form apical lumina shared by numerous well-polarized epithelial cells (~8–9 in a section, thus ~50 per lumen), showing basal lamina indicative of a basolateral plasma membrane domain. When endothelial cells were depleted (cKO) or absent (SU5416-treated explants), ezrin+ structures were much smaller and remained frequently intracellular, and cells lacked laminin staining at their opposite pole. Although these cells could still form "rosettes", the lumen was never shared by more than 4 epithelial cell profiles. These observations shed light on the molecular and cellular processes of follicles formation during thyroid development. We propose that folliculogenesis starts by the reorganization of the epithelial cells mass. At this stage, only peripheral cells are in contact with the extracellular matrix and epithelial cells are not polarized. Some epithelial cells display intracellular vesicles surrounded by ezrin. Reorganization of the cellular mass generates prefollicular structures, or "rosettes", in which ~8 epithelial cells have clustered, in a concerted and oriented way, so that ezrin+ vesicles assume a subapical position, i.e. have become the subapical compartment, a well-known intermediate during epithelial polarization (Hoekstra et al., 2004). Coordinated fusion then generates a lumen, which expands as follicles mature into independent angio-follicular units and organize a tight basal lamina.

These in vivo processes are thus remarkably similar to those reported using 3D-cultures of MDCK epithelial cells (Madin–Darby canine kidney) (Bryant and Mostov, 2008). When cultured in matrigel, individual MDCK cells gather and assemble into polarized spherical monolayer surrounding a central lumen, i.e. follicular-like structure. Before lumen formation, intracellular vesicles containing the apical traffic regulators Rab8, Rab11 and Cdc42, as well as proteins of the exocyst complex, appear in the aggregated cells. These vesicles converge towards the cell pole opposite to the extracellular matrix. Oriented and concerted fusion of the vesicles generates a central lumen (Bryant et al., 2010). Knocked-down or dominant-negative Rab8, Rab11 or exocyst components prevent the formation of the central lumen. Instead, MDCK cells display small multi-lumina shared by few cells of the aggregate (Bryant et al., 2010). Besides the MDCK molecular machineries involved in lumen generation, initiating signals from matrigel have been pinpointed (Yu et al., 2005). Whether the same sets of molecules are involved in thyroid follicle formation, as proposed in our model presented at Fig. 9, is now accessible to experimentation. In a remarkable recent paper, the group of Costagliola recently showed that transient expression of NKX2.1 and Pax8 in ES cells, followed by TSH treatment, stimulated non only their thyroid differentiation but also their organization into follicles (Antonica et al., 2012). To achieve tridimensional organization in follicles, the authors cultured ES cells in matrigel, further underlining initiating or facilitating signals from the extracellular matrix. Although the authors looked for endothelial cells in their culture and found none, based on PECAM labelling, this observation does not rule out the presence of endothelial progenitors. Indeed, we here show that, in the absence of PECAM+ endothelial cells, eEPCs, which are PECAM-, VEGFR2- and Tie-2+ (Fig. 8), induced follicle formation. Alternatively, growth factors present in the matrigel could promote follicle formation in conjunction with TSH.

Validity of thyroid explants. Based on our expertise on pancreas and submandibular glands development (Hick et al., 2009), we developed and extensively used in this study an original *ex vivo* thyroid explants culture system that faithfully reproduces in vivo thyroid development: bilobation, endothelial cells invasion, remodeling of epithelial mass into fully differentiated follicles, as well as C-cells attraction from ultimobranchial bodies and differentiation into calcitonin-producing cells. We propose that, albeit technically demanding, this innovative culture system can be a powerful tool to study thyroid development. So far, most *ex vivo* studies have used adult thyroid-derived cells, grown either on 2D plastic dishes or in 3D matrices. In these conditions, differentiated follicular cells either remain as follicles or reacquire a three-dimensional organization (Toda et al., 2001; Eggo et al., 2003). However, pure epithelial cell cultures ignore interactions with extracellular matrix, cytokines, growth factors and other cell types such as the endothelial or nerves cells. Moreover, commercial matrices contain uncontrolled concentrations of growth factors that may interfere with the process of follicle formation.

To provide instead a comprehensive set of actors for in vitro development studies, we microdissected a fragment of tissue localized rostral to the pharyngeal arch arteries, and containing the trachea, but not the esophagus. During culture, the median anlage migrates laterally and fuses with the ultimobranchial bodies to generate the two lobes connected by a narrow isthmus. Epithelial cells proliferate, reorganize from a mass into polarized monolayers and differentiate into thyrocytes and C-cells, depending on their origin. Importantly, endothelial cells in the microdissected tissue proliferate, migrate into the thyroid lobes, and closely associate with the epithelial cells as in vivo, without any need for blood supply—nor interference by circulating factors.

We further showed that this culture system is amenable to loss- and gain-of-function experiments via the addition of specific inhibitors, blocking antibodies, growth factors, cytokines, or even cells. To address the contribution of endothelial cells by loss-of-function, these were ablated by treating thyroid explants with a VEGFR2 inhibitor (apoptosis was detected within 8 h). For gain-of-function, ablated explants were washed and co-cultured with embryonic endothelial progenitor cells (eEPCs). The defect of epithelial reorganization caused by the absence of blood vessels was over-rescued by the addition of eEPCs to the explants, indicating a dosage effect or the lack of appropriate antagonist. Interestingly, rescued follicle formation *ex vivo* did not require contact since eEPCs-conditioned media were as effective as eEPCs to promote epithelial follicle formation and calcitonin expression.

In conclusion, our work demonstrates that reciprocal interactions between epithelial and endothelial cells govern thyroid gland development. Epithelial-derived VEGF-A is necessary to recruit and allow expansion of a dense endothelial network in the thyroid. In turn, endothelial cells are necessary for follicular cells reorganization into follicles and for the differentiation of the C-cells. We now focus on the identification of the instructive factor(s) released by endothelial cells.

Acknowledgements

The authors thank E. Marbaix for expert analysis of histological staining, F. Lemaigre for critical comments and continuous support and M. Busslinger for Pax8-cre mouse strain. The work was supported by grants from the Université catholique de Louvain (Actions de recherche concertées), the Fund for Scientific Medical Research (Belgium) and the Interuniversity Attraction Poles Program-Belgian Science Policy (Belgium). A.-C.H. held a fellowship from the Fonds pour la formation à la Recherche dans l' Industrie et dans l'Agriculture (Belgium), CEP, PS and JFC are senior research associates and OF is research director of the F.R.S.—FNRS (Belgium). The funders had no role in study design, data collection and analysis, decision to publish, or preparation of the manuscript.

Appendix A. Supporting information

Supplementary data associated with this article can be found in the online version at http://dx.doi.org/10.1016/j.ydbio.2013.04.022.

References

Alt, B., Elsalini, O.A., Schrumpf, P., Haufs, N., Lawson, N.D., Schwabe, G.C., Mundlos, S., Gruters, A., Krude, H., Rohr, K.B., 2006. Arteries define the position of the thyroid gland during its developmental relocalisation. Development 133, 3797–3804.

Andersson, L., Westerlund, J., Liang, S., Carlsson, T., Amendola, E., Fagman, H., Nilsson, M., 2011. Role of EphA4 receptor signaling in thyroid development: regulation of folliculogenesis and propagation of the C-cell lineage. Endocrinology 152, 1154–1164.

Antonica, F., Kasprzyk, D.F., Opitz, R., Iacovino, M., Liao, X.-H., Dumitrescu, A.M., Refetoff, S., Peremans, K., Manto, M., Kyba, M., Costagliola, S., 2012. Generation of functional thyroid from embryonic stem cells. Nature 491, 66–71.

Bouchard, M., Souabni, A., Busslinger, M., 2004. Tissue-specific expression of cre recombinase from the Pax8 locus. Genesis 38, 105–109.

Bryant, D.M., Datta, A., Rodriguez-Fraticelli, A.E., Peranen, J., Martin-Belmonte, F., Mostov, K.E., 2010. A molecular network for de novo generation of the apical surface and lumen. Nat. Cell Biol. 12, 1035–1045.

Bryant, D.M., Mostov, K.E., 2008. From cells to organs: building polarized tissue. Nat. Rev. Mol. Cell Biol. 9, 887–901.

Chen, A., Cuevas, I., Kenny, P.A., Miyake, H., Mace, K., Ghajar, C., Boudreau, A., Bissell, M.J., Boudreau, N., 2009. Endothelial cell migration and vascular endothelial growth factor expression are the result of loss of breast tissue polarity. Cancer Res. 69, 6721–6729.

Cleaver, O., Dor, Y., 2012. Vascular instruction of pancreas development. Development 139, 2833–2843.

Cleaver, O., Melton, D.A., 2003. Endothelial signaling during development. Nat. Med. 9, 661–668.

De Felice, M., Di Lauro, R., 2004. Thyroid development and its disorders: genetics and molecular mechanisms. Endocr. Rev. 25, 722–746.

Dunn, J.T., Dunn, A.D., 2001. Update on intrathyroidal iodine metabolism. Thyroid 11, 407–414.

Eggo, M.C., Quiney, V.M., Campbell, S., 2003. Local factors regulating growth and function of human thyroid cells in vitro and in vivo. Mol. Cell Endocrinol. 213, 47–58.

Eremina, V., Sood, M., Haigh, J., Nagy, A., Lajoie, G., Ferrara, N., Gerber, H.P., Kikkawa, Y., Miner, J.H., Quaggin, S.E., 2003. Glomerular-specific alterations of VEGF-A expression lead to distinct congenital and acquired renal diseases. J. Clin. Invest. 111, 707–716.

Fagman, H., Andersson, L., Nilsson, M., 2006. The developing mouse thyroid: embryonic vessel contacts and parenchymal growth pattern during specification, budding, migration, and lobulation. Dev. Dyn. 235, 444–455.

Fagman, H., Grande, M., Gritli-Linde, A., Nilsson, M., 2004. Genetic deletion of sonic hedgehog causes hemiagenesis and ectopic development of the thyroid in mouse. Am. J. Pathol. 164, 1865–1872.

Fagman, H., Nilsson, M., 2009. Morphogenesis of the thyroid gland. Mol. Cell Endocrinol. 323, 35–54.

Fong, G.H., 2009. Regulation of angiogenesis by oxygen sensing mechanisms. J. Mol. Med. (Berl.) 87, 549–560.

Frezzetti, D., Reale, C., Cali, G., Nitsch, L., Fagman, H., Nilsson, O., Scarfo, M., De Vita, G., Di Lauro, R., 2012. The microRNA-processing enzyme dicer is essential for thyroid function. Plos One 6, e27648.

Gaide Chevronnay, H.P., Cornet, P.B., Delvaux, D., Lemoine, P., Courtoy, P.J., Henriet, P., Marbaix, E., 2008. Opposite regulation of transforming growth factors-beta2 and -beta3 expression in the human endometrium. Endocrinology 149, 1015–1025.

Gerard, A.C., Many, M.C., Daumerie, C., Costagliola, S., Miot, F., DeVijlder, J.J., Colin, I. M., Denef, J.F., 2002. Structural changes in the angiofollicular units between active and hypofunctioning follicles align with differences in the epithelial expression of newly discovered proteins involved in iodine transport and organification. J. Clin. Endocrinol. Metab. 87, 1291–1299.

Gerber, H.P., Hillan, K.J., Ryan, A.M., Kowalski, J., Keller, G.A., Rangell, L., Wright, B.D., Radtke, F., Aguet, M., Ferrara, N., 1999. VEGF is required for growth and survival in neonatal mice. Development 126, 1149–1159.

Hick, A.C., van Eyll, J.M., Cordi, S., Forez, C., Passante, L., Kohara, H., Nagasawa, T., Vanderhaeghen, P., Courtoy, P.J., Rousseau, G.G., et al., 2009. Mechanism of primitive duct formation in the pancreas and submandibular glands: a role for SDF-1. BMC. Dev. Biol. 9, 66.

Hoekstra, D., Tyteca, D., van, IJzendoorn S.C., 2004. The subapical compartment: a traffic center in membrane polarity development. J. Cell Sci. 117, 2183–2192.

Jacquemin, P., Pierreux, C.E., Fierens, S., van Eyll, J.M., Lemaigre, F.P., Rousseau, G.G., 2003. Cloning and embryonic expression pattern of the mouse Onecut transcription factor OC-2. Gene Expr. Patterns 3, 639–644.

Jacquemin, P., Yoshitomi, H., Kashima, Y., Rousseau, G.G., Lemaigre, F.P., Zaret, K.S., 2006. An endothelial-mesenchymal relay pathway regulates early phases of pancreas development. Dev. Biol. 290, 189–199.

Kameda, Y., Nishimaki, T., Chisaka, O., Iseki, S., Sucov, H.M., 2007. Expression of the epithelial marker E-cadherin by thyroid C cells and their precursors during murine development. J. Histochem. Cytochem. 55, 1075–1088.

Kusakabe, T., Kawaguchi, A., Hoshi, N., Kawaguchi, R., Hoshi, S., Kimura, S., 2005. Thyroid-specific enhancer-binding protein/NKX2.1 is required for the maintenance of ordered architecture and function of the differentiated thyroid. Mol. Endocrinol. 20, 1796–1809.

Lammert, E., Cleaver, O., Melton, D., 2001. Induction of pancreatic differentiation by signals from blood vessels. Science 294, 564–567.

Lania, G., Zhang, Z., Huynh, T., Caprio, C., Moon, A.M., Vitelli, F., Baldini, A., 2009. Early thyroid development requires a Tbx1-Fgf8 pathway. Dev. Biol. 328, 109–117.

Lazarus, A., Del-Moral, P.M., Ilovich, O., Mishani, E., Warburton, D., Keshet, E., 2011. A perfusion-independent role of blood vessels in determining branching stereotypy of lung airways. Development 138, 2359–2368.

Liao, J., Kochilas, L., Nowotschin, S., Arnold, J.S., Aggarwal, V.S., Epstein, J.A., Brown, M.C., Adams, J., Morrow, B.E., 2004. Full spectrum of malformations in velo-cardio-facial syndrome/DiGeorge syndrome mouse models by altering Tbx1 dosage. Hum. Mol. Genet. 13, 1577–1585.

Morreale de Escobar, G., Jesus Obregon, M., Escobar del Rey, F., 2000. Is neuropsychological development related to maternal hypothyroidism or to maternal hypothyroxinemia. J. Clin. Endocrinol. Metab. 85, 3975–3987.

Ohuchi, H., Hori, Y., Yamasaki, M., Harada, H., Sekine, K., Kato, S., Itoh, N., 2000. FGF10 acts as a major ligand for FGF receptor 2 IIIb in mouse multi-organ development. Biochem. Biophys. Res. Commun. 277, 643–649.

Olivieri, A., Stazi, M.A., Mastroiacovo, P., Fazzini, C., Medda, E., Spagnolo, A., De Angelis, S., Grandolfo, M.E., Taruscio, D., Cordeddu, V., et al., 2002. A population-based study on the frequency of additional congenital malformations in infants with congenital hypothyroidism: data from the Italian Registry for Congenital Hypothyroidism (1991–1998). J. Clin. Endocrinol. Metab. 87, 557–562.

Pierreux, C.E., Cordi, S., Hick, A.C., Achouri, Y., Ruiz de Almodovar, C., Prevot, P.P., Courtoy, P.J., Carmeliet, P., Lemaigre, F.P., 2010. Epithelial: endothelial cross-talk regulates exocrine differentiation in developing pancreas. Dev. Biol. 347, 216–227.

Pierreux, C.E., Poll, A.V., Kemp, C.R., Clotman, F., Maestro, M.A., Cordi, S., Ferrer, J., Leyns, L., Rousseau, G.G., Lemaigre, F.P., 2006. The transcription factor hepatocyte nuclear factor-6 controls the development of pancreatic ducts in the mouse. Gastroenterology 130, 532–541.

Revest, J.M., Suniara, R.K., Kerr, K., Owen, J.J., Dickson, C., 2001. Development of the thymus requires signaling through the fibroblast growth factor receptor R2-IIIb. J. Immunol. 167, 1954–1961.

Rodriguez, W., Jin, L., Janssens, V., Pierreux, C., Hick, A.C., Urizar, E., Costagliola, S., 2012. Deletion of the RNAseIII enzyme dicer in thyroid follicular cells causes hypothyroidism with signs of neoplastic alterations. PLoS One 6, e29929.

Sbaa, E., Dewever, J., Martinive, P., Bouzin, C., Frerart, F., Balligand, J.L., Dessy, C., Feron, O., 2006. Caveolin plays a central role in endothelial progenitor cell mobilization and homing in SDF-1-driven postischemic vasculogenesis. Circ. Res. 98, 1219–1227.

Silberschmidt, D., Rodriguez-Mallon, A., Mithboakar, P., Cali, G., Amendola, E., Sanges, R., Zannini, M., Scarfo, M., De Luca, P., Nitsch, L., Di Lauro, R., De Felice, M., 2011. In vivo role of different domains and of phosphorylation in the transcription factor Nkx2-1. BMC. Dev. Biol. 11, 9.

Taulli, R., Accornero, P., Follenzi, A., Mangano, T., Morotti, A., Scuoppo, C., Forni, P.E., Bersani, F., Crepaldi, T., Chiarle, R., et al., 2005. RNAi technology and lentiviral delivery as a powerful tool to suppress Tpr-Met-mediated tumorigenesis. Cancer Gene Ther. 12, 456–463.

Toda, S., Koike, N., Sugihara, H., 2001. Cellular integration of thyrocytes and thyroid folliculogenesis: a perspective for thyroid tissue regeneration and engineering. Endocr. J. 48, 407–425.

Toublanc, J.E., 1992. Comparison of epidemiological data on congenital hypothyroidism in Europe with those of other parts in the world. Horm. Res. 38, 230–235.

van Eyll, J.M., Pierreux, C.E., Lemaigre, F.P., Rousseau, G.G., 2004. Shh-dependent differentiation of intestinal tissue from embryonic pancreas by activin A. J. Cell Sci. 117, 2077–2086.

Yu, W., Datta, A., Leroy, P., O'Brien, L.E., Mak, G., Jou, T.S., Matlin, K.S., Mostov, K.E., Zegers, M.M., 2005. Beta1-integrin orients epithelial polarity via Rac1 and laminin. Mol. Biol. Cell 16, 433–445.

Supplementary figures

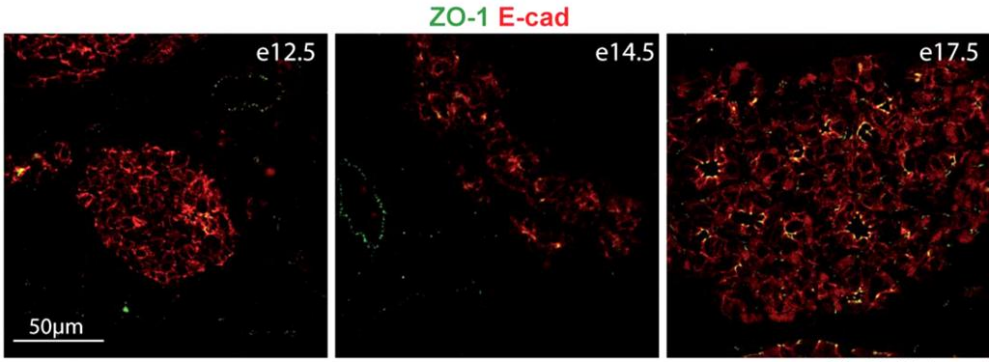

Fig. S1 (complementary to Fig. 1B, C) Tight junction maturation. Double immunofluorescence of control thyroid sections from e12.5 to e17.5. The e12.5 thyroid bud is composed of a mass of non-polarized epithelial cells (E-cad^{+}; ZO-1^{-}). Small dots of ZO-1 staining appear at e14.5. At e17.5, epithelial cells are organized in follicular-like structures or "rosettes", composed of polarized monolayers surrounding small lumina delineated by ZO-1 labeled apico-basolateral boundaries.

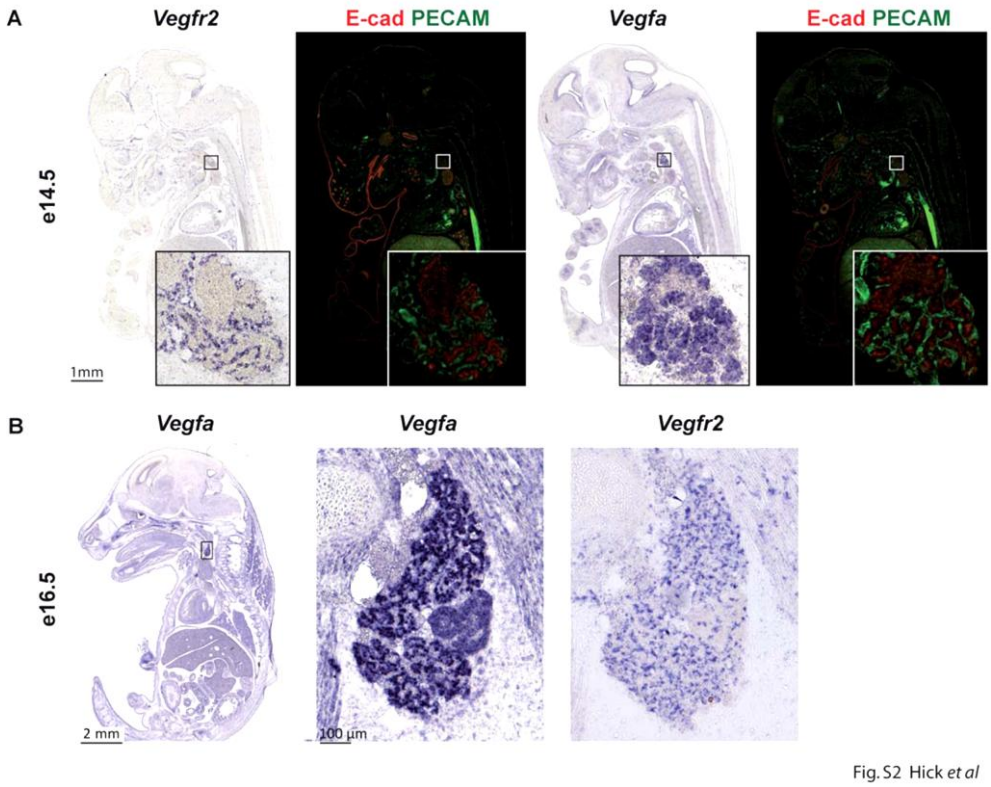

Fig. S2 (complementary to Fig. 2) Whole-embryo views of fields selected at Fig. 2B. (A) *In situ* hybridization and double immunofluorescence on adjacent sagittal sections of the thyroid bud from a **e14.5** WT embryo emphasize the complementary expression pattern of Vegfa, expressed by E-cadherin^{+} epithelial cells, and Vegfr2 in invading PECAM^{+} endothelial cells. **(B)** *In situ* hybridization on adjacent sagittal sections of a **e16.5** WT embryo shows persistence of this complementary expression pattern.

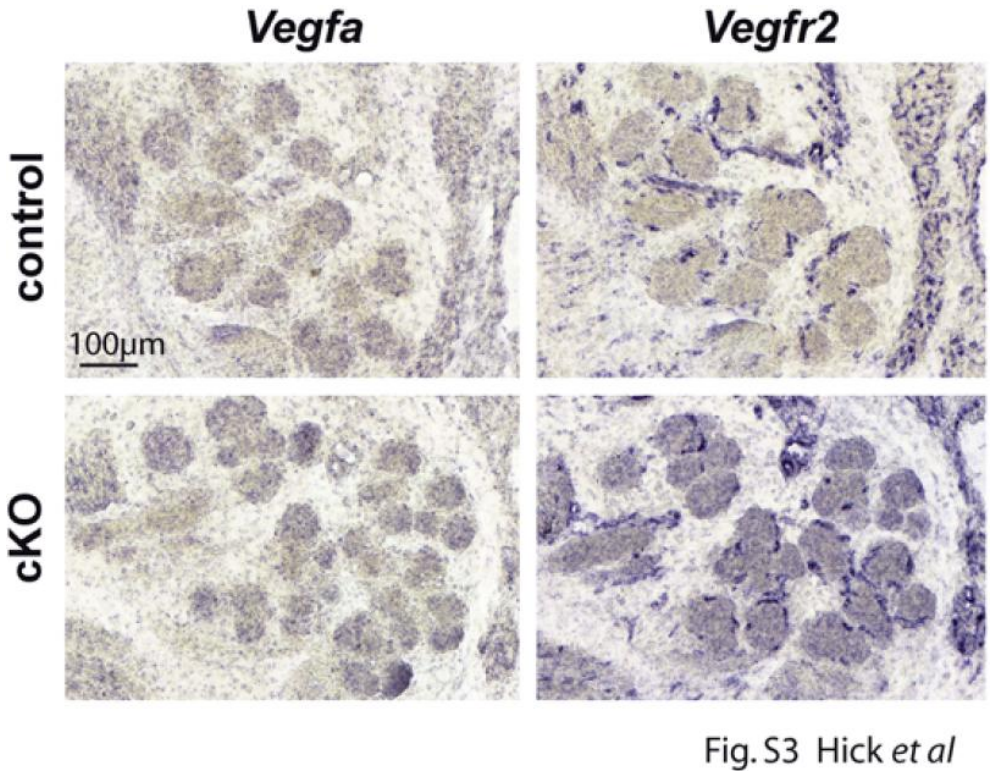

Fig. S3 Normal expression of Vegfa and Vegfr2 in the submandibular glands of Vegfa cKO. *In situ* hybridization showing similar expression of Vegfa and Vegfr2 in control and Vegfa cKO (thyroid-specific) submandibular glands at e14.5.

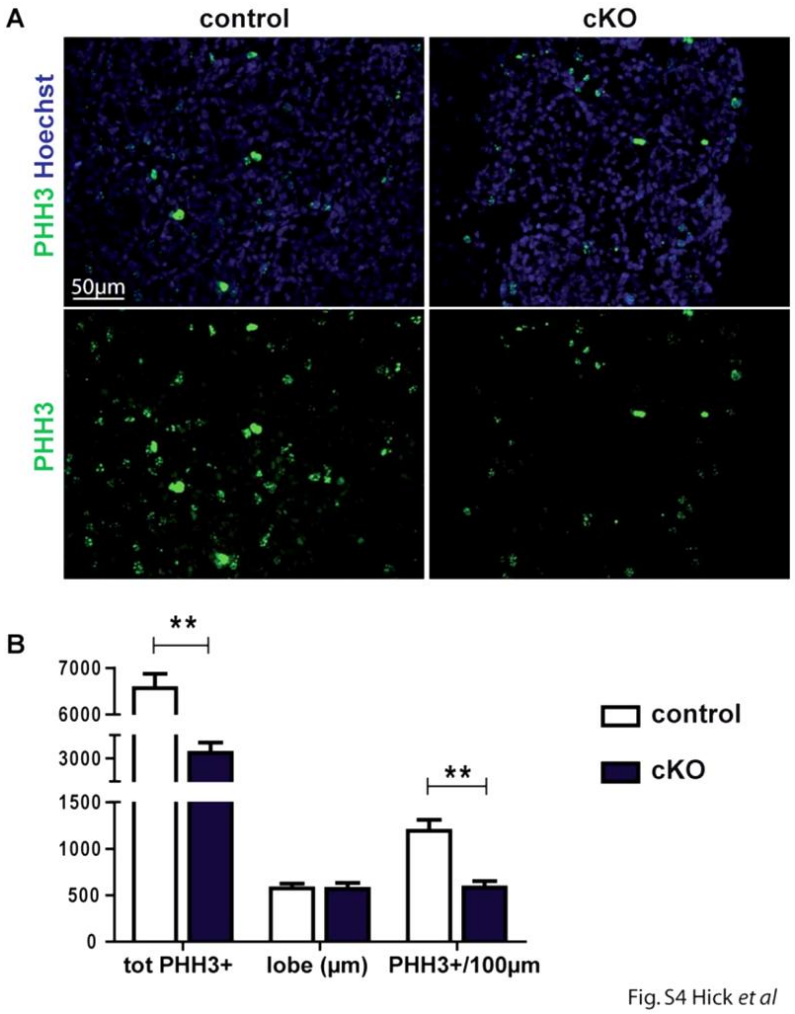

Fig. S4 Proliferation is still restricted to the periphery of e17.5 cKO thyroids. (A) Immunofluorescence for phosphohistoneH3 (pHH3) with (upper row) and without (lower panel) nuclei counterstaining by Hoechst of control and cKO frontal thyroid sections. Proliferating cells ($pHH3^+$) are numerous and widely distributed within control glands, but less abundant and restricted to the periphery in cKO. **(B) Quantification** (3 glands per condition). Although lobe size is similar, total number of $PHH3^+$ cells is reduced by 2-fold in cKO.

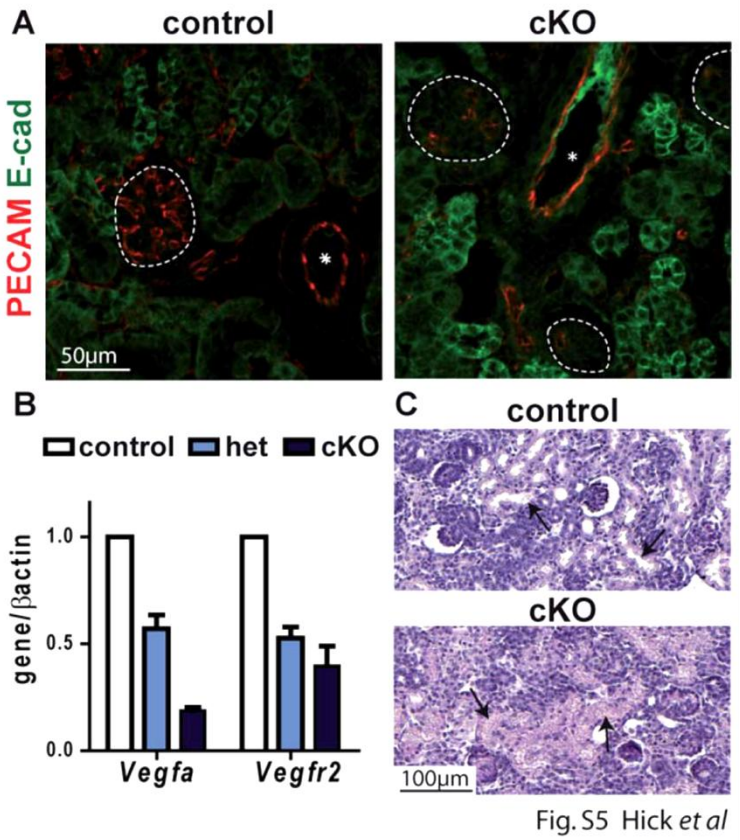

Fig. S5 Conditional (Pax8-Cre) Vegfa inactivation also strongly reduces vascular density in kidney embryos at P0. (A) Reduced vascular density in glomerular tufts. Immunofluorescence for PECAM in control and cKO kidneys (general tissue structure is shown by E-cadherin). In cKO, large blood vessels appear normal (asterisks) but endothelial cells in glomerular tufts (dotted lines) are almost absent. **(B) Decreased Vegfa and Vegfr2 by RT-qPCR.** Loss of one (het, for heterozygous) or two Vegfa alleles (cKO) causes a dose-dependent reduction in the expression of Vegfa (> 80 % Cre activity), and, to a lesser extent, of the endothelial marker Vegfr2. **(C) Altered kidney histology.** P.A.S. histological staining shows absence of normal glomeruli and closed tubules (arrows) in cKO.

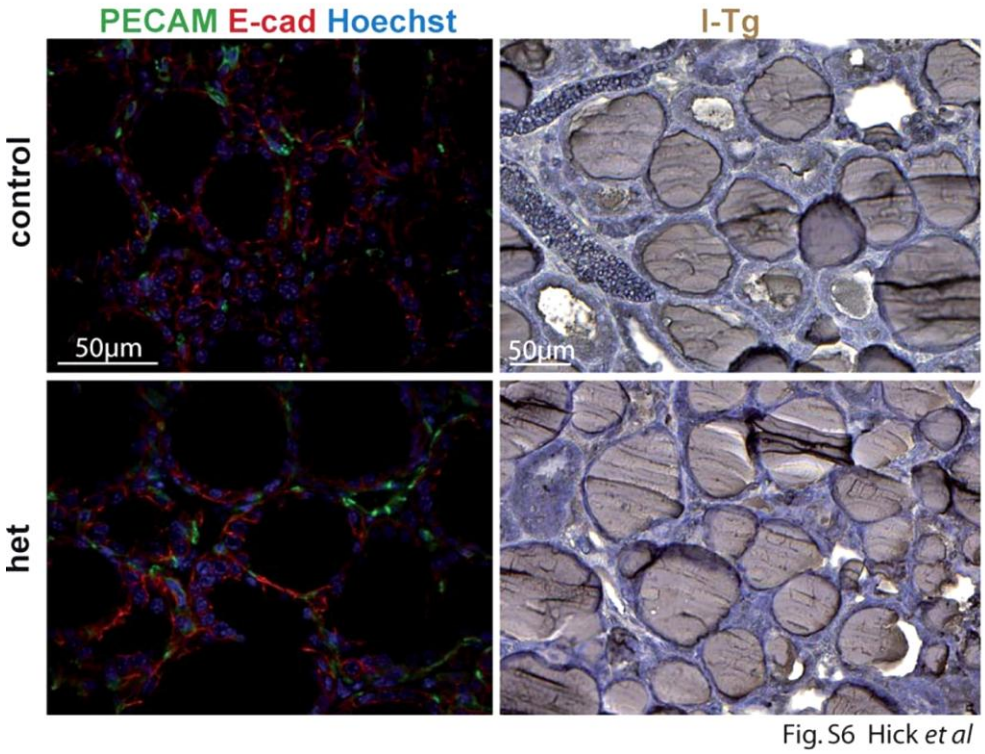

Fig. S6 Thyroid of adult heterozygotes for Vegfa is normal. Triple fluorescence on WT and heterozygous ($Pax8^{cre}$ $Vegf^{fl/+}$) thyroids sections at 2 months. No difference can be seen in follicular organization and size, vascularization and iodothyroglobulin storage.

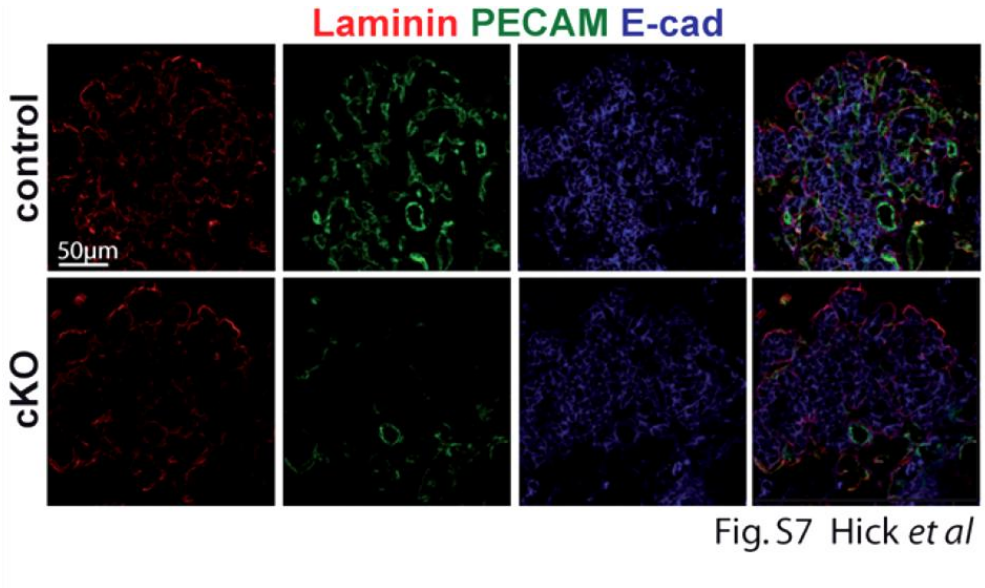

Fig. S7 Reduced vascular density in cKO is associated with impaired basement membrane formation. Triple immunofluorescence of e15.5 control and cKO thyroid sections. Laminin labeling surrounds individual epithelial clusters in WT but is mainly found at the periphery of cKO thyroids.

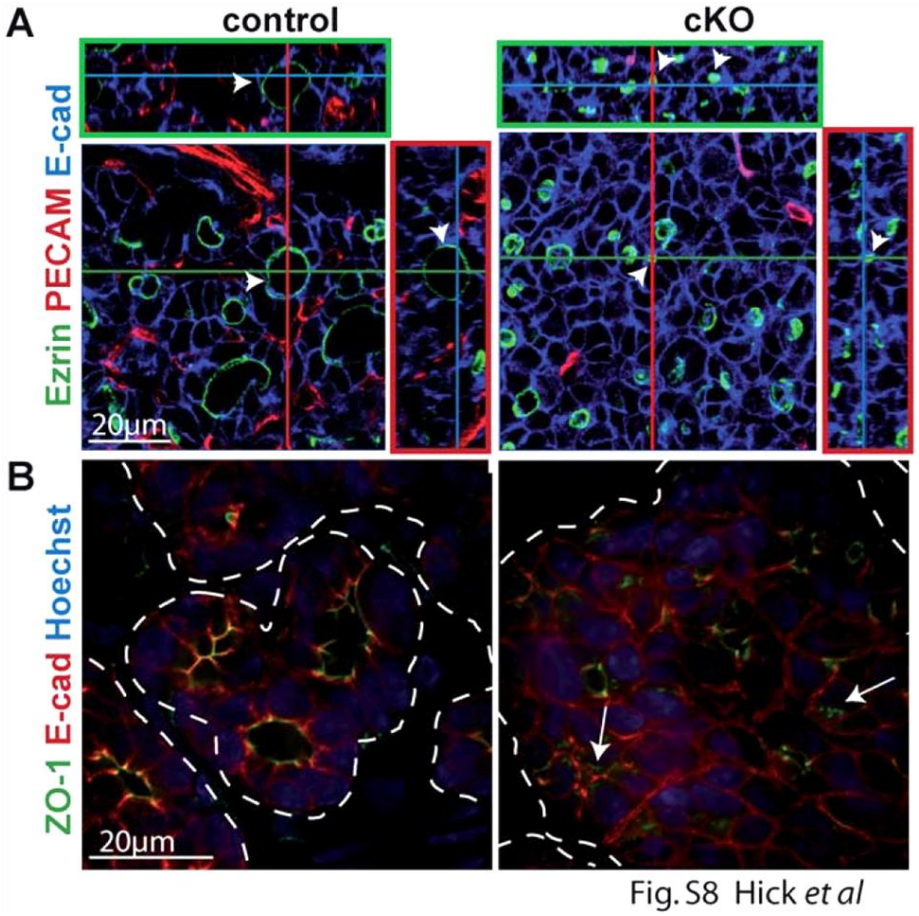

Fig. S8 (complementary to Fig. 7) Epithelial organization in follicles is perturbed in cKO thyroid glands. Triple fluorescence labeling of P0 control and cKO thyroid sections. **(A) Orthogonal views** of stacks of 65 (control) and 53 (cKO) confocal images show several large lumina surrounded by ezrin lumina in control, but much smaller ezrin+ structures in cKO newborns (arrowheads). **(B) ZO-1 immunolabeling in confocal sections.** In controls, ZO-1 is restricted to the tight junctional belts of epithelial (E-cad+) "rosettes". In thyroid of cKO pups, "rosettes" are rarely observed and ZO-1 labeling is mostly associated with clusters of dots under the epithelial plasma membrane (arrow).

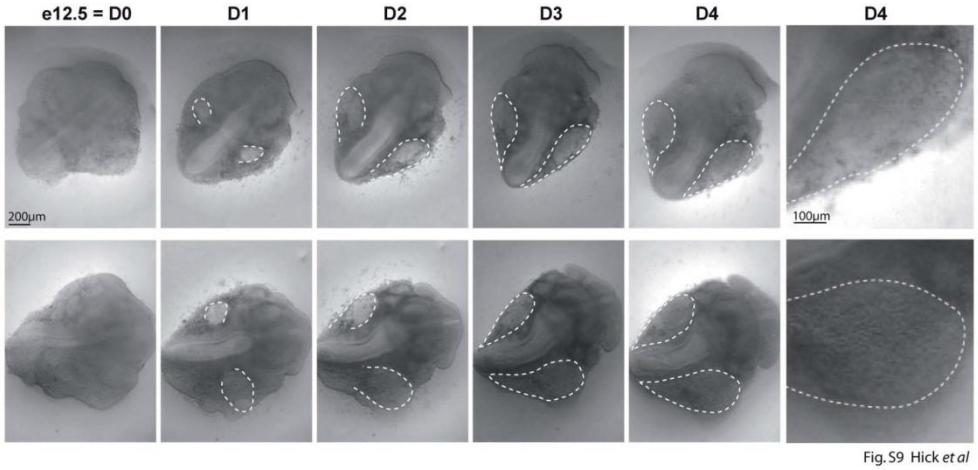

Fig. S9 *Ex vivo* bilobation and development of thyroid explants. Bright-field image of e12.5 thyroid explants before and during 4 days of culture. In freshly dissected tissue (D0), thyroid anlagen are hardly visible. The two thyroid lobes (dotted lines) become visible already after one day of culture (D1), then expand continuously from D1 to D4. Even at higher magnification (right panel), follicular structures are still not visible in the thyroid lobes.

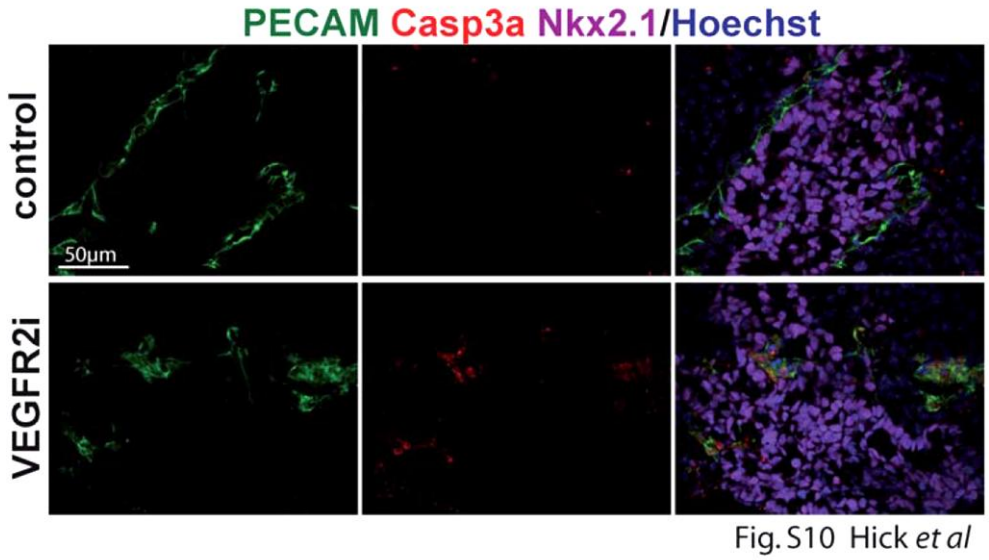

Fig. S10 Pharmacological inhibition of VEGFR2 (VEGFR2i) in e12.5 explants triggers systematic apoptosis specifically in endothelial cells. Quadruple fluorescence labeling of endothelial cells ($PECAM^{+}$), thyrocytes (Nkx2.1), and apoptotic cells (Casp3a) of e12.5 thyroid explants treated or not with VEGFR2i for 16h shows activated caspase-3 in all explants, limited to endothelial cells.

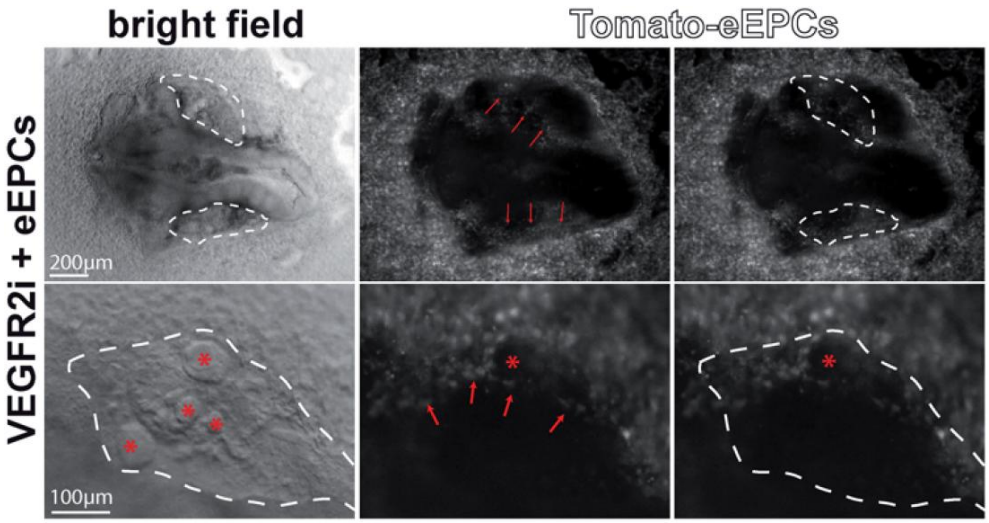

Fig. S11 Addition of endothelial precursor cells (eEPCs) around explants deprived of endogenous endothelial cells causes enlargement of follicular lumina. E12.5 explants were treated for 40 h with VEGFR2i to ablate endogenous endothelial cells, washed, then incubated with Tomato-eEPCs for 2 days. **Left panels: Bright-field views** of thyroid explants after 4 days in culture show large peripheral refractile disks corresponding to enlarged follicles (asterisks) in the two lobes. **Center and right panels: Tomato-EPCs fluorescence** shows clustering of eEPCs around the explants and their partial invasion on the lobes (upper panel, small arrows; same field with dotted lines define the two lobes), with possible enrichment around enlarged follicles (lower panel, asterisks).

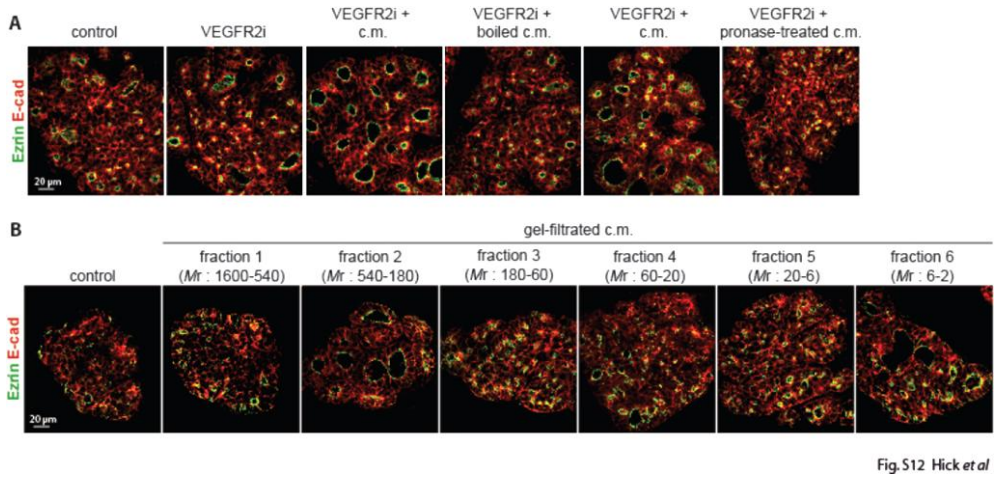

Fig. S12 The endothelial progenitor cell-derived folliculogenic activity has a proteinaceous nature and is found in both high- and a low-molecular weight fractions. E12.5 thyroid explants were treated with the VEGFR2 inhibitor (VEGFR2i) for 40 h to ablate endogenous endothelial cells, washed, then incubated with the indicated conditioned media (c.m.) for 2 days. (A) Immunolabeling. As compared to control explants, lumina (ezrin^{+}) of c.m.-treated explants are larger. Boiling or pronase treatment of the c.m. abolishes most of the foliculogenic activity. (B) Immunolabeling. As compared to control explants, we observed that two fractions (#2 and #6) of gel-filtrated c.m. displayed folliculogenic activity. Molecular weight ranges (in kDa) are based on the position of calibrators

2. An *ex vivo* culture system to study thyroid development

Anne-Sophie Delmarcelle, Mylah Villacorte, Anne-Christine Hick, Christophe E. Pierreux

Although purely “technical”, this work is an essential contribution for the lab and for collaborators. In this paper, we describe microdissection of the thyroid gland at E12.5 and E14.5 and the culture of the thyroid explants on semi-permeable filters but also on fibronectin- or collagen-coated dishes. I was the main artisan of this experimental paper, which is accompanied by a movie illustrating critical steps of the thyroid microdissection and culture. The movie is available on request.

Video Article

An *Ex vivo* Culture System to Study Thyroid Development

Anne-Sophie Delmarcelle[1], Mylah Villacorte[1], Anne-Christine Hick*[1], Christophe E. Pierreux*[1]

[1]Pole of Cell Biology, Université catholique de Louvain & de Duve Institute

*These authors contributed equally

Correspondence to: Christophe E. Pierreux at Christophe.pierreux@uclouvain.be

URL: http://www.jove.com/video/51641
DOI: doi:10.3791/51641

Keywords: Cellular Biology, Issue 88, Development, cellular biology, thyroid, organ culture, epithelial morphogenesis, immunostaining, imaging, RNA

Date Published: 6/6/2014

Citation: Delmarcelle, A.S., Villacorte, M., Hick, A.C., Pierreux, C.E. An *Ex vivo* Culture System to Study Thyroid Development. *J. Vis. Exp.* (88), e51641, doi:10.3791/51641 (2014).

Abstract

The thyroid is a bilobated endocrine gland localized at the base of the neck, producing the thyroid hormones T3, T4, and calcitonin. T3 and T4 are produced by differentiated thyrocytes, organized in closed spheres called follicles, while calcitonin is synthesized by C-cells, interspersed in between the follicles and a dense network of blood capillaries. Although adult thyroid architecture and functions have been extensively described and studied, the formation of the "angio-follicular" units, the distribution of C-cells in the parenchyma and the paracrine communications between epithelial and endothelial cells is far from being understood.

This method describes the sequential steps of mouse embryonic thyroid anlagen dissection and its culture on semiporous filters or on microscopy plastic slides. Within a period of four days, this culture system faithfully recapitulates *in vivo* thyroid development. Indeed, (i) bilobation of the organ occurs (for e12.5 explants), (ii) thyrocytes precursors organize into follicles and polarize, (iii) thyrocytes and C-cells differentiate, and (iv) endothelial cells present in the microdissected tissue proliferate, migrate into the thyroid lobes, and closely associate with the epithelial cells, as they do *in vivo*.

Thyroid tissues can be obtained from wild type, knockout or fluorescent transgenic embryos. Moreover, explants culture can be manipulated by addition of inhibitors, blocking antibodies, growth factors, or even cells or conditioned medium. *Ex vivo* development can be analyzed in real-time, or at any time of the culture by immunostaining and RT-qPCR.

In conclusion, thyroid explant culture combined with downstream whole-mount or on sections imaging and gene expression profiling provides a powerful system for manipulating and studying morphogenetic and differentiation events of thyroid organogenesis.

Video Link

The video component of this article can be found at http://www.jove.com/video/51641/

Introduction

The thyroid gland is a collection of independent epithelial spheres, called follicles, surrounded by a dense network of endothelial capillaries. This organization allows thyroid function: endothelial capillaries provide thyrocytes with iodine, required for T3 and T4 hormone synthesis, and distribute these latter to the whole body. Scattered in between the follicles and capillaries, C-cells produce the hypocalcemic hormone calcitonin[1]. Although adult thyroid architecture and functions are well known, the cellular and molecular mechanisms involved in thyroid embryonic development (follicle formation and differentiation) are far from being understood.

During embryogenesis, thyrocytes progenitor originates as a thickening (the midline anlage) of the ventral wall of the foregut endoderm at embryonic day (e) 8.5 in the mouse embryo, while C-cells progenitors originate at e11.5 as droplet-shaped protrusions (the ultimobranchial bodies) of the fourth pharyngeal pouches[2-6]. The midline bud then detaches from the endoderm, expands bilaterally to fuse at e13.5 with the ultimobranchial bodies on each side of the trachea. Finally, thyrocytes organize into follicles and C-cells differentiate.

Current knowledge on thyroid formation mainly comes from histological analysis of fixed tissues, but the morphogenetic events involved in thyroid formation are highly dynamic and involve communications and interactions between different cell types and with the extracellular matrix. Recent work showed that thyrocyte progenitors produce high levels of VEGF to recruit endothelial cells to the developing thyroid, and, in turn, recruited endothelial cells promote follicle formation and C-cells differentiation[7].

Most *ex vivo* studies on the thyroid have been performed on isolated adult thyroid-derived cells, grown either on 2D tissue culture plastic dishes or in 3D matrices. Using these types of cultures, differentiated follicular cells either remain polarized and organized as follicles or reacquire a 3D organization[8-10]. However, these pure epithelial cells, explanted from their physiological environment, and cultured in 2D, ignore interactions with extracellular matrix, cytokines, growth factors and with other cell types such as the endothelial or nerves cells that they normally encounter

in vivo. A very nice study recently described a differentiation protocol of ES cells into thyroid follicles using a final culture step in 3D matrigel[11]. However, these 3D cultures lack contact with other cell types.

Based on previous expertise on pancreas and salivary glands organ culture[12-14], a method for dissecting mouse embryonic thyroid anlagen and culturing the explants on semiporous filters or on microscopy plastic slides was developed.

When working with e12.5 embryos, the dual origin of the thyroid anlagen (the midline anlage and the two lateral ultimobranchial bodies) imposed the microdissection of a large fragment of tissue. This contained the trachea, but not the esophagus, and extended from the pharyngeal arch arteries up to the arytenoid swelling. When cultured on filters, the midline anlage extends laterally on each side of the trachea, where they fuse with the ultimobranchial bodies to form the two thyroid lobes, still connected by a narrow isthmus.

In culture, epithelial cells proliferate, organize into follicles and differentiate into thyrocytes and C-cells, depending on their origin. Endothelial cells contained in the microdissected tissue also proliferate and invade the thyroid lobes to finally associate closely with the epithelial follicular structure, independently of blood flow or circulating factors. As development of the explants faithfully recapitulates *in vivo* development, this culture system is optimal to study morphogenetic and differentiation events occurring during thyroid development.

Thyroid tissues can be obtained from wild type, knockout or fluorescent transgenic embryos, and the culture system is amenable to loss- and gain-of-function experiments. Finally, time-lapse imaging of fluorescently labeled thyroid explants on microscopy plastic dishes could be exploited to better investigate the kinetics and continuity of morphogenetic movements that occur *in vivo*. Time-lapse imaging has already been used to study branching morphogenesis of the pancreas[15,16] or the ureteric bud[17].

Protocol

Mice were raised and treated according to the principles of laboratory animal care of the University Animal Welfare Committee. All procedures and protocols were approved by this Committee.

1. Coating of Microscopy Plastic Culture Chambers

NOTE: Perform all the following steps under sterile conditions in a laminar flow hood. The two types of coating are functionally equivalent.

1. Coat plastic culture chambers with fibronectin one day prior to isolation of thyroid tissues:
    1. Dilute sterile fibronectin to a 50 µg/ml final concentration in M199 medium supplemented with 100 U/ml penicillin, 100 µg/ml streptomycin, 0.25 µg/ml fungizone and 2 mM glutamine[12].
    2. Cover the wells with 200 µl of diluted fibronectin and incubate overnight in a 4 °C refrigerator.
    3. On the day of the dissection, aspirate the fibronectin, rinse the wells once with M199 and add a minimum volume of 200 µl of M199 supplemented with antibiotics, glutamine and 10% fetal calf serum.
    4. Leave the coated chambers in the incubator until ready to plate the explants.
2. Coat plastic culture chambers with type I collagen 2 hr before isolation of thyroid tissues:
    1. Dilute sterile type I collagen to a 50 µg/ml final concentration in 10 mM HCl. NOTE: Keep collagen stock solution on ice.
    2. Cover the wells with 200 µl of diluted type I collagen and incubate for 2 hr at room temperature (RT).
    3. Aspirate the type I collagen solution, rinse the wells once with M199 and add a minimum volume of 200 µl of M199 supplemented with antibiotics, glutamine and 10% fetal calf serum.
    4. Leave the coated chambers in the incubator until ready to plate the explants.

2. Dissection of Thyroid Anlagen-containing Tissues (e12.5) or Thyroid Lobes (e13.5-e14.5)

NOTE: Use clean dissecting tools and Petri/culture plates. The general steps and incisions described below are the same for e12.5 and e14.5 embryos.

1. Sacrifice timed-pregnant female mice at the desired embryonic (e) day (from e12.5 to e14.5) and remove the uterus using dissecting instruments.
2. Place the dissected uterus in a 10 cm plate containing HBSS.
3. Hold one extremity of the uterus with forceps and open the uterus with small scissors to liberate progressively all the embryos.
4. Separate the embryos from the placenta with scissors and transfer the embryos with their extraembryonic membranes in a new 10 cm plate containing HBSS.
5. Remove the yolk sac and the amnion. NOTE: From this point, work under a stereomicroscope with transillumination from below; increasing magnification with dissection steps. Use tungsten needles in glass capillaries as dissecting tools.
6. Using the needles like a knife and fork, remove the upper part of the head, including the upper jaw and the ears (**Figure 1A**, cut along a).
7. Hold the embryo on its back and remove first an extra piece of the neural tube (**Figure 1A**, cut along b), then the lower part of the embryo, just under the anterior limbs and above the heart (**Figure 1B**).
8. Transfer the embryo slice containing the tongue (to orient the tissue) and neck region in a new 10 cm plate containing HBSS.
9. Remove the neural tube and tissues posterior to the esophagus/trachea (**Figure 1C**, cut along a).
10. Gently section the tissue slice along both sides of the tongue (**Figure 1C**, cut along b and b').
11. Locate the esophagus and trachea, in the prolongation of the tongue, and dissect away the tongue, leaving the arytenoid swelling (**Figure 1D**, cut along a), and the tissue on both sides of the esophagus/trachea (**Figure 1D**, cut along b and b').
12. Remove the esophagus, and place the trachea with its ventral side facing up.

13. Dissect away the undesired tissues such as the thymus (**Figure 1E**) and all the tissues located laterally to the pharyngeal arch arteries. For e13.5 or e14.5 embryos, visualize the thyroid lobes on each side of the trachea (**Figure 1F**; red dotted lines) and further dissect the lobes from the trachea.
14. Transfer the isolated e12.5 trachea region, or the e13.5-e14.5 thyroid lobes into a 35 mm culture plate containing pre-warmed M199 medium supplemented with antibiotics, glutamine and 10% fetal calf serum. Transfer explants using a prewetted filter tip on a P-200 micropipette. For e12.5 explants, cut the extremity of the tip to widen the opening. NOTE: Routinely, and if embryos have the same genotype, perform steps 6 & 7 on all the embryos, then 9-11, and finally 12 & 13.

3. Plating and Culture of Thyroid Explants

1. Wash the explants by successive transfer in three wells of a 24-well plate containing 1 ml of pre-warmed culture medium (= M199 supplemented with antibiotics, glutamine and 10% fetal calf serum).
2. Plating of thyroid lobes on coated microscopy plastic culture chambers:
    1. Aspirate M199 culture medium from the coated chambers.
    2. Carefully, transfer the thyroid explants into the culture chambers using a micropipette and filter tips. Place one explant in the center of each chamber.
    3. Remove excess medium and place the culture chamber in a tissue culture incubator (37 °C; 5% CO_2) for 2 hr to let the explants attach to the matrix.
    4. Gently add 200 to 300 µl of pre-warmed culture medium to each well.
    5. Incubate for long-term culture in the tissue culture incubator.

3. Plating of trachea region or thyroid lobes on semiporous filters:
    1. Fill the number of wells of a 24-well plate required with 330 µl of pre-warmed culture medium.
    2. Place filters (*e.g.* 0.4 µm Millipore filter) on the medium, taking care to avoid trapping of air bubbles below the culture filter.
    3. Carefully, using a micropipette and filter tips, transfer the thyroid explants with a minimal volume of medium onto the center of the filters (maximum 4/filter).
    4. Remove the excess of medium and space out the explants with a tungsten needle.
    5. Incubate for long-term culture in the tissue culture incubator. NOTE: Change culture medium every other day under the laminar flow hood. Culture the explants up to 7 days.

4. Whole-mount Immunofluorescence Staining Protocol for Thyroid Explants

Dislodge explants grown on filters (after step 2 below) using tungsten needles or fine forceps and transfer in a 24-well plate for all the steps, except for primary (step 5) and secondary (step 7) antibody incubations (96-well plate). For adherent explants cultured on microscopy plastic chambers, perform all the steps in the culture chambers.

1. Aspirate M199 culture medium and fix the explant with ice-cold 4% paraformaldehyde (PFA) for 20 min (500 µl in 24-well dish and 300 µl in microscopy slides).
2. Wash 2x 10 min in Tris Buffered Saline with Triton (TBST; 50 mM Tris HCl pH 7.5, 150 mM NaCl, 0,1% Triton X-100) at RT.
3. Process the explants immediately or store at -20 °C. NOTE: For long-term storage at -20 °C, dehydrate the explants in methanol by gradually increasing methanol concentration in TBST to reach 100% methanol. When ready to continue with the immunostaining (step 4), rehydrate the explants by gradually adding TBST to methanol.
4. Replace TBST with the blocking solution (10% normal Goat Serum in TBST) and incubate on a sea-saw rocker for 30-60 min at RT.
5. Dilute primary antibody in blocking solution (100-200 µl per condition). Transfer the "filter" explants from a 24-well plate to a 96-well plate. Incubate explants with the primary antibodies on a sea-saw rocker overnight at 4 °C.
6. The next day, discard the primary antibody solution, transfer the "filter" explants back in a 24-well plate, and wash at least five times with TBST on a sea-saw rocker for 45-60 min each at RT.
7. Dilute secondary antibody (*e.g.* Goat anti-X-Alexa Fluor at 1:2,000 dilution) in TBST containing 1% of normal goat serum and incubate the explants with this dilution overnight on a sea-saw rocker at 4 °C and in the dark. For nuclear counterstaining, include 1 µg/ml of bis-Benzimide (Hoechst) together with the secondary antibody solution.
8. The next day, discard the secondary antibody solution and wash 5x with TBST on a sea-saw rocker for 45-60 min each at RT. During the washes, keep the explants in the dark.
9. Perform an additional wash in TBST gently swirling overnight at 4 °C in the dark.
10. Postfix the immunostained explants in 4% PFA at 4 °C for 10 min.
11. Wash 2x 10 min with TBST.
12. Transfer the explants either gradually in methanol 100% for long-term storage at -20 °C, or analyze immediately. For explants cultured on filters, and immunostained in a 24-well plate, transfer in a microscopy chamber (*e.g.* LabTek or Ibidi) with TBST or better fluorescent mounting medium prior to analysis with a Multiphoton or confocal microscope.

5. Extraction of RNA from Thyroid

Work in an RNase-free environment. Therefore, use nucleic acid and nuclease free pipette tips and clean both bench and equipment from contaminants and RNases. This protocol being based on phenol/chloroform, perform the first steps (1 to 7) under a chemical hood.

1. Homogenize one thyroid explant or two thyroid lobes with 300 µl of RNA extraction solution using a disposable pestle for 1.5 ml tube. In between samples, wash the pestle in 2% SDS, then water, then ethanol.
2. Add another 100 µl of RNA extraction solution, vortex 10 sec and incubate at RT for 10 min.

3. Vortex for 30 sec and add 20 ng of tRNA to each sample.
4. Vortex for 1 min and add 80 µl of chloroform.
5. Vortex vigorously for 30 sec and incubate 15 min at RT.
6. Spin for 15 min at 19,000 x g in a refrigerated (4 °C) centrifuge.
7. Transfer carefully the colorless upper aqueous phase in a fresh tube containing 20 µg of glycogen as coprecipitant.
8. Vortex and add 200 µl of 100% isopropanol alcohol.
9. Vortex vigorously for 15-30 sec and let RNA precipitate at -20 °C for 2-3 hr or at -80 °C for 1 hr.
10. Spin for 30 min at 19,000 x g at 4 °C, and eliminate supernatant.
11. Wash the pellet with 450 µl of cold 75% ethanol and vortex to dislodge the pellet.
12. Spin for 10 min at 19,000 x g at 4 °C, and eliminate supernatant.
13. Dry the pellet under the hood for 5 min.
14. Resuspend the pellet with 10 µl of RNase-free water and incubate 10 min at RT.
15. Assay RNA concentration, store at -80 °C or reverse transcribe for gene expression analysis.

Representative Results

Thyroid anlages (midline and UB, together with surrounding tissues), and thyroid lobes are dissected from mouse embryos at e12.5 and e13.5/e14.5, respectively (**Figure 1**). After one day in culture on filter, the midline anlage is visible (**Figure 2A**) as an elongated tissue spanning on top of the trachea. It progressively forms two lobes on each side of the trachea. If isolated thyroid lobes (e13.5 or e14.5) are cultured, they will expand, undergo morphogenesis and epithelial cells will organize into macroscopically visible follicular structures (**Figure 2B**).

Organization and polarization of epithelial cells, labeled with E-cadherin, can be visualized by ezrin immunolabeling (**Figure 3A**). Ezrin-positive intracellular structures progressively, and in a concerted way, fuse with one pole of the cell that will become the apical pole. During this process, endothelial cells positive for PECAM proliferate and organize around the developing follicles to form angio-follicular units (**Figure 3B**). To quantify differentiation of thyrocytes and C-cells, RNA can be isolated from the cultured thyroid lobes, and gene expression assayed by RT-qPCR (**Figure 3C**). While the expression of the thyroid transcription factor Nkx2.1 does not change during the culture, expression of thyrocyte-specific thyroglobulin and of C-cell-specific calcitonin dramatically increased, indicating functional differentiation.

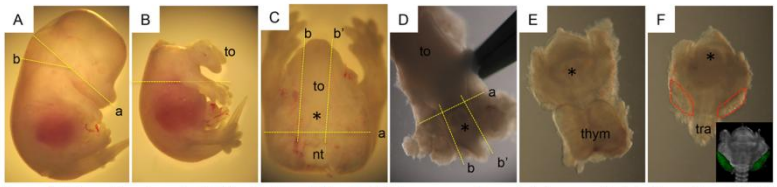

Figure 1. Dissection steps to isolate the thyroid from e14.5 mouse embryo. Incisions are depicted by yellow dotted lines. (**A**) The upper part of the head is removed by two incisions to expose the tongue. (**B**) The neck region is separated from the rest of the body by sectioning the embryo below the upper limbs and above the heart. (**C**) Keeping the tongue (to) as a guide, remove the neural tube (nt) and the lateral tissues and limbs. (**D**) The tongue, arytenoid swelling (*) and the esophagus/trachea are perfectly aligned. First remove the tongue and then tissues lateral to the esophagus/trachea region. (**E**) The thyroid lobes are partly hidden by the thymus (thym) which should be discarded. (**F**) Thyroid lobes are visible on each side of the trachea (red dotted ovoids), or better visualized using fluorescent reporter embryos (Pax8-Cre; Rosa-stop-YFP; inset). Abbreviations: to (tongue), thym (thymus), tra (trachea), * (arytenoid swelling). Please click here to view a larger version of this figure.

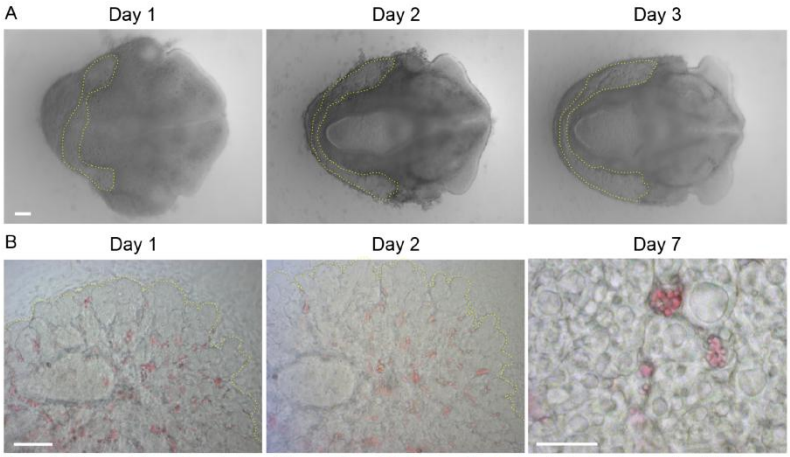

Figure 2. Dissected thyroid explants on filter and thyroid lobes on fibronectin nicely develop *ex vivo*. (**A**) Photographs of an e12.5 thyroid explant cultured for 1, 2 and 3 days on semiporous filter, at the air-medium interface. Thyroid epithelial cells migrate bilaterally on each side of the trachea and form two growing thyroid lobes. (**B**) Brightfield images on day 1 and day 2 of an e14.5 thyroid lobe cultured on microscopy plastic culture chambers. Note the expansion and remodeling of the epithelium that ultimately form large (20-100 µm) follicles around day 7. Yellow dotted line delineates the epithelial periphery of the thyroid. Scale bars, 100 µm. Please click here to view a larger version of this figure.

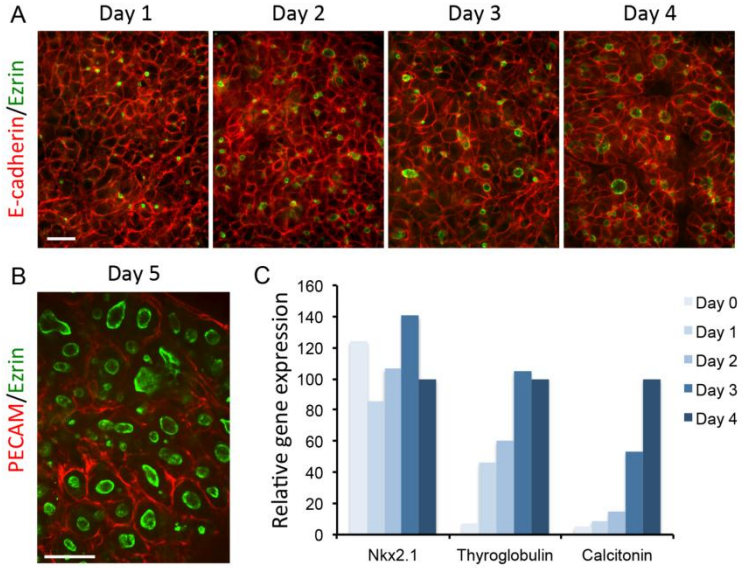

Figure 3. Folliculogenesis, angiogenesis and differentiation of thyroid in culture. Thyroid lobes were cultured for the indicated time. (**A**) Fixed tissues were whole-mount immunostained with antibodies against the basolateral marker E-cadherin, and the subapical membrane marker Ezrin. After one day in culture, epithelial cells of the thyroid parenchyma present small ezrin-positive structures that correspond to intracellular vesicles[7]. Concerted fusion of the vesicles from adjacent cells will form small lumen at day 2; their progressive growth, and organization of the surrounding cells around the lumen will delineate pre-follicular structures after 4 days. Scale bar, 20 µm. (**B**) Thyroid lobe immunostained with antibodies against the Platelet and Endothelial Cell Adhesion Molecule (PECAM) and Ezrin. Follicles are surrounded by endothelial structures. Scale bar, 50 µm. (**C**) RNA, extracted from thyroid lobes, was reverse transcribed before quantitative PCR. The expression of the thyroid transcription factor Nkx2.1, and of two differentiation genes, thyroglobulin and Calcitonin, was measured using specific primer pairs. To calculate the relative gene expression, the ΔΔ Ct method was used, using E-cadherin as the reference gene and the last time point of the culture as 100%. Images shown in **A** and **B** are single confocal optical sections of whole-mount immunostained thyroid lobes. Please click here to view a larger version of this figure.

Discussion

This paper describes a method for dissecting and culturing thyroid explants (e12.5) or lobes (e14.5) in order to study and better understand the complex events leading to thyroid formation. Due to the dual origin of the thyroid anlagen (the midline anlage and the two lateral ultimobranchial bodies), and their small size, a fragment of e12.5 tissue localized rostral to the pharyngeal arch arteries, and containing the trachea, but not the esophagus is microdissected. As illustrated, within a period of four days, this culture system faithfully recapitulates *in vivo* thyroid development since: (i) the midline anlage migrates bilaterally and expands to form, with the UB, two thyroid lobes connected by a narrow isthmus (**Figure 2A**), (ii) thyroid precursors reorganize from a mass of cells into follicles and ultimately polarize (**Figures 2B** and **3A**), (iii) endothelial cells present in the microdissected tissue proliferate, migrate into the thyroid lobes, and closely associate with the epithelial cells (**Figure 3B**), and (iv) thyrocytes and C-cells differentiate qualitatively (**Figure 3C**), as they do *in vivo*[7]. As dissection physically interrupts *in utero* development and explanted tissue has to adapt to culture condition, the morphological and differentiation events are slightly delayed as compared to the *in vivo* situation.

Critical steps within the protocol

The critical aspect of this method is in the dissection. First, it is essential to remove lateral tissues, as well as the right and left lobes of the thymus gland from the e12.5 explants, as their expansion in culture hinder proper development of the thyroid lobes. Second, rapidity is also critical if one wants to maintain endothelial cells alive. If dissection is not performed under a sterile atmosphere, it is important to wash several times the explants in sterile culture medium. Finally, when culturing explants on semiporous filters, it is important to use a small volume of medium and to place the explants on the center of the filter. Too much medium will flow to the periphery of the filter and create a meniscus with the filter wall. In this case, the explant will follow the medium and reaches the meniscus; its development will be in medium rather than at the air/medium interface.

Possible modifications and limitations

The protocol described here applies to e12.5 thyroid explants and to e13.5 and e14.5 isolated thyroid lobes. Younger and older developmental stages could be tested in function of the scientific question addressed. Other culture conditions could also be tested: thyroid explants or lobes could be grown in 3D matrigel, or the medium could be complemented with Insulin/Transferrin/Selenium rather than with 10% serum.

An important aspect of tissue culture is oxygen concentration. When grown on microscopy plastic slides, oxygen concentration is difficult to appreciate as it will decrease with the height of medium above the explants. When grown on filters, at the air/medium interface, explants are in contact with the atmosphere, hence with 21% of oxygen. In this latter case, one could try to reproduce the "hypoxic" *in utero* environment using lower pO_2 concentration inside the incubator.

If tissular complexity of the e12.5 explants is an advantage for correct development, it is also a main drawback as the epithelial cells are not accessible to viruses or transfection reagents. Manipulation can be performed with diffusible reagents (inhibitors, blocking antibodies, growth factors, cytokines, conditioned medium), keeping in mind that the exogenous compound affects all cell types. Moreover, tissue complexity and the small size of the lobes relative to the entire tissue explant (see **Figure 2A**, right panel), reduces the purity of the extracts (RNA or protein) prepared.

Although most of the data presented in this paper were obtained from 4-5 days cultured explants, it is possible to keep the organ in culture for longer time, up to 10 days on plastic, with a continuous development of the follicles (see **Figure 2B** at day 7). If longer cultures have to be performed, one should verify that all the cell types, including endothelial cells, survive in the explants.

Significance of the technique with respect to existing methods or other alternative methods

Compared to culture of pure populations of thyrocytes in 2D dishes or 3D matrices, this organ culture system presents the advantage of maintaining the natural and physiological composition of the microdissected fragments. Indeed, in addition to thyrocytes and C-cells progenitors, explants contain mesenchymal and endothelial cells as well as extracellular matrix. As already demonstrated with salivary glands, kidney, lung or pancreas, organ cultures nicely mimic *in vivo* development. Moreover, it provides a way to rapidly analyze and manipulate (gain or loss-of-function) wild type and knockout organs.

Future applications or directions after mastering this technique

This paper shows that the cellular and molecular aspects of thyroid development can be analyzed with a microscope or by RT-qPCR; *in situ* hybridization or western blotting could also be performed. This culture system is amenable to gain- and loss-of-function experiments via the addition of specific inhibitors, blocking antibodies, growth factors, cytokines, or even cells in the culture medium[7]. However, all the cell types present in the tissue are affected. It would be interesting to develop virus-based cell-type specific targeting.

The use of a fluorescent reporter strain, with a fluorescent dissecting microscope, facilitates the microdissection of the tissue piece (**Figure 1F**, inset), but also, as reported by others using a membrane-tagged fluorescent protein[16], allows to perform real-time imaging of the developing organ in 3D[15,16], or to follow a particular cell population in the culture. Development of new fluorescent reporter strains will be necessary to carefully visualize morphogenetic events.

Disclosures

The authors have nothing to disclose.

Acknowledgements

The work was supported by grants from the Université catholique de Louvain (Action de recherché concertées) and the Fund for Scientific Medical Research (F.R.S.-FNRS, Belgium). A.-S.D. is a doctoral fellow from Télévie, A.-C.H. held a fellowship from the Fonds pour la formation à la Recherche dans l'Industrie et dans l'Agriculture (Belgium), M.V. is supported by the de Duve Institute and C.E.P. is a senior research associate of the F.R.S.-FNRS (Belgium).

References

1. Colin, I.M., Denef, J.-F., Lengelé, B., Many, M.-C., & Gérard, A.-C. Recent insights into the cell biology of thyroid angiofollicular units. *Endocr. Rev.* 34 (2), 209-238, http://dx.doi.org/10.1210/er.2012-1015 (2013).
2. Fagman, H., Andersson, L., & Nilsson, M. The developing mouse thyroid : embryonic vessel contacts and parenchymal growth pattern during specification, budding, migration, and lobulation. *Dev. Dyn.* 235(2), 444-455, http://dx.doi.org/10.1002/dvdy.20653 (2006).
3. Fagman, H., & Nilsson, M. Morphogenesis of the thyroid gland. *Mol. Cell. Endocrinol.* 323(1),35-54, http://dx.doi.org/10.1016/j.mce.2009.12.008 (2010).
4. Fagman, H., & Nilsson, M. Morphogenetics of early thyroid development. *J. Mol. Endocrinol.* 46(1), R33-42, http://dx.doi.org/10.1677/JME-10-0084 (2011).
5. De Felice, M., & Di Lauro, R. Thyroid development and its disorders : genetics and molecular mechanisms. *Endocr. Rev.* 25(5), 722-746, http://dx.doi.org/10.1210/er.2003-0028 (2004).
6. De Felice, M., & Di Lauro, R. Intrinsic and extrinsic factors in thyroid gland development : an update. *Endocrinology.* 152(8), 2948-2956, http://dx.doi.org/10.1210/en.2011-0204 (2011).
7. Hick, A.-C., *et al.* Reciprocal epithelial :endothelial paracrine interactions during thyroid development govern follicular organization and C-cells differentiation. *Dev. Biol.* 381(1), 227-240, http://dx.doi.org/10.1016/j.ydbio.2013.04.022 (2013).

8. Toda, S., Koike, N., & Sugihara, H. Cellular integration of thyrocytes and thyroid folliculogenesis: a perspective for thyroid tissue regeneration and engineering. *Endocr. J.* 48, 407-425, http://dx.doi.org/10.1507/endocrj.48.407 (2001).
9. Toda, S., *et al.* Culture models for studying thyroid biology and disorders. *ISRN Endocrinol.* 2011:275782, http://dx.doi.org/10.5402/2011/275782 (2011).
10. Eggo, M. C., Quiney, V. M., & Campbell, S. Local factors regulating growth and function of human thyroid cells in vitro and *in vivo*. *Mol. Cell. Endocrinol.* 213, 47-58, http://dx.doi.org/10.1016/j.mce.2003.10.034 (2003).
11. Antonica, F., *et al.* Generation of functional thyroid from embryonic stem cells. *Nature* 491, 66-71, http://dx.doi.org/10.1038/nature11525 (2012).
12. van Eyll, J.M., Pierreux, C.E., Lemaigre, F.P., & Rousseau, G.G. Shh-dependent differentiation of intestinal tissue from embryonic pancreas by activin A. *J. Cell Sci.* 117, 2077-2086, http://dx.doi.org/10.1242/jcs.01067 (2004).
13. Hick, A.-C., *et al.* Mechanism of primitive duct formation in the pancreas and submandibular glands: a role for SDF-1. *BMC Dev. Biol.* 9, 66, http://dx.doi.org/10.1186/1471-213X-9-66 (2009).
14. Pierreux, C.E., *et al.* Epithelial:Endothelial cross-talk regulates exocrine differentiation in developing pancreas. *Dev. Biol.* 347, 216-227, http://dx.doi.org/10.1016/j.ydbio.2010.08.024 (2010).
15. Puri, S., & Hebrok, M. Dynamics of embryonic pancreas development using real-time imaging. *Dev. Biol.* **306** 82-93, http://dx.doi.org/10.1016/j.ydbio.2007.03.003 (2007).
16. Petzold, K.M., & Spagnoli, F.M. A system for ex-vivo culturing of embryonic pancreas. *J. Vis. Exp.* 27(66):e3979, http://dx.doi.org/10.3791/3979 (2012).
17. Watanabe, T., & Costantini, F. Real-time analysis of ureteric bud branching morphogenesis *in vitro*. *Dev. Biol.* 271, 98-108, http://dx.doi.org/10.1016/j.ydbio.2004.03.025 (2004).

3. Thyroid follicle development requires Smad1/Smad5 and endothelial-dependent basement membrane assembly

Mylah Villacorte*, Anne-Sophie Delmarcelle*, Manon Lernoux, Mahé Bouquet, Jennifer Bolsée, Lieve Umans, Susana Chuva de Sousa Lopes, Patrick Van Der Smissen, Takako Sasaki, Guido Bommer, Samuel Refetoff, Frédéric P. Lemaigre, An Zwijsen, Pierre J. Courtoy, Christophe E. Pierreux (* Equal first authors)

My project merged with the project led by Dr. Mylah Villacorte on the characterization of Smad1/5^{dKO} and both projects complemented one another. Indeed, we noticed several similarities between Smad1/5^{dKO} and Vegfa^{KO}: (i) defective folliculogenesis, (ii) impaired basement membrane assembly, and (iii) rescue by conditioned medium from eEPC. My main contribution was the identification of laminins present in the conditioned medium as a folliculogenic factor. I also re-analyzed Vegfa^{KO} by focusing on basement membrane protein expression and assembly and I studied the regulation of Vegfa expression by BMP ligands.

Thyroid follicle development requires Smad1/Smad5- and endothelial-dependent basement membrane assembly

Mylah Villacorte[1†], Anne-Sophie Delmarcelle[1†], Manon Lernoux[1], Mahé Bouquet[1], Jennifer Bolsée[1], Lieve Umans[2,3], Susana Chuva de Sousa Lopes[5], Patrick Van Der Smissen[1], Takako Sasaki[6], Guido Bommer[1], Samuel Refetoff[7], Frédéric P. Lemaigre[1], An Zwijsen[2,4], Pierre Courtoy[1], and Christophe E. Pierreux[1*]

[1] de Duve Institute and Université Catholique de Louvain, Brussels, Belgium, [2] VIB Center for the Biology of Disease, KU Leuven, Belgium, [3] Laboratory of Molecular Biology (Celgen), Stem Cell Biology and Embryology, KU Leuven, Belgium, [4]Department of Human Genetics, KU Leuven, Belgium, [5]Department of Anatomy and Embryology, Leiden University Medical Center, Leiden, The Netherlands, [6]Department of Matrix Medicine, Faculty of Medicine, Oita University, Oita, Japan, [7]Department of Medicine, Pediatrics and Genetics, The University of Chicago, Chicago, IL, USA.

† Equally contributing first authors

*corresponding author. Fax : +32 2 764 75 43

E-mail address: christophe.pierreux@uclouvain.be

Keywords:

Thyroid, Smad1/5, follicles, epithelium, extracellular matrix

Summary

Epithelial BMP-Smad1/5 signaling and associated endothelial cells are required for reorganization of thyroid progenitor cell mass into mature follicles via deposition of basement membrane proteins.

Abstract

Thyroid follicles, the functional units of the thyroid gland, are delineated by a monolayer of thyrocytes, which rest on a basement membrane. During embryonic development, follicles are formed by reorganization of an unstructured mass of non-polarized cells, but regulatory mechanisms driving folliculogenesis remain largely unknown. Here we show that assembly of the basement membrane is critical for folliculogenesis and is controlled by endothelial cells and BMP-Smad signaling in thyrocytes. Thyroid-specific double Smad1 and Smad5 knockout mice (Smad1/5^{dKO}) display growth retardation, hypothyroidism and defective follicular architecture. In Smad1/5^{dKO} embryonic thyroids the epithelial cells remain associated in large clusters and form small follicles. Although similar follicular defects are found in Vegfa^{KO} thyroids, Smad1/5^{dKO} thyroids have normal endothelial cell density but show reduced expression of several endothelial markers. Interestingly, we found that both Smad1/5^{dKO} and Vegfa^{KO} thyroids displayed impaired basement membrane assembly. Furthermore, conditioned medium (CM) from embryonic endothelial progenitor cells (eEPC) rescues the folliculogenic defects of Smad1/5^{dKO} and Vegfa^{KO} thyroids. Laminin α1β1γ1 is abundantly released by eEPC into CM, and is critically required for folliculogenesis. These results support that thyrocytes cooperate with endothelial cells to promote folliculogenesis via assembly of the basement membrane.

Introduction

Thyroid follicles are the functional units of the thyroid gland. Each follicle is composed of a polarized monolayer of epithelial cells delineating a close lumen where thyroglobulin (TG) is stored as colloid. Thyrocytes differentiate from thyroid progenitors that bud from the foregut endoderm as a mass of non-polarized epithelial cells, which reorganize to form pre-follicular structures by acquisition of apico-basal polarity (Fagman et al., 2006; Hick et al., 2013). Differentiated thyrocytes face the lumen at the apical pole, and are attached to the basement membrane at their basal pole. In the mature thyroid, a dense network of blood vessels surrounds each follicle. Together, they form angio-follicular units responsible for T_3 and T_4 thyroid hormone synthesis and storage within TG, and then hormone secretion into the bloodstream (Colin et al., 2013; Nilsson and Fagman, 2013). A limited number of transcription factors (Nkx2.1, Pax8, Foxe1 and Hhex) and signalling molecules are known to control thyroid development (Fagman and Nilsson, 2010), but factors regulating follicle formation remain largely unknown.

Several studies have demonstrated the importance of epithelial-endothelial interactions in organs developing from the endoderm (Hick et al., 2013; Lammert et al., 2001; Lazarus et al., 2011; Pierreux et al., 2010). In the thyroid, we found that endothelial cells are recruited in response to epithelial-derived VEGFa and are essential for the organization of thyroid epithelial cell mass into follicles (Hick et al., 2013). However, the identity and mode of action of folliculogenic factor(s) are still unknown.

Bone/body morphogenetic proteins (BMP) are members of the transforming growth factor (TGF-β) family that control many developmental processes such as epithelial differentiation and tissue morphogenesis (Macias et al., 2015). Upon BMP ligand binding to its receptor, the intracellular signal transducers, Smad1/5/8 become activated by c-terminal phosphorylation. Phosphorylated Smad1/5/8 bind Smad4 and translocate to the nucleus where they regulate expression of target genes, such as *Id* genes. BMP also interacts with members of apico-basal polarity complex as exemplified by early events of neural tube closure (Eom et al., 2011). Loss of Twisted gastrulation gene, encoding a BMP modulator, causes craniofacial defects and affects foregut endoderm and reduced

expression of *Hhex*, a transcription factor required for early thyroid development (Petryk et al., 2004). Interestingly, reports on ES cell differentiation have shown that modulation of BMP signalling is critical for efficient lineage specification of Nkx2.1 endodermal progenitors (Green et al., 2011; Longmire et al., 2012). Since Smads often function redundantly, we studied the role of BMP signalling in the thyroid gland by combined genetic inactivation of Smad1 and Smad5. We found that Smad1/5^{dKO} mice have retarded growth, suffer from hypothyroidism and display a major perturbation in follicle formation. Defective follicle formation, highly reminiscent of that observed in Vegfa^{KO} mice, was associated with impaired assembly of basement membrane proteins and could be rescued by laminin-rich conditioned medium. Our results indicate that epithelial BMP-Smad1/5 signaling and endothelial cells of the thyroid promote folliculogenesis via assembly of the basement membrane.

Results

Active BMP signaling in thyrocyte progenitors during thyroid development

We first analyzed BMP signaling in thyroid development at the time of follicle formation (from E14.5 to E18.5). Several BMP ligands, among which *Bmp2*, *-4*, *-5* and *-7* were the most abundantly expressed (Fig. 1A). BMP type I and type II receptors, intracellular *Smad1, -5* and *-8* as well as the common mediator *Smad4*, were also well-expressed (Fig. 1A). Measurement of the absolute copy number of Smad1/5/8 in E14.5 thyroid glands (Fig. 1B) showed that *Smad8* mRNA is approximately four times less abundant than *Smad1* and *Smad5*.

We next assessed whether BMP signaling was active during thyroid development. We could not detect phosphorylated forms of Smad1/5/8 by immunolabeling of embryonic thyroid sections, but found that thyroid epithelial cells were BMP responsive. Indeed, treatment of microdissected E14.5 thyroid lobes with BMP4 induced Smad1/5/8 phosphorylation and nuclear translocation (Fig. 1C). We further recorded *in vivo* BMP signaling activity using a transgenic line expressing Green Fluorescent Protein (GFP) under the control of BMP Response Elements (Monteiro et al., 2008). At E14.5, GFP expression was restricted to elongated structures running along and in-between thyroid epithelial cell masses, likely endothelial cells from blood vessels. In contrast, non-polarized thyroid epithelial cells (E-cadherin+) did not show detectable GFP (Fig. 1D). One day later, GFP was detected in some thyroid epithelial cells, and by E16.5 in almost all of them. This indicated that BMP signaling was turned on in epithelial cells of developing thyroid between E14.5 and E15.5, i.e. at the start and during follicle formation.

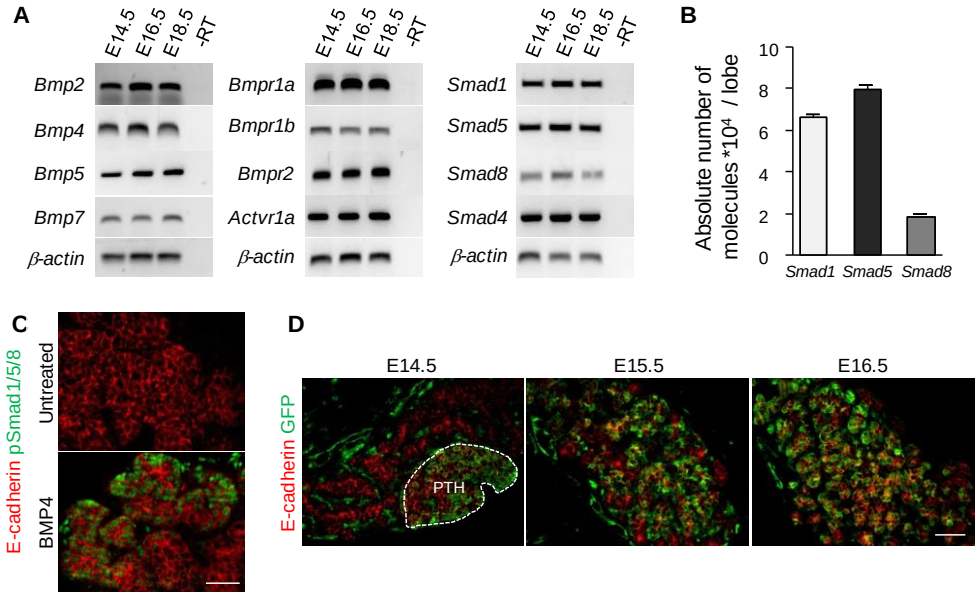

Figure 1. Active BMP signaling in thyrocyte progenitors during thyroid development. (A) *BMP ligands, receptors and Smad intracellular mediators are expressed in the thyroid during follicle formation, from E14.5 to E18.5. Bmp-2, -4, -5, -7 are the most abundant mRNAs in the thyroid (n≥3).* ***(B)*** *Absolute quantification of Smad1/5/8 mRNAs at the initiation of follicle development (E14.5) reveals that Smad1 and Smad5 are the most abundant intracellular mediators of BMP signaling in the thyroid (n≥3).* ***(C)*** *Detection of pSmad1/5/8 (green) is increased on sections of E14.5 explants treated for 30 min with 20 ng/ml BMP4, as compared to untreated samples.* ***(D)*** *Thyroid sections from BRE-GFP reporter mouse line reveal the presence of GFP (green) at E14.5 in blood vessels and parathyroid (PT, delineated by white dotted line) but not in immunolabeled thyroid epithelial cells (E-cadherin, red). From E.15.5 onwards, most epithelial cells of the developing thyroid display GFP activity. Data are presented as means ± S.E.M. Bar, 50 µm.*

Smad1/5^{dKO} mice display growth retardation, abnormal follicles and hypothyroidism

To determine the role of BMP signaling in the thyroid, we deleted the most abundant Smads, Smad1 and Smad5, in the thyroid by crossing mice with conditional alleles of Smad1 (Smad1$^{fl/fl}$) and Smad5 (Smad5$^{fl/fl}$) with Pax8-Cre mice (Bouchard et al., 2004). Single Smad1^{KO} and Smad5^{K0}, as well as double Smad1/5^{dKO} mice were viable and born at normal Mendelian ratios. Only Smad1/5^{dKO} displayed smaller body size and significantly reduced body weight at 10 weeks (Fig. 2A). Histological analysis of control thyroids at 10 weeks showed a collection of large follicles composed of a monolayer of epithelial cells delineating a round lumen (Fig. 2Ba). Single Smad1^{KO} and Smad5^{KO} looked comparable to the control thyroid, although follicles in Smad5^{KO} were somewhat smaller (Fig. 2Bb, Bc). In marked contrast, the thyroid structure of Smad1/5^{dKO} was completely disorganized with much fewer, irregular follicles delineated by taller thyrocytes (Fig. 2Bd). This was accompanied with adipogenesis in Smad1/5^{dKO} which occurred also to a lesser extent in Smad1^{KO} (data not shown). To evaluate thyroid function, we immunolabeled sections with iodinated thyroglobulin (Tg) using immunoperoxidase. This led to homogeneous staining filling the colloid of all follicles of control and single KO thyroids (Fig. 2Be-g). In Smad1/5^{dKO}, iodinated Tg was limited to a peripheral rim, suggesting colloid depletion (Fig. 2Bh). These data suggested that although some thyroid differentiation can occur in Smad1/5^{dKO}, functionality was dramatically affected. Because Smad1/5^{dKO} displayed growth-retardation and histological alterations of the thyroid glands, we next analyzed their thyroid hormonal status at 10 weeks. Plasma T_3 and T_4 concentrations were decreased by five-fold in Smad1/5^{dKO} (Fig. 2C), and accordingly, TSH concentrations were dramatically increased up to 20,000 fold (Fig. 2C). Thus, this major feedback response was insufficient to maintain plasma T_3 and T_4 concentrations (Fig. 2C), demonstrating thyroid unresponsiveness. Taken together, these data indicate that Smad1 and Smad5 are redundantly required for thyroid follicle formation and function.

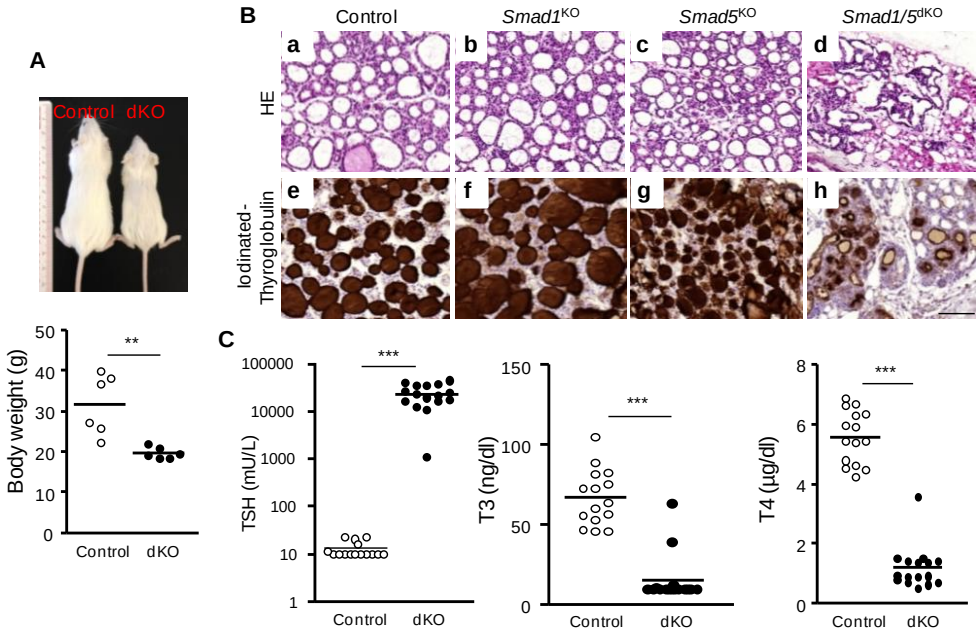

Figure 2. Smad1/5^{dKO} mice display growth retardation, abnormal follicles, and hypothyroidism. *Ten weeks-old single and double (d) KO mice were compared to age-matched control.* ***(A)*** *Smad1/5^{dKO} mice have smaller body size and lower body weight as compared to control.* ***(B)*** *H&E staining of control (a) Smad1^{KO} (b) and Smad5^{KO} (c) thyroids reveals abundant mature follicles lined with flat thyrocytes, while Smad1/5^{dKO} (d) thyroids exhibit severe disorganization of the thyroid parenchyma, with fewer and abnormal follicular structures lined with thicker thyrocytes suggesting high TSH level. Control (e), Smad1^{KO} (f) and Smad5^{KO} (g) thyroids show homogeneous and dense signal for iodinated-Tg in the colloid. (h) In the Smad1/5^{dKO}, iodinated-Tg is limited to a peripheral rim.* ***(C)*** *TSH, T_3 and T_4 concentrations were measured in plasma of control (open circles) and Smad1/5^{dKO} mice (filled circles) (n≥15). Most Smad1/5^{dKO} mice exhibit very high plasma or serum TSH and low T_3 and T_4. **p<0.001; ***p<0.0001 using Mann Whitney U test. Data are presented as means ± S.E.M. Bar, 100 µm.*

Smad1/5 are efficiently inactivated in thyrocytes progenitors

The severe follicular alterations and major hypothyroidism of adult Smad1/5^{dKO} mice suggested that follicle formation and/or differentiation might be affected in embryonic thyroid. We first verified Cre-mediated Smad1 and Smad5 recombination by measuring the abundance of *Smad1/5/8* mRNA during early stages of embryonic thyroid development (Fig. 3A). As compared to controls, Smad1/5^{dKO} thyroid showed a 50% reduction in the abundance of *Smad1* and *Smad5* mRNA as early as E14.5, and this reduction persisted until the end of gestation (Fig. 3A). As expected, *Smad8* expression was not affected at E14.5, but significantly decreased at E18.5, suggesting positive regulation by BMP-Smad1/5 signaling during thyroid development. Based on epithelial-specific Pax8-Cre expression, we hypothesized that the 50% global reduction in Smad1/5 reflected loss of expression in the developing thyrocytes but persistent expression in other cell types. Further, treating cultured thyroid lobes with BMP4 revealed phosphorylation of Smad1 and Smad5 in controls but not in a large majority of Smad1/5^{dKO} (Fig. 3B). These data indicate that Smad1/5 were successfully inactivated in thyroid epithelial cells and suggest that the remaining 50% expression is attributed to Smad1/5 presence in other cell types of the thyroid where the Cre is not active.

Smad1/5 inactivation impairs thyroid folliculogenesis

Follicle formation from an original mass of non-polarized epithelial cells involves a complex morphogenetic process starting around E14.5. Careful analysis of thyroid gland development reveals progressive fragmentation of the epithelial mass, organization of the epithelial cells in independent spherical structures or rosettes, acquisition of apico-basal polarity and finally lumen expansion (Fagman et al., 2006; Hick et al., 2013). To test when BMP signaling impacts on follicle formation, we analyzed thyroid development in control and Smad1/5^{dKO} mouse embryos from E14.5 to E18.5 (Fig. 3C, E). In controls, small clusters of the apical marker ezrin first became apparent in the thyroid mass at E14.5, just underneath or fused with the membrane of epithelial progenitors (Fig. 3Ca). These clusters could correspond to vesicles coated with ezrin and targeted to the membrane to initiate apical pole development. At this stage, the basal marker laminin was only found between thyroid peripheral cells and the stroma (Fig. 3Ea). At E16.5, coordinated

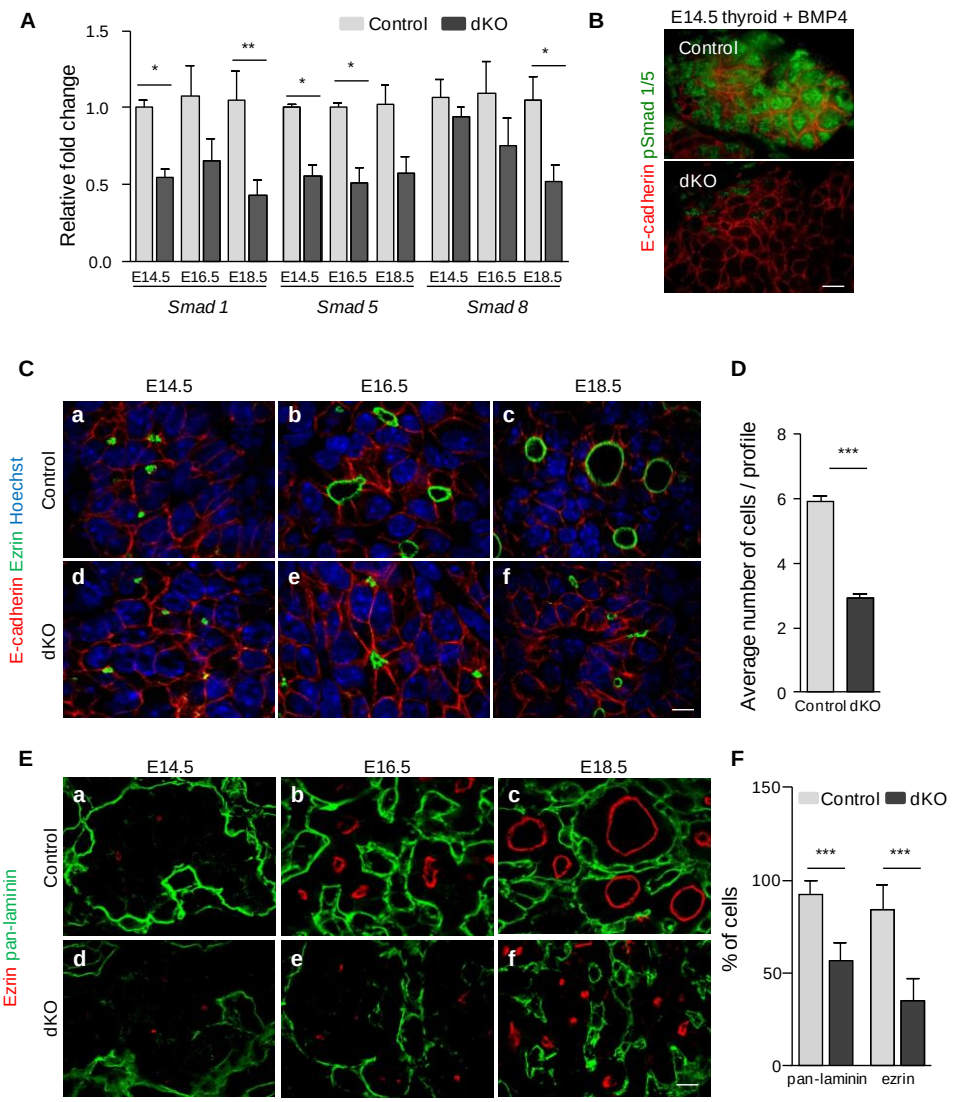

Figure 3. Smad1/5 are efficiently inactivated in thyrocyte progenitors. (A) *As compared to control thyroid lobes (grey bars), Smad 1/5^{dKO} (black bars) show a ~50% reduction in Smad1 and Smad5 mRNA levels from E14.5 onwards. Expression of Smad8 is affected at E18.5 (n≥5).* ***(B)*** *pSmad1/5 labeling reveals Smad activation in control, but not in Smad1/5^{dKO} thyroid lobes at E14.5 treated in parallel with 20 ng/ml of BMP4.* ***(C)*** *Organization of epithelial progenitor cells (E-cadherin; red) in monolayers surrounding a lumen (ezrin; green) is impaired in Smad1/5^{dKO} thyroid glands.* ***(D)*** *The number of cells per luminal profile of well-*

defined Par3^{+} structures (n≥13) is decreased by ~2-fold in thyroid glands of Smad1/5^{dKO} as compared to control. ***(E)*** *Defective apical (ezrin; red) and basal specification (pan-laminin; green) in Smad1/5^{dKO}, as compared to control thyroid glands* ***(F)****. The number of cells in contact with pan-laminin and with ezrin is decreased in Smad1/5^{dKO}. *p<0.05; ** p<0.001; *** p<0.0001 0001 using Mann Whitney U test. All mRNAs were normalized to RPL27. Data are presented as means ± S.E.M. Bar, 10 µm. See also Fig. S1 in the Supplementary materials.*

fusion of vesicles from several epithelial cells progressively separated cell membranes and delineated small lumina. Thyrocyte progenitors organized in pre-follicular structures progressively assembled a laminin-rich basement membrane, appearing as a dense meshwork, which fragmented the mass (Fig. 3Cb, Eb). By the end of gestation, follicular structures were individualized, i.e. completely surrounded by laminin and ezrin^{+} lumina had expanded (Fig. 3Cc, Ec). At E14.5 in the absence of Smad1 and Smad5, thyroid epithelial cells also contained small clusters of ezrin and the thyroid mass was delineated by laminin (Fig. 3Cd, Ed). Fusion of vesicles with the membrane occurred, but lumina of pre-follicular structures were smaller in Smad1/5^{dKO} at E16.5 (Fig. 3Ce, Ee). In addition, the percentage of epithelial cells showing ezrin^{+} membrane revealed a two-fold decrease (84% ± 13.8 *versus* 35% ± 11.7; Fig. 3F). Fragmentation of the thyroid mass of Smad1/5^{dKO} was also impaired: epithelial cells remained associated in large clusters and the percentage of epithelial cells in contact with pan-laminin was reduced (92% ± 7.7 *versus* 57% ± 9.5; Fig. 3F). At E18.5, the difference between control and Smad1/5^{dKO} was even more evident. Most epithelial cells remained associated, pre-follicular structures were composed of a reduced number of cells, only partially delineated by laminin and their lumen did not expand (Fig. 3Cf, Ef, D). Altogether, these results indicate that BMP signaling is essential for epithelial reorganization of the thyroid progenitor mass into individualized follicles with large lumina.

Despite the reduced number of ezrin^{+} epithelial cells and the smaller lumina, we noticed that ezrin was correctly localized to the apical pole in Smad1/5^{dKO}. This suggested that apical polarity was preserved. To further support this interpretation we analyzed control and Smad1/5^{dKO} thyroid for Par3, a key

component of the apical polarization machinery, and F-actin for cytoskeleton organization, and found no obvious difference between controls and Smad1/5^{dKO} (Fig. S1A). Furthermore, transmission electron microscopy revealed that the cells surrounding small lumina in Smad1/5^{dKO} still developed tight junctions and microvilli projecting into the lumen space, as in control follicles (Fig. S1B). However, intracellular microvilli inclusion bodies were observed in Smad1/5^{dKO}, suggesting defective apical delivery of intracellular vesicles (Fig. S1B, inset). Altogether, these data indicated that BMP-Smad signaling controls folliculogenesis downstream of the initial apical specification but upstream of basement membrane assembly, epithelial reorganization and lumen expansion.

Smad1/5 signaling in thyrocytes stimulates *Vegfa* expression and affects gene expression in neighboring endothelial cells

Previous work from our group has shown that endothelial cell recruitment into the developing thyroid is required for follicle formation. The folliculogenic effect of endothelial cells was contact-independent and could be mimicked with medium conditioned by endothelial cells (Hick et al., 2013). We thus tested whether defective folliculogenesis in Smad1/5^{dKO} could either be due to lack of endothelial cells, or of a signal derived therefrom. We identified endothelial cells by immunolabeling for PECAM, a cell adhesion molecule specifically expressed by endothelial cells, in control and Smad1/5^{dKO} thyroids from E14.5 to E18.5 (Fig. 4A). In control and Smad1/5^{dKO} thyroids abundance and localization of blood vessels were unaffected at the three stages analyzed (Fig. 4A). Quantification of endothelial surface and epithelial to endothelial surface ratio did not reveal any significant difference.

To evaluate endothelial cell differentiation in Smad1/5^{dKO}, we measured the expression of selected endothelial-specific genes. We found that expression of *vascular endothelial cadherin-1* (*Cdh5*) and *-2* (*Pcdh12*) as well as of *Tie1* was significantly reduced at E16.5 (Fig. 4B), but expression of *Vegfr2*, *Pecam1* and *endothelial cell-specific molecule 1* (*Esm1*) were normal. *Vegfa* controls endothelial cell development and BMP-Smad1/5 signaling is known to control *Vegfa* expression in several cell types (Bai et al., 2013; Shao et al., 2009); (Deckers et al., 2002); (Shimizu et al., 2012a). Therefore we measured *Vegfa* in developing Smad1/5^{dKO} thyroids and found that it was reduced starting at E14.5; this

reduction reached statistical significance starting at E16.5 (Fig. 4C). We thus directly analyzed the effect of BMP addition on *Vegfa* expression in E14.5 thyroid lobes and in the thyroid follicular cell line FRTL-5. Treatment of thyroid lobes with the specific BMP inhibitor, DMH1(Hao et al., 2010), led to a reduction in *Vegfa* expression and of the BMP-Smad1/5 signaling target gene *Id2* (Fig. 4D). Incubation of wild-type thyroid lobes with BMP ligands induced *Id2*, but did not modify the already high *Vegfa* expression (Hick et al., 2013). To circumvent BMP accessibility issue we incubated the thyroid cell line FRTL-5 with a combination of the most abundant BMP ligands in the thyroid (BMP2, -4, -5 and -7) and noticed a dose-dependent stimulation of the expression of *Vegfa* and *Id2* (Fig. 4E). These results indicated that epithelial Smad1/5 signaling regulates endothelial gene expression, potentially via VEGFa expression.

Figure 4. Normal blood vessel density but altered VEGFa and endothelial cell gene expression upon Smad1/5 inactivation. (A) *Immunolabeling for E-cadherin (red) and platelet endothelial cell adhesion molecule 1 (PECAM, green) reveals preserved blood vessel density in Smad1/5^{dKO} mice from E14.5 to E18.5.* ***(B)*** *Expression of endothelial VE-cadherin (Cdh5), Protocadherin 12 (Pcdh12) and Tyrosine Kinase with Immunoglobulin-like and EGF-like domains 1 (Tie1) are significantly reduced after epithelial inactivation of Smad1/5 at E16.5.* ***(C)*** *Vegfa expression is reduced in Smad 1/5^{dKO} thyroid (black bars) as compared to control (grey bars).* ***(D)*** *E14.5 thyroid lobes treated with 3 µM of the BMPR inhibitor, DMH1, for 16 hours have reduced Id2 and Vegfa mRNA levels.* ***(E)*** *Expression of Id2 and Vegfa in FRTL-5 cells is rapidly (8 hours) stimulated by a mix of BMP-2, -4, -5, -7 ligands in a dose-dependent manner. *p<0.05; ** p<0.001; *** p<0.0001 using Mann Whitney U test (n≥5). All mRNAs were normalized to either RPL27 or* β*-actin. Data are presented as means ± S.E.M. Bar, 50 µm.*

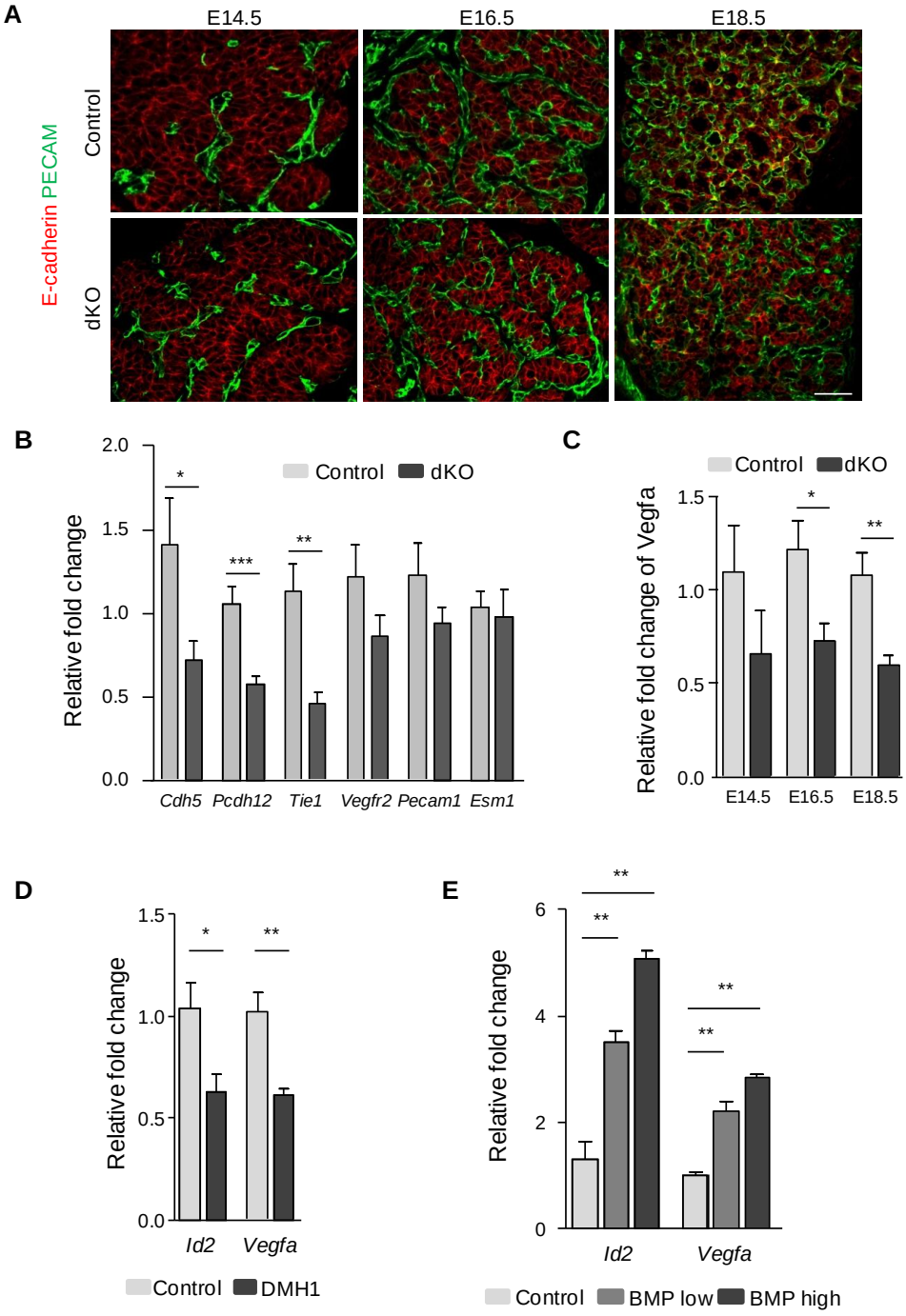
A
E14.5
E16.5
E18.5
Control
dKO
E-cadherin PECAM
B
Relative fold change
Control
dKO
Cdh5
Pcdh12
Tie1
Vegfr2
Pecam1
Esm1
C
Relative fold change of Vegfa
E14.5
E16.5
E18.5
D
Relative fold change
Id2
Vegfa
Control
DMH1
E
Relative fold change
Id2
Vegfa
Control
BMP low
BMP high

Production of the basement membrane proteins laminin and type IV collagen, is decreased in Smad1/5^{dKO} and Vegfa^{KO} thyroid glands

We next turned to the identification of the follicle promoting factor(s). Knowing that thyrocytes and endothelial cells form their own continuous basement membrane, that extracellular matrix components promote epithelial cell organization, and that contact with laminin was partly impaired in Smad1/5^{dKO}, we postulated that the basement membrane could stimulate folliculogenesis. We first looked for a possible defect of *laminin* and *type IV collagen* expression in Smad1/5^{dKO} and Vegfa^{KO} (Fig. S2). Laminins are a family of 5 α, 3 β and 3 γ chains forming αβγ heterotrimers that span the basement membrane. Collagen type IV family has 6 α chains forming trimers interconnected with the laminin network.

In Smad1/5^{dKO}, expression of *laminins* α*2*, α*3,* β*1* and β*3* chains were significantly albeit transiently reduced (Fig. S2A, B). Expression of laminin α3 and α4 was significantly reduced in Vegfa^{KO} (Fig. S2C). Of note, laminin α4 displays an endothelial-specific pattern in E16.5 embryos (Matrixome). A similar analysis revealed a reduction of most of *type IV collagen* genes in Smad1/5^{dKO} (Fig. S2D). There was an important and sustained reduction in *collagen* α*3-6 (IV)* chains. *Collagen* α*1(IV)* and α*2(IV)* were modestly reduced or delayed. In Vegfa^{KO}, expression of *collagen* α*1(IV)* and α*2(IV)* was significantly reduced (Fig. S2E); both genes being reportedly endothelial-specific (Matrixome). In conclusion, gene expression analysis revealed decreased expression of a number of basement membrane proteins in Smad1/5^{dKO} and Vegfa^{KO}.

We next examined by immunofluorescence staining whether decreased gene expression resulted in impaired basement membrane assembly. In line with the gene expression analysis, collagen type IV signals were severely affected in both KO (Fig 5Ab, d). Pan-laminin signals were also reduced in Smad1/5^{dKO} and only modestly in Vegfa^{KO} (Fig 5Af, h). Taken together, these data indicated that expression and/or deposition of basement membrane proteins depends on endothelial cells and Smad1/5 signaling in thyrocytes, and suggested an essential role for basement membrane assembly in folliculogenesis.

Epithelial laminin production is affected in Smad1/5^{dKO}

Mature angio-follicular units are characterized by the close proximity between endothelial and epithelial cells. To determine the respective contribution of epithelial and endothelial cells to basement membrane proteins synthesis, we analyzed the expression of laminin and collagen type IV genes in FACS-sorted epithelial population (Fig. S3). Epithelial thyrocyte progenitors were selected based on YFP expression after Pax8-cre mediated recombination of ROSA-STOP-YFP locus. This population was compared to YFP$^-$ cells, which thus included C-cells, endothelial and mesenchymal cells but also non-recombined thyrocyte progenitors. *Yfp* mRNA was only found in the YFP$^+$ cells. *Pax8* and the epithelial marker *E-cadherin* showed a two-fold enrichment in this population, while *Vegfr2* was enriched four-fold in the YFP$^-$ population as expected (Fig. S3A). mRNAs for all collagens type IV as well as *laminins* α*3*, β*1-3* and γ*1-2* were equally distributed in YFP$^+$ and YFP$^-$ thyroid cells. In contrast, *laminin* α*1* and α*5* chains were enriched in the YFP$^+$ epithelial population while *laminin* α*2* and α*4* chains showed a strongest expression in YFP$^-$ population (Fig. S3B).

Since laminins α1 and α5 were enriched in the epithelial population, we studied their expression by immunolabeling using specific antibodies. In control thyroid glands, epithelial follicular structures were surrounded by almost continuous laminin α1 and α5 signal. In Smad1/5^{dKO} thyroids, laminin α1 signal was severely reduced (Fig. 5B), supporting the RT-qPCR analysis (Fig. S2A). Laminin α5 signal was comparable to controls, although the pattern was affected due to epithelial organization defect (Fig. 5C). These data indicated that the basement membrane proteins, laminin and collagen type IV, are naturally produced by epithelial and endothelial cells of angio-follicular units, and that Smad1/5^{dKO} epithelial cells have impaired ability to produce and assemble laminin α1-containing heterotrimers.

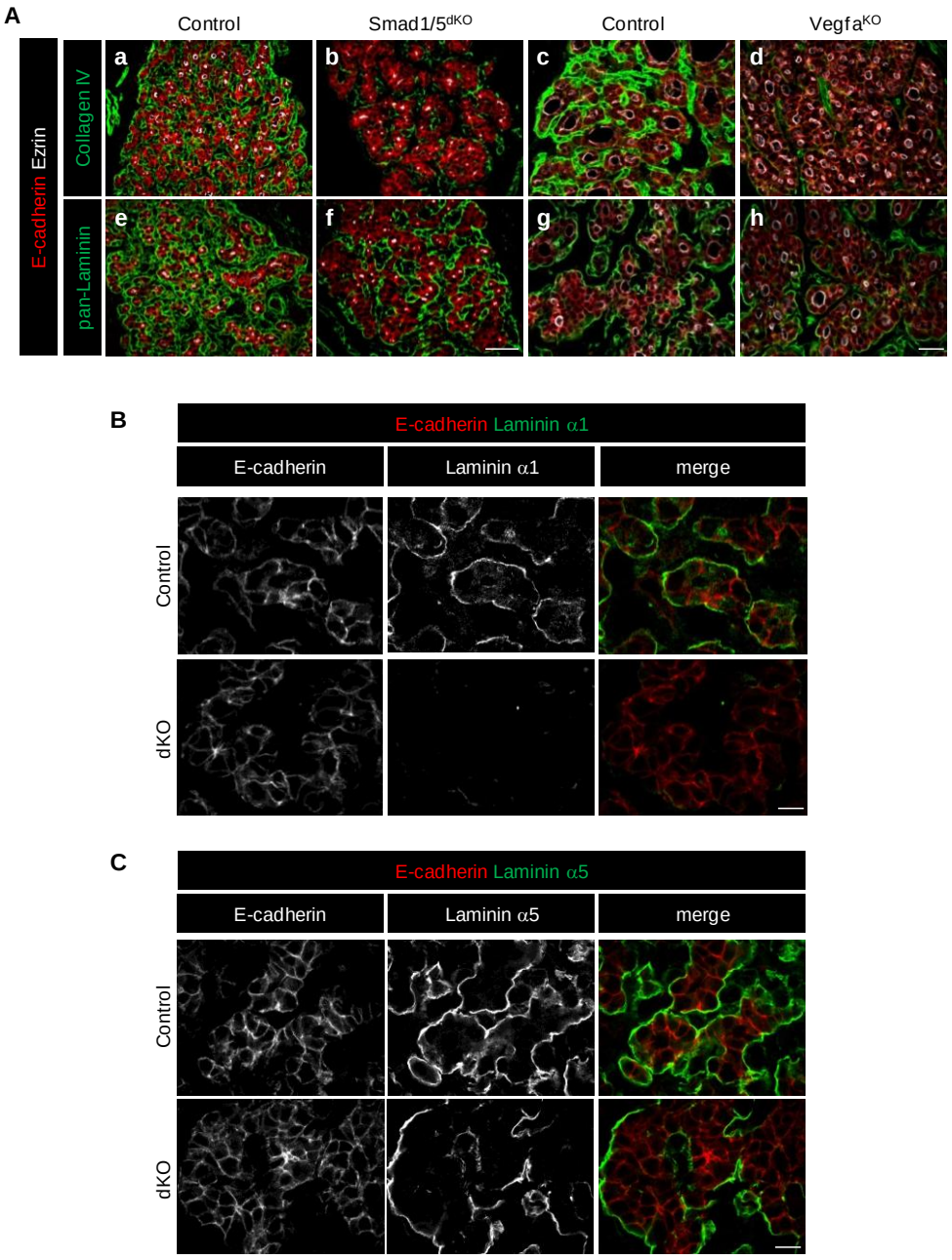

Figure 5. Production of the basement membrane proteins laminin and type IV collagen, is decreased in Smad1/5^{dKO} and in Vegfa^{KO} thyroid glands. *Thyroid gland sections from Smad1/5^{dKO} at E16.5 and Vegfa^{KO} at P0 were analyzed by*

immunolabeling for basement membrane markers and compared to age-matched control thyroid. ***(A)*** *Comparative multiplex immunolabeling for thyrocyte epithelial E-cadherin (red), polarity marker, ezrin (white) and basal markers, pan-laminin or type IV collagen (green). Type IV collagen signal is decreased in Smad1/5^{dKO} and Vegfa^{KO}. Pan-laminin signal shows subtle changes as compared to that in control mice. (**B**) Immunolabeling of laminin α1 (white, green), found around epithelial cells (E-cadherin; white, red) in control, is markedly decreased in Smad1/5^{dKO} at E16.5.* ***(C)*** *Immunolabelling of laminin α5 (white, green), found around epithelial cells (E-cadherin; white, red) in control is marginally affected in Smad1/5^{dKO} at E16.5. Bars, (A) 50 µm, (B, C) 10 µm. See also Fig.S2 and S3 in the Supplementary materials.*

Medium conditioned by endothelial cells contains folliculogenic factor(s) and rescues follicle formation defect of Smad1/5^{dKO} and Vegfa^{KO}

To investigate the mechanism of follicle formation, we resorted to an *ex vivo* culture system of thyroid lobes. Pharmacological depletion of endothelial cells in E12.5 thyroid explants prevents folliculogenesis. Addition of CM by embryonic endothelial progenitor cells (eEPC), herein referred to as eEPC-CM, can rescue and stimulate follicle formation (Hick et al., 2013). Using an improved thyroid lobe culture system (Delmarcelle et al., 2014), we now demonstrated that addition of eEPC-CM to wild-type thyroid lobes promotes follicle formation within 3 days of culture (Fig. 6A). This medium thus contains folliculogenic factor(s). We thus addressed whether eEPC-CM can rescue defective folliculogenesis of Smad1/5^{dKO} and Vegfa^{KO}. We first confirmed that E14.5 Smad1/5^{dKO} thyroid lobes have impaired follicle formation in *ex vivo* culture. Only very small ezrin^{+} structures could be observed in untreated Smad1/5^{dKO} lobes (Fig. 6B). Incubation of control thyroid lobes with eEPC-CM stimulated folliculogenesis up to six-fold (Fig. 6C). Most importantly, eEPC-CM significantly induced follicle formation not only in Smad1/5^{dKO} thyroid lobes (Fig. 6B, C), but also in Vegfa^{KO} (Fig. S4). We concluded that eEPC-CM contains folliculogenic factor(s) able to rescue the follicle formation defect of Smad1/5^{dKO} and Vegfa^{KO} thyroid glands, consistent with the model that eEPC-derived folliculogenic factor(s) act downstream of epithelial Smad1/5 signaling and of endothelial cells.

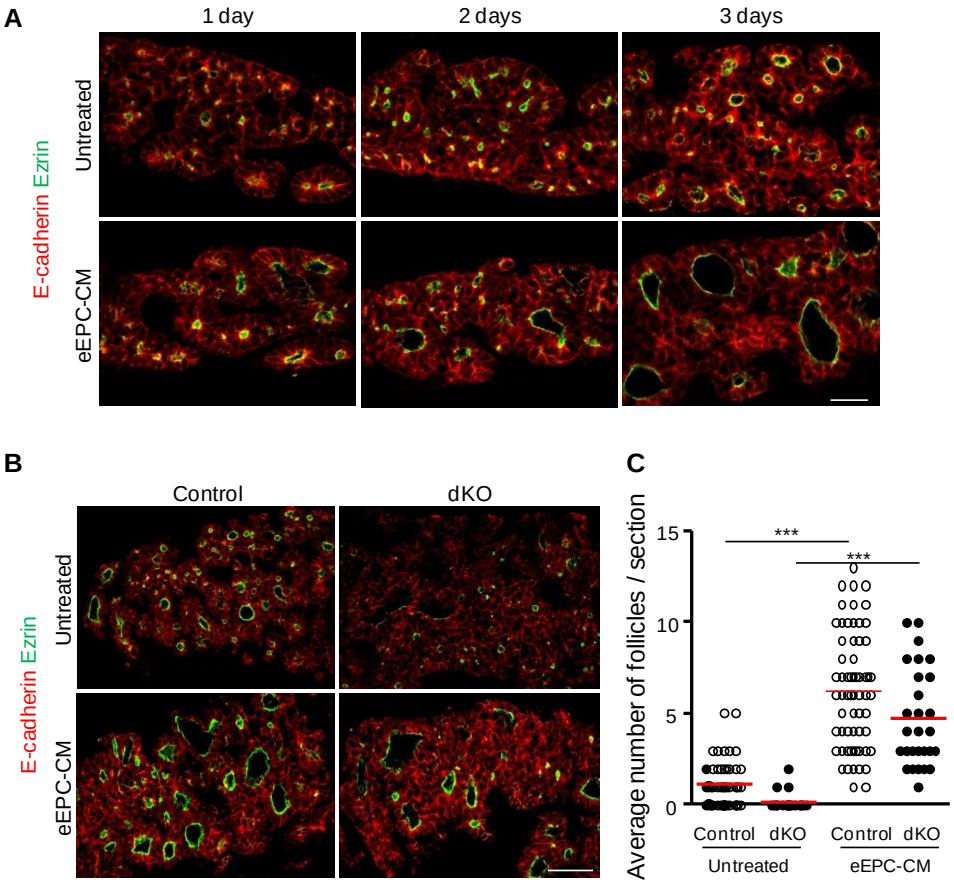

Figure 6. Medium conditioned by endothelial cells contains folliculogenic factor(s) and rescues follicle formation defect of Smad1/5^{dKO} and Vegfa^{KO}. (A) *Within 3 days of culture, epithelial cells (E-cadherin^{+}, red) from wild-type E14.5 thyroid lobes polarize apically (ezrin^{+}, green) and form small follicles. Addition of eEPC-CM to the culture stimulates polarization and follicle formation.* ***(B)*** *As compared to control, ezrin^{+} (green) structures are smaller in untreated Smad1/5^{dKO} thyroid lobes, but are enlarged when cultured with eEPC-CM.* ***(C)*** *The number of large ezrin^{+} luminal follicles per thyroid explants section was calculated. *** p<0.0001 using One-way ANOVA followed by Bonferroni's multiple comparison test (n≥23). Data are presented as means ± S.E.M. Bars, (A) 20 µm and (B) 50 µm. See also Fig. S4 in the Supplementary materials.*

Laminins deposited and assembled around thyroid epithelial cells, promote folliculogenesis

As the eEPC-CM can rescue folliculogenesis in these two thyroid mutants, we examined whether eEPC express and release basement membrane proteins in the medium. We first determined the expression of all laminin and collagen type IV genes in eEPC. We found that eEPC express very high level of *laminin* α*1,* β*1* and *γ1* mRNAs, which almost reached the level of β-*actin* housekeeping gene (Fig. 7A). Among collagen type IV genes, α*6* showed the highest level of expression, albeit approximately 1000X lower than *laminin* β*1*. To verify that eEPC can secrete laminins in the medium, most probably as laminin-111 (heterotrimer of α1, β1 and γ1), we analyzed eEPC-CM by silver staining, western blotting and mass spectrometry. Silver staining revealed a band migrating at a similar M*r* as purified laminin-111 (Fig. 7B). Western blotting with anti-laminin α1 antibody demonstrated that laminin α1 is detected in eEPC-CM (Fig. 7B). Mass spectrometry easily detected laminin α1, laminin β1 and laminin γ1 peptides in the CM (Table S1). Next, we asked whether laminin-111 from eEPC-CM was deposited on cultured E14.5 thyroid lobes. Immunolabeling for laminin α1 revealed a much stronger signal after 1 day of incubation with the CM, as compared to untreated explants. Laminin α1 signal further increased after 2 and 3 days of culture and became organized around epithelial structures (Fig. 7C). These data indicated that laminin-111, which is expressed and secreted by eEPC in the medium, can be assembled around epithelial structure of thyroid lobes.

To confirm that laminin-111 acts as a folliculogenic factor we inhibited its production in eEPC. Silencing of laminin α1 in eEPC by shRNA yielded CM with no folliculogenic activity on thyroid lobes (Fig. 7D, E), and no increased deposition of laminin α1 in thyroid lobes (Fig. 7E). Similar results were obtained with laminin β1 and laminin γ1 shRNAs (data not shown). These data indicated that laminin-111 in eEPC-CM is a key actor of thyroid folliculogenesis.

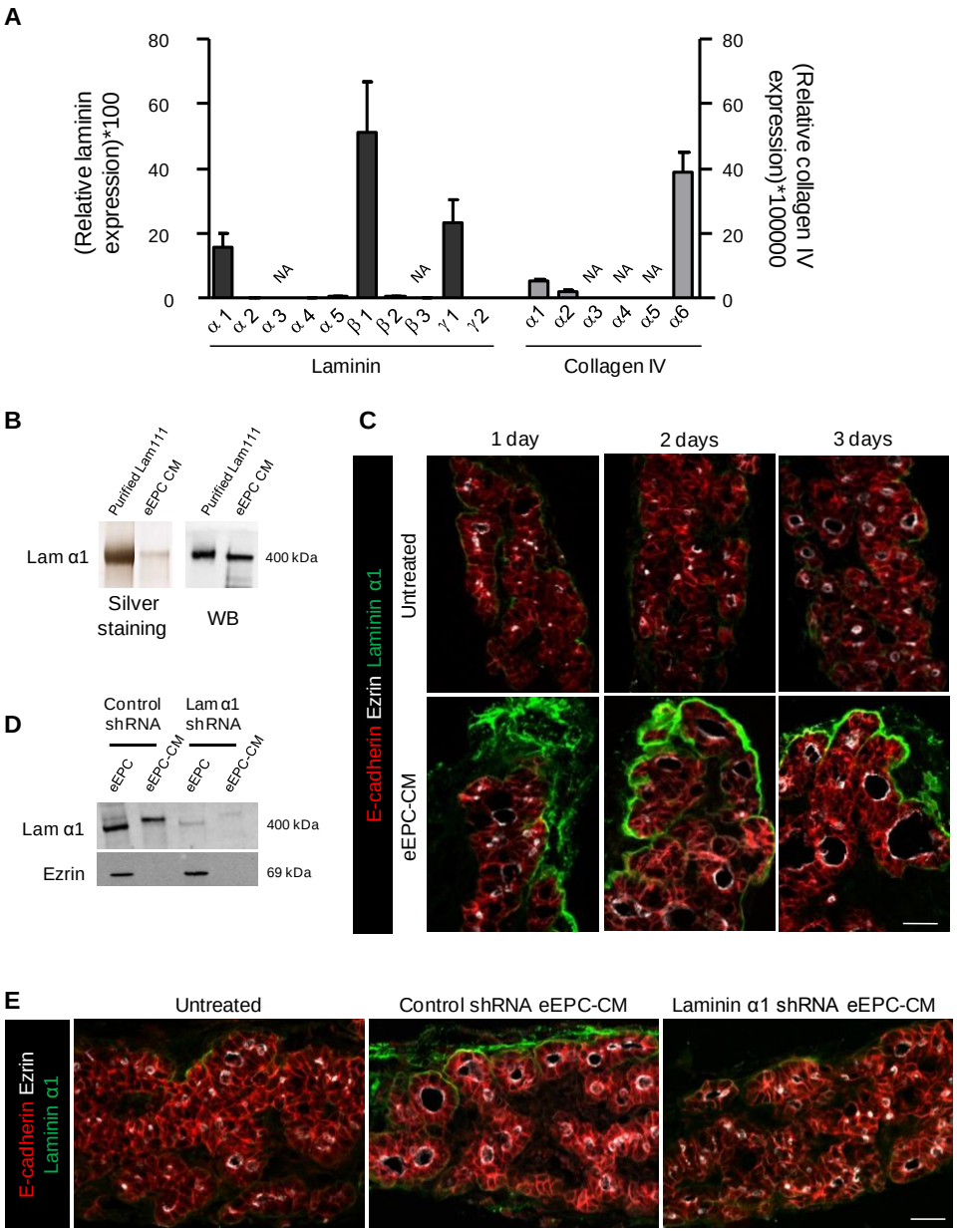

Figure 7. Laminins deposited and assembled around thyroid epithelial cells, promote folliculogenesis. (A) *eEPC cells express high level of selected laminin genes and much lower level of collagen IV genes. All mRNAs were normalized to* β*-actin. Data are presented as means ± S.E.M. (n≥3)* ***(B)*** *Laminin α1 (400 kDa) is*

secreted by eEPC and accumulates in eEPC-CM. ***(C)*** *E14.5 thyroid lobes cultured with eEPC-CM show intense signal for laminin α1 (green) around thyroid epithelial cells (E-cadherin, red), and larger follicles (ezrin, white) as compared to untreated lobes.* ***(D)*** *shRNA-mediated laminin α1 silencing in eEPC decreases laminin α1 in eEPC extract and CM, as compared to control shRNA. Ezrin is used as a loading control for eEPC extracts.* ***(E)*** *As compared to thyroid lobes cultured with control shRNA eEPC-CM, lobes cultured in the presence of CM from laminin α1 shRNA eEPC do not show laminin α1 deposition and have small follicles, similar to those of untreated lobes. Bar, 20 μm*.

Discussion

In this paper, we examined if and how BMP/Smad signalling is required for thyroid follicle formation. We found that BMP signalling was activated in thyroid epithelial cells at the time of follicle formation. Inactivation of Smad1/5 in thyroid epithelium caused major alterations of follicular structures, hypothyroidism and growth retardation but no loss of viability. Defective follicular formation was associated with impaired basement membrane assembly, and was highly reminiscent of the follicle formation defect of $Vegfa^{KO}$ embryos, in which endothelial cells are absent. Follicle formation defects in $Smad1/5^{dKO}$ and $Vegfa^{KO}$ could be rescued with laminin-rich conditioned medium. Taken together, our findings support a model in which thyroid follicle formation depends on basement membrane assembly, a process controlled by epithelial Smad1/5 signaling and endothelial cells.

Ten weeks old $Smad1/5^{dKO}$ were smaller and had a reduced body weight as compared to their control littermates. Failure to grow is readily explained by the very low levels of thyroid hormones, T_3 and T_4, and extremely high TSH values demonstrated non-compensated hypothyroidism. Thyroid unresponsiveness despite huge TSH values is well known in KOs mice for the TSH receptor, Nkx2.1, Foxe1 and Pax8 (De Felice and Di Lauro, 2004). Defects of folliculogenesis due to absence of Smad1 and Smad5, followed by thyroid involution with adipogenesis explain TSH unresponsiveness and emphasize the need for follicle formation for proper thyroid hormone production.

Our work reveals that follicle formation occurs by reorganization of the thyroid primordium epithelial cells mass into polarized monolayers surrounding a central lumen. This process is thus comparable to the cord hollowing model of *de novo* lumen formation (Andrew and Ewald, 2010) and apico-basal polarization during *de novo* lumen formation in MDCK cells cultured in matrigel. In this culture system, fusion of vesicles to the Apical Membrane Initiation Site (AMIS) allows apical lumen opening and cyst formation (Bryant et al., 2010). In thyroid, we also observed $ezrin^{+}$ intracellular vesicles and their exocytosis towards the center of cell clusters to generate apical lumen. However, *de novo* thyroid lumen formation *in vivo* requires concomitant individualization and vascularization of the pre-follicular structures or rosettes. In $Smad1/5^{dKO}$, $ezrin^{+}$ vesicles appeared, fused

with membranes, but fragmentation of the mass, individualization of pre-follicular structures and lumen expansion were affected, despite endothelial invasion.

Follicle formation defect observed in the absence of Smad1 and Smad5 is reminiscent of the defect observed in the absence of endothelial cells, upon Vegfa inactivation in thyroid epithelium (Hick et al., 2013). Although endothelial cell density in Smad1/5^{dKO} was comparable to that of control thyroid glands, expression of several endothelial cell identity markers (*Cdh5*, *Pcdh12* and *Tie1)* was impaired, consistent with reciprocal paracrine communications. BMP/Smad signaling in thyroid epithelial cells indeed controlled the expression of *Vegfa*. BMP are known to control *Vegfa* gene expression in different cell types (Bai et al., 2013; Deckers et al., 2002; Shao et al., 2009; Shimizu et al., 2012b) and this regulation can be positive or negative, as demonstrated in zebrafish for Smad1 and Smad5, respectively (He and Chen, 2005). BMP9 repressed VEGF expression during angiogenesis (Shao et al., 2009). BMP also directly influence endothelial cells. Functional deletion of BMP4 and the BMP type I receptor in mice impairs differentiation of mesoderm precursors, which are necessary for vascular development (Beets et al., 2013; Mishina et al., 1995; Winnier et al., 1995). Smad1^{KO} and Smad5^{KO} are embryonic lethal and exhibit angiogenesis defects (Lechleider et al., 2001; Yang et al., 1999). Smad1 and Smad5 have been implicated in endothelial cell "fate" decision during angiogenesis (Moya et al., 2012). Our findings in developing thyroid suggest instead that BMPs could control endothelial gene expression program indirectly, at least by regulating *Vegfa* expression. Besides decreased expression of several endothelial cell identity markers, few endothelial-enriched basement membrane proteins (*type IV collagen α1*, α*2* and *laminin α3*) were also affected. Collagen α1 and α2 indeed showed an endothelial-specific expression pattern (Matrixome), and expression of collagen α1, α2 and laminin α3 was also decreased in Vegfa^{KO}, i.e. in the absence of endothelial cells. Gene expression changes in endothelial cells could in turn impact on follicle formation. Several studies have emphasized the critical role played by endothelial cells via angiocrine factors in the regulation of organ morphogenesis (Ramasamy et al., 2015). Taken together, this supports a reciprocal paracrine communication in which thyrocyte progenitors, under the influence of BMP, participate in the maturation of thyroid endothelial cells via VEGFa. In turn, endothelial cells could modify thyroid environment, at least by

producing their own basement membrane proteins, which facilitate folliculogenesis.

Defective follicle formation in both $Vegfa^{KO}$ and $Smad1/5^{dKO}$ was rescued by CM containing laminin-111. Although only $Smad1/5^{dKO}$ showed reduced laminin α1 expression, the expression and assembly of type IV collagen was significantly affected both in $Smad1/5^{dKO}$ and $Vegfa^{KO}$. Besides laminins, type IV collagens are essential for integrity, stability and functionality of the basement membrane (Poschl et al., 2004; Yurchenco, 2011). Since laminin deposition is indeed a primary event in basement membrane formation and triggers assembly of a type IV collagen network (Morrissey and Sherwood, 2015; Poschl et al., 2004), we suggest that exogenous laminin-111 stimulated the organization of epithelial cells in follicles in control thyroids and rescued follicle formation defect in $Smad1/5^{dKO}$ and $Vegfa^{KO}$ by promoting assembly of endogenous laminins and type IV collagens scaffold.

The importance of the extracellular environment for cell polarization in tissue culture experiments has long been recognized (Wang et al., 1990a; Wang et al., 1990b). Culture of epithelial cells such as the MDCK (Madin-Darby Canine Kidney) in collagen-rich gel or matrigel triggers production of laminin and assembly of a basement membrane, then formation of cystic structures, which can be directly compared to thyroid follicles (Bryant et al., 2010). Moreover, ES cells, forced to transiently co-express Pax8 and Nkx2.1 transcription factors, differentiate into thyrocytes progenitors that can form functional follicles when further cultured in matrigel (Antonica et al., 2012; Ma et al., 2015). These *in vitro* studies support the critical role of basement membrane and extracellular matrix proteins in development of a 3D, cyst-like, follicular structure.

In vivo, we observed reduced expression and immunoreactivity on sections from $Smad1/5^{dKO}$ for laminin α1 and collagen type IV. Few reports have suggested a direct role for BMP signaling in basement membrane synthesis and deposition. During ductus arteriosus closure BMP9 and BMP10 are required to stimulate endothelial cell differentiation and extracellular matrix deposition (Levet et al., 2015). Smad1 directly controls the expression of collagen type IV α1 and α2, and in mesangial cells this leads to glomerular basement membrane thickening (Abe et al., 2004; Matsubara et al., 2015). Thus, cumulative evidences

indicate that BMP and Smad can regulate tissue morphogenesis by controlling expression and/or deposition of extracellular matrix proteins.

In conclusion, we present evidence that BMP-Smad signaling is essential in thyrocyte progenitors for follicle formation, together with endothelial cells. Besides positively controlling *Vegfa* expression, and indirectly endothelial-specific gene expression, epithelial BMP signaling also regulate the expression and assembly of laminins and type IV collagens. Altogether, we propose that epithelial BMP-Smad signaling and endothelial cells control thyroid follicle formation via basement membrane production.

Materials and Methods

Animals

Smad1/5-floxed, Vegfa-floxed, Pax8-Cre and BRE-YFP mice were obtained from A. Zwijsen and E.J. Robertson (Arnold et al., 2006; Umans et al., 2003), N. Ferrara (Genentech) (Gerber et al., 1999), M. Busslinger (Bouchard et al., 2004) and S.M. Chuva de Sousa Lopes (Monteiro et al., 2008), respectively. All other mice were of the CD1 strain. Mice were raised and treated according to the guidelines of laboratory animal care of the University Animal Welfare Committee, UCL.

Dissection and culture of thyroid explants

Thyroid lobes were microdissected from E14.5 mouse embryos and processed as described (Delmarcelle et al., 2014). DMH1 (Sigma-Aldrich) was dissolved in DMSO and used at 3 or 10 µM. Recombinant mouse BMP4 (R&D Systems) was reconstituted at 100 µg/ml in 4 mM HCl containing 0.1% BSA and added at 20 ng/ml in the culture medium. Control explants were exposed to the same concentration of vehicle as the test samples. Thyroid lobes were maintained in culture during 3 or 4 days, and processed for RNA extraction and immunolabeling as described (Delmarcelle et al., 2014).

Histology, Oil Red O, immunolabeling and morphometric analyses

Thyroids were microdissected and fixed for 1 hour with 4% formaldehyde in PBS and processed for paraffin embedding. 8 µm-thick sections were stained with hematoxylin and eosin staining. Immunofluorescence on sections thyroid gland sections from embryos or explants was performed as described previously (Pierreux et al., 2006) . Antibodies and dilutions are shown in Table S2. Nuclei were counterstained with Hoechst (Sigma) in PBS during incubation with secondary antibody. For immunoperoxidase, the envision system (Dako) was used. Whole histological sections were recorded with Mirax Scan (Zeiss). Fluorescence on sections was observed with a Zeiss Cell Axiovert 200 inverted fluorescence microscope or with a Zeiss Cell Observer Spinning Disk (COSD). For quantification of follicles, at least 18 sections in 4 independent explants were counted. Endothelial and epithelial surface was quantified using the Axiovision 4.8.2 software (Zeiss). Briefly, images were prepared as binary mask, filled and the

surface area was calculated on 6 images/sections spanning 360 µm of 3 controls and 3 Smad1/5^{dKO} thyroids. The epithelial: endothelial surface ratio was finally calculated.

T3, T4 and TSH level measurements

T_3 and T_4 concentrations were measured by coated-tube RIA (Siemens Medical Solution Diagnostics). Plasma Thyroid-stimulating hormone (TSH) concentrations were measured using a sensitive, heterologous, disequilibrium double-antibody precipitation RIA as described previously (Pohlenz et al., 1999). Hormone levels were measured in 16 female and 15 male mice.

RNA extraction and Real-time RT-PCR

Total RNA was extracted from microdissected thyroid lobes, cultured explants or FRTL-5 cells using Trizol reagent and phenol/chloroform extraction (Delmarcelle et al., 2014). RNA (0.5–1 µg) was reverse-transcribed with random hexamers using Moloney Murine Leukemia Virus reverse transcriptase (Invitrogen). Real-time quantitative PCR was performed by using KAPA^{TM} SYBR® Fast qPCR kit (Sopachem). Primers sequences are described in Table S3. β-*actin* and *RPL27* were used as reference genes and relative changes in target gene/reference gene mRNA ratio were determined by transformation of threshold cycles to absolute mRNA numbers (Dupasquier et al., 2014) or using the ΔΔCt method.

Endothelial progenitor cells (EPCs) conditioned medium (CM)

Previously established mouse embryonic EPCs (Hatzopoulos et al., 1998; Kupatt et al., 2005) were used for no more than 6 months after being thawed, as described (Sbaa et al., 2006). The preparation of CM was adapted from (Hick et al., 2013). Briefly, 90% confluent cells were incubated for 24 h in M199 medium without serum (6 ml for a 7.8 cm^2 dish). Supernatant was first centrifuged at 1900 *g* for 5 min to remove floating cells or large debris, then at 17000 *g* for 20 min and finally concentrated 10-x by centrifugation at 1900 *g* for 5 min in Amicon Ultra 50K units. 10-x concentrated medium was supplemented with 10% FCS before use. Mass spectrometry was performed as described (Cho et al., 2014).

Cell culture

Fisher rat thyroid follicular FRTL-5 cells (Sigma) were cultured in Coon's modified F12 medium as previously described (Craps et al., 2015) and were used within 6 months of purchase. Cells were grown in 12-well tissue culture dishes for 24 h before treatment with BMP ligands. Recombinant mouse BMP 2, -4, -5 and -7 (R&D Systems) were reconstituted in 4 mM HCl containing 0.1% BSA at 100 – 150 µg/ml and used as a mix of 25 ng/ml (BMP2), 5 ng/ml (BMP4), 150 ng/ml (BMP5) and 75 ng/ml (BMP7). After 8 h, cells were lysed in Trizol reagent and RNA was extracted.

Lentiviral infection

Lentiviral constructs driving expression of shRNA against laminin α1 were generated as described previously (Gerin et al., 2010). Briefly, the pGIPZ lentiviral vectors containing a shRNA against laminin α1, α5, β1 and γ1 or the pGIPZ empty vector (Openbiosystems) were transfected in HEK293T for lentiviral production. Packaging was performed using a second generation plasmid system (psPAX2 and pMD2.G; Addgene plasmids 12,259 and 12,260, respectively) by transient transfection with the calcium phosphate co-precipitation method. We used 8.4 µg of lentiviral vectors, 8.4 µg of psPAX2 and 4.2 µg of pMD2.G per 6-cm tissue culture dish. After 24 h of transfection, EPC cells were infected with filtrated lentiviral particles and 4mg/ml of Polybrene (Sigma). Infected cells were selected for 4 days with 2 µg/ml of puromycin (Merck). CM was prepared as above.

Western blotting

Western blotting was performed as described (Cominelli et al., 2014). Briefly, cells were lysed in RIPA buffer and protein concentration was measured using bicinchoninic acid. 30 µg of cell protein extract or a corresponding volume of 10-x CM was loaded with 2% SDS and 10 mM DTT sample buffer on 5% polyacrylamide gels (4% stacking gel), resolved by SDS-PAGE and transferred onto PVDF membrane (Polyscreen ® PVDF Transfer Membrane, Perkin Elmer). Blots were blocked and incubated overnight at 4°C with the primary antibody (rabbit anti-laminin α1, 1/1000, gift from Takako Sasaki; mouse anti-ezrin, 1/1000, Thermo Scientific). After washes and incubation with the appropriate secondary antibody, immunoreactive bands were visualized using chemiluminescence (Supersignal

West Femto Maximum sensitivity substrate mixed with Supersignal West Pico chemiluminescent substrate, Thermo Scientific) and acquired using a 2000MM Kodak Image Station (Eastman Kodak Co.). For silver staining, gels are stained using the Silverquest Staining Kit (Invitrogen).

Electron microscopy

Control and Smad1/5^{dKO} thyroid lobes were rinsed with 155 mM NaCl, fixed by 2% (v/v) glutaraldehyde in 0.1 M sodium cacodylate buffer, pH 7.4 for 30 min at 4^{o}C and washed thrice with 50 mM Tris-HCl, pH 6.0 for 10 min. Cells were post-fixed with 1% (w/v) OSO_4-2%KFe(CN)6 solution (reduced osmium) and stained "en bloc" with 1% uranyl acetate for 2 h and pelleted in 2% agar. Pellets were dehydrated in graded ethanol and embedded in Spurr. Ultrathin (70 nm nominal) sections were obtained with a Reichert ultramicrotome (Reichert), collected on rhodanium 400 mesh grids and contrasted with 3% uranyl acetate followed by lead citrate, each for 10 min. Grids were washed with water, dried, and analyzed in a FEI CM12 electron microscope operating at 80 kV.

Statistics

Sample size was defined based on previous expertise. Mann Whitney U test and One-way ANOVA followed by Bonferroni's multiple comparison tests were performed using Prism software.

Acknowledgements:

We thank T. Sasaki for purified laminin and antibodies, J. Miner for anti-laminin antibodies and Ris-Stalpers for iodo-thyroglobulin antibody. We also thank J-F. Collet and D. Vertommen for biochemical assistance, J. Craps for the FRTL-5 cell line, S. Costagliola and S. Ascenzo for discussions and S. Cordi for technical advices. This work was supported in part by grants from F.R.S.-FNRS, ARC, Fondation Roi Baudouin, Interuniversity Attraction Poles-Phase VII [IUAP/PAI P7/14], Belgium and DK15070 from the National Institutes of Health, USA. MV was supported by FSR-UCL, ASD by Télévie, and GB and CEP are Research Associate of the F.R.S.-FNRS.

Author Contributions

MV and ASD designed and performed the experiments and wrote the manuscript. ML, MB, JB, LU, PVDS and SR performed experiments. SCSL provided the BRE mouse line. TS, GB, FL, SR, AZ and PC contributed intellectually and edited the manuscript. CEP conceived the project, contributed experimental and intellectual advice and edited the manuscript.

Conflict of Interest

The authors declare that they have no conflict of interest.

References

Abe, H., Matsubara, T., Iehara, N., Nagai, K., Takahashi, T., Arai, H., Kita, T. and Doi, T. (2004). Type IV collagen is transcriptionally regulated by Smad1 under advanced glycation end product (AGE) stimulation. *J Biol Chem* **279**, 14201-14206.

Antonica, F., Kasprzyk, D. F., Opitz, R., Iacovino, M., Liao, X. H., Dumitrescu, A. M., Refetoff, S., Peremans, K., Manto, M., Kyba, M., et al. (2012). Generation of functional thyroid from embryonic stem cells. *Nature* **491**, 66-71.

Bai, Y., Wang, J., Morikawa, Y., Bonilla-Claudio, M., Klysik, E. and Martin, J. F. (2013). Bmp signaling represses Vegfa to promote outflow tract cushion development. *Development* **140**, 3395-3402.

Beets, K., Huylebroeck, D., Moya, I. M., Umans, L. and Zwijsen, A. (2013). Robustness in angiogenesis: notch and BMP shaping waves. *Trends Genet* **29**, 140-149.

Bouchard, M., Souabni, A. and Busslinger, M. (2004). Tissue-specific expression of cre recombinase from the Pax8 locus. *Genesis* **38**, 105-109.

Bryant, D. M., Datta, A., Rodriguez-Fraticelli, A. E., Peranen, J., Martin-Belmonte, F. and Mostov, K. E. (2010). A molecular network for de novo generation of the apical surface and lumen. *Nat Cell Biol* **12**, 1035-1045.

Cho, S. H., Szewczyk, J., Pesavento, C., Zietek, M., Banzhaf, M., Roszczenko, P., Asmar, A., Laloux, G., Hov, A. K., Leverrier, P., et al. (2014). Detecting envelope stress by monitoring beta-barrel assembly. *Cell* **159**, 1652-1664.

Colin, I. M., Denef, J. F., Lengele, B., Many, M. C. and Gerard, A. C. (2013). Recent insights into the cell biology of thyroid angiofollicular units. *Endocr Rev* **34**, 209-238.

Cominelli, A., Gaide Chevronnay, H. P., Lemoine, P., Courtoy, P. J., Marbaix, E. and Henriet, P. (2014). Matrix metalloproteinase-27 is expressed in CD163+/CD206+ M2 macrophages in the cycling human endometrium and in superficial endometriotic lesions. *Mol Hum Reprod* **20**, 767-775.

Costello, I., Biondi, C. A., Taylor, J. M., Bikoff, E. K. and Robertson, E. J. (2009). Smad4-dependent pathways control basement membrane deposition and endodermal cell migration at early stages of mouse development. *BMC Dev Biol* **9**, 54.

De Felice, M. and Di Lauro, R. (2004). Thyroid development and its disorders: genetics and molecular mechanisms. *Endocr Rev* **25**, 722-746.

Deckers, M. M., van Bezooijen, R. L., van der Horst, G., Hoogendam, J., van Der Bent, C., Papapoulos, S. E. and Lowik, C. W. (2002). Bone morphogenetic proteins stimulate angiogenesis through osteoblast-derived vascular endothelial growth factor A. *Endocrinology* **143**, 1545-1553.

Delmarcelle, A. S., Villacorte, M., Hick, A. C. and Pierreux, C. E. (2014). An ex vivo culture system to study thyroid development. *J Vis Exp*.

Eom, D. S., Amarnath, S., Fogel, J. L. and Agarwala, S. (2011). Bone morphogenetic proteins regulate neural tube closure by interacting with the apicobasal polarity pathway. *Development* **138**, 3179-3188.

Fagman, H., Andersson, L. and Nilsson, M. (2006). The developing mouse thyroid: embryonic vessel contacts and parenchymal growth pattern during specification, budding, migration, and lobulation. *Dev Dyn* **235**, 444-455.

Fagman, H. and Nilsson, M. (2010). Morphogenesis of the thyroid gland. *Mol Cell Endocrinol* **323**, 35-54.

Gao, Y., Duran, S., Lydon, J. P., DeMayo, F. J., Burghardt, R. C., Bayless, K. J., Bartholin, L. and Li, Q. (2015). Constitutive activation of transforming growth factor Beta receptor 1 in the mouse uterus impairs uterine morphology and function. *Biol Reprod* **92**, 34.

Gerber, H. P., Hillan, K. J., Ryan, A. M., Kowalski, J., Keller, G. A., Rangell, L., Wright, B. D., Radtke, F., Aguet, M. and Ferrara, N. (1999). VEGF is required for growth and survival in neonatal mice. *Development* **126**, 1149-1159.

Gerin, I., Clerbaux, L. A., Haumont, O., Lanthier, N., Das, A. K., Burant, C. F., Leclercq, I. A., MacDougald, O. A. and Bommer, G. T. (2010). Expression of miR-33 from an SREBP2 intron inhibits cholesterol export and fatty acid oxidation. *J Biol Chem* **285**, 33652-33661.

Green, M. D., Chen, A., Nostro, M. C., d'Souza, S. L., Schaniel, C., Lemischka, I. R., Gouon-Evans, V., Keller, G. and Snoeck, H. W. (2011). Generation of anterior foregut endoderm from human embryonic and induced pluripotent stem cells. *Nat Biotechnol* **29**, 267-272.

He, C. and Chen, X. (2005). Transcription regulation of the vegf gene by the BMP/Smad pathway in the angioblast of zebrafish embryos. *Biochem Biophys Res Commun* **329**, 324-330.

Hick, A. C., Delmarcelle, A. S., Bouquet, M., Klotz, S., Copetti, T., Forez, C., Van Der Smissen, P., Sonveaux, P., Collet, J. F., Feron, O., et al. (2013). Reciprocal epithelial:endothelial paracrine interactions during thyroid development govern follicular organization and C-cells differentiation. *Dev Biol* **381**, 227-240.

Kogai, T., Endo, T., Saito, T., Miyazaki, A., Kawaguchi, A. and Onaya, T. (1997). Regulation by thyroid-stimulating hormone of sodium/iodide symporter gene expression and protein levels in FRTL-5 cells. *Endocrinology* **138**, 2227-2232.

Koh, W., Mahan, R. D. and Davis, G. E. (2008). Cdc42- and Rac1-mediated endothelial lumen formation requires Pak2, Pak4 and Par3, and PKC-dependent signaling. *J Cell Sci* **121**, 989-1001.

Lammert, E., Cleaver, O. and Melton, D. (2001). Induction of pancreatic differentiation by signals from blood vessels. *Science* **294**, 564-567.

Lazarus, A., Del-Moral, P. M., Ilovich, O., Mishani, E., Warburton, D. and Keshet, E. (2011). A perfusion-independent role of blood vessels in determining branching stereotypy of lung airways. *Development* **138**, 2359-2368.

Lechleider, R. J., Ryan, J. L., Garrett, L., Eng, C., Deng, C., Wynshaw-Boris, A. and Roberts, A. B. (2001). Targeted mutagenesis of Smad1 reveals an essential role in chorioallantoic fusion. *Dev Biol* **240**, 157-167.

Levet, S., Ouarne, M., Ciais, D., Coutton, C., Subileau, M., Mallet, C., Ricard, N., Bidart, M., Debillon, T., Faravelli, F., et al. (2015). BMP9 and BMP10 are necessary for proper closure of the ductus arteriosus. *Proc Natl Acad Sci U S A* **112**, E3207-3215.

Longmire, T. A., Ikonomou, L., Hawkins, F., Christodoulou, C., Cao, Y., Jean, J. C., Kwok, L. W., Mou, H., Rajagopal, J., Shen, S. S., et al. (2012). Efficient derivation of purified lung and thyroid progenitors from embryonic stem cells. *Cell Stem Cell* **10**, 398-411.

Ma, R., Latif, R. and Davies, T. F. (2015). Human embryonic stem cells form functional thyroid follicles. *Thyroid* **25**, 455-461.

Macias, M. J., Martin-Malpartida, P. and Massague, J. (2015). Structural determinants of Smad function in TGF-beta signaling. *Trends Biochem Sci* **40**, 296-308.

Matsubara, T., Araki, M., Abe, H., Ueda, O., Jishage, K., Mima, A., Goto, C., Tominaga, T., Kinosaki, M., Kishi, S., et al. (2015). Bone Morphogenetic

Protein 4 and Smad1 Mediate Extracellular Matrix Production in the Development of Diabetic Nephropathy. *Diabetes* **64**, 2978-2990.

Mishina, Y., Suzuki, A., Ueno, N. and Behringer, R. R. (1995). Bmpr encodes a type I bone morphogenetic protein receptor that is essential for gastrulation during mouse embryogenesis. *Genes Dev* **9**, 3027-3037.

Monteiro, R. M., de Sousa Lopes, S. M., Bialecka, M., de Boer, S., Zwijsen, A. and Mummery, C. L. (2008). Real time monitoring of BMP Smads transcriptional activity during mouse development. *Genesis* **46**, 335-346.

Morrissey, M. A. and Sherwood, D. R. (2015). An active role for basement membrane assembly and modification in tissue sculpting. *J Cell Sci* **128**, 1661-1668.

Moya, I. M., Umans, L., Maas, E., Pereira, P. N., Beets, K., Francis, A., Sents, W., Robertson, E. J., Mummery, C. L., Huylebroeck, D., et al. (2012). Stalk cell phenotype depends on integration of Notch and Smad1/5 signaling cascades. *Dev Cell* **22**, 501-514.

Nilsson, M. and Fagman, H. (2013). Mechanisms of thyroid development and dysgenesis: an analysis based on developmental stages and concurrent embryonic anatomy. *Curr Top Dev Biol* **106**, 123-170.

Nolan, D. J., Ginsberg, M., Israely, E., Palikuqi, B., Poulos, M. G., James, D., Ding, B. S., Schachterle, W., Liu, Y., Rosenwaks, Z., et al. (2013). Molecular signatures of tissue-specific microvascular endothelial cell heterogeneity in organ maintenance and regeneration. *Dev Cell* **26**, 204-219.

Petryk, A., Anderson, R. M., Jarcho, M. P., Leaf, I., Carlson, C. S., Klingensmith, J., Shawlot, W. and O'Connor, M. B. (2004). The mammalian twisted gastrulation gene functions in foregut and craniofacial development. *Dev Biol* **267**, 374-386.

Pierreux, C. E., Cordi, S., Hick, A. C., Achouri, Y., Ruiz de Almodovar, C., Prevot, P. P., Courtoy, P. J., Carmeliet, P. and Lemaigre, F. P. (2010). Epithelial: Endothelial cross-talk regulates exocrine differentiation in developing pancreas. *Dev Biol* **347**, 216-227.

Pierreux, C. E., Poll, A. V., Kemp, C. R., Clotman, F., Maestro, M. A., Cordi, S., Ferrer, J., Leyns, L., Rousseau, G. G. and Lemaigre, F. P. (2006). The transcription factor hepatocyte nuclear factor-6 controls the development of pancreatic ducts in the mouse. *Gastroenterology* **130**, 532-541.

Pohlenz, J., Maqueem, A., Cua, K., Weiss, R. E., Van Sande, J. and Refetoff, S. (1999). Improved radioimmunoassay for measurement of mouse thyrotropin in serum: strain differences in thyrotropin concentration and thyrotroph sensitivity to thyroid hormone. *Thyroid* **9**, 1265-1271.

Poschl, E., Schlotzer-Schrehardt, U., Brachvogel, B., Saito, K., Ninomiya, Y. and Mayer, U. (2004). Collagen IV is essential for basement membrane stability but dispensable for initiation of its assembly during early development. *Development* **131**, 1619-1628.

Ramasamy, S. K., Kusumbe, A. P. and Adams, R. H. (2015). Regulation of tissue morphogenesis by endothelial cell-derived signals. *Trends Cell Biol* **25**, 148-157.

Sbaa, E., Dewever, J., Martinive, P., Bouzin, C., Frerart, F., Balligand, J. L., Dessy, C. and Feron, O. (2006). Caveolin plays a central role in endothelial progenitor cell mobilization and homing in SDF-1-driven post-ischemic vasculogenesis. *Circ Res* **98**, 1219-1227.

Shao, E. S., Lin, L., Yao, Y. and Bostrom, K. I. (2009). Expression of vascular endothelial growth factor is coordinately regulated by the activin-like kinase receptors 1 and 5 in endothelial cells. *Blood* **114**, 2197-2206.

Shimizu, F., Sano, Y., Takahashi, T., Haruki, H., Saito, K., Koga, M. and Kanda, T. (2012a). Sera from neuromyelitis optica patients disrupt the blood-brain barrier. *J Neurol Neurosurg Psychiatry* **83**, 288-297.

Shimizu, T., Magata, F., Abe, Y. and Miyamoto, A. (2012b). Bone morphogenetic protein 4 (BMP-4) and BMP-7 induce vascular endothelial growth factor expression in bovine granulosa cells. *Anim Sci J* **83**, 663-667.

Umans, L., Vermeire, L., Francis, A., Chang, H., Huylebroeck, D. and Zwijsen, A. (2003). Generation of a floxed allele of Smad5 for cre-mediated conditional knockout in the mouse. *Genesis* **37**, 5-11.

van Eyll, J. M., Pierreux, C. E., Lemaigre, F. P. and Rousseau, G. G. (2004). Shh-dependent differentiation of intestinal tissue from embryonic pancreas by activin A. *J Cell Sci* **117**, 2077-2086.

Wang, A. Z., Ojakian, G. K. and Nelson, W. J. (1990a). Steps in the morphogenesis of a polarized epithelium. I. Uncoupling the roles of cell-cell and cell-substratum contact in establishing plasma membrane polarity in multicellular epithelial (MDCK) cysts. *J Cell Sci* **95 (Pt 1)**, 137-151.

---- (1990b). Steps in the morphogenesis of a polarized epithelium. II. Disassembly and assembly of plasma membrane domains during reversal of epithelial cell polarity in multicellular epithelial (MDCK) cysts. *J Cell Sci* **95 (Pt 1)**, 153-165.

Winnier, G., Blessing, M., Labosky, P. A. and Hogan, B. L. (1995). Bone morphogenetic protein-4 is required for mesoderm formation and patterning in the mouse. *Genes Dev* **9**, 2105-2116.

Yang, X., Castilla, L. H., Xu, X., Li, C., Gotay, J., Weinstein, M., Liu, P. P. and Deng, C. X. (1999). Angiogenesis defects and mesenchymal apoptosis in mice lacking SMAD5. *Development* **126**, 1571-1580.

Yurchenco, P. D. (2011). Basement membranes: cell scaffoldings and signaling platforms. *Cold Spring Harb Perspect Biol* **3**.

Supplementary figures

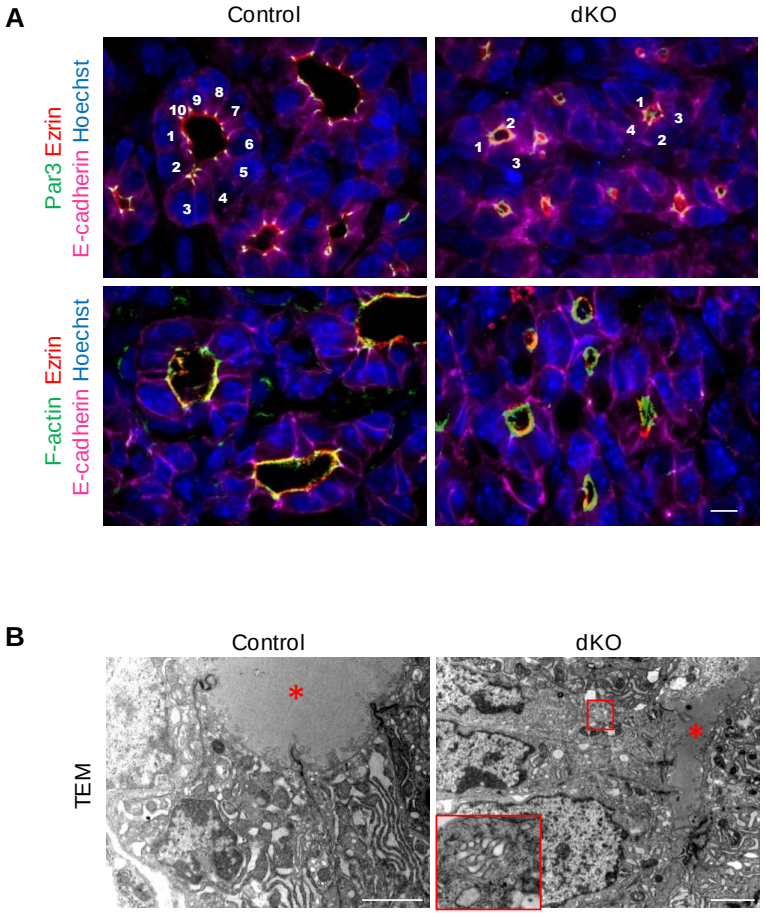

Figure S1. Apical polarity is not affected in Smad1/5^{dKO} at E18.5. (A) Apical polarity marker, Par3 and cytoplasmic stratification marker, F-actin, show no difference in signal intensity and localization between Smad1/5^{dKO} and control. Numbers illustrate counting of cells facing lumina (see Fig. 3D). **(B)** Transmission electron microscopy of control thyroid reveals cuboidal epithelial cells surrounding a large lumen filled with homogeneous colloid (*), in which tight junctions and apical microvilli are projecting. In Smad1/5^{dKO}, columnar thyrocytes also display tight junctions and apical microvilli projecting in non-expanded and smaller lumen (*). Inset illustrates microvilli inclusion body at a distance from apical lumen. Bar, (A) 10 µm and (B) 2 µm.

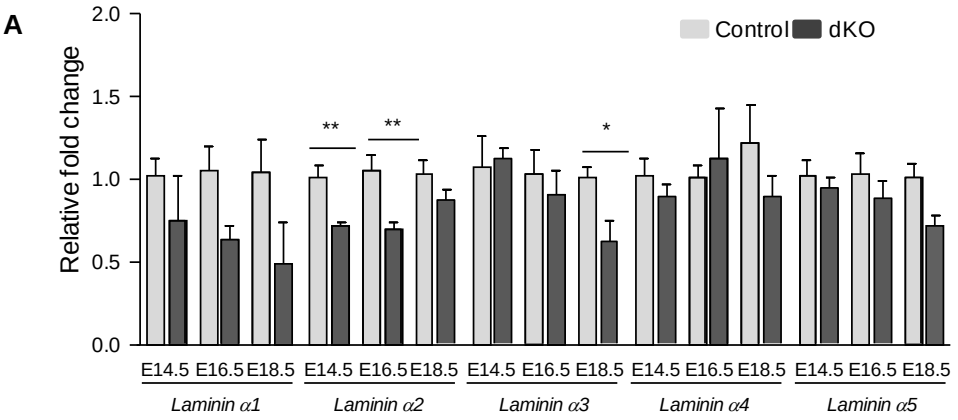
A
Control
dKO
Relative fold change
2.0
1.5
1.0
0.5
0.0
**
**
*
E14.5 E16.5 E18.5 E14.5 E16.5 E18.5 E14.5 E16.5 E18.5 E14.5 E16.5 E18.5 E14.5 E16.5 E18.5
Laminin α1
Laminin α2
Laminin α3
Laminin α4
Laminin α5

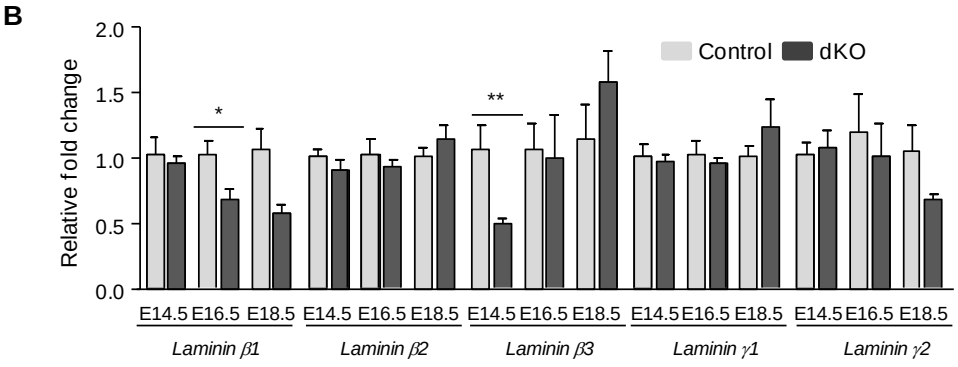
B
Control
dKO
Relative fold change
2.0
1.5
1.0
0.5
0.0
*
**
E14.5 E16.5 E18.5 E14.5 E16.5 E18.5 E14.5 E16.5 E18.5 E14.5 E16.5 E18.5 E14.5 E16.5 E18.5
Laminin β1
Laminin β2
Laminin β3
Laminin γ1
Laminin γ2

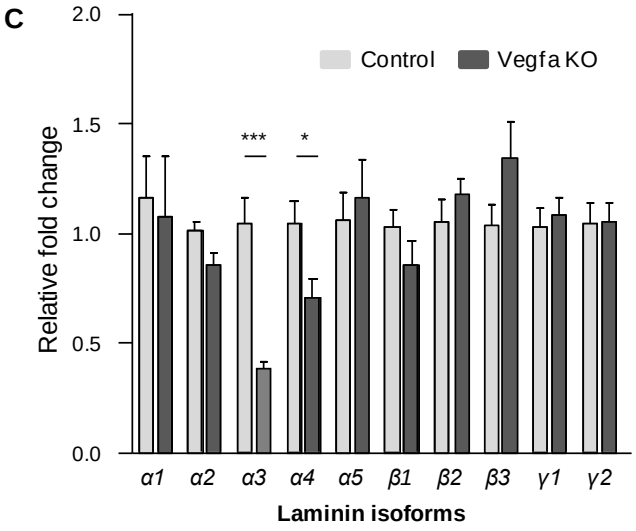
C
Control
Vegfa KO
Relative fold change
2.0
1.5
1.0
0.5
0.0
***
*
α1 α2 α3 α4 α5 β1 β2 β3 γ1 γ2
Laminin isoforms

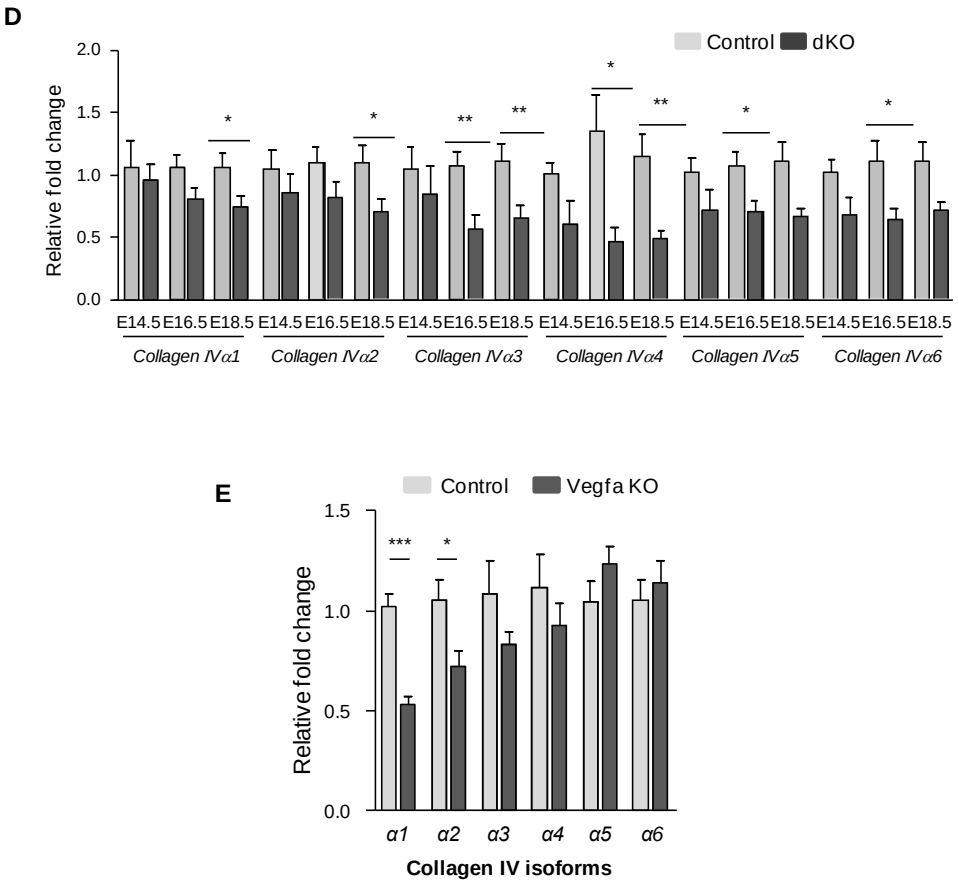

Figure S2. Expression of *laminin α,* β and γ chains in Smad1/5^{dKO} and Vegfa^{KO} mice. (A) Quantification of *laminin α* in control and Smad1/5^{dKO} from E14.5 to E18.5. Expression of *laminin α1* shows a trend to a decrease from E14.5 to E18.5. Variability may come from remaining parathyroid cells, highly expressing this laminin isoform. *Laminin α2* expression was significantly reduced at E14.5 and E16.5 but was normal at E18.5. *Laminin α3* was significantly reduced at E18.5. Expression levels of *laminin α4* and *α5* were statistically not different from E14.5 to E18.5. **(B)** Quantification of *laminin* β *and γ* in control and Smad1/5^{dKO} from E14.5 to E18.5. Expression of *laminin* β*1* was reduced from E16.5. Expression of *laminin* β*3* showed 50% reduction at E14.5 and no change at E18.5. *Laminin* β*2*, *γ1* and *γ2* expression were comparable to control. **(C)** Quantification of *laminins* in Vegfa^{KO} at P0. *Laminin α3* and *α4* were significantly reduced as compared to control. All the other *laminins* were normally expressed. **(D)** Quantification of

collagen IV genes in Smad1/5^{dKO} from E14.5 to E18.5. Expression of *collagen IVα1* and *IVα2*, showed no change at E14.5 and E16.5 but their expression levels were significantly reduced at E18.5. *Collagen IVα3* and *IVα4* showed no difference at E14.5 but significantly reduced at E16.5 and E18.5. C*ollagen IVα5* and *IVα6* were reduced from E14.5 onwards, but only statistically at E16.5. **(E)** Quantification of *collagen IV* genes in Vegfa^{KO} at P0. *Collagen IVα1*, *α2* were significantly reduced as compared to control. All the other *collagen IV* genes were normally expressed. All mRNAs were normalized to either *RPL27* or β-*actin* *p<0.05; ** p<0.001; *** p<0.0001 using Mann Whitney U test (n≥3). Data are presented as means ± S.E.M.

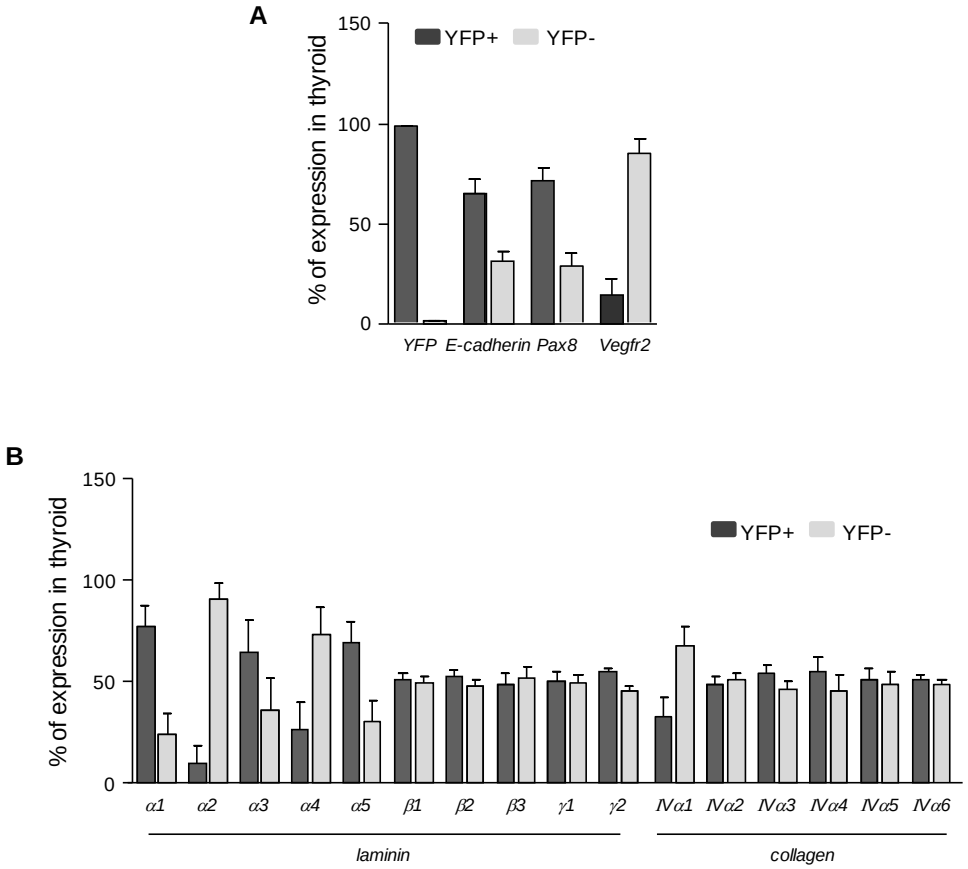

Figure S3. Expression of *laminin* and *collagen* in FACS-sorted Pax8/CRE$^+$ cells. (A) Percent of expression of selected genes in YFP$^+$ and YFP$^-$ populations reveals enrichment of *YFP*, *E-cadherin* and *Pax8* in YFP$^+$ (i.e. thyrocytes progenitors) population and absence of *Vegfr2* in this population. (B) Percent of expression of *laminin* α, β, and γ and *collagen type IV* in YFP$^+$ and YFP$^-$ populations reveals enrichment of *laminin α1* and *α5* in YFP$^+$ population and enrichment of *laminin α2*, α*4* and *collagen α1(IV)* in YFP$^-$ population. All mRNAs were normalized to β-*actin.* Data are presented as means ± S.E.M. (n=4).

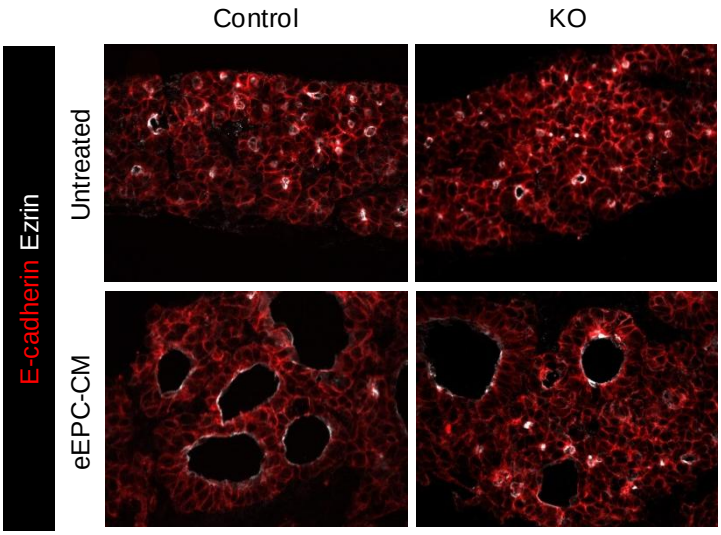

Figure S4. **eEPC-CM rescues follicle formation defect in Vegfa^{KO} thyroid glands.** Treatment of E14.5 thyroid glands of control and Vegfa^{KO} mice with eEPC-CM during 3 days, stimulates follicle formation and lumen size enlargement, as visualized by ezrin (white) and E-cadherin (red) labeling. Bar, 20 µm.

SUPPLEMENTARY TABLES

Table S1. List of candidate folliculogenic factors found by mass spectrometry analysis of eEPC-CM.

Accession	Name	Score	MW (kDa)
Q5NCU4	SPARC	71.04	34.3
P07724	Serum albumin	67.97	68.6
F8VQJ3	Laminin subunit gamma 1	60.83	177.1
P06151	L-lactate dehydrogenase A chain	53.01	36.5
P09103	Protein disulfide-isomerase	50.57	57.0
P02469	Laminin subunit beta 1	48.94	197.0
P08113	Endoplasmin	40.42	92.4
G3x9D5	Histone H2B	35.83	13.4
P14211	Calreticulin	35.32	48.0
F8VQ40	Laminin subunit alpha-1	34.57	337.9
P60710	Actin, cytoplasmic1	31.37	41.7
P68033	Actin, alpha cardiac muscle	25.63	42.0
Q01768	Nucleoside diphosphate kinase B	23.24	17.4
P20029	78kDa glucose-regulated protein	21.38	72.4
Q5SQB0	Nucleophosmin	19.06	29.5

Table S2. List of primary antibodies used.

Primary antibody	Species	Dilution	Source	Catalog number
E-cadherin	mouse	1/200	BD Biosciences	610182
Pan-Laminin	rabbit	1/100	Sigma	L9393
PECAM	rat	1/100	BD Biosciences	550274
PECAM	rat	1/20	Dianova	DIA 310
Ezrin	mouse	1/300	Thermo sceintific	MS-661
Calcitonin	rabbit	1/1000	Dako	A0576
GFP	rabbit	1/200	Cell Signaling	2956S
Par3	rabbit	1/200	Merck/Millipore	07-330
Laminin α1	rabbit	1/1000	Gift from Dr. T. Sasaki	
Laminin α5	rabbit	1/1000	Gift from Dr. T. Sasaki	
Collagen IV	rabbit	1/500	Merck/Millipore	AB756P

Thyroglobulin	mouse	1/500	Dako	M0781
pSmad158	rabbit	1/100	Cell Signaling	9511S
pSmad15	rabbit	1/100	Cell Signaling	9516S
iodo-thyroglobulin	mouse	1/100	Gift from Dr. Ris-Stalpers	

Table S3. List of primer sequences

Gene	Primer sequences (5'-3')	Fragment size (bp)
E-cadherin	AGGGAGCTGTCTACCAAAGTG CCAGTCTCGTTTCTGTCTTC	146
Ve-cadherin	GGATGTGGTGCCAGTAAACC ACCCCGTTGTCTGAGATGAG	173
Vegfr2	GCATGGAAGAGGATTCTGGA CGGCTCTTTCGCTTACTGTT	142
Vegfa mouse	GTACCTCCACCATGCCAAGT CTGCATGGTGATGTTGCTCT	265
Vegfa rat	GAGTATATCTTCAAGCCGTCCTGT TTTTCTGGCTTTGTTCTATCTTC	193
β-actin	TCCTGAGCGCAAGTACTCTGT CTGATCCACATCTGCTGGAAG	77
Nkx2.1	ATCTGAGCTGGGGTGCTGGG GCCCTGTCTGTACGCTGCGA	244
Pax8	TGCCTTTCCCCATGCTGCCTCCGTGTA GGTGGGTGGTGCGCTTGGCCTTGATGTAG	298
Foxe1	GGCGGCATCTACAAGTTCAT GGATCTTGAGGAAGCAGTCG	115
Hhex	TCAGAATCGCCGAGCTAAAT ACTGCGAACGATCCAAAGAG	152
Tpo	TGCCAACAGAAGCATGGGCAAC GCACAAAGTTCCCATTGTCCAC	424
Tg	TGGGACGTGAAAGGGGAATGGTGC GTGAGCTTTTGGAATGGCAGGCGA	394
Nis	AGCAGGCTTAGCTGTATCCC AGCCCCGTAGTAGAGATAGGAG	235
Tshr	CTGCGGGGCAAAGAGTGTGC AGGGGAGCTCTGTCAAGGCA	325

Calcitonin	TGGTTGTCAGCATCTTGCTC CTTAGATCTGGGGCTGTCCA	221
Smad1	GCCTCTGGAATGCTGTGAGT GAACTGAGCCAGAAGGCTGT	137
Smad5	GCAGAGCCATCACGAGCTAA CCAGAAGGCTGTGTTGTGGA	169
Smad8	CACCGACCCTTCCAATAAC CTGGACAAAGATGCTGCTG	153
RPL27	GCCCTGGTGGCTGGAATTGACC AAACTTGACCTTGGCCTCCCGC	233
ID2	CATCCTGTCCTTGCAGGCAT CCATTCAACGTGTTCTCCTGG	199
PECAM	ATAGGCATCAGCTGCCAGTC TCCGCTCTGCACTGGTATTC	157
Pcdh12	TGCCCCTCACCACCAATTAC GTGCTGCCCCAACAACATTT	171
Tie1	CAGGGACCTTGACCTTGACC ATCATGGCCCGGATCACTTG	135
Esm1	ACCTTCGGGATGGAATGCAA AGAGGTCCTGCTGGGAGATT	125
YFP	CCTCGTGACCACCTTCGG CTCAGGTAGTGGTTGTCGG	400
BMP2	CAGCGCAATCTCCATGTTG GGGAAATATTAAAGTGTCAGCTGG	197
BMP4	GGATCTTTACCGGCTCCAG CCAGATGTTCTTCGTGATGG	130
BMP5	TTCCACATGGAGAAGCAGTG AAGCCCAAATTGTTCTGTGG	246
BMP7	TCCGGTTTGATCTTTCCAAG TGGCTGTGATGTCAAACACC	224
Laminin α1	AGCTGTGTGCTTCTGGCTAC TCACTGTCACCTTCCACGAC Or CCGACAACCTCCTCTTCTACC TCTCCACTGCGAGAAAGTCA	123 Or 59
Laminin α2	CTGGAGTTGGTCCTCTCAGC TGAACATCAACCTCACGGGC Or TTGCCCTCTGCCAACTGAAT TGAACATCAACCTCACGGGC	240 Or 135

Laminin α3	ATGAACAGTGAGGCAGGTGG GGACGCCTCCAATGTGTAGT	198
Laminin α4	ACGGGGAATACCTGAACGTG TCTGTGCCATCTGCCATCAC	124
Laminin α5	ACCCAAGGACCCACCTGTAG TCATGTGTGCGTAGCCTCTC	168
Laminin β1	TGGACAAGAGCAACGAGGAC TTCTGTAACTGCTGTGGCGT	147
Laminin β2	GTGTGGCTTGCATAGCCCT TCCGATGACTATTTGGGTTGTCT	121
Laminin β3	GGGAGACCATGGAAATGATG GATCTGCTCCACACGCTTCT	121
Laminin γ1	TGCCGGAGTTTGTTAATGCC CTGGTTGTTGTAGTCGGTCAG	184
Laminin γ2	GGCAGTCAGCATCAGAACAG CCCCACGTAGTGCTCAGAAG	125
Integrin α3	CCCTTCCAGACACCTCCAAC ACCACAGCTCAATCTCAGCC	230
Integrin α6	TGGACATTCTCCTGAGGGCT TGAGGGAAACACCGTCACTC	100
Integrin α7	AAGGTGGAGCCTAGCACATC TCAAAGCTGTAGAGTGGGCAG	121
Integrin β1	ATGGCCGGGGTATTTGTGAA GAAGTGGGAGCACTCCTGTG	181
Integrin β4	CAGGGAGGCTGGCTTTCAAT TTCTTGGGGTTGTCCACGAG	171
Collagen IV α1	AACAACGTCTGCAACTTCGC CTTCACAAACCGCACACCTG	135
Collagen IV α2	GGATGCCAGGGCTTAAAGGT CTGTCTCCAGGCAAACCTCC	159
Collagen IV α3	GGCCCTGAGTGGAAGGAAAG GACTCCTTGGGCTCCCTTTG	138
Collagen IV α4	GCCAGAAAGGACCAATGGGA TACTGGCCCTTTTCTGCCTG	106
Collagen IV α5	CCCCAGGACCAGATGGATTG TACTGAAGCGACGAAGGCAG	224
Collagen IV α6	GGCCTGAAAGGAGACCAAGG CTCAAATGTGCGACCAGGTG	128

VIII. DISCUSSION AND CONCLUSION

1. Discussion and perspectives

Adult thyroid is composed of polarized epithelial monolayers organized in closed spherical structures, the follicles. Epithelial cells rest on a basement membrane, are closely encircled by endothelial cell and surround a closed lumen, the colloid, where iodo-thyroglobulin is formed and stored. This epithelial architecture and close association with blood vessels dictates the ultimate endocrine thyroid function, which is the production and secretion of thyroid hormones (T_3-T_4) in the bloodstream. Our first study not only demonstrated that epithelial VEGF-A is necessary for the recruitment of endothelial cells during thyroid development: recruited endothelial cells penetrate and invade the thyroid mass to become finally closely associated with follicles, but also that endothelial cells are required for thyrocytes organization in follicles even in the absence of blood supply in explants. Indeed, in the absence of *Vegfa* ($Vegfa^{KO}$), endothelial cell density is reduced and follicles are smaller. Pharmacological ablation of endothelial cells in wild-type thyroid explant culture also impaired follicle formation. Of greatest interest, addition of embryonic endothelial progenitor cells (eEPC), or medium conditioned (CM) by these cells, rescued and stimulated folliculogenesis. This indicated that folliculogenic activity of endothelial cells is contact-independent and that eEPC produce and secrete one (or several) folliculogenic factor(s). Most of my thesis work was devoted to the identification of the soluble folliculogenic factor(s) secreted by eEPC and to the comprehension of its mode of action.

Several complementary approaches abundantly highlighted the importance of laminins during folliculogenesis. I found that laminins α1, β1 and γ1 were produced by WT-eEPC, secreted in the CM and assembled around thyroid explants in culture. Conversely, eEPC specifically silenced for laminin α1 did not stimulate folliculogenesis. Another piece of the puzzle was that thyroid-specific $Smad1/5^{dKO}$ displayed smaller follicle lumina, similarly to the $Vegfa^{KO}$ and we found that both KO had defective basement membrane assembly, due to reduced expression of type IV collagen and laminins. Bringing the two pieces of evidence together, addition of laminin-rich eEPC-CM to $Smad1/5^{dKO}$ and $Vegfa^{KO}$ rescued

and stimulated folliculogenesis. We conclude that basement membrane assembly is necessary for follicle formation during thyroid development.

To avoid repetitions with discussions from the papers, I decided to focus this last section on data not presented in the papers and on the comparison of *de novo* lumen formation in the well-studied MDCK system with our *ex vivo* culture system.

1.1. Thyroid explant culture

1.1.1. System improvement

The first thyroid culture system, developed by Anne-Christine Hick, used thyroid dissected at E12.5 and cultured during 4 days (Hick et al., 2013). This stage was chosen because culture of pancreas and submandibular gland, routinely performed in the lab, were performed at this stage. However, E12.5 thyroid is still very small and cannot be visualized under standard stereomicroscope. Moreover, the different anlagen (the midline thyroid bud and the two lateral ultimobranchial bodies) have not yet fused. Hence, the microdissected tissue had to encompass a large region containing part of the trachea, which extended from the pharyngeal arch arteries up to the arytenoid swelling and its surrounding mesenchymal tissue. Upon culture on filter, the E12.5 midline anlage continued its extension laterally on each side of the trachea and merged with the ultimobranchial bodies to form two thyroid lobes connected by the isthmus. After 4 days, histological analysis of the explants revealed the presence of two vascularized lobes, containing follicles. Thus, culture of thyroid explant at this stage allows bilobation, angiogenesis and folliculogenesis. Nevertheless, this culture system has a major drawback: the dissected tissue is strongly heterogeneous. In particular, when extracting RNA for gene expression analyses, we measure RNAs not only from the thyroid but also from the trachea and other surrounding tissues present in the explant.

We improved this system by using thyroid microdissected at E14.5. At this developmental stage, thyroid lobes are located at their final positions, on each side of the trachea, and fused with the ultimobranchial bodies. Thyrocyte progenitors are also at the start of folliculogenesis and differentiation. This E14.5 thyroid lobe culture system is thus more adequate to study folliculogenesis. In

addition, at this stage, we obtain two separated lobes (useful for comparison) larger and easier to visualize.

In our initial study on the role of endothelial cells during thyroid development, we used an inhibitor of VEGFR-2 (SU5416), which prevents endothelial cell survival. Treatment with SU5416 lasted 40h to allow ablation of endothelial cells, and was followed for rescue by the addition of eEPC or conditioned medium during 56h. We can estimate that the age of the explants treated with eEPC or CM was approximately at E14 (E12.5 + 40h), i.e. at the start of folliculogenesis. When thyroid lobes were microdissected at E14.5, we tested the CM without pretreatment with SU5416. Since follicle formation was stimulated as compared to untreated explants, depletion of endothelial cells was no longer necessary. This indicated that the folliculogenic activity present in eEPC-CM is strong. As endothelial cell density was not affected by the CM, we favored a model in which folliculogenic factor(s) act downstream of endothelial cells. To analyze the time window in which the CM can stimulate folliculogenesis, it would be interesting to test if follicle formation is also stimulated in E12.5 explants directly treated with CM.

Culture of thyroid explants on semi-permeable filters provides several advantages as compared to other systems in which thyrocytes are grown in monolayers or in 3D collagen gels. First, the natural composition and topological relation of the dissected tissue which encompasses thyrocytes, C-cells, endothelial and mesenchymal cells but also extracellular matrix, is maintained in culture. Secondly, our 3D organ culture faithfully reproduces *in vivo* development, thus allows studying the apico-basal polarization process of thyrocyte progenitors. Thirdly, an important aspect is the oxygen concentration. Grown on filters, thyroid explants are at the interface between air and medium. On the contrary, when grown on coated plastic culture chambers or in collagen gels, oxygen concentration is difficult to evaluate due to the presence of medium or collagen around the explants. It was demonstrated that when E13.5 rat pancreas are cultured in collagen gels, cells suffer from hypoxia and endocrine differentiation is compromised. On the contrary, E13.5 rat pancreas cultured on filter are not hypoxic and endocrine differentiation is preserved (Heinis et al., 2010). Finally, immunolabeling of our explants cultured on filters is direct, easy and antibody penetration is very efficient. Indeed, in the course of a collaboration with Russian

scientists (3D Bioprinting Solutions), we observed that thyroids lobes grown in collagen were not correctly labeled in whole-mount: the collagen around thyroid lobes impaired antibodies penetration. Whole-mount protocol should thus be adapted, by increasing primary antibody incubation time from 16h to 24, if not 48h.

1.1.2. Embryonic endothelial progenitor cells (eEPC)

To demonstrate the implication of endothelial cells on follicle formation in thyroid explants, we tested rescue of the folliculogenic defect of SU-treated explants with different endothelial cell lines; eEPC, Bend3 (Brain endothelial cells) and HUVEC (Human Umbilical Vein Endothelial Cells). In our hands, only eEPC stimulated lumen formation and we thus focused on this cell line. eEPC were isolated from murine embryos at E7.5. These cells have endothelial characteristics: they express *Tie-2* (Angiopoietin-1 receptor) and *Thbd* (Thrombomodulin*)*, display cobblestone morphology and form tubes in Matrigel (Hatzopoulos et al., 1998). eEPC enhance vascularization and tissue recovery after ischemia, and, according to their transcriptome, they express factors known to induce angiogenesis, organogenesis and tissue remodeling (Kupatt et al., 2005). These observations supported our choice of eEPC as an interesting cell line for the identification of the folliculogenic factor(s). In addition to these theoretical considerations, a technically important issue is that eEPC are easily cultured and grow rapidly.

Other cell lines have been used to prepare conditioned medium to study morphogenetic activities. For example, medium conditioned by human hair follicle-derived mesenchymal stem cells enhances cell organization and multilumen formation in mouse submandibular gland (Maruyama et al., 2015). Medium conditioned by HUVEC stimulates branching morphogenesis in lung explants (Lazarus et al., 2011). A recent review highlights the role of factors secreted by endothelial cells, collectively called *angiocrine* factors, in development and regeneration (Ramasamy et al., 2015).

1.1.3. Preparation and manipulation of conditioned medium (eEPC-CM)

Apart from a slight increase in the duration of conditioning time (prolonged from 16 to 24h) and cell confluence (85-90% instead of 50-70%), preparation of CM remained unchanged during my PhD.

eEPC are cultured in DMEM containing 20% of serum (FBS) while our explants are cultured on M199 medium with only 10% FBS. For conditioning, DMEM was thus aspirated and replaced by M199 without FBS. Traces of FBS remained and appeared critical. Indeed, we observed that if eEPC were thoroughly washed with PBS to remove all traces of FBS and albumin (i.e. for mass spectrometry analysis) before conditioning in M199, folliculogenic activity was strongly reduced. This suggested that the presence of low amount of FBS was required for the production or for the stability/activity of the folliculogenic factor. Addition of low amount of FBS (up to 2%) at the end of the conditioning did not restore folliculogenic activity. We thus concluded that efficient production by eEPC of bioactive folliculogenic factor requires traces of FBS in the conditioning medium.

To initiate characterization of the folliculogenic factor, we first wished to determine the biological nature of the factor (RNA or protein). eEPC-CM was thus incubated with either RNase or trypsine/pronase, to degrade RNA or proteins respectively. RNase treatment had no effect. When we tried to test the protease-treated CM on culture, we faced rapid degradation of the explants by pronase (even after inactivation). After several rounds of dilution/concentration to eliminate pronase activity, folliculogenic activity of the CM was lost. Although not perfect, these experiments suggested that the folliculogenic factor was most probably a protein.

We then focused on the estimation of the molecular weight of the active folliculogenic protein(s). Separation of the CM into sedimentable and soluble material by ultracentrifugation revealed that both materials stimulated folliculogenesis in thyroid explant culture (Hick et al., 2013). The sedimentable folliculogenic fraction, currently studied by Jonathan Degosserie, could contain exosomes and/or microvesicles. We also fractionated the CM based on protein

size (Superdex 75 column) and tested the fractions on thyroid lobes. We focused on two reproducible extreme fractions containing part of the folliculogenic activity: one fraction of high (433-902 kDa) and one fraction of low (5-11 kDa) molecular weight (Figure 19). The high-molecular weight fraction led us on the track of laminins, a large component of the basement membrane, with a molecular weight from 400 to 800kDa for heterotrimers. The very low molecular weight fraction could contain growth factors such as EGF (~5kDa), Activin (~15kDa) or BMP (~15kDa). However, we did not consider a candidate approach on this low molecular weight fraction, as the list of candidate factors was very long. Instead we focused on laminins as they are required for polarization and lumen formation in MDCK (O'Brien et al., 2001) and we found abundant laminin peptides by mass spectrometry analysis of the CM.

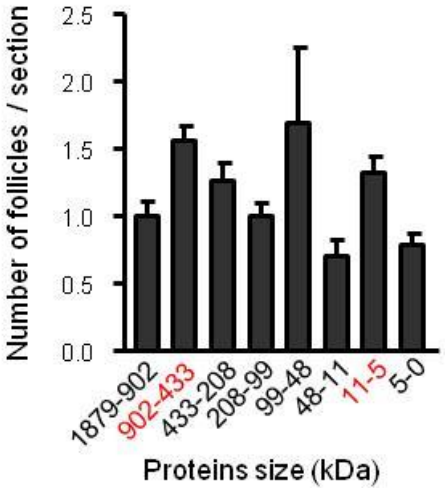

Figure 19. CM fractionation highlights two fractions with higher folliculogenic activity. Large follicles were counted in explants and divided by the number of section. We compared the activity of each fraction to the first fraction (902-1879). We observed that three fractions are pro-folliculogenic. A high-molecular weight fraction (433-902), a low-molecular weight fraction (5-11) and a less reproducible intermediate molecular weight fraction (48-99) (note higher standard deviation).

The difficulty of this biochemical approach resides in its complexity (volume of CM, concentration before and after fractionation, “sterile” condition) and the variability in the distribution of fractions collected. Not only very

demanding, this biochemical fractionation approach, yielded less solid information on the candidate folliculogenic factor than mass spectrometry. *A posteriori*, I would recommend analyzing CM by mass spectrometry, and if no obvious candidate emerges then, start fractionation experiments.

1.2. CM is endowed with different activities

1.2.1. CM effect on the thyroid

A priori, stimulation of follicle formation by CM could be the result of increased proliferation of cells around a developing lumen, of increased differentiation of thyrocyte progenitors, then combination or just another mechanism. We tested these possibilities in E14.5 explants cultured for 3 days and found that proliferation (as measured by phosphohistone H3 immunolabeling) was actually decreased in CM-treated thyroid explants as compared to control. We concluded that increased size of follicles was not caused by an increase in thyrocyte proliferation. We also observed that differentiation markers (Na/I symporter, thyroglobulin and thyroperoxidase) were also reduced in CM-treated explants based on mRNA (Figure 20 A.) and immunofluorescence (thyroglobulin) (Figure 20 B.). These results indicate that eEPC-CM prevents thyrocytes differentiation and that the stimulation of follicle formation is not caused by increased differentiation.

As CM stimulates neither proliferation nor differentiation, we turned our attention on the polarization process. In explants incubated with CM we found larger ezrin^{+} lumina, accumulation of Par3 protein at the apical pole and abundant F-actin localization in the subapical region and increased basal laminin α1 signal (see below).

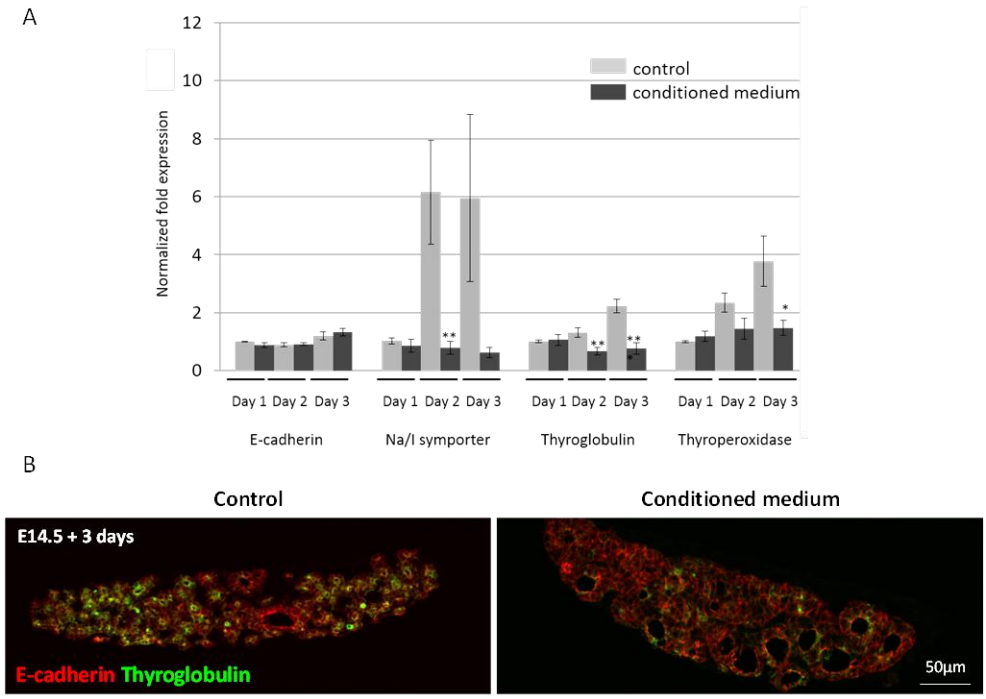

Figure 20. Reduced thyroid differentiation by eEPC-CM. A. Thyrocytes differentiation genes are decreased in thyroid lobes treated with CM after 2 and 3 days in culture, as compared to control. B. Thyroglobulin immunolabeling signal was decreased by eEPC-CM at E14.5+3 days.

In most biological systems and in development in particular, an inverse correlation between proliferation and differentiation/polarization is often observed. Along embryonic development, proliferation decreases when tissue differentiate and polarize. For example, our lab showed that the transcription factor ZONAB simultaneously stimulates proliferation and represses differentiation in renal proximal tubular cells (Lima et al., 2010), indicating that ZONAB behaves as a master gene oppositely controlling proliferation and differentiation (i.e. switch). During thyroid development, only after intense proliferation of thyrocyte progenitors do thyrocytes acquire polarity and differentiate. In thyroid lobes treated with eEPC-CM, we observed a decrease in proliferation in parallel with a stimulation of polarization, but surprisingly, differentiation was also decreased. Thus, upon eEPC-CM treatment, polarization

seems to be uncoupled from differentiation and CM may be a mixture of pro-polarization factor(s) and anti-differentiation factor(s).

Candidate proteins for these pro-polarization and anti-differentiation activites could come from mass spectrometry analyses of the CM. Indeed, we reproducibly found the presence of the protein SPARC (secreted protein acidic cysteine rich) as a very abundant protein in our EPC-CM. SPARC, also called osteonectin, is an ECM-associated protein which binds collagen and is required for the assembly and organization of basement membrane (Bradshaw, 2009). SPARC has also been shown to act as a positive regulator of angiogenesis (Rivera et al., 2011). Thus, SPARC could act in concert with, or independently from, laminin on the folliculogenic process. However, we did not study the role of SPARC during folliculogenesis as mass spectrometry results were obtained at the very end of my experimental work. It would be interesting to measure its expression in both Smad1/5^{dKO} and Vegfa^{KO} mice and analyze its localization in CM-treated explants.

1.2.2. CM effect on the pancreas

Our group has shown that pancreatic endothelial cells, localized closed to ductal cells in the developing organ, prevent these to differentiate into acinar cells. Targeted overexpression of VEGFa in acinar progenitors induces endothelial cells recruitment and repression of acinar differentiation (Pierreux et al., 2010). In this context, the goal of the master thesis of Charlotte Heymans was to further understand the mechanisms of acinar differentiation by endothelial cells. I supervised her work at the bench and we demonstrated that eEPC-CM can indeed limit acinar differentiation (Figure 21 A. and B.), and that this effect is probably mediated by the downregulation of a trimeric transcription factor complex (Ptf1a, Rbpjl and E-protein) required for pancreas acinar differentiation (Figure 21 C.). This suggests that the CM here limits acinar differentiation by preventing expression of an acinar-specific transcriptional complex.

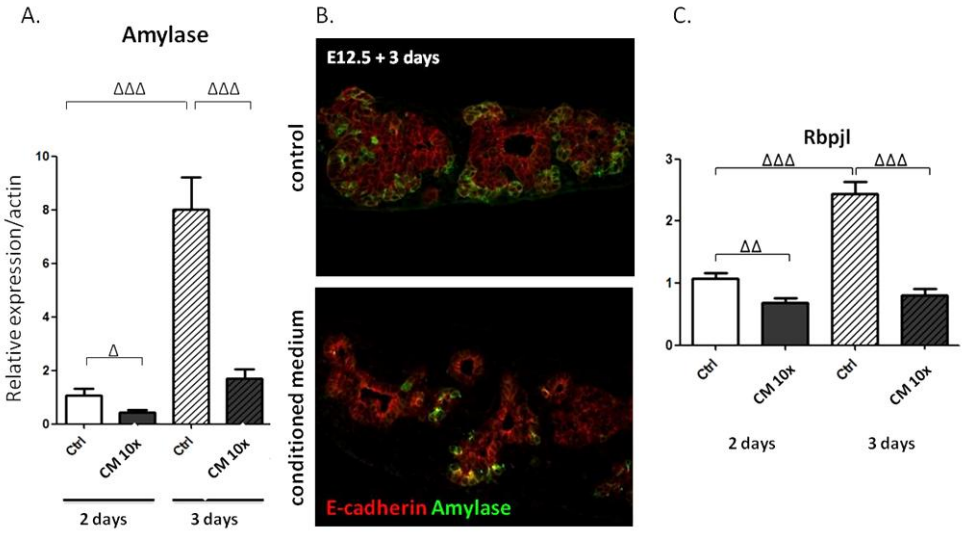

Figure 21. Inhibition of acinar differentiation by eEPC-CM. A. Amylase mRNA expression is increased about 8 fold in control pancreas explants from day 2 to day 3. CM abrogates this induction. B. Amylase immunolabelling is reduced at E12.5+3 days in the presence of CM, as compared to control pancreas. C. As for amylase, expression of the transcription factor Rbpjl does not increase from 2 to 3 days of culture in the presence of eEPC-CM.

Rbpjl is a paralog of Rbpj, the vertebrate Suppressor of Hairless and Notch dependent transcriptional regulator. During pancreas development, Rbpjl progressively replaces Rbpj in the heterotrimeric complex with Ptf1a and the E-protein, thereby triggering acinar differentiation at the expense of a progenitor fate. Nothing is known about the expression of Rbpj and Rbpjl in the thyroid, but since we observed a repression of thyroid differentiation by eEPC-CM, it could be interesting to study if these factors, and Notch signaling, are implicated in thyroid development. Along this line, the expression of the four transcription factors critical for thyroid development (Nkx2.1, Hhex, Foxe1 and Pax8) should also be measured.

1.3. Laminin-111 from CM is a stimulator of follicle formation

Based on the proteic nature of the folliculogenic factor and the bioactivity of the high-molecular weight fraction, we postulated that laminins with a

molecular weight comprised between 400 and 800kDa in trimers, could be a critical folliculogenic factor.

Various experiments were performed to test the involvement of laminins in folliculogenesis. First, we demonstrated by RT-qPCR that eEPC highly express laminins isoforms, especially laminin α1, β1 and γ1. Second, mass spectrometry, silver staining and western blotting revealed the presence of laminin α1, β1 and γ1 in the CM. Third, abundant laminin α1 was deposited and assembled around thyroid lobes cultured with eEPC-CM. Lastly, CM from laminin α1-silenced eEPC did not stimulate follicle formation. In addition, two different KO mice ($Vegfa^{KO}$ and $Smad1/5^{dKO}$), which display defective folliculogenesis and basement membrane formation, were rescued by eEPC-CM. Altogether, these results pointed towards a critical role of laminins in folliculogenesis.

Despite several trials, gain-of-function experiments were not conclusive. Replacement of eEPC-CM by commercial and non-commercial (Sasaki et al., 2010) purified laminin 111 on thyroid lobes neither increased laminin α1 deposition/assembly in the explants and nor stimulated folliculogenesis. Misassembly of purified laminin might result from loss of a post-translational modification or absence of a critical partner. It is also possible that purified laminin still assembled around the explants but did not properly organize, thereby preventing recognition by anti-laminin antibody, as reported previously (O'Brien et al., 2001).

Laminin α1 and α5 are recognized as the main epithelial laminins and their expression varies during embryonic development: laminin α1 appearing first, then being replaced by laminin α5. During thyroid development, we also observe decreasing expression levels for laminin α1, suggesting that laminin α1 is essential at the beginning of folliculogenesis then becomes less important at the end of gestation, reminiscent of bile duct development where laminin α1 is necessary to start, and laminin α5 to complete, epithelial morphogenesis (Tanimizu et al., 2012). Type IV collagen is also important for basement membrane stability (Pöschl et al., 2004). In thyroid explants, no change in type IV collagen labeling was observed in the presence of CM. Rescue of folliculogenesis in $Vegfa^{KO}$ and $Smad1/5^{dKO}$, which display reduced collagen IV labeling, could be explained by the large quantities of laminin 111 present in the eEPC-CM. Laminin 111 abundance

could allow its assembly and stabilization around KO thyrocytes and be sufficient even in the absence of type IV collagen, to stimulate folliculogenesis.

We also tested the involvement of integrin signaling in lumen formation and observed that treatment with a blocking anti-integrin β1 antibody did not prevent folliculogenesis triggered by the CM. However, immunofluorescence on sections of thyroid explants incubated with the blocking antibody failed to detect it in the tissue, raising the possibility of poor penetration into the explant and preventing one to conclude on to the implication of integrin β1 in transducing the effects of eEPC-CM. Second, utilization of inhibitors against integrin downstream signaling kinases such as Src and Fak showed only a partial blockade of the folliculogenic effect with the Src inhibitor, PP2. Despite non-conclusive results, we keep the possibility open that integrins transduce signal received from laminins through the Src pathway.

1.4. A role for CM in lumen expansion?

After *de novo* lumen formation, expansion is necessary for physiological functions. Lumen expansion requires two activities: (1) deposition at the apical membrane of anti-adhesive factors such as podocalyxin or glycosylated mucins, which avoid lumen collapse, and (2) fluid secretion and induction of hydrostatic pressure by activation of apical channels and pumps such as Na^+/K^+ ATPase or CFTR (Sigurbjörnsdóttir et al., 2014). Two studies in zebrafish gut lumen and in mouse salivary glands have shown the role of CFTR activation by cAMP/PKA in opening and expansion of lumen (Bagnat et al., 2010; Nedvetsky et al., 2014). We thus tested if eEPC-CM could act on lumen expansion through CFTR. Although CFTR expression was increased from the first day of culture in the presence of eEPC-CM, pharmacological inhibition of CFTR or of cAMP/PKA did not prevent eEPC-CM to stimulate folliculogenesis. This suggests that the increase in CFTR expression could be a consequence rather than a cause of lumen expansion.

1.5. *De novo* lumen formation in *in vitro* and *ex vivo* culture systems

A widely used system to study *de novo* lumen formation is the MDCK cell line. MDCK are derived from immortalized kidney distal tubular cells. Grown in 2D,

these cells form a monolayer with apical surface facing the culture medium. In suspension, they form cysts with an inverted polarity, i.e. with apical pole facing the culture medium and basolateral surface in the center of the cystic structure. In 3D collagen, cysts are correctly polarized with the apical pole facing the central lumen and the basolateral membrane contacting the collagen matrix (Sigurbjörnsdóttir et al., 2014; Zegers et al., 2003). I thought it would be informative to compare *de novo* lumen formation in MDCK cultured in collagen with our thyroid lobe culture system and thus summarize here the main steps already described in the introduction (Figure 22). Initially, single MDCK cell seeded in collagen has no surface polarity: apical and basolateral proteins are randomly distributed throughout the cell surface (1), and the cell contacts the surrounding stroma rich in fibrillar collagen (2). After one cell division, the new cell-cell contact together with cell-ECM contact give cues to promote polarized secretion and production/assembly of a laminin-rich basement membrane (red), and to allow endocytosis of apical proteins and lipids (red vesicles) of the cell membrane facing the ECM (3). Increased cell-basement membrane (red & yellow) contacts and asymmetric targeting of intracellular polarity complexes Par, Crumbs and Scribble trigger lumen opening (4, 5). Polarity complexes and stabilized basement membrane (yellow) provide further information for oriented organization of the cytoskeleton (6), and polarized membrane trafficking contributes to *de novo* lumen formation and expansion (7). Cyst growth is maintained via oriented cell division (8).

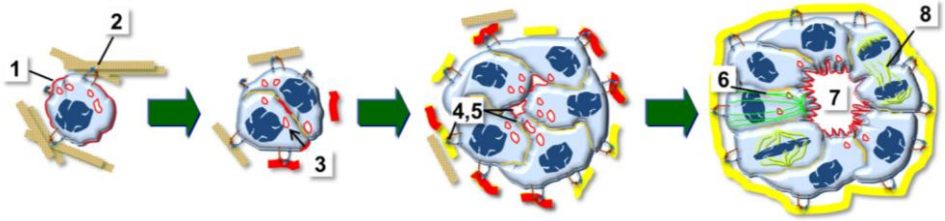

Figure 22. Schematic representation of steps involved in *de novo* lumen formation and polarity acquisition in epithelial cells. See details in the text (Manninen, 2015).

A cystic organization with a closed lumen is an abnormal architecture for MDCK cells, originating from distal tubules of the kidney and better resembles to a closed thyroid follicle than to an open kidney tubule. Indeed, comparison of

MDCK *de novo* lumen formation to thyroid folliculogenesis reveals some telling differences. First, at two cells stage MDCK are already polarized, quite different from thyrocyte progenitors which first expand as a mass without polarity markers up to the start of folliculogenesis. Indeed, after their budding from the endoderm (E10.5), thyrocyte progenitors form a mass of non-polarized cells, which will migrate collectively and reach their final localization at approximately E13.5. At E13.5-E14.5, only the rim of cells at the periphery is in contact with laminin-rich basement membrane and is thus partially polarized with a basal, but no apical pole. Within the mass, ezrin positive clusters (vesicles) and tight junction proteins (ZO-1) progressively appear in some cells. Thus, during thyroid development, we do not observe the apical marker ezrin all around the cell surface of progenitors, and we do not observe inverse polarity. As a consequence, transcytosis of future apical proteins recaptured from the (basal) cell surface contacting the extracellular matrix, to be redirected to the opposite (apical) membrane is not observed in our *ex vivo* culture system.

The formation of the apical pole (initiated around E14.5 in some cells) (steps 4-5) occurs when intracellular ezrin^{+} vesicles fuse with a membrane, which will become the apical membrane. An intrinsic or an extrinsic program could trigger the formation of these vesicles in cells within the mass. Our observations suggest that this early apical specification, i.e. appearance of ezrin^{+} clusters, is not controlled by extrinsic signal since ezrin^{+} structures preferentially appear in cells localized deep within the mass, not predominantly in the peripheral cells, as is the case in the pancreas (Hick et al., 2009).

Later on, signal for polarization are probably controlled or reinforced by extrinsic cues. During mass reorganization, thyrocytes secrete VEGF-A to recruit endothelial cells (Hick et al., 2013). Invasion of endothelial cells into the thyroid mass results in disruption of epithelial cell-cell junctions. Involvement of C-cells in this process could also be hypothesized. The loss of epithelial cell-cell contacts and the development of contact with the stroma provide thyrocytes with signals to develop their basolateral membrane. Maturation and stabilization of the latter will further contribute to lumen opening and apico-basal polarization. Indeed, solutes injection into the apical lumen first requires basolateral transporters and pumps in contact with the internal milieu.

A last difference is that MDCK cells receive the polarization signal from the ECM, and polarization then occurs from basal to apical. In thyroid, our analysis suggested that apical specification either appears within the mass, in response to an intrinsic signal, or stochastically. Upon fusion of ezrin^{+} vesicles with a membrane, different scenarios can be proposed from that cell with a newly formed apical pole. First, formation of the apical lumen disrupts cell-cell contact with neighboring cell(s) and induces in these cells a polarization signal starting from the new apical surface. Secondly, fusion of ezrin^{+} vesicles with a membrane in one cell, can induce polarization of its neighboring cells through tight junction formation. In both cases, polarization would develop from apical to basal. Reinforcement and maturation of apico-basal polarity would require basement membrane assembly. Simultaneously, and as in MDCK, gain of cell-matrix interaction at the expense of cell-cell contact, in the mass or at its periphery, will cause polarization from basal to apical.

In conclusion, MDCK cell is an excellent system to study and identify molecules implicated in *de novo* lumen formation. However, we believe that steps 1, 2 and 3 are *in vitro* artefacts that do not occur *in vivo* in the presence of non-polarized progenitors. In thyroid, ezrin and apical markers are not present *ad initio* but appear during lumen formation. This was also observed during pancreas (Hick et al., 2009; Villasenor et al., 2010) and bile duct development (Antoniou et al., 2009). However, in these two organs, acquisition of apico-basal polarity occurs predominantly at the periphery of the parenchyme; that is in progenitor cells in contact with the surrounding stroma or the portal mesenchyme. Thus, *in vivo* lumen formation requires basement membrane assembly and stabilization (similar to steps 4 to 8 in the MDCK) and *de novo* appearance of apical markers.

1.6. Intracellular lumen: microvillus inclusion disease?

In the early stage (E14.5) of folliculogenesis, we observed clusters of the apical protein ezrin localized just underneath of the future apical pole. We believe that these are intracellular vesicles loaded with apical proteins, as observed in MDCK system, and that their fusion with the membrane triggers first lumen formation and then expansion. Both Vegfa^{KO} and Smad1/5^{dKO} have reduced follicle lumen size and this is associated with the presence of an “intracellular lumen”, as visualized by electron microscopy (Figure 23 A.). These appear as round

structures, delineated by a membrane but not in contact with tight junctions. Their lumen is filled with microvilli similar to those normally facing the follicular lumen (Hick et al., 2013) (Villacorte*, Delmarcelle* et al., in revision).

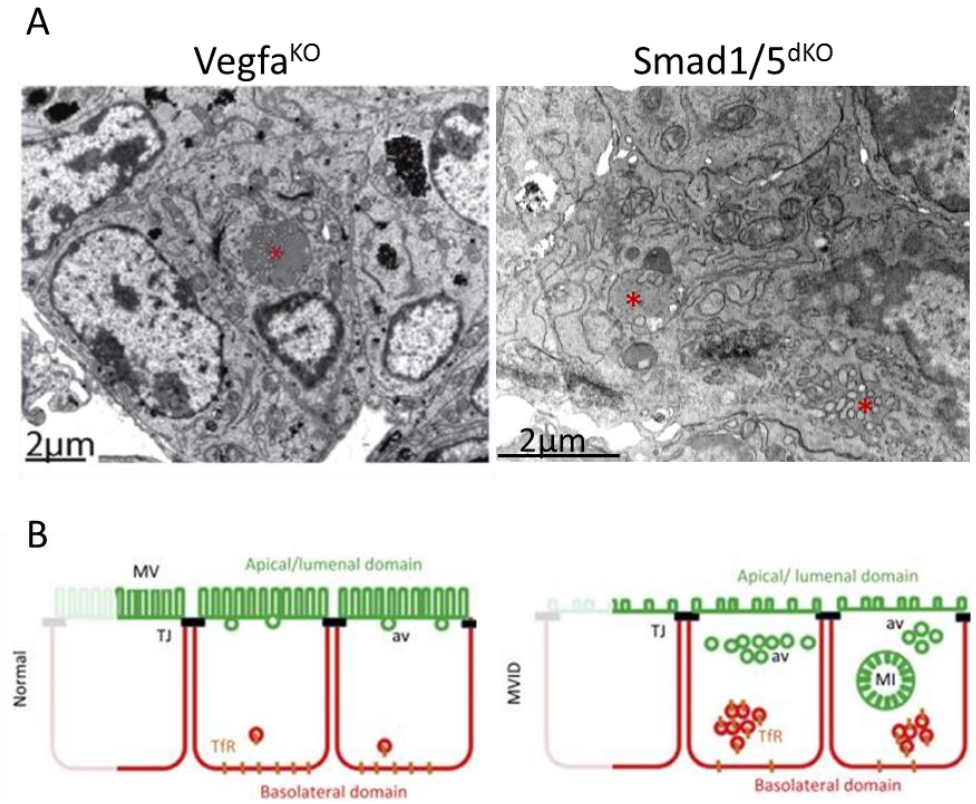

Figure 23. *De novo* lumen formation and MIVD. A. Visualization of intracellular lumen (red asterisk) by electronic microscopy in Vegfa^{KO} and Smad1/5^{dKO}. B. Schematic representation of intestinal epithelial polarity in normal and MIVD conditions. In normal intestine, microvilli are present in high number at the apical domain facing the lumen and apical vesicles (av) fuse with the apical membrane. In MIVD, the apical endocytic trafficking is defective and microvilli inclusion vacuoles and apical vesicles accumulate in the cell. In few cases, the accumulation of basolateral vesicles is also observed (Overeem et al., 2015).

Similar structures have been observed and mainly described in the so called microvillus inclusion disease (MIVD) (Figure 23 B.). In this rare intestinal disease, intestinal cells have defective microvilli at the apical pole, thereby causing

nutrient malabsorption and severe diarrhea. The lack of apical microvilli is explained by the presence of microvilli-containing intracellular structures. MIVD is mostly associated with mutation in the myosin-VB gene or in few case, in the syntaxin-3 gene. Myosin-VB is a motor protein, which interacts with actin filaments and enables trafficking of intracellular vesicles toward the apical membrane. Syntaxin-3 is an apical SNARE involved in fusion of intracellular vesicles with the apical membrane. Mutations in these two genes cause accumulation of microvillus inclusion bodies and subapical vesicles in the cell (Overeem et al., 2015; Szperl et al., 2011; Wiegerinck et al., 2014). Mechanistically, it would thus be interesting to measure the expression of myosin-VB and syntaxin-3, or visualize their localization in $Vegfa^{KO}$ and $Smad1/5^{dKO}$. Intracellular lumina have also been observed in cancer cell lines: in intestinal cell line (Caco-2) after pharmacological inhibition of microtubules polymerization (Gilbert and Rodriguez-Boulan, 1991), and in breast cancer cell line (MCF-7), when cell adhesion is not yet established (Vega-Salas et al., 1993). A common defective mechanism leading to the presence of intracellular vesicles in both $Vegfa^{KO}$ and $Smad1/5^{dKO}$ may exist. We could hypothesize that the defect in basement membrane assembly prevents production of an intracellular signal required for actin filaments or microtubules polymerization/stabilization, or for the fusion of vesicles with the apical membrane. Although we did perform few experiments, in another context, on microtubules stability in CM-treated thyroid, we never analyzed microtubules integrity in the two KO.

2. General conclusion

In conclusion, our work refines the developing thyroid model presented in the introduction (Compare Figure 3; see chapter 1.2.1., with Figure 24). First, we demonstrated that soon after thyroid bud formation, epithelial production of VEGF-A allows recruitment of endothelial cells (red) around the bud (blue). Around E14, some thyrocyte progenitors within the mass acquire apical markers, visualized as intracellular $ezrin^{+}$ clusters (green dots). Concomitantly, endothelial cells progressively invade the thyroid mass (blue), thereby disrupting epithelial cell-cell contacts and creating new cell-matrix contacts and development of a laminin-rich basement membrane (orange). Further development and maturation of apico-basal polarity require (i) fusion of $ezrin^{+}$ vesicles, containing microvilli and loaded with apical proteins (transporters, channels and pumps) with the apical

membrane, and (ii) stabilization of basement membrane scaffold. Extended contacts with endothelial cells and concerted and oriented apico-basal polarization of adjacent thyrocytes are critical aspects for thyroid function (Figure 24).

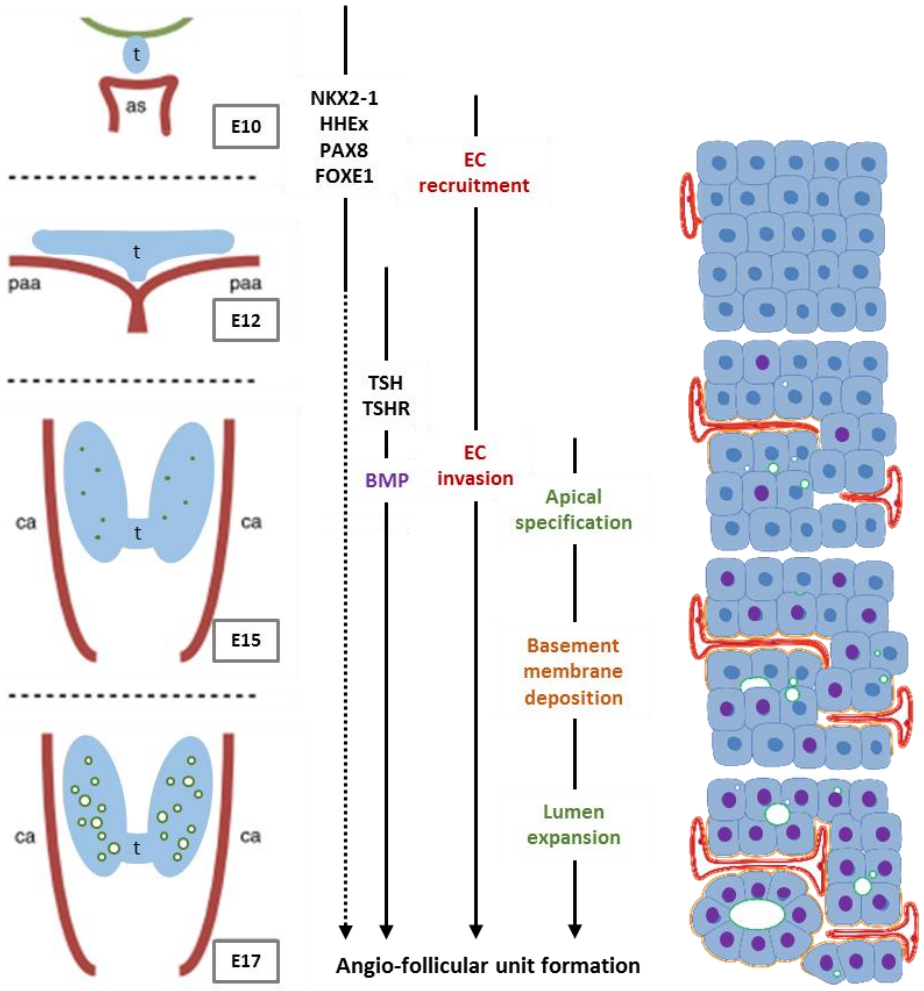

Figure 24. Refinement in thyroid development and folliculogenesis models. On the left: global thyroid morphogenesis, on the right: cellular behavior. Endothelial cells (red) are recruited upon VEGF-A secretion and progressively invade the thyroid cell mass (blue). Their presence and invasion are required for follicle formation. In parallel, cell polarization by apical specification (green) and basement membrane (orange) deposition and assembly allows lumen formation and expansion. BMP signaling (purple), active from E15 is also required for follicle formation (adapted from (Fagman and Nilsson, 2010)).

We propose the following model based on our cellular and molecular observations. During folliculogenesis, follicular epithelial cells (blue) produce the pro-angiogenic factor VEGF-A which will bind VEGFR2 on endothelial cells (red) to recruit them around thyroid bud. With invasion and penetration of endothelial cells in the mass, epithelial cell contacts will be disrupted and new ECM-epithelial cell contacts will be created. This physical role is necessary for cell polarization and reorganization. In addition, endothelial cells may secrete a factor (X) required for folliculogenesis. Following contact disruptions, epithelial cells will assemble their own basement membrane (orange) by production and secretion of laminins and type IV collagen. This assembled BM will reinforce polarization signals. In parallel, BMP-Smad1/5 signaling (purple) is active during thyroid development and is also required for correct follicular reorganization of thyroid cells. Smad1/5 pathway supports endothelial cells function by controlling VEGFA expression, in addition to promoting basement membrane production. *In vitro*, we discovered that endothelial progenitor cells directly produce laminin 111 which promotes follicles formation. We hypothesize that *in vivo*, the X factor could be laminins (Figure 25).

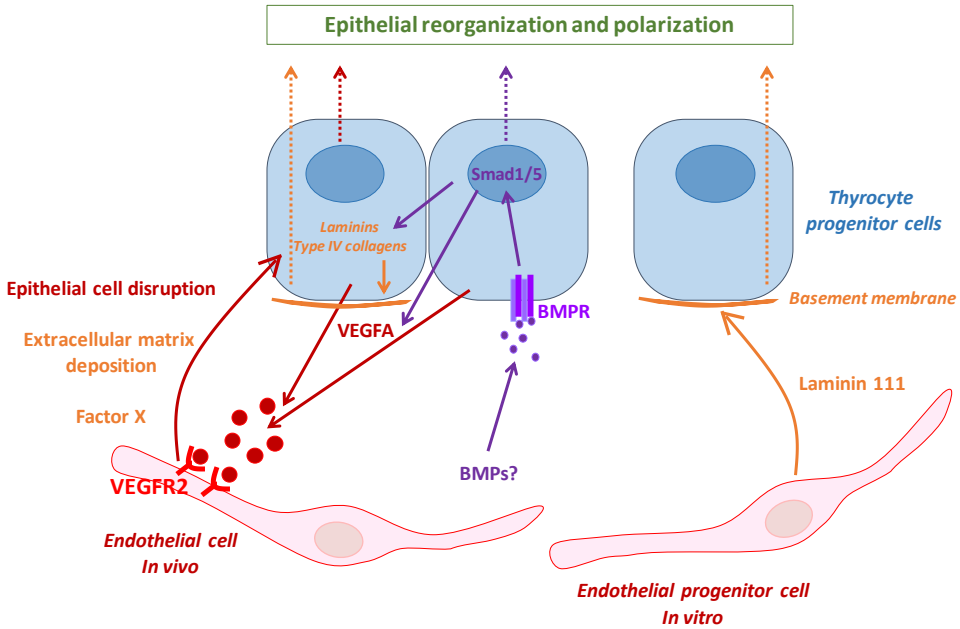

Figure 25. Reciprocal paracrine interactions during epithelial cell reorganization into follicles. See text for details.

IX. Bibliography

Akhtar, N. and Streuli, C. H. (2013). An integrin–ILK–microtubule network orients cell polarity and lumen formation in glandular epithelium. *Nature cell biology* **15**, 17-27.

Andersson, L., Westerlund, J., Liang, S., Carlsson, T., Amendola, E., Fagman, H. and Nilsson, M. (2011). Role of EphA4 receptor signaling in thyroid development: regulation of folliculogenesis and propagation of the C-cell lineage. *Endocrinology* **152**, 1154-1164.

Andrew, D. J. and Ewald, A. J. (2010). Morphogenesis of epithelial tubes: Insights into tube formation, elongation, and elaboration. *Developmental biology* **341**, 34-55.

Antonica, F., Kasprzyk, D. F., Opitz, R., Iacovino, M., Liao, X.-H., Dumitrescu, A. M., Refetoff, S., Peremans, K., Manto, M. and Kyba, M. (2012). Generation of functional thyroid from embryonic stem cells. *Nature* **491**, 66-71.

Antoniou, A., Raynaud, P., Cordi, S., Zong, Y., Tronche, F., Stanger, B. Z., Jacquemin, P., Pierreux, C. E., Clotman, F. and Lemaigre, F. P. (2009). Intrahepatic bile ducts develop according to a new mode of tubulogenesis regulated by the transcription factor SOX9. *Gastroenterology* **136**, 2325-2333.

Aszodi, A., Legate, K. R., Nakchbandi, I. and Fässler, R. (2006). What mouse mutants teach us about extracellular matrix function. *Annu. Rev. Cell Dev. Biol.* **22**, 591-621.

Aumailley, M. (2013). The laminin family. *Cell adhesion & migration* **7**, 48-55.

Bagnat, M., Cheung, I. D., Mostov, K. E. and Stainier, D. Y. (2007). Genetic control of single lumen formation in the zebrafish gut. *Nature Cell Biology* **9**, 954-960.

Bagnat, M., Navis, A., Herbstreith, S., Brand-Arzamendi, K., Curado, S., Gabriel, S., Mostov, K., Huisken, J. and Stainier, D. Y. (2010). Cse1l is a negative regulator of CFTR-dependent fluid secretion. *Current biology* **20**, 1840-1845.

Balda, M. S. and Matter, K. (2009). Tight junctions and the regulation of gene expression. *Biochimica Et Biophysica Acta (BBA)-Biomembranes* **1788**, 761-767.

Barczyk, M., Carracedo, S. and Gullberg, D. (2010). Integrins. *Cell and tissue research* **339**, 269-280.

Bradshaw, A. D. (2009). The role of SPARC in extracellular matrix assembly. *Journal of cell communication and signaling* **3**, 239-246.

Bryant, D. M., Datta, A., Rodríguez-Fraticelli, A. E., Peränen, J., Martín-Belmonte, F. and Mostov, K. E. (2010). A molecular network for de novo generation of the apical surface and lumen. *Nature cell biology* **12**, 1035-1045.

Bryant, D. M. and Mostov, K. E. (2008). From cells to organs: building polarized tissue. *Nature reviews Molecular cell biology* **9**, 887-901.

Chambard, M., Gabrion, J. and Mauchamp, J. (1981). Influence of collagen gel on the orientation of epithelial cell polarity: follicle formation from isolated thyroid cells and from preformed monolayers. *The Journal of cell biology* **91**, 157-166.

Colin, I. M., Denef, J.-F., Lengelé, B., Many, M.-C. and Gérard, A.-C. (2013). Recent insights into the cell biology of thyroid angiofollicular units. *Endocrine reviews* **34**, 209-238.

Dai, F., Lin, X., Chang, C. and Feng, X. (2010). Coupled Actions of PPM1A and RanBP3 Terminate TGFβ/SMAD Tumor Suppressor Functions. *Journal of Surgical Research* **158**, 333.

Datta, A., Bryant, D. M. and Mostov, K. E. (2011). Molecular regulation of lumen morphogenesis. *Current Biology* **21**, R126-R136.

De Felice, M. and Di Lauro, R. (2004). Thyroid development and its disorders: genetics and molecular mechanisms. *Endocrine reviews* **25**, 722-746.

De Felice, M. and Di Lauro, R. (2007). Murine models for the study of thyroid gland development.

De Felice, M. and Di Lauro, R. (2011). Minireview: intrinsic and extrinsic factors in thyroid gland development: an update. *Endocrinology* **152**, 2948-2956.

Delmarcelle, A.-S., Villacorte, M., Hick, A.-C. and Pierreux, C. E. (2014). An Ex vivo Culture System to Study Thyroid Development. *JoVE (Journal of Visualized Experiments)*, e51641-e51641.

Di Palma, T., Filippone, M., Pierantoni, G., Fusco, A., Soddu, S. and Zannini, M. (2013). Pax8 has a critical role in epithelial cell survival and proliferation. *Cell death & disease* **4**, e729.

Domogatskaya, A., Rodin, S. and Tryggvason, K. (2012). Functional diversity of laminins. *Annual review of cell and developmental biology* **28**, 523-553.

Domyan, E. T., Ferretti, E., Throckmorton, K., Mishina, Y., Nicolis, S. K. and Sun, X. (2011). Signaling through BMP receptors promotes respiratory identity in the foregut via repression of Sox2. *Development* **138**, 971-981.

Dunn, J. T. and Dunn, A. D. (2001). Update on intrathyroidal iodine metabolism. *Thyroid* **11**, 407-414.

Durbeej, M., Ekblom, P., Henry, M. D., Campbell, K., Talts, J. and Yurchenco, P. (2001). Dystroglycan binding to laminin α1LG4 module influences epithelial morphogenesis of salivary gland and lung in vitro. *Differentiation* **69**, 121-134.

Eggo, M. C., Quiney, V. M. and Campbell, S. (2003). Local factors regulating growth and function of human thyroid cells in vitro and in vivo. *Molecular and cellular endocrinology* **213**, 47-58.

Fagman, H., Andersson, L. and Nilsson, M. (2006). The developing mouse thyroid: embryonic vessel contacts and parenchymal growth pattern during specification, budding, migration, and lobulation. *Developmental dynamics* **235**, 444-455.

Fagman, H., Grände, M., Gritli-Linde, A. and Nilsson, M. (2004). Genetic deletion of sonic hedgehog causes hemiagenesis and ectopic development of the thyroid in mouse. *The American journal of pathology* **164**, 1865-1872.

Fagman, H. and Nilsson, M. (2010). Morphogenesis of the thyroid gland. *Molecular and cellular endocrinology* **323**, 35-54.

---- (2011). Morphogenetics of early thyroid development. *Journal of molecular endocrinology* **46**, R33-R42.

Fernández-Santos, J. M., Martín-Lacave, I., Morillo-Bernal, J., Utrilla, J. C. and García-Marín, R. (2012). *Paracrine regulation of thyroid-hormone synthesis by C cells*: INTECH Open Access Publisher.

Ferrari, A., Veligodskiy, A., Berge, U., Lucas, M. S. and Kroschewski, R. (2008). ROCK-mediated contractility, tight junctions and channels contribute to the conversion of a preapical patch into apical surface during isochoric lumen initiation. *Journal of cell science* **121**, 3649-3663.

Filippone, M. G., Di Palma, T., Lucci, V. and Zannini, M. (2014). Pax8 modulates the expression of Wnt4 that is necessary for the maintenance of the epithelial phenotype of thyroid cells. *BMC molecular biology* **15**, 21.

Gassama-Diagne, A., Yu, W., ter Beest, M., Martin-Belmonte, F., Kierbel, A., Engel, J. and Mostov, K. (2006). Phosphatidylinositol-3, 4, 5-trisphosphate regulates the formation of the basolateral plasma membrane in epithelial cells. *Nature cell biology* **8**, 963-970.

Gérard, A.-C., Many, M.-C., Daumerie, C., Costagliola, S., Miot, F., DeVijlder, J. J., Colin, I. and Denef, J.-F. (2002). Structural changes in the angiofollicular units between active and hypofunctioning follicles align with differences in the epithelial expression of newly discovered proteins involved in iodine transport and organification. *The Journal of Clinical Endocrinology & Metabolism* **87**, 1291-1299.

Gilbert, T. and Rodriguez-Boulan, E. (1991). Induction of vacuolar apical compartments in the Caco-2 intestinal epithelial cell line. *Journal of cell science* **100**, 451-458.

Goruppi, S. and Dotto, G. P. (2013). Mesenchymal stroma: primary determinant and therapeutic target for epithelial cancer. *Trends in cell biology* **23**, 593-602.

Govindan, J. and Iovine, M. K. (2015). Dynamic remodeling of the extra cellular matrix during zebrafish fin regeneration. *Gene Expression Patterns*.

Haigh, J. J. (2008). Role of VEGF in organogenesis. *Organogenesis* **4**, 247-256.

Harrison, C. A., Al-Musawi, S. L. and Walton, K. L. (2011). Prodomains regulate the synthesis, extracellular localisation and activity of TGF-β superfamily ligands. *Growth factors* **29**, 174-186.

Harunaga, J. S., Doyle, A. D. and Yamada, K. M. (2014). Local and global dynamics of the basement membrane during branching morphogenesis require protease activity and actomyosin contractility. *Developmental biology* **394**, 197-205.

Hatzopoulos, A. K., Folkman, J., Vasile, E., Eiselen, G. K. and Rosenberg, R. D. (1998). Isolation and characterization of endothelial progenitor cells from mouse embryos. *Development* **125**, 1457-1468.

Heinis, M., Simon, M.-T., Ilc, K., Mazure, N. M., Pouysségur, J., Scharfmann, R. and Duvillié, B. (2010). Oxygen tension regulates pancreatic β-cell differentiation through hypoxia-inducible factor 1α. *Diabetes* **59**, 662-669.

Hick, A.-C., Delmarcelle, A.-S., Bouquet, M., Klotz, S., Copetti, T., Forez, C., Van Der Smissen, P., Sonveaux, P., Collet, J.-F. and Feron, O. (2013). Reciprocal epithelial: endothelial paracrine interactions during thyroid development govern follicular organization and C-cells differentiation. *Developmental biology* **381**, 227-240.

Hick, A.-C., van Eyll, J. M., Cordi, S., Forez, C., Passante, L., Kohara, H., Nagasawa, T., Vanderhaeghen, P., Courtoy, P. J. and Rousseau, G. G. (2009). Mechanism of primitive duct formation in the pancreas and submandibular glands: a role for SDF-1. *BMC developmental biology* **9**, 66.

Hohenester, E. and Yurchenco, P. D. (2013). Laminins in basement membrane assembly. *Cell adhesion & migration* **7**, 56-63.

Iruela-Arispe, M. L. and Beitel, G. J. (2013). Tubulogenesis. *Development* **140**, 2851-2855.

Kalhuri, R. (2003). Basement membranes: Structure, assembly and role in tumor angiogenesis. *Nat. Rev. Cancer* **3**, 422-433.

Kameda, Y., Nishimaki, T., Chisaka, O., Iseki, S. and Sucov, H. M. (2007). Expression of the epithelial marker E-cadherin by thyroid C cells and their precursors during murine development. *Journal of Histochemistry & Cytochemistry* **55**, 1075-1088.

Kim, S.-H., Turnbull, J. and Guimond, S. (2011). Extracellular matrix and cell signalling: the dynamic cooperation of integrin, proteoglycan and growth factor receptor. *Journal of Endocrinology* **209**, 139-151.

Klein, R. (2012). Eph/ephrin signalling during development. *Development* **139**, 4105-4109.

Koh, W., Mahan, R. D. and Davis, G. E. (2008). Cdc42-and Rac1-mediated endothelial lumen formation requires Pak2, Pak4 and Par3, and PKC-dependent signaling. *Journal of cell science* **121**, 989-1001.

Koh, W., Sachidanandam, K., Stratman, A. N., Sacharidou, A., Mayo, A. M., Murphy, E. A., Cheresh, D. A. and Davis, G. E. (2009). Formation of endothelial lumens requires a coordinated PKCϵ-, Src-, Pak-and Raf-kinase-dependent signaling cascade downstream of Cdc42 activation. *Journal of cell science* **122**, 1812-1822.

Kolpak, E., Kabrits, S. and Bubalo, V. (2015). The follicle function and thyroid gland cancer. *Biology and Medicine* **7**.

Kostourou, V. and Papalazarou, V. (2014). Non-collagenous ECM proteins in blood vessel morphogenesis and cancer. *Biochimica et Biophysica Acta (BBA)-General Subjects* **1840**, 2403-2413.

Kupatt, C., Horstkotte, J., Vlastos, G. A., Pfosser, A., Lebherz, C., Semisch, M., Thalgott, M., Büttner, K., Browarzyk, C. and Mages, J. (2005). Embryonic endothelial progenitor cells expressing a broad range of proangiogenic and remodeling factors enhance vascularization and tissue recovery in acute and chronic ischemia. *The FASEB journal* **19**, 1576-1578.

Kusakabe, T., Kawaguchi, A., Hoshi, N., Kawaguchi, R., Hoshi, S. and Kimura, S. (2006). Thyroid-specific enhancer-binding protein/NKX2. 1 is required for the maintenance of ordered architecture and function of the differentiated thyroid. *Molecular endocrinology* **20**, 1796-1809.

Lania, G., Zhang, Z., Huynh, T., Caprio, C., Moon, A. M., Vitelli, F. and Baldini, A. (2009). Early thyroid development requires a Tbx1–Fgf8 pathway. *Developmental biology* **328**, 109-117.

Lazarus, A., Del-Moral, P. M., Ilovich, O., Mishani, E., Warburton, D. and Keshet, E. (2011). A perfusion-independent role of blood vessels in determining branching stereotypy of lung airways. *Development* **138**, 2359-2368.

Levet, S., Ouarné, M., Ciais, D., Coutton, C., Subileau, M., Mallet, C., Ricard, N., Bidart, M., Debillon, T. and Faravelli, F. (2015). BMP9 and BMP10 are necessary for proper closure of the ductus arteriosus. *Proceedings of the National Academy of Sciences* **112**, E3207-E3215.

Li, S., Harrison, D., Carbonetto, S., Fässler, R., Smyth, N., Edgar, D. and Yurchenco, P. D. (2002). Matrix assembly, regulation, and survival functions of laminin and its receptors in embryonic stem cell differentiation. *The Journal of cell biology* **157**, 1279-1290.

Lima, W. R., Parreira, K. S., Devuyst, O., Caplanusi, A., Francisca, N., Marien, B., Van Der Smissen, P., Alves, P. M., Verroust, P. and Christensen, E. I. (2010). ZONAB promotes proliferation and represses differentiation of proximal tubule epithelial cells. *Journal of the American Society of Nephrology* **21**, 478-488.

Lin, X., Duan, X., Liang, Y.-Y., Su, Y., Wrighton, K. H., Long, J., Hu, M., Davis, C. M., Wang, J. and Brunicardi, F. C. (2006). PPM1A functions as a Smad phosphatase to terminate TGFβ signaling. *Cell* **125**, 915-928.

Lohela, M., Bry, M., Tammela, T. and Alitalo, K. (2009). VEGFs and receptors involved in angiogenesis versus lymphangiogenesis. *Current opinion in cell biology* **21**, 154-165.

Lubarsky, B. and Krasnow, M. A. (2003). Tube morphogenesis: making and shaping biological tubes. *Cell* **112**, 19-28.

Ma, R., Latif, R. and Davies, T. F. (2013). Thyroid follicle formation and thyroglobulin expression in multipotent endodermal stem cells. *Thyroid* **23**, 385-391.

---- (2015). Human embryonic stem cells form functional thyroid follicles. *Thyroid* **25**, 455-461.

Macias, M. J., Martin-Malpartida, P. and Massagué, J. (2015). Structural determinants of Smad function in TGF-β signaling. *Trends in biochemical sciences* **40**, 296-308.

Manninen, A. (2015). Epithelial polarity–Generating and integrating signals from the ECM with integrins. *Experimental cell research* **334**, 337-349.

Mansouri, A., Chowdhury, K. and Gruss, P. (1998). Follicular cells of the thyroid gland require Pax8 gene function. *Nature genetics* **19**, 87-90.

Marotta, P., Amendola, E., Scarfò, M., De Luca, P., Zoppoli, P., Amoresano, A., De Felice, M. and Di Lauro, R. (2014). The paired box transcription factor Pax8 is essential for function and survival of adult thyroid cells. *Molecular and cellular endocrinology* **396**, 26-36.

Martin-Belmonte, F., Gassama, A., Datta, A., Yu, W., Rescher, U., Gerke, V. and Mostov, K. (2007). PTEN-mediated apical segregation of phosphoinositides controls epithelial morphogenesis through Cdc42. *Cell* **128**, 383-397.

Martín-Belmonte, F. and Rodríguez-Fraticelli, A. E. (2009). Acquisition of Membrane Polarity in Epithelial Tube Formation: Patterns, Signaling Pathways, Molecular Mechanisms, and Disease. *International review of cell and molecular biology* **274**, 129-182.

Maruyama, C., Leigh, N., Nelson, J., McCall, A., Mellas, R., Lei, P., Andreadis, S. and Baker, O. (2015). Stem Cell–Soluble Signals Enhance Multilumen Formation in SMG Cell Clusters. *Journal of dental research* **94**, 1610-1617.

Mauchamp, J., Mirrione, A., Alquier, C. and André, F. (1998). Follicle-like structure and polarized monolayer: role of the extracellular matrix on thyroid cell organization in primary culture. *Biology of the Cell* **90**, 369-380.

Miosge, N., Holzhausen, S., Zelent, C., Sprysch, P. and Herken, R. (2001). Nidogen-1 and nidogen-2 are found in basement membranes during human embryonic development. *The Histochemical journal* **33**, 523-530.

Miyazono, K., Kamiya, Y. and Morikawa, M. (2010). Bone morphogenetic protein receptors and signal transduction. *Journal of biochemistry* **147**, 35-51.

Miyazono, K., Maeda, S. and Imamura, T. (2005). BMP receptor signaling: transcriptional targets, regulation of signals, and signaling cross-talk. *Cytokine & growth factor reviews* **16**, 251-263.

Morrissey, M. A. and Sherwood, D. R. (2015). An active role for basement membrane assembly and modification in tissue sculpting. *Journal of cell science* **128**, 1661-1668.

Moya, I. M., Umans, L., Maas, E., Pereira, P. N., Beets, K., Francis, A., Sents, W., Robertson, E. J., Mummery, C. L. and Huylebroeck, D. (2012). Stalk cell phenotype depends on integration of Notch and Smad1/5 signaling cascades. *Developmental cell* **22**, 501-514.

Nedvetsky, P. I., Emmerson, E., Finley, J. K., Ettinger, A., Cruz-Pacheco, N., Prochazka, J., Haddox, C. L., Northrup, E., Hodges, C. and Mostov, K. E. (2014). Parasympathetic innervation regulates tubulogenesis in the developing salivary gland. *Developmental cell* **30**, 449-462.

Nelson, C. M. and Bissell, M. J. (2006). Of extracellular matrix, scaffolds, and signaling: tissue architecture regulates development, homeostasis, and cancer. *Annual review of cell and developmental biology* **22**, 287.

Nikolova, G., Jabs, N., Konstantinova, I., Domogatskaya, A., Tryggvason, K., Sorokin, L., Fässler, R., Gu, G., Gerber, H.-P. and Ferrara, N. (2006). The vascular basement membrane: a niche for insulin gene expression and β cell proliferation. *Developmental cell* **10**, 397-405.

O'Brien, L. E., Jou, T.-S., Pollack, A. L., Zhang, Q., Hansen, S. H., Yurchenco, P. and Mostov, K. E. (2001). Rac1 orientates epithelial apical polarity through effects on basolateral laminin assembly. *Nature cell biology* **3**, 831-838.

Ohuchi, H., Hori, Y., Yamasaki, M., Harada, H., Sekine, K., Kato, S. and Itoh, N. (2000). FGF10 acts as a major ligand for FGF receptor 2 IIIb in mouse multi-organ development. *Biochemical and biophysical research communications* **277**, 643-649.

Ojakian, G. K. and Schwimmer, R. (1994). Regulation of epithelial cell surface polarity reversal by beta 1 integrins. *Journal of cell science* **107**, 561-576.

Opitz, R., Maquet, E., Zoenen, M., Dadhich, R. and Costagliola, S. (2011). TSH receptor function is required for normal thyroid differentiation in zebrafish. *Molecular endocrinology* **25**, 1579-1599.

Overeem, A. W., Bryant, D. M. and van IJzendoorn, S. C. (2015). Mechanisms of apical–basal axis orientation and epithelial lumen positioning. *Trends in cell biology* **25**, 476-485.

Parlato, R., Rosica, A., Rodriguez-Mallon, A., Affuso, A., Postiglione, M. P., Arra, C., Mansouri, A., Kimura, S., Di Lauro, R. and De Felice, M. (2004). An integrated regulatory network controlling survival and migration in thyroid organogenesis. *Developmental biology* **276**, 464-475.

Pierreux, C. E., Cordi, S., Hick, A.-C., Achouri, Y., de Almodovar, C. R., Prévot, P.-P., Courtoy, P. J., Carmeliet, P. and Lemaigre, F. P. (2010). Epithelial: Endothelial cross-talk regulates exocrine differentiation in developing pancreas. *Developmental biology* **347**, 216-227.

Plosa, E. J., Young, L. R., Gulleman, P. M., Polosukhin, V. V., Zaynagetdinov, R., Benjamin, J. T., Im, A. M., van der Meer, R., Gleaves, L. A. and Bulus, N. (2014). Epithelial β1 integrin is required for lung branching morphogenesis and alveolarization. *Development* **141**, 4751-4762.

Pöschl, E., Schlötzer-Schrehardt, U., Brachvogel, B., Saito, K., Ninomiya, Y. and Mayer, U. (2004). Collagen IV is essential for basement membrane stability but dispensable for initiation of its assembly during early development. *Development* **131**, 1619-1628.

Pozzi, A. and Zent, R. (2011). Extracellular matrix receptors in branched organs. *Current opinion in cell biology* **23**, 547-553.

Ramasamy, S. K., Kusumbe, A. P. and Adams, R. H. (2015). Regulation of tissue morphogenesis by endothelial cell-derived signals. *Trends in cell biology* **25**, 148-157.

Ramel, M.-C. and Hill, C. S. (2012). Spatial regulation of BMP activity. *FEBS letters* **586**, 1929-1941.

Rebustini, I. T., Patel, V. N., Stewart, J. S., Layvey, A., Georges-Labouesse, E., Miner, J. H. and Hoffman, M. P. (2007). Laminin α5 is necessary for submandibular gland epithelial morphogenesis and influences FGFR expression through β1 integrin signaling. *Developmental biology* **308**, 15-29.

Revest, J.-M., Spencer-Dene, B., Kerr, K., De Moerlooze, L., Rosewell, I. and Dickson, C. (2001). Fibroblast growth factor receptor 2-IIIb acts upstream of Shh and Fgf4 and is required for limb bud maintenance but not for the induction of Fgf8, Fgf10, Msx1, or Bmp4. *Developmental biology* **231**, 47-62.

Rivera, L. B., Bradshaw, A. D. and Brekken, R. A. (2011). The regulatory function of SPARC in vascular biology. *Cellular and Molecular Life Sciences* **68**, 3165-3173.

Robinson, C. J. and Stringer, S. E. (2001). The splice variants of vascular endothelial growth factor (VEGF) and their receptors. *Journal of cell science* **114**, 853-865.

Sasaki, T., Takagi, J., Giudici, C., Yamada, Y., Arikawa-Hirasawa, E., Deutzmann, R., Timpl, R., Sonnenberg, A., Bächinger, H. P. and Tonge, D. (2010).

Laminin-121—recombinant expression and interactions with integrins. *Matrix Biology* **29**, 484-493.

Shattil, S. J., Kim, C. and Ginsberg, M. H. (2010). The final steps of integrin activation: the end game. *Nature reviews Molecular cell biology* **11**, 288-300.

Sigurbjörnsdóttir, S., Mathew, R. and Leptin, M. (2014). Molecular mechanisms of de novo lumen formation. *Nature Reviews Molecular Cell Biology* **15**, 665-676.

Silberschmidt, D., Rodriguez-Mallon, A., Mithboakar, P., Calì, G., Amendola, E., Sanges, R., Zannini, M., Scarfò, M., De Luca, P. and Nitsch, L. (2011). In vivo role of different domains and of phosphorylation in the transcription factor Nkx2-1. *BMC developmental biology* **11**, 9.

Szperl, A. M., Golachowska, M. R., Bruinenberg, M., Prekeris, R., Thunnissen, A.-M. W., Karrenbeld, A., Dijkstra, G., Hoekstra, D., Mercer, D. and Ksiazyk, J. (2011). Functional characterization of mutations in the myosin Vb gene associated with microvillus inclusion disease. *Journal of pediatric gastroenterology and nutrition* **52**, 307.

Tanimizu, N., Kikkawa, Y., Mitaka, T. and Miyajima, A. (2012). α1-and α5-containing laminins regulate the development of bile ducts via β1 integrin signals. *Journal of Biological Chemistry* **287**, 28586-28597.

Toda, S., Aoki, S., Uchihashi, K., Matsunobu, A., Yamamoto, M., Ootani, A., Yamasaki, F., Koike, E. and Sugihara, H. (2011). Culture models for studying thyroid biology and disorders. *ISRN endocrinology* **2011**.

Toda, S., Koike, N. and Suoihara, H. (2001). Cellular integration of thyrocytes and thyroid folliculogenesis: a perspective for thyroid tissue regeneration and engineering. *Endocrine journal* **48**, 407-425.

Toda, S., Watanabe, K., Yokoi, F., Matsumura, S., Suzuki, K., Ootani, A., Aoki, S., Koike, N. and Sugihara, H. (2002). A new organotypic culture of thyroid tissue maintains three-dimensional follicles with C cells for a long term. *Biochemical and biophysical research communications* **294**, 906-911.

Trueba, S. S., Augé, J., Mattei, G., Etchevers, H., Martinovic, J. l. e. n., Czernichow, P., Vekemans, M., Polak, M. and Attié-Bitach, T. (2005). PAX8, TITF1, and FOXE1 gene expression patterns during human development: new insights into human thyroid development and thyroid dysgenesis-associated malformations. *The Journal of Clinical Endocrinology & Metabolism* **90**, 455-462.

Turner, N. and Grose, R. (2010). Fibroblast growth factor signalling: from development to cancer. *Nature Reviews Cancer* **10**, 116-129.

Vega-Salas, D. E., San Martino, J. A., Salas, P. J. and Baldi, A. (1993). Vacuolar apical compartment (VAC) in breast carcinoma cell lines (MCF-7 and

T47D): failure of the cell-cell regulated exocytosis mechanism of apical membrane. *Differentiation* **54**, 131-141.

Villasenor, A., Chong, D. C., Henkemeyer, M. and Cleaver, O. (2010). Epithelial dynamics of pancreatic branching morphogenesis. *Development* **137**, 4295-4305.

Wang, A., Ojakian, G. and Nelson, W. (1990). Steps in the morphogenesis of a polarized epithelium. II. Disassembly and assembly of plasma membrane domains during reversal of epithelial cell polarity in multicellular epithelial (MDCK) cysts. *Journal of Cell Science* **95**, 153-165.

Wang, H., Lacoche, S., Huang, L., Xue, B. and Muthuswamy, S. K. (2013). Rotational motion during three-dimensional morphogenesis of mammary epithelial acini relates to laminin matrix assembly. *Proceedings of the National Academy of Sciences* **110**, 163-168.

Wang, R. N., Green, J., Wang, Z., Deng, Y., Qiao, M., Peabody, M., Zhang, Q., Ye, J., Yan, Z. and Denduluri, S. (2014). Bone Morphogenetic Protein (BMP) signaling in development and human diseases. *Genes & diseases* **1**, 87-105.

Wang, X., Harris, R. E., Bayston, L. J. and Ashe, H. L. (2008). Type IV collagens regulate BMP signalling in Drosophila. *Nature* **455**, 72-77.

Wiegerinck, C. L., Janecke, A. R., Schneeberger, K., Vogel, G. F., van Haaften–Visser, D. Y., Escher, J. C., Adam, R., Thöni, C. E., Pfaller, K. and Jordan, A. J. (2014). Loss of syntaxin 3 causes variant microvillus inclusion disease. *Gastroenterology* **147**, 65-68. e10.

Wu, M. Y. and Hill, C. S. (2009). TGF-β superfamily signaling in embryonic development and homeostasis. *Developmental cell* **16**, 329-343.

Yang, B., Sonawane, N. D., Zhao, D., Somlo, S. and Verkman, A. (2008). Small-molecule CFTR inhibitors slow cyst growth in polycystic kidney disease. *Journal of the American Society of Nephrology* **19**, 1300-1310.

Yang, X. P. and Chiba, S. (1999). Effects of prolonged cold storage on double peaked vasoconstrictor responses to periarterial nerve stimulation in isolated canine splenic arteries. *Br J Pharmacol* **126**, 1810-1814.

Yousif, L. F., Di Russo, J. and Sorokin, L. (2013). Laminin isoforms in endothelial and perivascular basement membranes. *Cell adhesion & migration* **7**, 101-110.

Yu, W., Datta, A., Leroy, P., O'Brien, L. E., Mak, G., Jou, T.-S., Matlin, K. S., Mostov, K. E. and Zegers, M. M. (2005). β1-integrin orients epithelial polarity via Rac1 and laminin. *Molecular biology of the cell* **16**, 433-445.

Yurchenco, P. D. (2011). Basement membranes: cell scaffoldings and signaling platforms. *Cold Spring Harbor perspectives in biology* **3**, a004911.

---- (2015). Integrating Activities of Laminins that Drive Basement Membrane Assembly and Function. *Current Topics in Membranes* **76**.

Zannini, M., Acebron, A., De Felice, M., Arnone, M. I., Martin-Pérez, J., Santisteban, P. and Di Lauro, R. (1996). Mapping and functional role of phosphorylation sites in the thyroid transcription factor-1 (TTF-1). *Journal of Biological Chemistry* **271**, 2249-2254.

Zegers, M. M., O'Brien, L. E., Yu, W., Datta, A. and Mostov, K. E. (2003). Epithelial polarity and tubulogenesis in vitro. *Trends in cell biology* **13**, 169-176.

Books references

Alberts B., Johnson A., Lewis J. (2002). Molecular Biology of the Cell, 4th edition. New York: Garland Science.

Koeppen B. M., Stanton B. A. (2010). Berne & Levy Physiology, updated edition, 6th edition.

Weiss A. S. (2011). The science of elastin, Copyright Elastagen Pty Ltd.